Generating patient-derived models of soft-tissue sarcoma for the evaluation of therapy response and resistance

William Gabriel John Kerrison

A thesis submitted for the degree of Doctor of Philosophy

The Institute of Cancer Research

University of London

Declaration

The work presented in this thesis was completed under the supervision of Dr Paul Huang in the Molecular and Systems Oncology team at the Institute of Cancer Research, London, United Kingdom.

I, William Kerrison, confirm that the work presented in this thesis is my own. Information that has been derived from other sources is clearly indicated within the thesis.

Abstract

For the majority of patients, advanced soft-tissue sarcoma (STS) is fatal, with an overall survival of 14-19 months. Systemic chemotherapy has remained the cornerstone of advanced STS control for more than 30 years and prognosis has seen little change in the past decade, highlighting the urgent need for novel treatment modalities. In order to improve clinical efficacy of targeted therapies, identification of response and resistance mechanisms and candidate biomarkers of response are vital. However, a major obstacle in the study of STS drug response mechanisms is the lack of models that closely represent patient tumours. This obstacle restricts our ability to develop effective treatment strategies for advanced sarcoma that can be translated into clinical benefit.

This project seeks to address this issue by first establishing a patient-derived model pipeline, starting with STS patient tumour biopsies, and using this to develop a panel of patient-derived xenografts (PDXs) as well as 2D and 3D in vitro PDX-derived cell cultures, with a particular focus on the leiomyosarcoma (LMS) subtype. These models have been characterised via proteomic profiling, by measuring growth kinetics and, in the case of in vitro cultures, tumourigenicity by in vivo injection. These models were used in cell-based and in vivo assays to assess the degree of sensitivity to standard of care chemotherapies such as doxorubicin, gemcitabine or docetaxel as well as a panel of small molecule inhibitors targeting key oncogenic signalling pathways. This analysis was followed by functional assessment of candidate drug response mechanisms. Through these means, I reported the mechanisms of response to standard of care therapeutics and targeted therapies such as PI3K/mTOR and PARP inhibitors while highlighting predictive biomarkers of response including phosphatase and tensin homolog (PTEN) deletion. Additionally, the impact of chemo-resistance on subsequent response to targeted therapies was investigated to inform future drug treatment regimens.
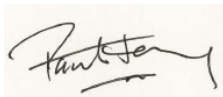
COVID-19 impact statement

Following the government "Stay at Home" order, I met with my primary supervisor (Paul Huang) on 20/03/20 and planned to immediately stop experiments. The Institute of Cancer Research (ICR) laboratories were closed on 23/03/20. The initial lockdown resulted in having to cease all ongoing experiments, which included the establishment of PDX-derived cell cultures and drug dose escalation studies. Unfortunately, some of these cultures were primary cells which were still under early stages of expansion. Upon cryopreserving these early cultures and thawing no viable cells remained. There was therefore a need to re-derive these primary cell models (~2 months of work lost) post-lockdown whilst work to establish new *in vitro* cultures had to be postponed due to time constraints. PDX-engraftment of patient biopsies was also halted and patient biopsies were instead frozen for the duration of lockdown, delaying the establishment of these models. ICR laboratories were reopened on 08/06/20 at a reduced capacity of 30% until 16/08/21 and during this time, shift-work was implemented due to social distancing rules. From June to August 2020, tissue culture laboratories were operating at 25% capacity and from August 2020 until September 2021 tissue culture laboratories were operating at 50% capacity which both significantly impacted productivity. Due to the impact of COVID on the laboratory closure as well as extended social distancing rules, a deadline extension was granted from 30/9/22 to 30/12/22.

Will Kerrison

Dr. Paul Huang

Acknowledgments

Firstly, I would like to thank my supervisor, Dr. Paul Huang, for giving me the opportunity to work in his lab, and for his support, dedication and guidance throughout my project. I would also like to thank the Molecular and Systems Oncology team, both past and present who have helped me throughout my PhD, offering advice and reassurance. All of them have make the lab a wonderful place to work.

Outside of work I would like to thank my parents and brothers who have given me constant support and encouragement. To my partner Alihan, I would like to say thank you for your unwavering patience with me throughout this entire PhD journey, and for never once failing to cheer me up after experiments go awry.

Table of contents

List of figures

List of tables

Abbreviations and acronyms

4EBP1	Eukaryotic initiation factor 4E (elF-4E) binding protein 1
ABC	ATP-binding cassette
ACTB	β-actin
ACTG2	Actin gamma smooth muscle 2
ADIRF	Adipogenesis Regulatory Factor
ADP	Adenosine diphosphate

ALDH1	Aldehyde dehydrogenase 1
ALK	Anaplastic lymphoma kinase
ALT	Alternative lengthening of telomeres
ARMS	Alveolar rhabdomyosarcoma
ASPS	Alveolar soft part sarcoma
ATM	Ataxia telangiectasia mutated
ATP	Adenosine triphosphate
ATR	Ataxia telangiectasia and Rad3-related protein
ATRX	Alpha-thalassemia/intellectual disability syndrome, X-linked
BAK	BCL2 Antagonist/Killer 1
BAX	Bcl-2-associated X protein
BCA	Bicinchoninic acid
BCL-2	B-cell lymphoma 2
BCL-w	Bcl-2-like protein 2
BCL-xL	B-cell lymphoma-extra large
BCR/ABL	Breakpoint cluster region/Abelson
BER	Base excision repair
BET	Bromo- and extra-terminal domain
bFGF	Basic FGF
BME	Basement membrane extract
BRCA1/2	Breast cancer gene
BSA	Bovine serum albumin
CAF	Cancer associated fibroblast
CAIX	Carbonic anhydrase IX
CALD1	Caldesmon gene
CC3	Cleaved caspase 3
CCND1	Cyclin D1
CCND3	Cyclin D3
CCS	Clear cell sarcoma
CDK	Cyclin-dependent kinases

CDKN2A	Cyclin Dependent Kinase Inhibitor 2A
cDNA	complementary DNA
CHD4	Chromodomain helicase DNA-binding protein 4
CHEK1	Checkpoint kinase 1
CHEK2	Checkpoint kinase 2
CHRDL2	Chordin Like 2
Cmax	Peak plasma concentration
CRISPR	Clustered Regularly Interspaced Short Palindromic Repeats
CtIP	Carboxy-terminal binding protein
DCN	Decorin
DDLPS	De-differentiated liposarcoma
DDR	DNA damage response
DMEM	Dulbecco's Modified Eagle Medium
DMSO	Dimethylsulfoxide
DNA-PK	DNA-dependent protein kinase catalytic subunit
DOR	Duration of repsonse
DSB	Double strand break
E2F1	E2 promoter binding factor 1
EBV	Epstein-Barr virus
ECM	Extracellular matrix
EDTA	Ethylenediamine tetraacetic acid
eEF2K	Eukaryotic elongation factor 2 kinase
EGF	Epidermal growth factor
EGFR	Epidermal growth factor receptor
eIF-4A	Eukaryotic translation initiation factor 4A
eIF-4B	Eukaryotic translation initiation factor 4B
eIF-4E	Eukaryotic translation initiation factor 4E
eIF-4G	Eukaryotic translation initiation factor 4G
EORTC	European Organisation for Research and Treatment of Cancer
EORTC-STBSG	European organisation for Research and Treatment of Cancer-Soft Tissue and Bone Sarcoma group

ERK	Extracellular signal-regulated kinase
ES	Epithelioid sarcoma
ESR1	Estrogen receptor 1
EZH2	Enhancer of zeste homolog 2
FAK	Focal adhesion kinase
FANCA	Fanconi anemia complementation group A
FASP	Filter-aided sample preparation
FBS	Foetal bovine serum
FDA	Food and Drug Administration
FDR	False discovery rate
FFPE	Formalin fixed paraffin embedded
FGF	Fibroblast growth factor
FGFR	Fibroblast growth factor receptor
FIGO	Federation of Gynaecology and Obstetrics
FNCLCC	Fédération Nationale des Centres de Lutte Contre le Cancer
FOXO	Fork head box O
GEMM	Genetically engineered mouse models
GINS1	GINS Complex Subunit 1
GIST	Gastrointestinal stromal tumour
GRB2	Growth factor receptor-bound protein 2
GSK3	Glycogen synthetase 3
H&E	Hematoxylin and eosin
H2AX	H2A histone family member X
HEPES	4-(2-hydroxyethyl)-1-piperazineethanesulfonic acid
HER2	Human epidermal growth factor receptor 2
HGFR	Hepatocyte growth factor receptor
HHV8	Human herpesvirus 8
HIF-1α	Hypoxia-inducible factor 1α
HR	Homologous recombination
HRD	Homologous recombination deficiency

HRP	Horseradish peroxidase
HSP90	Heat shock protein 90
IC50	Half-maximal inhibitory concentration
ICI	Immune checkpoint inhibitor
IGF	Insulin growth factor
IGFR	Insulin growth factor receptor
IHC	Immunohistochemical
IL2	Interleukin-2
IR	Ionising radiation
IRS	Insulin receptor substrate
JAK-2	Janus kinase 2
LFS	Li-Fraumeni syndrome
LMS	Leiomyosarcoma
LPS	Liposarcoma
MACS	Magnetic-activated cell sorting
MAPK	Mitogen-activated protein kinase
MDM2	Murine double minute 2
MDR1	Multi-drug resistance protein 1
MEK	Mitogen-activated protein kinase kinase
MELK	Maternal embryonic leucine zipper kinase
mOS	Median overall survival
mPFS	Median progression free survival
MPNST	Malignant peripheral nerve sheath tumour
MRE11	Meiotic recombination 11 homolog 1
mRNA	Ribonucleic acid
mTOR	Mammalian target of rapamycin
mTORC1	Mammalian target of rapamycin complex 1
mTORC2	Mammalian target of rapamycin complex 2
NAD	Nicotinamide adenine dinucleotide
Nbs1	Nijmegen breakage syndrome protein 1

NF1	Neurofibromin 1
NF-1	Neurofibromatosis type 1
NF-kB	Nuclear factor κB
NG2	Neuron-glial antigen 2
NHEJ	Non-homologous end joining
Notch	Neurogenic locus notch homolog protein
NSCLC	Non-small cell lung cancer
NSG	NOD scid gamma
OCT3/4	Octamer-binding transcription factor 3/4
OS	Overall survival
p70S6K	P70 ribosomal protein S6 kinase
PAR	Poly ADP-ribosylation
PARP	Poly (ADP-ribose) polymerase
PBMC	Peripheral blood mononuclear cells
PBS	Phosphate buffered saline
PCR	Polymerase chain reaction
PDGF	Platelet-derived growth factor
PDGFR	Platelet-derived growth factor receptor
PDK1	Phosphoinositide-dependent protein kinase1
PDOX	Patient derived orthotpic xenograft
PDX	Patient derived xenograft
PFS	Progression free survival
P-gp	P-glycoprotein 1
PI3K	Phosphatidylinositol-3 kinase
PIP2	Phosphatidylinositol 4,5-bisphosphate
PIP3	Phosphatidylinositol 3,4,5-triphosphate
Plk1	Polo-like kinase 1
PNKP	Polynucleotide kinase-phosphatase
PR	Partial response
PRDM16	PR/SET domain 16

p-S6	Protein S6
PTB	Phosphotyrosine binding
PTEN	Phosphatase and tensin homolog
PTGER2	Prostaglandin E receptor 2
PVDF	Polyvinylidene fluoride
Rad50	RAD50 Double Strand Break Repair Protein
RAD51	RAD51 Recombinase
Raf-1	Rapidly accelerated fibrosarcoma 1
Rb	Retinoblastoma tumour suppressor protein
RB1	Retinoblastoma gene 1
RBC	Red blood cell
RBL2	RB Transcriptional Corepressor Like 2
RIPA	Radio-immunoprecipitation assay
RMS	Rhabdomyosarcoma
RNA	Ribonucleic acid
RNAseq	RNA sequencing
ROCK	Rho-associated protein kinase
RPA	Replication protein A
RTK	Receptor tyrosine kinase
S6RP	Ribosomal protein S6
SAM	Significant analysis of microarrays
SCF	Stem cell factor
SCS	Spindle cell sarcoma
SD	Stable disease
SH2	Src homology 2
SLFN11	Schlafen Family Member 11
SNAIL	Zinc finger protein SNAI1
SOX2	SRY-Box Transcription Factor 2
SP100	Speckled 100 kDa protein
SS	Synovial sarcoma

SSB	Single strand break
ssDNA	single stranded DNA
STAT-3	Signal transducer and activator of transcription 3
STAT5	Signal transducer and activator of transcription 5
STR	Short tandem repeat
STS	Soft-tissue sarcoma
STUMP	Uterine smooth muscle tumours of unknown malignant potential
SWATH	Sequential window acquisition of all theoretical mass spectra
SYNM	Synemin
TAM	Tumour associated macrophage
TBS	Tris-buffered saline
TCGA	The Cancer Genome Atlas
TERT	Telomerase reverse transcriptase
TGF-β1	Transforming growth factor beta-1
TIL	Tumour infiltrating lymphocyte
TKI	Tyrosine kinase inhibitor
TMB	Tumour mutation burden
TP53	Tumour protein 53
UPS	Undifferentiated pleomorphic sarcoma
UV	Ultraviolet
VEGF	Vascular endothelial growth factor
VEGFR	Vascular endothelial growth factor receptor
VIPR2	Vasoactive Intestinal Peptide Receptor 2
VPS34	Vacuolar protein sorting 34
WDLPS	Well-differentiated liposarcoma
WES	Whole exome sequencing
WGS	Whole genome sequencing
WHO	World Health organisation
Wnt	Wingless-related integration site
XRCC1	X-ray cross complementing group 1

XRCC3   X-Ray Repair Cross Complementing 3

α-SMA   α-Smooth muscle actin

Chapter 1 - Introduction

1.1 Sarcoma biology

Sarcomas are a group of rare and heterogenous mesenchymal malignancies, accounting for approximately 1% of adult cancers (**Figure 1.1**) and 10% of paediatric cancers (age 0-14) (Stiller et al. 2013). There are now over 150 recognised histological subtypes, each with their own distinct clinical presentation, molecular characteristics and prognosis (WHO classification of tumor editorial board 2020).
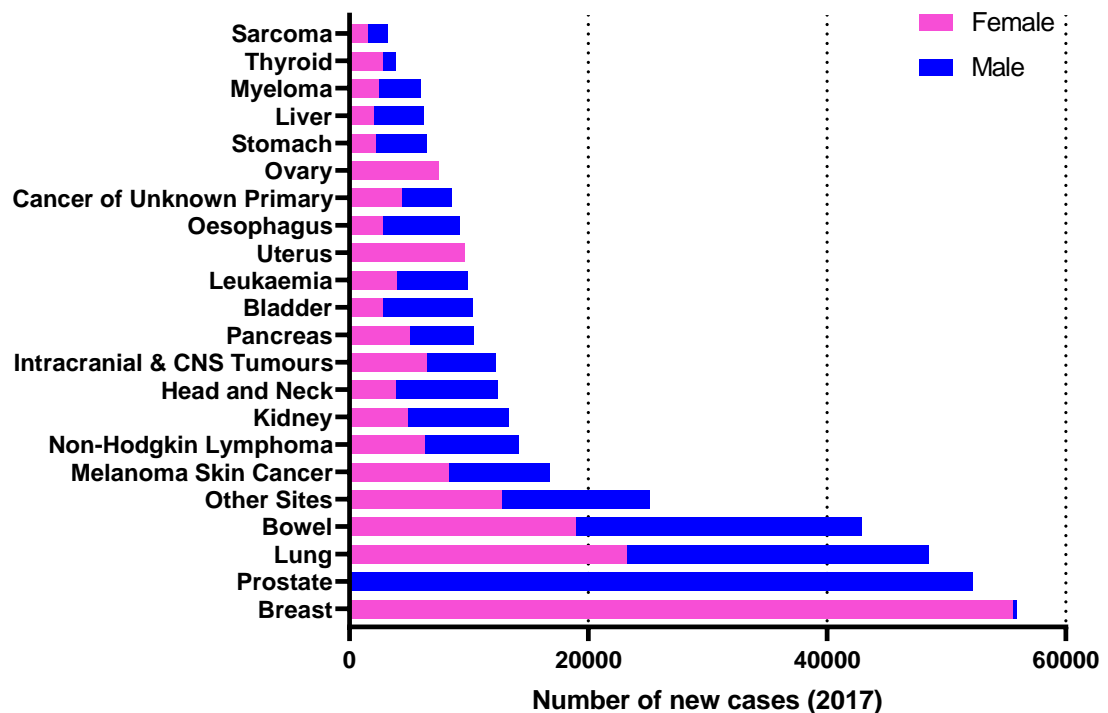
Figure 1.1. Incidence of sarcoma compared to other cancer types. Number of reported female and male cancer diagnosis in the UK in 2017 for sarcoma, liver, stomach and ovary cancer, cancers of unknown primary origin, oesophageal cancer, uterine cancer, leukaemia, bladder cancer, pancreatic cancer, intercranial && CNS tumours, head and neck cancer, kidney cancer, non-Hodgkin lymphoma, melanoma, cancers of other sites, bowel, lung, prostate and breast cancer (Cancer Research UK 2017c; 2017a; 2017b)

Sarcomas are cancers which all arise from cells derived from the embryonic mesenchyme. During the early stages of embryogenesis, pluripotent stem cells differentiate into three primordial germ layers: the ectoderm, the endoderm and the mesoderm. This makes up connective and soft-tissue which originate from the embryonic mesoderm. The ectoderm gives rise to the skin and nervous system, the endoderm gives rise to epithelial cells lining the digestive track and organs such as the lung and pancreas while the mesoderm and part of the neuroectoderm transiently form the mesenchyme.

The mesenchyme is composed of loosely organised mesenchymal cells surrounded with abundant extracellular matrix (ECM). Mesenchymal cells are noted for their ability to migrate throughout epithelial layers during embryogenesis and while the mesenchyme is a transient component of the developing embryo, mesenchymal stem cells are present in adults in tissues such as bone marrow and adipose tissue. Mesenchymal stem cells are multipotent and differentiate into tissues such as bone, cartilage, muscle, adipose tissue, stroma and blood vessels (Schoenwolf et al. 2020). Malignant cells of mesenchymal origin (sarcomas) can therefore arise in any of these tissues which are spread throughout the body, meaning they can occur in any anatomical location. Due to the wide range of tissue and anatomical location of origin, sarcomas are highly heterogeneous in histology and clinical presentation which makes treatment extremely challenging.

Mesenchymal stem cells differentiate into cell lineages such as osteocytes, chondrocytes, myoblasts, adipocytes, fibroblasts and endothelial cells in order to form the respective tissue types and so sarcomas are often categorised based on cell of origin such as osteosarcoma (osteocyte), chondrosarcoma (chondrocyte), leiomyosarcoma (myocyte), liposarcoma (adipocyte) fibrosarcoma (fibroblast) angiosarcoma (endothelial) (Hoang et al. 2018) **(Figure 1.2)**. Much knowledge of these lineage defined sarcoma subtypes stems from the similarity of molecular markers observed via immunohistochemical (IHC) staining as well as the transformation of respective normal cell types *in vitro* and *in vivo* via genetic modification to phenocopy tumours (Taylor et al. 2011). However, the specific cell of origin remains unknown for a significant number of histologically defined subtypes. Broadly, sarcomas can also be classified as bone and cartilage sarcomas or soft-tissue sarcomas, the latter arising from soft-tissues such as muscle, fat and connective tissue, although even this fundamental categorisation is not sufficient to include all subtypes such as Ewing's sarcoma which is comprised of both soft-tissue and bone or cartilage.
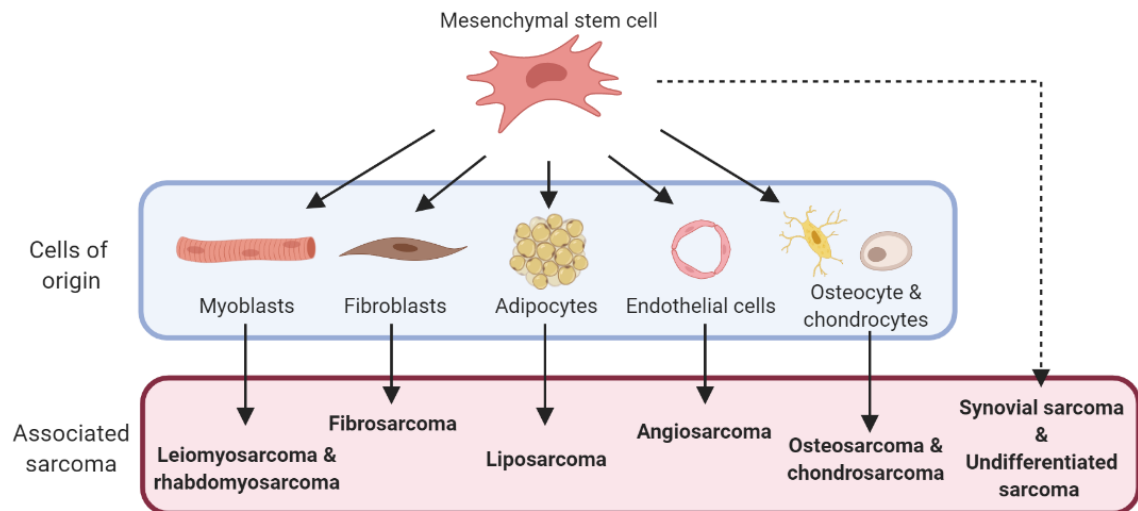
Figure 1.2 Mesenchymal stem cell differentiation patterns and associated sarcomas. Created using BioRender.

1.1.1 Soft-tissue sarcomas

Soft-tissue sarcomas (STS) make up the majority of sarcoma diagnoses, approximately 85% (Cancer Research UK 2017c; 2017a) and are comprised of over 80 histological subtypes (WHO classification of tumor editorial board 2020). Histological STS subtypes are distinct malignancies each presenting with different clinical characteristics, prognoses, histology and genetics (WHO classification of tumor editorial board 2020), The most common STS subtypes are leiomyosarcoma (LMS), undifferentiated pleomorphic sarcoma (UPS), well-differentiated liposarcoma (WDLPS), de-differentiated liposarcoma (DDLPS), and gastrointestinal stromal tumour (GIST), which make up 13%, 12%, 6%, 6% and 8% of all STS diagnosis respectively (**Figure 1.3**) (Gamboa, Gronchi, and Cardona 2020; J. Y. Blay et al. 2019). Additionally, approximately 20% of STS have been assigned as ultra-rare STS, with an incidence of ≤1 per 1,000,000 and are comprised of 56 different subtypes (Stacchiotti et al. 2021). General STS incidence rates increase with age, although some subtypes are more commonly seen in certain age groups. For example, approximately half of paediatric STS are rhabdomyosarcoma (RMS), of which embryonal RMS is almost exclusively seen in this age group, while geriatric STS are most commonly liposarcoma (LPS), LMS and UPS (WHO classification of tumor editorial board 2020).
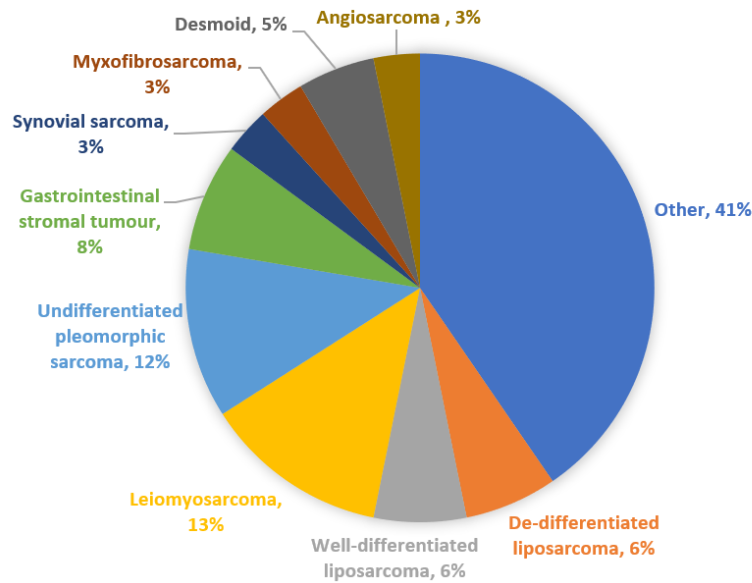
Figure 1.3. Distribution of STS subtypes in adult patients. Data from: (Gamboa, Gronchi, and Cardona 2020).

STS can arise almost anywhere in the body while presenting vastly different clinical characteristics, histologies and molecular profiles between and even within subtypes (Gamboa, Gronchi, and Cardona 2020). STSs are most commonly located in the lower extremities (35%) but can also occur in the trunk (13%), upper extremities (9%), retroperitoneum (7%), gastrointestinal tract (7%), head and neck (5%), uterus (4%) and other sites (20%) (J. Y. Blay et al. 2019; Brennan et al. 2014).

While rarely observed, benign soft-tissue tumours can contain areas of malignant transformation, causing serious complications. For example, leiomyomas (benign tumours of smooth muscle lineage) can occasionally contain distinct malignant areas and surgical resection of these uterine leiomyomas via morcellation can lead to dissemination of malignant disease following tissue disruption (George et al. 2014). Due to the far poorer prognosis of sarcoma in comparison to benign soft-tissue tumours, accurate initial diagnosis of disease is vital in order for patients to receive the appropriate treatment and/or monitoring for progression (Pedra Nobre et al. 2021).

1.1.2 Aetiological factors of STS

The aetiology of STS is largely unknown and the majority of subtypes are believed to arise spontaneously, with no clear cause. However, for a small proportion of STS subtypes (10%) a causative factor has been clearly documented, including hereditary

mutations, exposure to radiation and viral infection (American Cancer Society 2018; WHO classification of tumor editorial board 2020).

Hereditable cancer pre-disposition syndromes such as Li-Fraumeni syndrome (LFS) can increase the risk of developing a range of STS subtypes anywhere in the body (Farid and Ngeow 2016; Ognjanovic et al. 2012). LFS is an autosomal dominant syndrome caused by germline mutations in tumour protein 53 (*TP53)* gene, which encodes the transcription factor P53 (Ognjanovic et al. 2012). P53 plays an important role in control of cell growth particularly in response to DNA damage, by regulating the expression of several genes involved in DNA repair, cell cycle arrest, senescence and apoptosis and therefore, P53 is classed as a tumour suppressor (Kruiswijk, Labuschagne, and Vousden 2015). Germline mutations affecting this protein can lead to aberrant transcription, causing deregulation of cell growth control and tumourigenesis, therefore people with LFS have a significantly increased lifetime risk of developing cancer and approximately 11.6-17.8% of patients with LFS develop STS (Bougeard et al. 2015). Consistent with the general age distribution of sarcoma subtypes, LFS patients who develop RMS are almost exclusively age <20 while LFS STS patients with LPS and LMS are almost all age >20. Interestingly, p53 null mutations in particular, including frameshifts, nonsense and splice site mutations are enriched in the leiomyosarcoma subtype and p53 mutations outside of the DNA binding domain are associated with a significantly increased risk of developing LMS (Ognjanovic et al. 2012).

Neurofibromatosis type 1 (NF-1) is another heritable syndrome which pre-disposes patients to STS and is also autosomal dominant. NF-1 is caused by mutations in the tumour suppressor gene Neurofibromin 1 (*NF1*) which encodes neurofibromin 1, a protein involved in the negative regulation of cell growth and survival signalling cascades such as the mitogen-activated protein kinase (MAPK) pathway (Gutmann et al. 2017; Emmerich et al. 2015). Inactivating mutations in *NF1* leads to aberrant MAPK pathway activation, increasing cell growth, proliferation and survival (Gottfried, Viskochil, and Couldwell 2010). *NF1* expression is particularly elevated in the peripheral nerve sheath and therefore, patients with NF-1 often develop multiple benign peripheral nerve sheath tumours (neurofibromas) which do not metastasise but can cause damage to surrounding nerves (Ryu et al. 2019; Farid et al. 2014). Additionally, approximately 5-13% of NF-1 patients develop STS in the form of a malignant peripheral nerve sheath tumour (MPNST) and around 5-7% of NF-1 patients develop STS as a GIST (Farid et al. 2014; Corless, Barnett, and Heinrich 2011; Nishida et al. 2016).

People with hereditary mutant Retinoblastoma gene 1 (*RB1)* have a 13.1% cumulative risk of developing STS including LMS, as secondary malignancies which mirrors *RB1* loss seen frequently in sporadic LMS tumours (Venkatraman et al. 2003). Thus, germline *RB1* alterations are another potential predisposing factor to STS development. *RB1* is a tumour suppressor gene encoding retinoblastoma tumour suppressor protein (Rb) which plays a pivotal role in the negative regulation of cell cycle progression, repressing the expression of genes required for G1 to S cell cycle phase progression and is also involved in DNA repair (P. H. Huang et al. 2016). Loss of Rb function can lead to cell cycle deregulation and malignant transformation (Giacinti and Giordano 2006).

In 2016, Ballinger et al. assessed the monogenic and polygenic determinants of sarcoma in patients across a range of subtypes and ages. The study concluded that around half of sarcoma patients harbour an excess of pathogenic germline alterations in both known and novel STS associated genes, suggesting the proportion of STS caused by inherited pre-disposing mutations might actually be far higher than previously documented (Ballinger et al. 2016). This result could potentially lead to improved risk stratification via familial genetic testing and screening, although further population-based studies will be necessary to conclude the extent of which these different genetic variants can increase the risk of STS development and establish a causative link (Ballinger et al. 2016; Benjamin and Futreal 2016) .

Approximately 2.5-5% of all sarcomas are associated with radiation exposure and most commonly these are secondary cancers, following radiotherapy treatment for breast cancer, lymphoma and cervical carcinoma (Brady, Gaynor, and Brennan 1992; Mito et al. 2019). Higher doses of radiation received is associated with a higher incidence of developing secondary cancers, however the incidence of radiation associated STS following radiotherapy is still rare, occurring in less than 1% of patients receiving radiotherapy (Mito et al. 2019; Berrington De Gonzalez et al. 2013). In terms of histological subtype, radiation associated STS most frequently occur as UPS or angiosarcoma and demonstrate more aggressive clinical behaviours and worse survival outcomes when compared to spontaneous STS of the same subtype (Cha et al. 2004; Brady, Gaynor, and Brennan 1992; Bjerkehagen et al. 2009).

Finally, STS can also arise due to viral infection. Kaposi sarcoma is the most well documented viral-associated STS and it is caused by the infection of an immunocompromised host with human herpesvirus 8 (HHV8), leading to cutaneous lesions which are highly aggressive (Cesarman et al. 2019; Mancuso et al. 2008). HHV8 has been shown to transform human endothelial cells by the expression of proteins that

can bind to Rb and P53 tumour suppressors, thus regulating cell proliferation and apoptosis (S. C. Verma and Robertson 2003). Additionally, smooth muscle neoplasms including leiomyomas and LMS can be caused by the infection of an immunocompromised host with Epstein-Barr virus (EBV) (Moore Dalal et al. 2008; Jenson et al. 2009) The precise mechanism by which EBV can cause smooth muscle neoplastic transformation is not fully understood although activation of mammalian target of rapamycin (mTOR)/Akt pathway as well as the increase expression of v-myc has been recorded (Jonigk et al. 2012; Ong et al. 2009; Q. Shen et al. 2011). It is important to identify if STS are associated with viral infection as these malignancies often require different treatment strategies compared to non-viral associated STS, often focussing on re-establishing a functional immune system within the patient in addition to the use of anti-retroviral therapy (Schneider and Dittmer 2017; Magg et al. 2018).

1.1.3 Genetic classification of STS

Historically, the classification and subsequent treatment of STS relied on gross morphology, histological characteristics and IHC staining for biomarkers of suspected tissue of origin (Hajdu 1981). However, it has since become clear that some subtypes harbour pathognomonic gene alterations or are more likely to present with certain gene mutations (Kawai et al. 1998; Galili et al. 1993). Genetic classification of STS refines the diagnostic process and gives an insight into the process of oncogenesis, helping to define distinct clinical subtypes which would have previously been grouped together based on histological appearance (Gounder et al. 2022). This is reflected in the most recent World Health Organisation (WHO) classification which puts a greater emphasis on the molecular characteristics of certain STS subtypes (Kallen and Hornick 2021).

In addition to the diverse histology of STS, these tumours are also genetically diverse. STS subtypes can be broadly categorised as genetically simple or those with complex karyotypes. Genetically simple STS tumours including subtypes such as alveolar rhabdomyosarcoma (ARMS), synovial sarcoma (SS) and GIST. These often display a low tumour-mutation burden (TMB) and near diploid karyotypes with only a few, recurring genetic alterations which drive tumourigenesis such as point mutations (e.g. KIT or platelet-derived growth factor receptor (PDGFR) mutations in GIST) or fusion genes (e.g. SSX18:SSX1/2/4 in SS) (Taylor et al. 2011; Gounder et al. 2022). Sarcomas with complex karyotypes including LMS, UPS and LPS excluding myxoid types, harbour rearranged genomes due to gene copy number alterations, translocations and ploidy (Abeshouse et al. 2017; Nacev et al. 2022). These subtypes often harbour alterations in

various tumour suppressor genes which leads to genomic instability. However some subtypes fall in between the binary classification of STS genomes, such as DDLPS which is driven by a recurrent murine double minute 2 (*MDM2*) amplification but also displays a complex karyotype consistent with genomic instability (**Figure 1.4)** (Nacev et al. 2022; Gounder et al. 2022) .
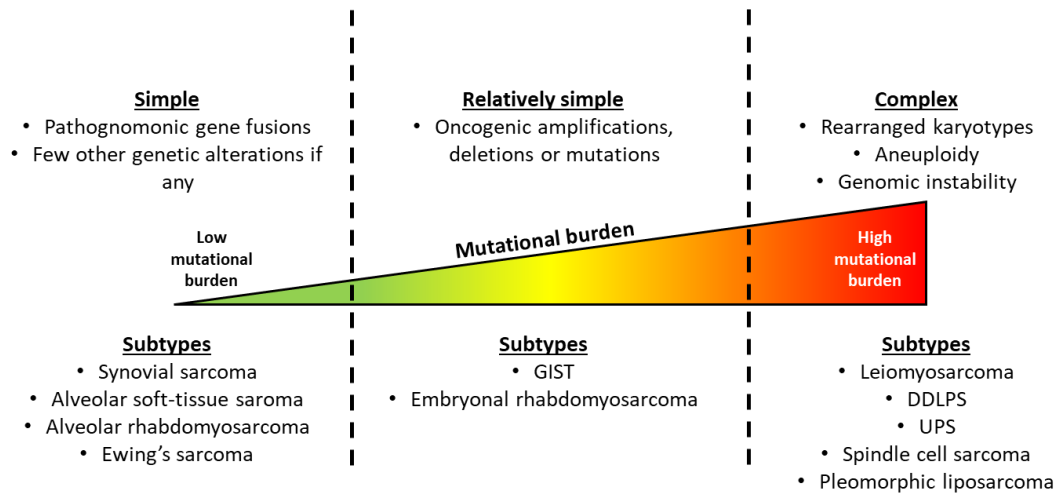
Figure 1.4 Spectrum of genetic characteristics and complexity in STS. Examples of subtypes falling under each genetic category. Genetically "simple" STS typically display pathognomonic gene translocations with low mutational burden and normal diploid karyotype. "Relatively simple" STS display recurrent oncogenic driver mutations with increased mutational burden occasionally with background genomic instability. "Complex" STS are characterised by rearranged karyotypes and caused by genomic instability which lack recurrent or consistent genetic alterations. (Abeshouse et al. 2017; WHO classification of tumor editorial board 2020). DDLPS; Dedifferentiated liposarcoma, GIST; Gastrointestinal stromal tumour, UPS; Undifferentiated liposarcoma.

1.2 Clinical and biological characteristics of LMS

This thesis will focus primarily on one of the subtypes of STS, LMS. Therefore the following sections will provide an overview of the current status of LMS research in the context of other STS subtypes and cancer types.

1.2.1 Presentation, diagnosis and prognosis of LMS

 LMS is one of the most common STS subtypes, occurring more frequently in middle-aged or older adults and with a slight female predominance (Kasper et al. 2021). LMS is

believed to form from smooth muscle or their pre-cursor cells and can therefore arise almost anywhere in the body but most frequently in the retroperitoneum, extremities or uterus. The disease is often divided into extra-uterine LMS (arising in the retroperitoneum, walls of blood vessels, gastrointestinal tract, extremities or subcutaneously) or uterine LMS as the two groups have distinct clinicopathological characteristics (Kasper et al. 2021; Bathan et al. 2013).

LMS is a particularly aggressive malignancy with distant metastases occurring in approximately half of all patients despite initial local control with resection and systemic therapy (Penel et al. 2009). Following surgical resection, the main pattern of control failure for LMS of the extremity, abdomen or trunk is distant metastatic recurrence, occurring in 93% of patients, with lower rates of recurrence at local sites (30%) compared to other STS subtypes such as liposarcoma where 50% of recurrences occur at local sites (Ikoma et al. 2017; Penel et al. 2011; Gladdy et al. 2013). Upon LMS dissemination, median survival is approximately 12 months (Gladdy et al. 2013)

Prognosis is based on both tumour staging and anatomical location as the ten year metastatic rate of LMS ranges from 31% in extremities, 58% in abdomen to 53-71% in the uterus (Gladdy et al. 2013; Mbatani, Olawaiye, and Prat 2018). Outcomes vary substantially between non-uterine and uterine LMS patients, although at the point of diagnosis, uterine LMS tumours are often larger with higher incidences of metastases and therefore it is unclear whether the molecular differences in uterine and non-uterine LMS can affect aggressiveness (Lamm et al. 2014). Additionally, outcomes can also vary widely within uterine or non-uterine LMS groups and prognosis based only on anatomical location is inaccurate, requiring further histological grading to improve accuracy of prognoses (Kasper et al. 2021).

As with other STS subtypes, the major clinicopathological factors which affect LMS patient outcomes are histological grade, tumour size and depth (Serrano and George 2013). In Europe, LMS tumours are histologically graded according to the three-tiered Fédération Nationale des Centres de Lutte Contre le Cancer (FNCLCC) grading system which considers tumour differentiation, extent of necrosis and mitotic counts (Guillou et al. 2016). However, this staging does not apply to gynaecological tumours. Uterine LMS tumours are not graded due to the limited evidence that tumour grade correlates with patient outcome and therefore, the International Federation of Gynaecology and Obstetrics (FIGO) staging system used for uterine LMS diagnosis does not account for tumour grade (Roberts, Aynardi, and Chu 2018).

1.2.2 Genetics of LMS

In contrast to genetically simple sarcomas, some STS subtypes with complex karyotypes can arise from benign pre-cursor tumours which increase in genomic complexity to progress into metastatic sarcoma such as the progression from atypical lipoma to WDLPS to DDLPS (Horvai et al. 2009; Rosai et al. 1996). However, despite the genomic complexity of LMS, there is no evidence that leiomyomas (the benign counterpart of LMS) undergo transformation to form malignant tumours, therefore LMS is still considered to arise *de novo* (Serrano and George 2013).

While frequent mutations in tumour suppressor genes can be observed in STS subtypes with complex karyotypes including *TP53,* phosphatase and tensin homolog (*PTEN*) and *RB1,* genetic classification plays a less significant role in diagnosis compared to that of STS subtypes with recurrent driver mutations and instead, diagnosis is based on ancillary histopathological analysis. (Abeshouse et al. 2017; Nacev et al. 2022; Gounder et al. 2022; Chudasama et al. 2018) . However, genomic sequencing can occasionally aid in diagnosis of STSs with complex karyotypes by distinguishing between benign and malignant tumours with the same cell of origin. For example, benign leiomyomas and LMS of the uterus display very similar histologies, often leading to the diagnosis of uterine smooth muscle tumours of unknown malignant potential (STUMPs) (Croce et al. 2015). Genomic hybridisation array analysis of these tumours or even of circulating tumour DNA has been able to distinguish between leiomyomas and LMS tumours by assigning a genomic rearrangement score, showing that STUMPS with high rearrangement scores have clinical characteristics of LMS tumours while STUMPs with low scores had favourable outcomes consistent with benign leiomyomas (Croce et al. 2015; Przybyl et al. 2018).

Recurrent somatic mutations identified in LMS tumours includes *TP53* (49%), *RB1* (27%), and Alpha-thalassemia/intellectual disability syndrome, X-linked (*ATRX)* (24%) while mutations in other genes were less common such as *PTEN* (4%) (Chudasama et al. 2018). Of the three recurrent mutant genes, *TP53* mutations were clustered in the DNA-binding domain and the tetramerization domain meanwhile mutations in *RB1* and *ATRX* were seen across the gene (Chudasama et al. 2018). Karyotyping of LMS samples have shown no recurrent aberrations at the chromosomal level while DNA copy number alteration (CNA) analysis demonstrates a complex genetic landscape with the extent of cytogenetic changes and copy number gains showing an association with tumour evolution and worse survival (Cuppens et al. 2018; Raish et al. 2012). Further genomic

studies of LMS have shown that genetic losses are often detected in certain chromosomal regions such as 10q11-21.2 encoding *PTEN*, 13q14.3-q21.1 encoding *RB1* and 17P13 which encodes *TP53* (Chudasama et al. 2018; Nacev et al. 2022; Cuppens et al. 2018). Together, inactivating genetic aberrations including mutations and gene deletions in *TP53* and *RB1* are almost universally seen in LMS tumours (92% and 94% respectively) while 57% of LMS tumours display inactivating aberrations in *PTEN* (Chudasama et al. 2018). Other studies have showed that aberrations in the RB1-cyclin D1 pathway including *RB1*, Cyclin D1 (*CCND1)*, Cyclin D3 (*CCND3)* and Cyclin Dependent Kinase Inhibitor 2A (*CDKN2A)* are seen in approximately 90% of LMS tumours and is associated with a worse prognosis (Dei Tos et al. 1996; Jilong Yang et al. 2009; Anderson et al. 2021). While far less common than *PTEN* alterations, gain of function aberrations in phosphatidylinositol-3 kinase (PI3K) can also be observed in a small subset of LMS tumours (2% of uterine and non-LMS tumours) (Nacev et al. 2022).

Deregulation in DNA damage response (DDR), especially homologous recombination (HR) repair, and DNA damage tolerance pathways leads to high genomic instability and thus promotes cancer progression (Bouwman and Jonkers 2012)**.** Germline heterozygous mutations in breast cancer gene 1/2 (*BRCA1/2*) genes, for example, confer a significantly increased risk of developing breast, ovarian, prostate and other cancers by pre-disposing the individual to bi-allelic loss of BRCA1/2 function via loss of heterozygosity (Rebbeck et al. 2018). Analysis of a pan-cancer cohort showed that uterine LMS frequently had HR deficiency including alterations in BRCA1/2, the majority of which was due to somatic homozygous deletion (Jonsson et al. 2019). In a cohort of 80 uterine LMS patients, 5% displayed a homozygous deletion of BRCA2 while another LMS cohort of 49 uterine or non-uterine tumours identified gene deletions in multiple components of the HR pathway, including *PTEN, BRCA2,* Ataxia telangiectasia mutated *(ATM),* Checkpoint kinase 1 (*CHEK1)*, X-Ray Repair Cross Complementing 3 *(XRCC3),* Checkpoint kinase 2 (*CHEK2), BRCA1* and RAD51 Recombinase (*RAD51)* with a prevalence of 57%, 53%, 22%, 22%, 18%, 12%, 10% and 10% respectively (Chudasama et al. 2018; Hensley et al. 2020). BRCA1/2 deletions were identified in 50% of the uterine cohort, 10% and 40% being homozygous or hemizygous BRCA1/2 deletions respectively (Chudasama et al. 2018)**.**

Genomic scarring, a particular pattern of mutations occurring when double strand breaks (DSBs) cannot be repaired via HR, was detected in most LMS tumours, suggesting impaired HR activity (Chudasama et al. 2018). Furthermore 214 STS patient samples from the Cancer Genome Atlas were assigned a HR deficiency score, taking into account loss of heterozygosity, telomeric allelic imbalance and large-scale state transitions, and

showed that patients with a low HR deficiency score had a significantly better prognosis compared to patients with a high HR deficiency score (H. Li et al. 2020). HR deficiency, as defined by the HR deficiency score was also detected in a panel of STS cell lines, including the uterine LMS model SK-LMS-1 (H. Li et al. 2020). In a larger study including 121 uterine LMS patients, 30 (25%) patients displayed DDR alterations which was lowered to 14% in a non-uterine LMS cohort of 90 patients suggesting that uterine LMS tumour might be particularly susceptible to therapeutic targeting of the DDR pathway (Rosenbaum et al. 2019). Meanwhile Nacev et al. showed that 24% of 165 uterine LMS tumour samples and 10% of 125 non-uterine LMS tumours display DDR gene alterations (Nacev et al. 2022). LMS patients with alterations in DDR associated genes, were found to have a worse prognosis compared to LMS patients without these DDR gene alterations and non-BRCA gene alterations in particular showed a significant negative correlation with OS (Rosenbaum et al. 2020).

1.2.3 Oncogenic pathways in LMS

Due to the range of oncogenes and tumour suppressor genes which are altered in LMS tumours, this subtype often shows several oncogenic signalling pathways including aberrant activation of receptor tyrosine kinase (RTK) cascades, aberrant PI3K-Akt-mTOR signalling and defective DNA repair pathways (Nacev et al. 2022)

1.2.3.1 Receptor tyrosine kinases

RTKs are cell surface receptors with intrinsic kinase activity and are crucial for a range of cellular processes such as proliferation, survival, motility, differentiation and metabolism (Blume-Jensen and Hunter 2001; Du and Lovly 2018). There are currently 58 known RTKs in the human genome all sharing a common protein domain organisation which is composed of an extracellular domain facilitating ligand binding, a transmembrane domain, an intracellular tyrosine kinase domain and a C-terminal tail (G. Manning et al. 2002). RTKs are activated upon ligand binding to their extracellular domain, often leading to receptor dimerisation (P. Liu et al. 2007). Prototypical RTKs include epidermal growth factor receptor (EGFR), vascular endothelial growth factor receptor (VEGFR), PDGFR, fibroblast growth factor receptor (FGFR), insulin growth factor receptor (IGFR) and c-KIT, which bind to their associated ligands; epidermal growth factor (EGF), vascular endothelial growth factor (VEGF), platelet-derived growth

factor (PDGF), fibroblast growth factor (FGF), insulin growth factor (IGF) and stem cell factor (SCF).

RTKs are activated upon ligand binding to their extracellular domain, leading to receptor dimerisation, although some RTKs exist as pre-formed dimers such as insulin-like growth factor 1 receptor (IGF1R) (P. Liu et al. 2007). Ligand-mediated dimerisation causes a conformational change in the intracellular kinase domain, resulting in auto-phosphorylation at various tyrosine residues along the C-terminal tail, which in turn recruits downstream signalling components such as phosphatidylinositol-3-kinase (PI3K), Src or docking proteins such as growth factor receptor-bound protein 2 (GRB2), all of which bind via Src homology 2 (SH2) or phosphotyrosine binding (PTB) domains to specific phosphorylated tyrosine residues. Subsequent phosphorylation of these components initiates crucial cell signalling pathways including MAPK, PI3K/Akt and Src (Lemmon and Schlessinger 2010).

Given the range of growth, survival and angiogenic pathways RTKs are able to initiate, it is unsurprising that deregulated RTKs can lead to cancer initiation and progression. In the context of sarcomas, previous reports have shown that cancer cell lines and tumours of various subtypes display overexpression and aberrant activation of RTKs and intracellular tyrosine kinases such as PDGFR, IGF1R and Src (J.-L. Yang et al. 2017; Y. Bai et al. 2012; S. S. Yoon et al. 2006). In LMS in particular, patient tissues and cell lines have shown strong expression of VEGFR1/2 as well as PDGFR-β (Gaumann et al. 2014; Cuppens, Annibali, et al. 2017). Cuppens et al. conducted IHC staining of a cohort of 153 uterine LMS tissue samples and demonstrated that 89% and 86% of uterine LMS tumours show expression of PDGFR-α. FGFR1 was seen to be amplified in case study of a patient with metastatic LMS meanwhile IGF1R was highly expressed in a subgroup of LMS, making up 49% of the LMS samples assessed, and IFG1R expression correlated with worse disease-specific survival suggesting that IGFR signalling is an recurring oncogenic pathway in a subset of LMS (Hemming et al. 2020; Chudasama et al. 2017).

1.2.3.2 PI3K-AKT-mTOR pathway

Many sarcomas display aberrant signalling network activation which converge on the PI3K-Akt-mTOR pathway (Y. Bai et al. 2012). Specifically, loss of PTEN expression is commonly observed in LMS tumours which can potentiate this pathway (**Figure 1.5**). The Cancer Genome Atlas (TCGA) study found *PTEN* gene mutations in 5% of LMS samples, deep PTEN gene deletions (therefore potentially homozygous) in 13% of LMS samples and a further 68% of LMS samples showed shallow *PTEN* gene deletions

(therefore potentially heterozygous) (Abeshouse et al. 2017). Additionally, in a small cohort of 17 LMS tumours, *PTEN* loss was associated with a poorer prognosis for LMS patients (J. Hu et al. 2005).
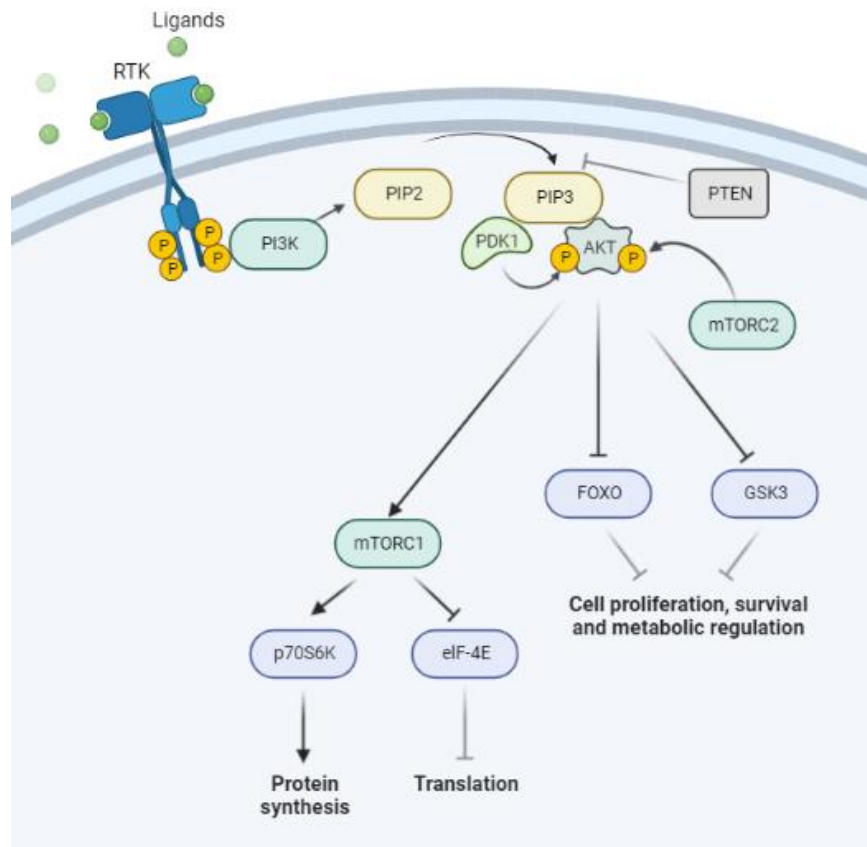
Figure 1.5. **Activated PI3K/Akt/mTOR signalling pathway.** Ligand induced RTK dimerization activates PI3K to convert PIP2 to PIP3 which accumulates in the absence of PTEN. PDK1 and Akt are recruited to PIP3, allowing for phosphorylation of Akt via PDK1 as well as mTORC2. Akt activation results in enhanced protein synthesis, translation, cell proliferation, cell survival and metabolic regulation. Figure was created using BioRender. eIF-4E; eukaryotic initiation factor 4E, FOXO;fork head box O, GSK3; glycogen synthetase 3, mTORC1/2; mammalian target of rapamycin complex 1/2, phosphoinositide-dependent protein kinase1; PDK1, phosphatidylinositol 4,5-biphosphate; PIP2, phosphatidylinositol 3,4,5-triphosphate; PIP3, Phosphoinositide 3-kinase; PI3K, Phosphatase and TENsin homolog; PTEN, p70 ribosomal S6 Kinase; p70S6K, Receptor Tyrosine Kinase; RTK.

Downstream of RTK activation by ligand binding, PI3K is recruited and subsequently activated by either direct or indirect binding to intracellular RTK domains, although PI3K

can also be activated via G protein-coupled receptors (Rascio et al. 2021; Law, White, and Hunzicker-Dunn 2016). PI3K is a lipid kinase which converts phosphatidylinositol 4,5-biphosphate (PIP2) to phosphatidylinositol 3,4,5-triphosphate (PIP3) on the intracellular membrane surface (**Figure 1.5**) (Vanhaesebroeck, Stephens, and Hawkins 2012; Jing Yang et al. 2019). PIP3 recruits the serine/threonine kinase Akt to the cell membrane in addition to phosphoinositide-dependent protein kinase1 (PDK1) where Akt is phosphorylated and activated by both PDK1 at Thr308 as well as mammalian target of rapamycin complex 2 (mTORC2) at Ser473 (Vanhaesebroeck, Stephens, and Hawkins 2012). Once activated, Akt is released from the cell membrane and is able to phosphorylate and subsequently activate or inhibit over 150 targets including mTOR, members of the fork head box O (FOXO) family of transcription factors as well as glycogen synthetase 3 (GSK3), driving cellular processes such as proliferation, cell survival and regulation of metabolism (B. D. Manning and Toker 2017; Rascio et al. 2021). Activated mTOR, specifically mammalian target of rapamycin complex 1 (mTORC1) in turn phosphorylates eukaryotic initiation factor 4E (eIF-4E) binding protein 1 (4EBP1) and p70 ribosomal S6 kinase 1 (p70S6K1) (D. E. Martin and Hall 2005). 4EBP1 is a translational repressor acting by binding and inhibiting the messenger ribonucleic acid (mRNA) cap binding protein eIF-4E. Upon activation mTOR signalling, hyperphosphorylation of 4EBP1 causes its dissociation from eIF-4E and eIF-4E is then free to bind to the scaffold protein Eukaryotic translation initiation factor 4G (eIF-4G), the adenosine triphosphate (ATP)-dependent RNA helicase Eukaryotic translation initiation factor 4A (eIF-4A) as well as Eukaryotic translation initiation factor 4B (eIF-4B) which initiates the translation of 5' cap mRNAs and ultimately leading to increased expression of several proteins associated with oncogenesis such as C-Myc, VEGF, cyclin D1 and hypoxia-inducible factor 1α (HIF-1α) (Song, Salmena, and Pandolfi 2012; Mamane et al. 2004) . Phosphorylation of p70S6K at Thr389 by mTORC1 leads to the subsequent phosphorylation of downstream targets involved in mRNA translation such as ribosomal protein S6, eIF-4B and eukaryotic elongation factor 2 kinase (eEF2K) (Ferrari et al. 1991; Redpath, Foulstone, and Proud 1996).

PTEN can function as both a protein and lipid phosphatase and acts as a negative regulator of the PI3K-Akt-mTOR pathway, converting PIP3 into PIP2 by dephosphorylation, and therefore preventing Akt activation. The loss of PTEN activity via gene mutations or deletions causes the excessive accumulation of PIP3 (Rascio et al. 2021). *PTEN* is therefore considered as a tumour suppressor gene (Song, Salmena, and Pandolfi 2012). Homozygous deletion of PTEN has been shown in smooth-muscle specific knockout mouse models to cause Akt upregulation and constitutive mTOR

activity, which was necessary for smooth muscle tumour formation, although suppression of P53 was additionally necessary for malignant progression. Treatment with the mTORC1 inhibitor rapamycin additionally decreased Akt activation and slowed tumour growth in these murine models (Hernando et al. 2007).

1.2.3.3 DNA repair pathways

Defects in the homologous recombination (HR) DNA repair pathway have been observed in several cancer types including breast, ovarian, colon and pancreatic cancer but also in certain sarcoma subtypes including LMS (Byrum, Vindigni, and Mosammaparast 2019; Yaeger et al. 2018; Raphael et al. 2017; Brenner et al. 2012). BRCAness is a term used to describe HR deficient cancer cells caused by mutations in *BRCA1/2* genes although this term has been expanded to include cancer cells which show HR deficiency that mimics *BRCA1/2* mutants. Maintaining genomic stability is essential to prevent accumulation of mutations and chromosomal aberrations. DNA damage can occur either exogenously via chemical mutagenesis, and ultraviolet (UV) and ionising radiation, or endogenously through reactive oxygen species (Chatterjee and Walker 2017). Different types of DNA damage have varying levels of associated cytotoxicity, with DSB being the most cytotoxic (Balmus et al. 2019). In order to repair DSBs, two main DNA repair pathways are employed by mammalian cells, HR repair and non-homologous end joining (NHEJ). HR utilises an undamaged complementary DNA strand as a template in order to faithfully repair the break without introducing errors and is therefore only observed in S and G2 cell cycle phases where replicated DNA is present (Mao et al. 2008; Brandsma and Gent 2012). Phosphorylated H2A histone family member X (H2AX), termed γ-H2AX, rapidly appears after exposure to DSB forming DNA damage and functions to accumulate DDR signalling and repair proteins at sites of DSBs (Paull et al. 2000). γ-H2AX is therefore widely used as a sensitive, robust marker of DSBs.

HR begins with the MRN-complex, composed of meiotic recombination 11 homolog 1 (MRE11), RAD50 Double Strand Break Repair Protein (Rad50) and Nijmegen breakage syndrome protein 1 (Nbs1), sensing DSBs and recruiting ATM kinase to phosphorylate histone H2AX (Rogakou et al. 1998). DSB ends are resected by the MRN-complex, CtBP-interacting protein (CtIP) and other exonucleases to generate 3' single stranded DNA (ssDNA) overhangs (Sartori et al. 2007). Replication protein A (RPA) binds to the ssDNA overhangs to remove secondary structures and prevent nucleotide loss. RPA is then displaced by Rad51, mediated by breast cancer and ovarian cancer susceptibility 1/2 (BRCA1/2), which forms a helical nucleoprotein filament on the ssDNA (Jensen,

Carreira, and Kowalczykowski 2010) in order to locate a homologous sequence on a sister chromatid and catalyse strand invasion. DNA synthesis is then initiated from the 3' end of the invading strand to extend the region of homology and the DNA crossovers, termed Holliday junctions, are resolved by cleavage and subsequent ligation to produce two repaired DNA molecules (Xue et al. 2013). A strong link has been established between BRCA1/2 proteins and HR function in mammalian cells with loss of function mutations causing impaired HR activity (Xia et al. 2001; Moynahan et al. 1999).

NHEJ is an alternative DSB repair pathway which does not require a sister chromatid template and can therefore occur at any stage of the cell cycle (Mao et al. 2008). NHEJ begins with the ring-shaped heterodimer Ku70/80 recognising and binding to DSBs in a sequence independent manner (Fell and Schild-Poulter 2015). Ku70/80 acts as a scaffold to recruit NHEJ specific repair proteins to DSB ends including DNA-dependent protein kinase catalytic subunit (DNA-PKcs) which forms the active DNA-PK complex. If the DSB ends cannot be directly ligated due to overhanging ends, they are resected or filled in with a variety of enzyme complexes including artemis, polynucleotide 3' phosphatase (PNKP) and DNA polymerases (Davis, Chen, and Chen 2014). Finally, DSB ends are ligated with DNA ligase IV. As DSB do not often have blunt ends and must first undergo end processing without a template strand, NHEJ is considered an error-prone form of DNA repair which can introduce short deletions or insertions, depending on the mechanism of end processing or even translocations if there are multiple DSBs across the genome and incorrect chromosomes are joined (Waters et al. 2014; Rothkamm et al. 2001).

1.2.4 Molecular and histological subclassification of LMS

Several histological variants exist for LMS and can be divided into spindle, myxoid and epithelioid histotypes, although occasionally a mix of these histotypes can be observed in the same tumour (Thway 2009; Oliva 2015). Well-differentiated LMS tumours commonly show spindle type histological characteristics analogous to smooth muscle and are composed of elongated spindle cells arranged in intersecting fascicular bundles with eosinophilic cytoplasm and variable numbers of pleomorphic cells (Demicco et al. 2015). Myxoid LMS tissue contain scant cytoplasm and nuclei of oval, spindle or stellate morphology and are often hypocellular, while epithelioid LMS tissues are often hypercellular, arranged in nests or sheets with eosinophilic cytoplasm and prominent cytologic atypia (Oliva 2015). Biomarkers of smooth muscle differentiation are used to aid in the diagnosis of LMS as most tumours show expression of α-smooth muscle actin

(α-SMA), desmin and caldesmon, of which α-SMA is most commonly observed from IHC staining across LMS tumours (Demicco et al. 2015). In a cohort of 202 non-uterine and 181 uterine LMS samples, 91%, 74% and 78% of tissues displayed α-SMA, desmin and caldesmon expression respectively (Demicco et al. 2015). However, there are no biomarkers exclusive to smooth muscle and expression of these markers can be observed in other tissues, meaning that IHC staining for smooth muscle markers should be interpreted with caution (Serrano and George 2013).

In addition to well-differentiated tumours, LMS can also present as moderately or poorly differentiated, display decreasing levels of smooth muscle characteristics (Oliva 2015). Some extremely poorly differentiated tumours are occasionally misdiagnosed as UPS, having lost common smooth muscle markers such as α-SMA, desmin and H-caldesmon (Demicco et al. 2015; Oliva 2015). Additionally, a significantly higher proportion of recurrent or metastatic LMS tumours are moderately or poorly differentiated compared to primary LMS tumours which show higher proportions of well-differentiated tissue (Demicco et al. 2015).

Based on histology, uterine LMS tumours are difficult to distinguish from benign myometrial leiomyomas and the criteria for differential diagnoses are controversial, such as number of acceptable mitoses before a tumour is considered malignant and degree of cellular atypia (C. Zhang et al. 2021; Sanada et al. 2022; Zheng et al. 2020). Due to the difficulty in distinguishing malignancy, non-uterine smooth muscle tumours are generally considered to be malignant with any amount of mitotic activity as benign leiomyomas very rarely occur extra-uterine (Kostov et al. 2021; D'Angelo and Prat 2010; Demicco et al. 2015). Some reports outline mitotic activity criteria for malignancy which is different depending on histotypes, set as at least ten, four or two mitoses per ten high-power fields for spindle, epithelioid and myxoid variants respectively (D'Angelo and Prat 2010; Demicco et al. 2015; Oliva 2015).

While histological and genetic classification of STS subtypes has remained the standard means of diagnosis for decades, it has become increasingly apparent that individual subtypes can have molecular subgroups with distinct clinical outcomes that conventional histological approaches might fail to detect (Beck et al. 2009; Merry et al. 2021; R. Shen et al. 2021; Chadha and Huang 2022; Milighetti et al. 2021; Chudasama et al. 2018; Guo et al. 2015). The successful identification and stratification of subgroups has led to an improved understanding of underlying biology and tailored therapeutic approach in multiple cancer types (Shai et al. 2003; Lapointe et al. 2004; Sørlie et al. 2001; Marisa et al. 2013; Asleh et al. 2022). A combination of genetic, transcriptomic and proteomic

profiling is therefore necessary to improve the stratification of patient subgroups within LMS, thus identifying subgroup specific therapies while increasing our understanding of the underlying disease biology.

Utilising gene expression microarrays, three distinct transcriptomic subgroups were identified from a cohort of 51 LMS tumours and these subgroups contained patterns of copy number alterations (Beck et al. 2009). The first subgroup, termed 'muscle-enriched LMS' was shown to have elevated expression of genes involved in muscle differentiation and function such as caldesmon gene (*CALD1)* and actin gamma smooth muscle 2 (*ACTG2)*. The majority of tumours in this group showed a loss of 16q24, containing Fanconi anemia complementation group A (*FANCA)* gene, which is involved in DNA repair, and loss of 1p36, containing PR/SET domain 16 (*PRDM16)*, the loss of which causes muscle differentiation (Benitez et al. 2018; Seale et al. 2008). The second group presented by Beck et al. had elevated or differential expression of genes relating to protein metabolism and regulation of cell proliferation while the third group were enriched for the elevated or differential expression of genes associated with extracellular proteins, wound response components, and protein synthesis (Beck et al. 2009). No significant difference in tumour grade was found between each subgroup and group 1 and 2 were found to have a higher percentage of non-uterine cases, making up 91 and 75% of each group respectively while group 3 showed an even distribution of uterine and non-uterine cases (Beck et al. 2009).

In a separate transcriptomic study of 37 LMS patient tumours, three subgroups were again identified (Chudasama et al. 2018). Gene ontology analysis revealed subgroup 1 to be enriched in biological functions such as platelet degranulation, complement activation and metabolism. Subgroup 2 was characterised by an enrichment in muscle function and development processes while subgroup 3 showed a low expression of genes which separated groups 1 and 2 but with slightly higher expression of genes associated with myofibril assembly, muscle filament action and cell-cell signalling. Subgroup 3 comprised of 70% of the sample cohort while groups 1 and 2 made up 14% and 16% of the sample cohort and uterine LMS tumours were not enriched or absent in any particular subgroup. The authors noted that subgroups 2 and 3 corresponded to the previously reported subgroups II and I from Beck and co-workers respectively (Chudasama et al. 2018). Analysis of 130 transcriptomes in a third study also revealed three distinct subgroups, where further genomic analysis showed these subgroups represent early evolutionary branches of LMS which arise from distinct lineages of smooth muscle such as vascular, digestive and gynaecological smooth muscle. The authors classed these subgroups as subtype 1 (dedifferentiated), 2a (abdominal), 2b

(abdominal or extremity) which together comprised the majority of samples in the cohort, and 3 (gynaecological) (Anderson et al. 2021).

Recently the gene expression profiles of LMS tumours in addition to other sarcoma subtypes, non-mesenchymal neoplasms and normal myogenic tissue were all compared. This analysis showed, once again, that there were three distinct LMS subgroups, this time classed as conventional LMS (cLMS) which was enriched in muscle associated processes, inflammatory LMS (iLMS) which was enriched in immune markers and uterogenic LMS (uLMS) which was enriched in a uterine-like gene expression program. By stratifying these subgroups a worse disease specific survival was associated with iLMS (Hemming et al. 2020). Despite the recurrent identification of three transcriptomic subgroups, the prognostic association of similar subgroups is not consistent between studies and after adjusting for clinicopathological variables, subgroups were not independent prognosticators of outcome (Hemming et al. 2020; Anderson et al. 2021; Beck et al. 2009). Therefore the clinical value of transcriptomic classification remains to be determined.

The use of proteomic profiling in LMS has so far been mainly limited to the analysis of cell lines relating to chemotherapy resistance mechanisms or identification of mesenchymal to epithelial markers in patient tumours (May et al. 2014; S. T. Lin et al. 2012; Jilong Yang et al. 2010), with only one study using proteomic profiling to identify LMS subgroups (Kirik et al. 2014). This study revealed at least two proteomic subgroups within a cohort of 31 LMS samples and subsequent pathway analysis revealed differing biological processes between these subgroups including cytoskeleton remodelling, apoptosis and telomere maintenance. However, the proteomes of LMS tumours were shown to poorly correlate with expression profiles, suggesting a complex interplay between gene copy number, and protein abundance (Kirik et al. 2014). This highlights the importance of proteomic analysis of subtypes characterised by copy number gains, such as LMS in order to accurately quantify protein, and therefore therapeutic target abundance.

1.3 Standard of care treatment pathways for LMS

Surgical resection with or without neo-adjuvant or adjuvant chemotherapy and/or radiotherapy remains the mainstay of treatment for local disease. Unfortunately, progression to advanced disease including local or distant recurrence is common, occurring in 10-30% and 30-40% of STS patients respectively (Frezza, Stacchiotti, and

Gronchi 2017; Rosa et al. 2016). For the majority of patients, advanced STS is fatal, with average survival of 14-17 months (Judson et al. 2014; Ryan et al. 2016).

1.3.1 Localised disease

The gold standard of LMS treatment for localised disease, which denotes primary tumours located at the site of origin, is surgical resection which for some less common STS subtypes is the only therapy which has been recorded as curative (Linch et al. 2014; Casali et al. 2018). The rationale behind neoadjuvant or adjuvant therapy is to reduce the size of tumours before surgical excision and/or prevent the likelihood of recurrence from residual disease after surgical excision (Kostov et al. 2021). Neoadjuvant radiotherapy is becoming standard of care for localised extremity LMS following several reports showing that radiotherapy can improve overall survival for patients undergoing surgery (Gennaro et al. 2021; Gingrich et al. 2017). For example, Gingrich et al showed that 90% of patients who had received neoadjuvant radiotherapy were able to achieve resection margins without residual disease (R0) while this was reduced to 75% and 80% in the adjuvant radiotherapy and no radiotherapy treatment arm upon disease resection, giving an odds ratio of 1.8 for R0 margins following neoadjuvant radiotherapy (Gingrich et al. 2017).

There are however, multiple conflicting results from clinical trials assessing the benefit of adjuvant chemotherapy following surgical excision, with or without radiotherapy to prevent recurrence. A meta-analysis of 18 trials including 1953 STS patients in total with localised resectable tumours showed that adjuvant chemotherapy led to a small but statistically significant decrease in both local and distant recurrence with an odds ratio of 0.73 and 0.69 respectively. Doxorubicin based adjuvant chemotherapy reduced overall recurrence with an odds ratio of 0.69 while combination doxorubicin and ifosfamide reduced overall recurrence with an odds ratio of 0.61. For overall survival, doxorubicin based adjuvant chemotherapy resulted in a non-significant decrease in mortality although doxorubicin and ifosfamide combination showed a decrease in mortality that was significant (Pervaiz et al. 2008). This benefit was not observed, however, in a pooled analysis of two trials from the European Organisation for Research and Treatment of Cancer (EORTC). From a total of 819 patients randomised to adjuvant or non-adjuvant therapeutic arms, adjuvant chemotherapy was not associated with improved outcomes in any STS subtype (A. Le Cesne et al. 2008).

A later EORTC trial randomised 351 intermediate to high grade STS patients without metastasis to receive adjuvant chemotherapy following excision but no benefit in overall

survival or relapse-free survival was observed compared to the control cohort (Woll et al. 2012). Due to these conflicting reports, adjuvant chemotherapy is not routinely recommended. The potential benefit of neoadjuvant chemotherapy is still under assessment although current studies also show limited benefit (A. Gronchi et al. 2021; Pasquali et al. 2022). Results from a randomised phase 3 trial showed that neoadjuvant chemotherapy did not lead to any complete response and only improved overall survival or disease free survival in patients treated with standard chemotherapy such as anthracyclines and ifosfamide, and not histology driven chemotherapy, showing a disease free survival odds ratio of 0.47 ((Alessandro Gronchi et al. 2020)

Treatment of advanced or metastatic, unresectable STS consists of monotherapy or a combination of systemic cytotoxic agents such as doxorubicin, ifosfamide, trabectedin, gemcitabine, docetaxel and eribulin. Systemic chemotherapy has remained the cornerstone of advanced STS control for more than 30 years and despite the emerging use of molecular-guided therapies such as tyrosine kinase inhibitors (TKIs) for select subtypes, prognosis has seen little change in the past decade, highlighting the urgent need for novel treatment modalities (Kasper et al. 2014).

1.3.2 First line chemotherapies

For advanced LMS patients, first line chemotherapy treatment is used primarily for disease control and palliative care but rarely with curative intent (Linch et al. 2014). Patients with higher grade tumours are more likely to response to chemotherapy, with a 65% relative improvement in response for each increase in tumour grade (Sleijfer et al. 2010; Savina et al. 2017). The anthracycline antibiotic doxorubicin is the most commonly used first-line therapy for advanced LMS as well as other STS subtypes and is one of the first agents seen to produce meaningful responses in patients with advanced disease. Response rates of 12-30% can be observed in metastatic LMS patients receiving doxorubicin based regimens and in addition to sarcoma, doxorubicin is also used for treatment of carcinomas (Judson et al. 2014; Tap et al. 2020; D'Ambrosio et al. 2020).

The mechanism of action for anthracycline based chemotherapies are not fully understood although there are two widely accepted hypotheses. The first is that anthracyclines such as doxorubicin can intercalate into DNA in rapidly dividing cells, leading to the disruption of DNA repair mediated by inhibiting the action of topoisomerase II. Topoisomerase II is an important component in DNA replication and acts by

generating transient double strand breaks (DSBs) to prevent DNA supercoiling, caused by strand separation (Nitiss 2009). By preventing the action of topoisomerase II, supercoiled DNA rapidly stalls DNA replication and also can lead to the formation of abnormal DNA structures (Pommier et al. 2010). The second widely accepted mechanisms of anthracycline action is via the generation of free radicals which can cause DNA damage, resulting in cell death (S. Y. Kim et al. 2006). Another potential mechanism is the enhancement of nucleosome turnover around promoters, caused by the intercalation of anthracyclines to DNA. Nucleosome turnover is defined by the successive alterations of histone proteins, and if occurring around promotor regions can effect gene transcription (F. Yang, Kemp, and Henikoff 2013).

While displaying potent dose dependant anti-tumour activity, the use of high dose doxorubicin is limited by its toxicity to non-malignant cells, particularly to cardiomyocytes, leading to short and long-term cardiotoxicity (Volkova and Russell 2012). This could possibly be due to the generation of free radical reactive oxygen species, a mechanism of action not limited to rapidly dividing cells (S. Zhang et al. 2012). Doxorubicin in addition to other anthracyclines, was also shown to induce apoptosis in cardiomyocytes via the upregulation of death receptors (L. Zhao and Zhang 2017).

The cardiotoxicity of anthracyclines has been recognised since the 1970s, where it was shown that cardiac risk increased with cumulative doxorubicin dose and therefore a maximum cumulative lifetime dose of 400-450 mg/m^2 for doxorubicin was recommended (von Hoff et al. 1979). However, the dosage of anthracycline based regimens used to treat advanced STS patients is often higher than patients with other malignancies and therefore the maximum lifetime dose is especially limiting for STS treatment (Loi et al. 2013). The co-administration of dexrazoxane, a cardio protectant, has since been shown to allow for a cumulative doxorubicin dose of 600 mg/m^2, with a low rate of cardiotoxicity and no reduction of efficacy. Dexrazoxane is believed to act as a cardio protectant by the chelation of iron thus reducing the formation of reactive oxygen species in myocardiocytes (R. L. Jones 2014).

Given that anthracycline based chemotherapy treatment is cemented as the backbone of advanced LMS management, many trials have sought to improve first line response rates or progression free survival (PFS) by combining doxorubicin with other chemotherapeutic agents which have shown some degree of activity as monotherapies **(Table 1.1)** (A. Gronchi et al. 2021).

The DNA alkylating agent, ifosfamide is another standard of care chemotherapy for STS, showing single agent, dose dependent, response rates of 5-25% (Tascilar et al. 2007;

Lorigan et al. 2007). Ifosfamide is a pro-drug which requires hepatic metabolism to generate the active cytotoxic agent. Once in its active form, ifosfamide can alkylate DNA to form DNA-DNA crosslinks, leading to inhibition of DNA replication and cell death. (Fleming 1997; J. Zhang, Tian, and Zhou 2008). However, ifosfamide dose is also limited by toxicity, most commonly neurotoxicity and leukotoxicity, and in a retrospective analysis it was shown that ifosfamide had limited activity in LMS patients and also when combined with doxorubicin showed no significant difference in overall survival compared to doxorubicin first-line treatment alone (**Table 1.1**) (Sleijfer et al. 2010; Judson et al. 2014). Further data from a meta-analysis of STS patients from European organisation for Research and Treatment of Cancer-Soft Tissue and Bone Sarcoma group (EORTC-STBSG) showed that LMS patients are less responsive to first-line treatment regimens containing ifosfamide, showing response rates of 19.5% and 25.6% for doxorubicin with ifosfamide or doxorubicin alone respectively. Additionally, the study showed that LMS patients receiving doxorubicin with ifosfamide had shorter overall survival compared to doxorubicin monotherapy (D'Ambrosio et al. 2020). Thus, ifosfamide is only routinely administered in combination therapy in select subtypes where a clear improvement in response was noted such as in SS.

While another alkylating agent, dacarbazine, has not been assessed as a first-line monotherapy agent in LMS, the agent has shown some activity as a first line treatment when combined with doxorubicin in advanced LMS patients, showing an improved response rate of 30.9% compared to doxorubicin and ifosfamide (19.5%) and doxorubicin monotherapy (25.6%) (**Table 1.1**) (D'Ambrosio et al. 2020). Dacarbazine is therefore recommended for multi-agent first line treatment for LMS patients specifically where ifosfamide shows limited activity as a first line therapy, either alone or in combination or (A. Gronchi et al. 2021).

Gemcitabine is another chemotherapy which has been assessed as a first-line treatment for advanced LMS and other STS subtypes, although initial results from a phase 2 trial showed minimal activity as a monotherapy (**Table 1.1**) (Von Burton et al. 2006). Gemcitabine is an analogue of the nucleoside deoxycytidine and is metabolised upon entry into cells via phosphorylation into the active triphosphate form. Gemcitabine triphosphate is incorporated into DNA instead of deoxycytidine which prevents DNA polymerases from elongating DNA strands (Plunkett, Huang, and Gandhi 1995). The gemcitabine triphosphate is locked onto the terminated DNA strand and is resistant to base excision repair, termed masked strand termination, therefore leading to cell death (Plunkett, Huang, and Gandhi 1995). The clinical efficacy of gemcitabine is dependent

on the accumulation of gemcitabine triphosphate in plasma which is achieved via intravenous infusion of a fixed dose per minute (Dileo et al. 2007).

The combination of gemcitabine with the taxane, docetaxel was suggested as a possible beneficial regimen due to the synergistic mechanisms of action (Merimsky et al. 2000; S. R. Patel et al. 2001). Docetaxel stabilises tubulin which leads to an inhibition of mitotic cell processes in addition to inducing the phosphorylation of B-cell lymphoma 2 (BCL-2) which promotes apoptosis (Pienta 2001). By terminating DNA synthesis with gemcitabine and upregulating apoptosis with docetaxel, an increase in response was hypothesised. In a phase 2 trial of first-line gemcitabine and docetaxel treatment, objective responses were observed in 35.8% of patients (**Table 1.1**) (Hensley, Blessing, Mannel, et al. 2008). Out of all evaluable patients, 4.8%% achieved a complete response while 31% achieved a partial response (PR) and 26.2% achieved stable disease (SD), demonstrating that gemcitabine and docetaxel combination can lead to high response rates and complete responses in uterine LMS patients as an initial chemotherapy regimen (Hensley, Blessing, Mannel, et al. 2008). However, more recently a phase 3 trial compared single agent doxorubicin treatment to combined gemcitabine and docetaxel in locally advanced or metastatic STS as a first line treatment and found that gemcitabine and docetaxel offered no improvement in OS or PFS compared to doxorubicin in any of the subtypes included such as LMS and additionally lead to higher toxicity in patients (Seddon et al. 2017). Therefore, gemcitabine and docetaxel treatment is not recommended in the first line setting for advanced STS but instead is recommended for LMS patients, particularly uterine LMS, who have progressed on first line treatment which will be discussed further in the following section.

Trabectedin is a marine-derived anticancer alkaloid and has also demonstrated clinical benefit in LMS as a first-line therapy, although almost all of these trials assess the first-line efficacy of trabectedin as a combinatorial therapy and not as a monotherapy (A. Gronchi et al. 2021; Patricia Pautier et al. 2022; 2015). The mechanism of action for trabectedin is complex, affecting both tumour cells and the tumour microenvironment It can bind to the minor groove of DNA and interferes with DNA binding proteins including transcription factors and DNA repair components. By inhibiting DNA repair, cells are unable to progress through G2 phase of the cell cycle, eventually triggering p53-independent apoptosis (D'Incalci and Galmarini 2010). Due to the interference with DNA repair, an increased sensitivity is noted for tumours which are deficient in certain DNA repair mechanisms due to synthetic lethal interactions (Monk et al. 2016). In addition, by interfering with trans-activated transcription, trabectedin modulates the expression of cytokines and chemokines produced by tumour cells and tumour-associated

macrophages, inhibiting immunosuppression and potentiating an anti-tumour immune microenvironment (Belgiovine et al. 2021). Trabectedin also displaces oncogenic transcription factors from promotor targets, ameliorating oncogenic signalling particularly from oncogenic fusion genes in subtypes such as Ewing's sarcoma (Harlow et al. 2019).

Combined first-line treatment of advanced LMS with trabectedin and doxorubicin (**Table 1.1**), showed an increase in response rate (38 vs 13%), median progression free survival (mPFS) (12.2 vs 6.2 months) and overall survival (30.5 vs 24.1 months) in the combination and doxorubicin monotherapy arms respectively, with an enhanced but manageable toxicity profile (P. Pautier, Italiano, et al. 2021; Patricia Pautier et al. 2022). The prolonged disease control in some LMS patients receiving trabectedin could potentially be explained by the effect on DNA repair mechanisms, whereby DNA damage repair signatures have been shown to predict responses of STS patients to trabectedin (Moura et al. 2021).

Authors	Type of study	N	Subtypes	Treatment	Response rate	mPFS (months)	mOS (months)
(Patricia Pautier et al. 2022)	Randomised phase 3	150	LMS	Doxorubicin & trabectedin vs doxorubicin	Uterine 36% vs 15%; non-uterine 37% vs 12%	6.2 vs 12.2	Not available
(P. Pautier, Floquet, et al. 2021)	Non-randomised phase 2	108	LMS	Trabectedin & doxorubicin 6 cycles	Uterine 59.6%; non-uterine 55.8%	Uterine 8.2; non-uterine 12.9	Uterine 20.2; non-uterine 34.5
(D'Ambrosio et al. 2020)	Retrospective	303	LMS	Doxorubicin & dacarbazine *vs.* doxorubicin & ifosfamide *vs.* doxorubicin	30.9% vs 25.6 % vs 19.5%	9.4 *vs.* 6.8 *vs.* 5.4	35.4 vs. 21.4 vs. 29.3
(Seddon et al. 2017)	Randomized, phase 3	257	STS (46% LMS)	Gemcitabine & docetaxel *vs.* doxorubicin	20% vs 19%	23.7 *vs.* 23.3 weeks	67.3 vs. 76.3 weeks
(Judson et al. 2014)	Randomized, phase 3	455	STS (25% LMS)	Doxorubicin & ifosfamide *vs.* doxorubicin	26% vs 14%	7.4 *vs.* 4.6	14.3 *vs.* 12.8
(Sleijfer et al. 2010)	Retrospective	1337	STS (42% LMS)	Ifosfamide & other vs doxorubicin	20.4% vs 24.7%	4.4 vs 3.5	12.4 vs 12.0
(Hensley, Blessing, Mannel, et al. 2008)	Phase 2	42	uLMS	Gemcitabine & docetaxel	35.8%	4.4	16
(Lorigan et al. 2007)	Randomised phase 3	326	STS (30% LMS)	Ifosfamide ($3*3g/m^2$) vs Ifosfamide ($9g/m^2$) vs doxorubicin	5.5% vs 8.4% vs 11.8%	2.16 vs 3.0 vs 2.52	10.92 vs 10.92 vs 12.0
(Von Burton et al. 2006)	Phase 2	48	STS (21% LMS)	Gemcitabine	4%	2.0	6.0

Table 1.1. Examples of clinical trials assessing systemic chemotherapies as a first line treatment for advanced LMS. LMS; leiomyosarcoma, mPFS; median progression-free survival, mOS; median overall survival.

1.3.3 Second line chemotherapies and beyond

Unfortunately many patients will fail to respond, develop secondary resistance or demonstrate treatment related toxicity to first line chemotherapy agents at which point patients will receive a different therapy as a second line treatment. Beyond the first-line setting, evidence for systemic chemotherapy response is less robust with several agents tested in phase 2 trial but fewer phase 3 trials reported (Sharma et al. 2013; A. Gronchi et al. 2021).

Gemcitabine is used in advanced or metastatic LMS as a second line chemotherapy with only modest activity when used alone **(Table 1.2)** (S. R. Patel et al. 2001). Gemcitabine displays a response rate ranging from 3.23%-18% in sarcomas across subtypes (Merimsky et al. 2000). However, an improved overall response rate was observed in metastatic STS patients including LMS patients who received gemcitabine and docetaxel (16%) compared to gemcitabine alone (8%) (Maki et al. 2007). Additionally, mPFS was 6.2 months and 3 months for combination or monotherapy treatment respectively and median overall survival (mOS) was also increased from 11.5 months in the monotherapy arm to 17.9 months in the combination arm, showing this regimen can lead to improved outcomes. However, combined gemcitabine and docetaxel did show an increase in toxicity (Maki et al. 2007).

In a retrospective study of bone or soft-tissue sarcoma patients treated with a combination of gemcitabine and docetaxel a response rate of 43% was reported. Responding subtypes included LMS, angiosarcoma, malignant fibrous histiocytomas, MPNST, osteosarcoma and Ewing's sarcoma (Leu et al. 2004). This study additionally showed *in vitro* that sequential treatment with gemcitabine followed by docetaxel produced synergy while simultaneous treatment led to antagonism in cancer cell lines (Leu et al. 2004). Therefore, gemcitabine infusion followed by docetaxel is the standard method of administering this combination in STS. In a phase 2 trial assessing the activity of gemcitabine and docetaxel in unresectable LMS patients either following progression on doxorubicin or as a first line treatment, an impressive response rate of 53% was reported, or 50% when only considering patients who had received prior doxorubicin (**Table 1.2**) (Hensley et al. 2002). Since this study, further phase 2 trials in the context of second line treatment have shown responses ranging from 21-27% in uterine or non-uterine LMS patients (**Table 1.2**) (Hensley, Blessing, DeGeest, et al. 2008; Patricia Pautier et al. 2012).

For advanced LMS, the alkylating agent trabectedin has recently shown promising results for patients who have progressed on doxorubicin or unsuited for anthracycline

treatment (Demetri et al. 2016). Initially in several phase 2 trials, trabectedin showed low response rates (8-11.1%) as a monotherapy for advanced chemo refractory STS, although these studies noted a lack of cumulative toxicity (**Table 1.2**) (Yovine et al. 2004; A. Le Cesne et al. 2005; Garcia-Carbonero et al. 2004). A phase 3 trial showed that trabectedin treatment lead to a 45% reduction in the risk of disease progression or death compared to dacarbazine for heavily pre-treated, advanced LMS or LPS with a response rate of 34% and 12% in trabectedin or dacarbazine treated patients respectively (Demetri et al. 2016). Based on these studies trabectedin is recommended as an option for LMS patients who have progressed on previous doxorubicin treatment (A. Gronchi et al. 2021).

Eribulin is another chemotherapeutic agent which has recently been suggested as an option for advanced LMS patients following failure on first line treatment regimens (**Table 1.2**) (Jean Yves Blay et al. 2019; Phillips et al. 2022). Eribulin is a non-taxane microtubule inhibitor which leads to mitotic arrest but has also showed other anti-tumour mechanisms of action including the suppression of transforming growth factor beta 1 (TGF-β1) which is a growth factor that promotes cell proliferation and metastasis (Ueda et al. 2016; Smith et al. 2010). Additionally eribulin can induce smooth muscle differentiation markers within LMS tumours (Kawano et al. 2016). A phase 2 trial of advanced STS patients who had previously received up to two single drugs for advanced disease showed a response rate of 5% in the LMS cohort although 32% of LMS patients demonstrated stable disease at 12 weeks after starting eribulin treatment (Schöffski et al. 2011). A later study focussed on LMS patients who had received at least 2 prior lines of chemotherapy treatment, assessing the outcomes of eribulin or dacarbazine treatment (Jean Yves Blay et al. 2019). This phase 3 trial reported similar response rates between eribulin and dacarbazine arms (5% vs 7% respectively) and also a similar mPFS (2.2 vs 2.6 months) and mOS (12.7 vs 13 months respectively) with manageable toxicity profiles, therefore both are used as second line or further treatment options (Jean Yves Blay et al. 2019; Axel Le Cesne, Martín-Broto, and Grignani 2022).

Authors	Type of study	N	Subtypes	Treatment	Response rate	mPFS (months)	mOS (months)
(Jean Yves Blay et al. 2019)	Randomised phase 3	309	LMS	Eribulin vs dacarbazine	5% vs 7%	2.2 vs 2.6	12.7 vs 13.0
(Demetri et al. 2016)	Randomized, phase 3	518	LPS and LMS (73% LMS)	Trabectedin vs. da carbazine	9.9% vs 6.9%	4.2 vs. 1.5	12.4 *vs*. 12.9
(Patricia Pautier et al. 2012)	Randomised phase 2	90	LMS	Gemcitabine vs Gemcitabine & docetaxel	Uterine 19% vs 24%; non-uterine 14% vs 5%	Uterine, 5.5 vs 4.7; non-uterine, 6.3 vs 3.8	Uterine, 20 vs 23; non-uterine, 15 vs 13
(Schöffski et al. 2011)	Nonramdomised phase 2	128	STS (31% LMS)	Eribulin	5% (LMS specific)	Not available	Not available
(Hensley, Blessing, DeGeest, et al. 2008)	Phase 2	51	Uterine LMS	Gemcitabine & docetaxel	27.1%	6.7	14.7
(Maki et al. 2007)	Randomised phase 2	122	STS (31% LMS)	Gemcitabine & docetaxel vs Gemcitabine	16% vs 8%	6.2 vs 3.0	17.9 vs 11.5
(A. Le Cesne et al. 2005)	Nonrandomised phase 2	104	STS (41% LMS)	Trabectedin	8.1%	3.5	9.2
(Garcia-Carbonero et al. 2004)	Phase 2	36	STS (36% LMS)	Trabectedin	8%	1.7	12.1
(Yovine et al. 2004)	Nonrandomised Phase 2	54	STS (48% LMS)	Trabectedin	11.1%	1.9	12.8
(Hensley et al. 2002)	Phase 2	34	LMS	Gemcitabine & docetaxel	53%	5.6	17.9
(Köstler et al. 2001)	Phase 2	27	STS (22% LMS)	Docetaxel	15%	2.4	7.7
(S. R. Patel et al. 2001)	Phase 2	56	STS (48% LMS)	Gemcitabine	18%	3	13.9

Table 1.2. Examples of clinical trials assessing systemic chemotherapies as a second or further line of treatment for advanced LMS. LMS; leiomyosarcoma, LPS; liposarcoma, mPFS; median progression-free survival, mOS; median overall survival, STS; soft-tissue sarcoma.

1.3.4 Chemotherapy resistance mechanisms in LMS

The major issues facing systemic chemotherapies as a treatment option is the accumulation of toxicity which leads to regimen discontinuation, and the development of multi-drug resistance. Multi-drug resistance poses a significant challenge to subsequent treatment, progressively lowering the response rates seen in patients receiving second line or further treatment regimens (Comandone et al. 2017). Mechanisms associated with chemotherapy resistance in other cancer types includes enhanced drug efflux, DNA repair, downregulation of apoptosis, ECM alterations, and angiogenesis (Tegze et al. 2012; Lovitt, Shelper, and Avery 2018; Gallego et al. 2022; Garcia-Ortega et al. 2022; Vaidyanathan et al. 2016). However, many of the mechanistic studies on LMS samples have so far mostly focused on drug efflux, DNA repair pathway alterations and anti-apoptotic mechanisms of chemotherapy resistance (De Graaff et al. 2016; Honoki et al. 2010; S. T. Lin et al. 2012; Martin-Broto et al. 2021) (**Figure 1.6**).
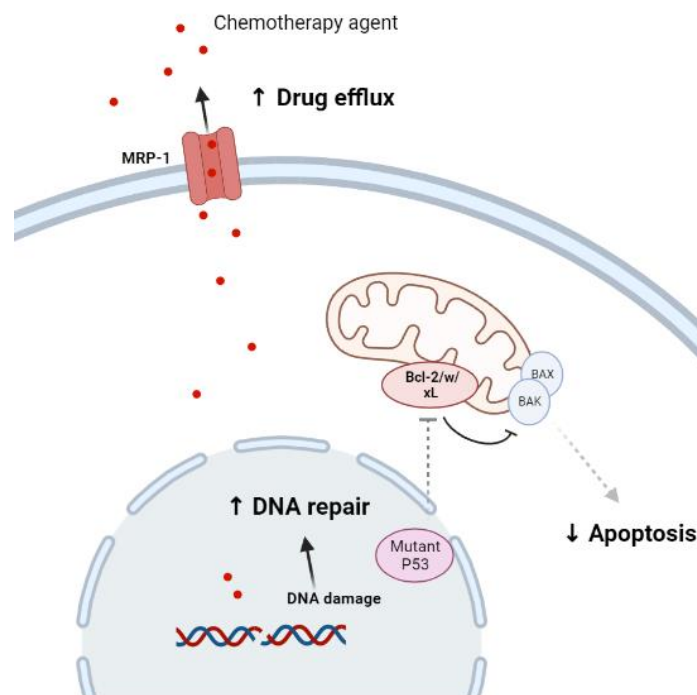
Figure 1.6. Overview of chemotherapy resistance mechanisms implicated in LMS. BAK; BCL2 Antagonist/Killer 1, BAX; Bcl-2-associated X protein, Bcl-2; B-cell lymphoma 2, Bcl-w; B-cell lymphoma 2 like protein 2, Bcl-2; B-cell lymphoma-extra large, MRP-1; multi-drug resistance protein-1. Created using BioRender.

In several cancer types, multi-drug resistance to chemotherapies has been shown to be promoted by the activation of ATP binding cassette (ABC) family of efflux transporters (Muriithi et al. 2020). The cellular function of ABC-transporters is to transport metabolites, toxics as well as essential molecules in and outside of the cell but can also actively

remove cytotoxic agents from the cell, resulting in reduced intracellular accumulation and thus, reduced anti-tumour activity (Rees, Johnson, and Lewinson 2009). The multi-drug resistance protein 1 (MDR1) or P-glycoprotein has been shown to actively remove doxorubicin from sarcoma cells, and an association between the degree of chemoresistance, expression of *MRP1,* and reduction of intracellular drug accumulation has been well documented in several subtypes including LMS (**Figure 1.6**) (Martin-Broto et al. 2021). In the LMS cell line SK-UT-1, doxorubicin treatment was found to cause an upregulation of the ABC transporter MRP-1 while co-treatent with the Breakpoint cluster region/Abelson (BCR/ABL) kinase inhibitor nilotinib reduced doxorubicin induced MRP-1 upregulation and also inhibited the efflux function MRP-1, leading to increase intracellular accumulation of doxorubicin (Villar et al. 2012). This effect was not seen in imatinib which is an inhibitor of BCR/ABL, c-KIT and PDGFRα but with less potency towards BCR/ABL compared to nilotinib, suggesting that BCR/ABL mediates an upregulation and enhanced activity of ABC transporters to induce doxorubicin resistance (Villar et al. 2012). P53 loss of function has also been shown to increase the expression of MRP-1, mediating chemotherapy resistance, whereby LMS cells transfected with wild type *TP53* reduced MRP-1 expression and led to an increased intracellular accumulation of doxorubicin (Zhan et al. 2001).

As doxorubicin exerts its anti-tumour effects via DNA damage, the alteration of DNA damage response and repair pathways is one of the main mechanisms implicated in chemotherapy resistance (**Figure 1.6**) (Boichuk et al. 2020; Gallego et al. 2022). For instance, osteosarcoma acquired doxorubicin resistant cells generated *in vitro* showed reduced DNA damage following doxorubicin exposure compared to parental cells (Gallego et al. 2022). Additionally Akt has been suggested as a potential mediator of enhanced DNA repair in doxorubicin resistant LMS cells based on the observation that Akt inhibition is able to re-sensitise cells to doxorubicin induced DNA damage, leading to enhanced apoptosis (Boichuk et al. 2020).

Downstream of induced DNA damage, upregulation of anti-apoptotic proteins such as Bcl-2 and parallel downregulation of pro-apoptotic proteins including Bcl-2-associated X protein (BAX) and BCL2 Antagonist/Killer 1 (BAK) is also associated with doxorubicin resistance (**Figure 1.6**) (Van oosterwijk et al. 2012). Anti-apoptotic proteins Bcl-2, B-cell lymphoma-extra large (Bcl-xL) and Bcl-2-like protein 2 (Bcl-w) bind to pro-apoptotic proteins BAX and BAK which prevents activity however, upon apoptotic signalling, anti-apoptosis proteins release BAX and BAK which are then able to oligomerize and form pores in the mitochondrial outer membrane, one of the main stages of mitochondria-mediated cell death (Kale, Osterlund, and Andrews 2017). De Graaf et al. reported that

77%, 84% and 42% of LMS tumours show a high expression of anti-apoptotic proteins Bcl-2, Bcl-xL and Bcl-w respectively and combination with Bcl-2 family inhibitor ABT-737, sensitised LMS cells to doxorubicin treatment (De Graaff et al. 2016). Proteomic analysis also demonstrated the upregulation of anti-apoptotic protein Bcl-w in acquired doxorubicin resistant LMS cell lines (S. T. Lin et al. 2012). Mechanistic investigation of chemoresistance in LMS cells showed that when LMS cells were transfected with maternal embryonic leucine zipper kinase (MELK) overexpression constructs, an upregulation of Bcl-2 via the activation of the Janus kinase 2 (JAK-2)/ Signal transducer and activator of transcription 3 (STAT-3) pathway was observed causing resistance to doxorubicin while the opposite was observed upon MELK suppression (Zhiwei Zhang et al. 2020). Furthermore high MELK expression in LMS patient tumours also correlated with poor survival outcomes (Zhiwei Zhang et al. 2020). Additionally, a recent study showed that primary STS cells including LMS with P53 mutations, a key regulator of apoptosis, demonstrate doxorubicin resistance via reduced apoptotic signalling (**Figure 1.6**) (Kirilin et al. 2022).

Clearly several chemoresistance mechanisms are active in LMS cells, however many of the studies investigating the molecular alterations of chemo-resistant LMS are largely confined to *in vitro* studies using commercial cell lines which may not fully encapsulate the variety of chemo resistant mechanisms employed by *in vivo* tumours (S. T. Lin et al. 2012; May et al. 2014). Therefore further work to investigate chemotherapy resistance mechanisms in patient-derived models is necessary.

1.4 Molecular targeted therapy for advanced LMS

To improve on the treatment options available for advanced LMS patients who have progressed on standard of care chemotherapy treatment, molecular targeted therapies are gaining increased interest in LMS. This is in part due to the recent large scale sequencing studies which have shown recurrent gene alterations and subsequently common oncogenic pathways which are active in LMS (Nacev et al. 2022; Gounder et al. 2022). Additionally, several therapies targeting the tumour microenvironment such as anti-angiogenics are under clinical assessment or have even been approved for LMS and other STS subtypes. Currently, pazopanib is the first and only targeted therapy approved for the treatment for multiple non-GIST soft-tissue sarcoma (STS) subtypes, (van der Graaf et al. 2012). Its use is limited to advanced or metastatic STS patients, excluding liposarcoma, who have progressed after receiving two or more lines of chemotherapy.

1.4.1 Tyrosine kinase inhibitors

Due to their elevated expression in LMS tissue, both RTKs and intracellular tyrosine kinases have therefore become attractive targets for anti-cancer therapies, such as small molecule tyrosine kinase inhibitors, which bind the kinase domain (either reversibly or irreversibly) within the ATP pocket or monoclonal antibodies which bind to receptors and prevent ligand-receptor interactions (Jiao et al. 2018; Gaumann et al. 2014; Cuppens, Annibali, et al. 2017). The majority of TKIs assessed so far in STS subtypes includes multi-target TKIs such as pazopanib and anlotinib which target can target both angiogenesis and also proliferation via the inhibition of RTKs such as VEGFR and PDGFR (van der Graaf et al. 2012; Wilhelm et al. 2011; Patwardhan et al. 2016; Xie et al. 2018). Most of these TKIs were first identified through biochemical screens for VEGFR2 inhibitors and later shown to potently inhibit the activation of VEGF mediated VEGFR2 activation, leading to a decrease in endothelial cell proliferation and tube formation (Wilhelm et al. 2011; Xie et al. 2018; Hu-Lowe et al. 2008).. In pre-clinical assessment, the multi-target TKI pazopanib showed anti-proliferative effects in STS cell lines and patient-derived models of LMS, rhabdoid tumours, SS and clear cell sarcoma which was frequently mediated by a reduction in PDGFR and Akt phosphorylation although some models also showed a reduction of MAPK pathway activation as well (Fleuren et al. 2017; Hosaka et al. 2012; Outani et al. 2014; Wong et al. 2016; Teicher et al. 2015). Additionally TKIs that targeted intracellular tyrosine kinases such as the Src inhibitor dasatinib also demonstrated anti-tumour activity in LMS cell lines as well as other subtypes (Teicher et al. 2015). However, further pre-clinical investigation into the mechanisms of LMS response to dasatinib has not been conducted.

Based on the encouraging pre-clinical observations that LMS and other STS models were sensitive to multi-target anti-angiogenic therapies, pazopanib underwent clinical assessment in a range of STS subtypes including LMS and eventually gained Food and Drug Administration (FDA) approval owing to the results of a randomised, double-blind, phase 3 clinical trial (PALETTE) (van der Graaf et al. 2012). This trial showed that pazopanib treated advanced STS patients who had previously received at least one line of anthracycline treatment prior to trial enrolment had significantly improved progression-free survival compared to a placebo-control group (4.6 vs 1.6 months respectively) with a hazard ratio of 0.31 ($p < 0.0001$) (van der Graaf et al. 2012). However, the study noted no significant difference in mOS between the two arms (12.5 vs 10.7 months) with a hazard ratio of 0.86 ($p = 0.25$). Upon approval it was observed that a subset of patients

did not respond to pazopanib or rapidly developed resistance after an initial response, and, on top of the lack of predictive clinicopathological factors for clinical response, eventually led to the removal of funding for pazopanib by the Cancer Drug Fund in 2015 (Amdahl et al. 2014).

This result highlights the continued difficulty in translating pre-clinical findings surrounding TKIs into meaningful, consistent clinical benefit in LMS and other STS subtypes. A similar outcome was seen in the first-in-class monoclonal antibody olaratumab which is highly specific to PDGFRα and inhibits PDGF mediated activation and downstream signalling once bound. LMS cell lines and xenograft models shown to express PDGFRα demonstrated a 35-67% reduction in tumour growth during olaratumab treatment, compared to a control antibody, indicating that this antibody may show clinical responses in LMS patients (Loizos et al. 2005). Indeed, an early phase 1b/2 clinical trial showed promising results when combined with doxorubicin in anthracycline naïve advanced STS patients, 38% of which were LMS patients (Tap et al. 2016). The combination of olaratumab and doxorubicin vastly improved mOS to 26.5 months compared to 6.6 months for doxorubicin treatment alone and this improvement was not dependent on subtype, although no significant difference in mPFS was seen (6.6 and 4.1 months respectively, p=0.615) (Tap et al. 2016). However, a later phase 3 trial with 509 STS patients, of which 46% were LMS, failed to reproduce the previous findings, showing no significant difference in mOS in patients treated with combined olaratumab and doxorubicin compared to patients treated with doxorubicin alone which in the LMS specific cohort was reported as 21.6 months and 21.9 months respectively (p=0.76) and additionally mPFS was slightly lower in the combined treatment arm compared to doxorubicin monotherapy particularly in the LMS cohort (4.3 months and 6.9 months respectively) (Tap et al. 2020).

Another multi-target anti-antiogenic TKI, anlotinib is currently a promising TKI candidate for advanced LMS and other STS based on phase 2 trial data which recruited patients with metastatic or advanced chemo refractory disease (Chi et al. 2018). The study showed anti-tumour activity with a mPFS of 5.6 months and an mOS of 12 months although in the LMS cohort mPFS and mOS was reported as 11 months and 15 months respectively with a 12 week PFS rate of 75% in LMS (Chi et al. 2018). A phase 3 trial is now ongoing, assessing anlotinib treatment in metastatic or advanced LMS, SS and alveolar soft part sarcoma (ASPS) and will be compared to dacarbazine treatment (NCT03016819). However pre-clinical studies assessing the mechanistic basis of anlotinib activity directly on LMS cells is lacking and so far only one study has aimed to identify direct anti-tumour mechanisms which was conducted on SS cells, showing

reduced cell proliferation which is mediated by the targeting of GINS complex subunit 1 (GINS1) which is a major component of DNA replication (Tang et al. 2019).

One of the major recurring issues for TKI therapy in LMS and other STS subtypes is the lack of well-defined predictive biomarkers of response in addition to the poor understanding of underlying biology of response and resistance (Wilding et al. 2019). To address these issues, translational work utilising panels of patient-derived models will be vital in order to fully capture heterogeneity of response as well taking into account potential variable responses due to prior multi-line treatment regimens.

1.4.2 PI3K/AKT/mTOR inhibitors

The PI3K/Akt/mTOR pathway is another key therapeutic target for LMS treatment due to the aberrant activity caused by frequent *PTEN* alterations (Chudasama et al. 2018; Nacev et al. 2022; Gounder et al. 2022; Cuppens, Annibali, et al. 2017). To target this pathway a range of PI3K inhibitors have been developed which are either pan-PI3K inhibitors or isoform-specific inhibitors. PI3K can be divided into three subclasses based on the subunit isoforms and substrate specificities (Thorpe, Yuzugullu, and Zhao 2015). Class I PI3Ks are stimulated by RTK and G protein-coupled receptors, and consist of a p110 catalytic subunit which can include p110α, p110β, p110δ or p110γ. Class II PI3Ks are not fully understood but only contain catalytic subunits while the single class III PI3K, vacuolar protein sorting 34 (VPS34) is involved in intracellular trafficking and autophagy (Vanhaesebroeck et al. 2010). In contrast to class II and class III, mutations in class I PI3Ks are commonly associated with cancer and while p110α and p110β isoforms are ubiquitously expressed, p110δ and p110γ expression is mainly observed in leukocytes (Okkenhaug and Vanhaesebroeck 2003). Therefore, p110δ mutations in particular is associated with haematological malignancies (Cornillet-Lefebvre et al. 2005).

Pan PI3K inhibitors target all four of the class I PI3K isoforms (α, β, δ, γ) and compete with ATP for the binding pocket in the catalytic subunits. However pan-PI3K inhibitors are associated with several adverse events and thus far only one pan-PI3K inhibitor, copanlisib, is approved by the FDA for use in non-Hodgkin lymphoma or chronic lymphocytic leukaemia (Mishra et al. 2021; Janku 2017; Dreyling et al. 2020). In contrast isoform specific PI3K inhibitors reduce off target effects at the expense of narrow patient selection and currently three small molecule isoform specific PI3K inhibitors are approved by the FDA: alpelisib (α-specific) which approved for breast cancer and idelalisib (δ-specific) and duvelisib (δ/γ -specific) which are approved for non-Hodgkin

lymphoma or chronic lymphocytic leukaemia (André et al. 2019; Q. Yang et al. 2015; K. Patel, Danilov, and Pagel 2019).

In LMS, a pan PI3K inhibitor ZSTK474 has shown efficacy in a non-uterine and uterine cell line, displaying reduced viability and a reduction in Akt activation, while ZSTK474 reduced LMS cell xenograft tumour growth comparable to that observed in doxorubicin treated xenografts (Namatame et al. 2018). Additionally a xenograft generated from the acquired doxorubicin resistant uterine-LMS cell line MES-SA/Dx5 showed a greater reduction in tumour growth compared to doxorubicin treatment, highlighting that this type of targeted therapy may show benefit in chemo refractory LMS patients (Namatame et al. 2018). Meanwhile a PI3Kα/δ selective inhibitor pictilisib also demonstrated anti-tumour activity in PDX LMS models by reducing tumour growth, although PDX tumour tissue demonstrated a similar intensity of staining for phosphorylated Ribosomal protein S6 (S6RP), a downstream marker of mTOR signalling, suggesting that mTOR signalling is still active in PI3K inhibitor treated LMS tumours (Fourneaux et al. 2017). Clinical trials assessing PI3K inhibitors in LMS are extremely limited due to the rarity of PI3K mutations in this disease, despite showing aberrant of the PI3K pathway via PTEN loss (Cuppens, Annibali, et al. 2017). One phase 2 trial included sarcoma patients when assessing the pan PI3K inhibitor buparlisib, although the subtypes of the sarcoma patients were not mentioned and only 1 out of 14 sarcoma patients showed clinical benefit from buparlisib treatment (Piha-Paul et al. 2019).

Given the downstream location of mTOR in the PI3K/Akt pathway, the inhibition of mTOR was considered an attractive therapeutic option for tumours which show an upregulation of this pathway and could potentially avoid side-effects caused by inhibition of upstream kinases (Chan 2004). Rapamycin is an allosteric, irreversible and highly specific inhibitor of mTOR, although rapamycin is limited by its poor solubility and pharmacokinetics which lead to the development of rapamycin analogues such as everolimus, temsirolimus and ridaforolimus (Chung et al. 1992; Kuo et al. 1992; Price et al. 1992; Jing Li, Kim, and Blenis 2014). In a panel of sarcoma cell lines, LMS cells were particularly sensitive to mTOR inhibition by everolimus and showed significantly higher sensitivity to mTOR inhibition compared to PI3K inhibition (Namatame et al. 2018). Additionally, everolimus has also showed anti-tumour activity in LMS PDX models by reducing tumour growth and showing a 30% reduction in staining intensity for phosphorylated S6RP downstream of mTOR (Fourneaux et al. 2017).

A small trial of LMS patients treated with temsirolimus reported stable disease or response in three of six patients although IHC status of PTEN or S6RP expression was not predictive of response (Italiano et al. 2011). Later a phase 2 clinical trial utilising the mTOR inhibitor temsirolimus combined with doxorubicin showed promising responses in relapsed or refractory sarcoma including LMS patients, reporting that 53% of patients achieved stable disease or better for 60 days after starting treatment (Trucco et al. 2018). The authors additionally showed that activated Akt detected in tissue biopsies 4 weeks after beginning treatment were a negative predictor of response (Trucco et al. 2018). However, despite clinical evidence of response in LMS, other clinical trials utilising first generation mTOR inhibitors were less successful than predicted (Demetri et al. 2013; Okuno et al. 2011). For example, Demetri et al reported in a phase 3 trial of metastatic sarcoma patients including LMS that treatment with the mTOR inhibitor ridaforolimus lead to only a modest increase in mPFS and mOS compared to placebo (17.7 and 90.6 weeks vs 14.6 and 85.3 weeks respectively) and a high toxicity profile was noted (Demetri et al. 2013). Meanwhile phase 2 study of gemcitabine and sirolimus in previously treated advanced STS patients, including LMS, showed no responses and dose limiting toxicity (Martin-Liberal et al. 2017).

The disappointing results of mTOR inhibitors in the clinic could be explained by the negative feedback loops inherent to the PI3K-Akt-mTOR pathway (Sathe et al. 2018). For example, one function of p70S6K following activation by mTORC1 is to cause the degradation of RTK substrates such as insulin receptor substrate (IRS) which leads to downregulated PI3K signalling and cessation of mTORC1 activation (Wan et al. 2006). When inhibited by rapamycin or analogues, IRS is no longer degraded by p70S6K, eventually leading to the upregulation of IRS mediated PI3K-Akt-mTOR pathway activation (Carracedo et al. 2008; Fourneaux et al. 2017; O'Reilly et al. 2006). P70S6K also inhibits mTORC2 by phosphorylation of the Rictor component, reducing the activation of Akt and serves as another negative feedback loop which is blocked by rapamycin (Laplante and Sabatini 2012).

Dual PI3K and mTOR inhibitors such as dactolisib (BEZ-235/NVP-BEZ235) were generated to overcome this PI3K-dependant feedback loop and have shown promising results *in vitro* both as a monotherapy or in combination with doxorubicin treatment, (Babichev et al. 2016). Fourneaux et al. demonstrated an elevated sensitivity to BEZ235 compared to mTOR or PI3K inhibition alone in three patient derived LMS cell lines and xenografts (Fourneaux et al. 2017). The authors established these models from tumours which displayed a loss of PTEN expression and strong p-S6RP[S240/244] staining, indicating aberrant activation of the PI3K/Akt/mTOR pathway (Fourneaux et al. 2017). However,

extracellular signal-regulated kinase (ERK) upregulation was still observed in LMS cells treated with the dual PI3K and mTOR inhibitor BEZ235, which was reduced upon the addition of a mitogen-activated protein kinase kinases (MEK) inhibitor and lead to a potent reduction on *in vivo* growth, suggesting an additional PI3K independent negative feedback loop might contribute to dual PI3K/mTOR inhibitor resistance via enhanced MAPK pathway activation (Fourneaux et al. 2016; H. K. Kim et al. 2016; Cuppens, Annibali, et al. 2017). Thus, while dual PI3K/mTOR inhibition is an attractive candidate therapy for LMS patients displaying *PTEN* loss, further research is necessary confirm the mechanisms of response to dual PI3K/mTOR inhibitors and whether negative feedback loops are broadly seen across patient samples.

A pre-clinical study generated several PI3K/mTOR inhibitor resistant LMS cell and xenograft models in order to investigate potential mechanisms of acquired resistance (Fourneaux et al. 2019). The authors found an upregulation of cancer stem cell associated markers SRY-box transcription tactor 2 (SOX2) and aldehyde dehydrogenase 1 (ALDH1) and, consistent with this observation, resistant LMS cells were better able to form spheroids in non-adherent culture, showing elevated self-renewal (Fourneaux et al. 2019). Additionally an enhancer of zeste homolog 2 (EZH2) inhibitor was able to re-sensitise LMS cells and xenografts to dual PI3K/mTOR inhibition by reducing ALDH1 expression, indicating that this drug combination could potentially delay the acquisition of resistance in LMS patients. BEZ235 has yet to be tested in the clinic for efficacy in LMS patients although based on promising pre-clinical results, warrants investigation as a second line or further treatment regimen.

Akt inhibitors are another class of drug which could be used to target LMS tumours with aberrant activation of the PI3K/Akt/mTOR pathway although there are fewer studies which have assessed AKT inhibitor response in LMS compared to PI3K and/or mTOR inhibitors. However, a pre-clinical study has demonstrated sensitivity of LMS cells to the Akt inhibitor MK-2206, showing that this can synergise with doxorubicin treatment and increase apoptosis compared to each monotherapy (Boichuk et al. 2020). Meanwhile, LMS cells with an acquired resistance to the cytotoxic chemotherapy eribulin showed sensitivity to combined MK-2206 and eribulin treatment (Hayasaka et al. 2019). Clinical studies of Akt inhibitors are limited, although a phase 1 pharmacokinetic study of MK-2206 did show stable disease in one out of three LMS patients included in the study, therefore further pre-clinical and clinical evaluation of Akt inhibition in LMS is warranted (Doi et al. 2015).

1.4.3 Synthetic lethality and PARP inhibitors

Deficiency in HR pathway or BRCAness is known to confer sensitivity to DNA-double strand break inducing drugs, including platinum based derivatives and poly (Adenosine diphosphate (ADP)-ribose) polymerase (PARP) inhibitors which have become standard of care therapies for *BRCA1/2* mutant breast and ovarian cancers (Helleday 2011)**.** The PARP family is comprised of 17 proteins involved in several aspects of the DDR including the detection of DNA damage and recruitment of repair components. Of these enzymes, PARP1 appears to play the most significant role in the DDR pathway. PARP1 is a major component of the base excision repair (BER) pathway which corrects small base lesions caused by oxidation, deamination or alkylation and is vital for the single strand DNA break (SSB) repair pathway (Fisher et al. 2007). In addition, both PARP1/2 have been shown to stabilise replication forks at BER intermediates and PARP1 further participates in nucleotide excision repair, NHEJ and HR (Ronson et al. 2018). PARP enzymes rapidly detects and binds to DNA damage, catalysing the polymerisation of poly ADP-ribosylation (PAR) from (nicotinamide adenine dinucleotide) NAD+ molecules. PARP1 is further activated by auto-PARylated which enables the PARylation of both histones and chromatin associated proteins. PARylation of these components results in the recruitment of DNA repair proteins including X-ray repair cross-complementing protein 1 (XRCC1) which repairs the single strand breaks (Brem and Hall 2005)**.**

PARP inhibitors are able to compete with NAD+ at the catalytic site of PARP and when PARP is inhibited, SSBs are unable to be repaired, leading to replication fork collapse, developing into a DSB. PARP inhibitors have been shown to inhibit SSB repair in all phases of the cell cycle (**Figure 1.7**) (Godon et al. 2008)**.** PARP inhibitors are, therefore, an example of synthetic lethality which is a concept where two individual mutations or aberrations are able to exist individually but are lethal when combined (Lord and Ashworth 2017). In this instance, normal HR proficient cells are able to repair the DSBs induced by PARP inhibition with relatively few errors, avoiding apoptosis and genetic alterations. HR deficient tumour cells on the other hand must repair DSBs via other repair pathways such as NHEJ which introduce mutations and genomic rearrangements, leading to cell death (Bryant et al. 2005; Farmer et al. 2005). In the clinical setting, remarkable tumour-specific responses are seen in BRCA1/2 mutant cancers. Several PARP inhibitors have now been approved for use in BRCA1/2 breast, ovarian, prostate and pancreatic cancers at varying stages of treatment (Geenen et al. 2018; Lord and Ashworth 2017). Olaparib was the first PARP inhibitor approved by the FDA in as a treatment for advanced BRCA1/2 mutated ovarian cancers (Kaufman et al. 2015) and

has now also been approved for treatment of BRCA1/2 mutated human epidermal growth factor receptor 2 (HER2)-negative breast cancer and advanced pancreatic cancer maintenance therapy (Robson et al. 2019; Golan et al. 2019)**.** PARP inhibitors have also shown activity beyond BRCA1/2 mutant tumours, in cancers which show HR deficiency or mutations in DDR associated genes. Olaparib has further been approved for the treatment of recurrent ovarian cancer regardless of BRCA1/2 mutation status and recently for the treatment of HR deficient prostate cancer (Pujade-Lauraine et al. 2017; de Bono et al. 2020).
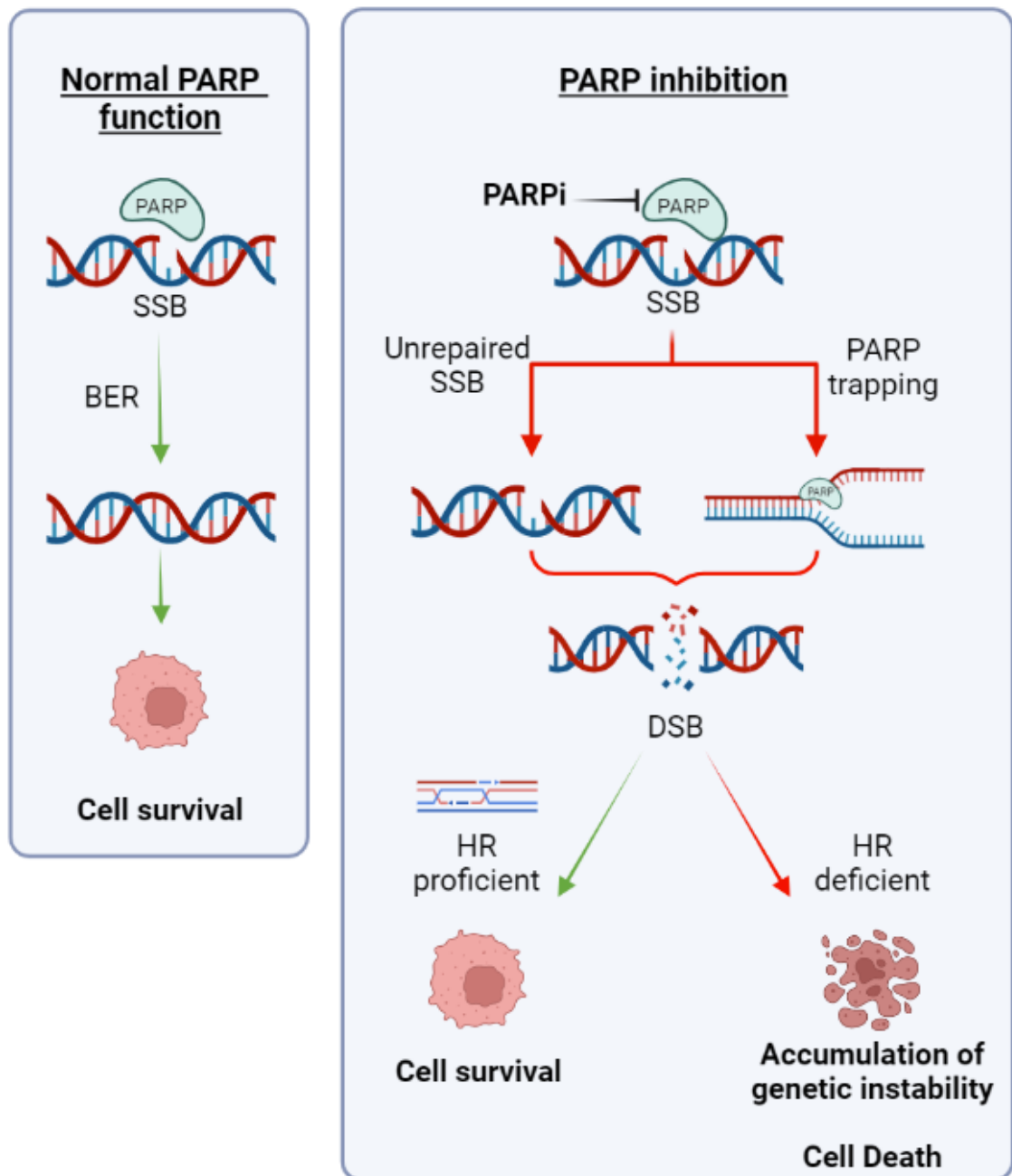
Figure 1.7. Mechanism of PARP inhibition compared to normal PARP function. PARP inhbitors prevent the action of BER and cause PARP trapping, converting SSBs into DDBs. HR proficient cells repair DSBs and survive PARP inhibition while HR deficient cells undergo cell death due to unrepaired DSBs and accumulation of genomic instability. Figure was created using BioRender. BER; Base Excision Repair, DSB; Double Strand Break, HR; Homologous Recombination, PARP; Poly (ADP-Ribose) Polymerase, PARPi; Poly (ADP-Ribose) Polymerase Inhibitor, SSB; Single Strand Break.

Other PARP inhibitors which have been approved for treatment in various cancer types includes niraparib, rucaparib and talazoparib. Talazoparib is another PARP inhibitor

approved for the treatment of BRCA1/2 mutant advanced HER2 negative breast cancer (Litton et al. 2018). Niraparib is approved for the treatment of recurrent ovarian cancer and primary peritoneal carcinomas that are HR deficient or showed a response to previous chemotherapy treatment and rucaparib is approved as a treatment for BRCA1/2 mutant advanced ovarian carcinoma, BRCA1/2 mutant metastatic prostate cancer and as a maintenance therapy for recurrent ovarian or primary peritoneal cancers (González-Martín et al. 2019; Oza et al. 2017; R. L. Coleman et al. 2017; Abida et al. 2019). Additionally, another PARP inhibitor, veliparib, is currently under assessment in clinical trials either as a monotherapy or combined with radiotherapy and chemotherapy (Kummar et al. 2009; Baxter et al. 2020).

1.4.3.1 Mechanisms of PARP inhibitors

The specific mechanism of action for the anti-tumour activity of PARP inhibitors is still not fully understood as PARP1 -/- mice are viable, do not develop tumours and are fertile, suggesting that PARP inhibitor-induced cell death is highly tumour-specific (Conde et al. 2001). There are currently several proposed mechanisms of action. One such mechanism is the inhibition of SSB repair activity of PARP, leading to replication fork collapse and accumulation of DNA lesions. This was tested in cell lines where PARP inhibitors induced γ-H2AX and Rad51 foci, markers of DSB and HR respectively, although a reduction in cell viability was only observed in BRCA2 knockdown cells (Bryant et al. 2005). However, contradicting the SSB repair inhibition theory, PARP inhibitor treatment does not lead to an increase in SSBs and PARP1 knockdown alone was not sufficient to induce γ-H2AX foci, representing DNA damage (Gottipati et al. 2010). Additionally, the cytotoxic capability of olaparib was elevated in wild-type PARP1 cells, with higher γ-H2AX foci, compared to PARP1 knockout cells, where olaparib had little effect on cell viability or γ-H2AX foci count (Murai et al. 2012). Therefore, the anti-tumour activity of PARP inhibitors might be mediated via alternative mechanisms.

Another proposed, and more widely accepted, mechanism of action of PARP inhibitors is PARP trapping. The activity of PARP has been shown to be necessary for the MRE-11 mediated restart of stalled replication forks which can be cause by SSBs (Bryant et al. 2009). Such stalled replication forks collapse if not restarted and repaired via HR, leading to a DSB (**Figure 1.7**) (Liao et al. 2018). Additionally, tumours displaying defective fork stabilisation showed a sensitivity to PARP inhibitors similar to HR defective tumours (Liao et al. 2018). However, the higher cytotoxicity of PARP inhibitors compared to PARP knockout can be explained by the potential of these inhibitors to trap PARP on DNA complexes. When inhibited, PARP1 is unable to undergo auto-parylation in order to eventually dissociate from DNA complexes, which is necessary or the completion of

DNA repair and inhibitor binding to the NAD+ site allosterically enhances the affinity of the N-terminal zinc finder domain to DNA (Satoh and Lindahl 1992), showing an increase in stabilised, cytotoxic PARP1/2-DNA complexes (Murai et al. 2012). Replication forks collapse upon encountering PARP1/2 DNA complexes which are repaired by HR in normal cells and cannot be repaired by NHEJ. Repair of these collapsed forks does not occur in HR deficient tumour cells, leading to cytotoxic DSB accumulation (Zhu et al. 2018).

Different clinically approved PARP inhibitors can have varying PARP trapping capabilities which may explain the difference in potency of each drug. The size of each PARP inhibitor molecule correlates with PARP trapping ability, with larger molecules such as talazoparib showing greater levels of PARP1/2-DNA trapped complexes, due to the greater allosteric effect on the N-terminal DNA binding zinc finger domain (Murai, Huang, et al. 2014). Talazoparib is also the most potent of the clinically approved PARP inhibitors when tested on cell lines, showing sub-micromolar anti-tumour activity compared to rucaparib which induces cytotoxicity at micromolar concentrations, suggesting that the PARP trapping ability of this class of drug correlates with potency of anti-tumour action (Hopkins et al. 2019). However, the correlation of PARP trapping ability and potency does not translate into *in vivo* studies, nor clinical practice where talazoparib treatment resulted in 50% and 42% response rate in BRCA mutant breast and ovarian cancer respectively, while a 65% response rate was observed in BRCA mutant or recurrent ovarian cancer patients treated with veliparib, a PARP inhibitor with the least PARP trapping ability (Hopkins et al. 2019; Steffensen, Adimi, and Jakobsen 2017). Talazoparib does however show a higher toxicity towards normal cells and therefore has a lower maximum tolerated dose (Bruin et al. 2022)

PARP inhibitors are also hypothesised to assert anti-tumour effects via the upregulation of NHEJ in tumour cells with HR deficiency. It was shown that PARP inhibitor treatment increased the phosphorylation of DNA-PK substrates which are major components of the NHEJ pathway, stimulating NHEJ activity specifically in HR deficient cells. Inhibition of DNA-PK activity reversed the genomic instability of these cells caused by PARP inhibitor treatment and additionally, chemical or genetic perturbation of NHEJ pathway was able to reduce the sensitivity of BRCA1/2 or ATM deficient cell lines to PARP inhibitors (A. G. Patel, Sarkaria, and Kaufmann 2011). PARP1 directly interacts with Ku70/80 to inhibit NHEJ and both PARP1 and Ku80 compete for the binding of DNA DSB ends (M. Wang et al. 2006). Therefore, PARP1 inhibition can lead to overactivation of NHEJ in response to DNA damage, generating chromosomal breaks and radial chromosome structures due to joining of incorrect chromosomes (Bunting et al. 2010). However, conflicting with this

hypothesis, combination treatment with a DNA-PK inhibitor, AZD7648, and olaparib did not reduce the anti-tumour effect of PARP inhibition but instead showed synergistic effects in ATM knockout non-small cell lung cancer (NSCLC) cells and xenografts, increasing genomic instability (Fok et al. 2019) . Thus, NHEJ activation does not fully explain the action of PARP inhibitors for all tumour cells. It is possible that the mechanism of action of PARP inhibitors leading to cell cytotoxicity depends on the genetic background of the tumour cell and which DDR associated genes are altered.

1.4.3.2 Pre-clinical assessment of PARP inhibitors in STS

Pre-clinical reports have demonstrated that some LMS cells are sensitive to PARP inhibition, although these studies have been limited to a few LMS cell lines which does not capture the full range of genetic heterogeneity in this subtype. Within a panel of STS cell lines, sensitivity to the PARP inhibitor niraparib was observed in the fibrosarcoma cell line HT-1080 and a uterine LMS cell line SK-LMS-1 which demonstrated HR deficiency but does not harbour BRCA1/2 mutations, suggesting that sensitivity in STS is not limited to BRCA1/2 mutants (H. Li et al. 2020). Additionally, temozolomide, a DNA alkylating chemotherapeutic agent, was also shown to synergise the most with PARP inhibitor treatment in HT-1080 and SK-LMS-1 when used in combination in comparison to PARP inhibition combined with doxorubicin, isosfamide or dacarbazine (H. Li et al. 2020). In a separate study the BRCA2 mutant uterine LMS cell lines SK-UT-1 and SK-UT-1b were shown to be sensitive to the PARP inhibitor olaparib in a clonogenic assay, an effect which was amplified by pre-treatment with cisplatin (Chudasama et al. 2018). Combination of rucaparib at micromolar concentrations with the alkylating agent trabectedin at picomolar concentrations showed synergy in LPS cell lines, resulting in accumulation in G2/M cell cycle phase with enhanced γ-H2AX formation and apoptosis particularly in the DDLPS cell line IB 115 compared to either monotherapy, though this effect was not seen in LMS cell lines (Laroche et al. 2017). Additionally, DDLPS IB 115 xenografts also showed a synergistic action of rucaparib and trabectedin combinatorial treatment (Laroche et al. 2017).

The relationship between *PTEN* alterations and PARP inhibitor sensitivity was explored in a panel of human tumour cell lines, showing that PTEN loss without *BRCA1/2* alterations causes HR deficiency, represented by the reduction of Rad51 foci in irradiated cells compared to PTEN WT controls (Mendes-Pereira et al. 2009). PTEN reduction also correlated with hypersensitivity of cell lines to PARP inhibitor treatment both *in vitro* and *in vivo* xenografts although the cell line panel tested did not include STS (Mendes-

Pereira et al. 2009). However, due to the common detection of *PTEN* alterations across STS subtypes, particularly in LMS it is possible PARP inhibitor treatment may benefit *PTEN* mutant LMS tumours in addition to *BRCA1/2* mutants.

1.4.3.3 Clinical data of PARP inhibitors in LMS

Thus far, there have only been a handful of STS clinical trials investigating PARP inhibitor therapies. However, these have shown promising initial results in the context of advanced disease following failure of first-line chemotherapy treatment, particularly in uterine LMS, where current options show little benefit (Asano et al. 2022).

A case series of four uterine LMS patients harbouring BRCA2 loss of function mutations were assessed for response to PARP inhibitor treatment. These patients had received at least four lines of treatment prior to initiation of PARP inhibitor treatment which led to SD for at least 12 months in three patients and PR in one patient (Seligson et al. 2019). In another case series, five high-grade uterine LMS patients, three harbouring biallelic *BRCA2* inactivation and two harbouring a somatic or germline truncating *BRCA2* mutations accompanied with loss of heterozygosity were treated with the PARP inhibitors in various clinical trials or off label. All five patients demonstrated a response with radiographic regression, with duration of treatment ranging from six to 28 months. Additionally, one patient demonstrated a complete response and remained on treatment at the time of the time of the report (Hensley et al. 2020). Furthermore, a case report identified a somatic BRCA2 mutation in a patient with advanced metastatic uterine LMS, previously treated with gemcitabine and docetaxel as a first-line therapy. Treatment with olaparib demonstrated a complete response, remaining disease free for two years at the point of the report, highlighting that BRCA mutation status informed PARP inhibitor treatment can lead to durable responses in uterine LMS patients despite progression on previous chemotherapy regimens (Shammas et al. 2022).

Preliminary results from a phase Ib trial utilising olaparib and concomitant radiotherapy in locally advance or unresectable STS showed that this treatment regimen was well tolerated with 3/22 unconfirmed PR (14%) and 12/22 SD (55%) outcomes reported, although the subtype information of these patients was not given (Sargos et al. 2022). Another phase Ib study instead assessed the combination of Olaparib and trabectedin in patients with advanced LMS (30%) but also other STS and bone sarcoma subtypes, showing a response rate of 14% with manageable toxicity (Grignani et al. 2018). The authors also investigated biomarkers of response and found that high PARP1 expression of tumours correlated with improved outcomes (Grignani et al. 2018). A phase 2 study

treated advanced uterine LMS patient with olaparib and temozolomide, observing an objective response rate of 27% (6/22) which met the prespecified primary efficacy endpoint (Ingham et al. 2021). Additionally, the mPFS and duration of response (DOR) was 6.9 and 12 months respectively, showing durable responses. Haematological toxicity was common, with grade 3/4 neutropenia and thrombocytopenia seen in 77% and 32% of patients respectively, although this was managed with dose modification (Ingham et al. 2021). Currently correlative analysis is underway to identify markers of HR deficiency which could underlie durable responses, including Rad51 foci scoring and Schlafen Family Member 11 (SLFN11) expression analysis, which is a predictive biomarker of DDR targeting therapy response in small cell lung cancer, prostate and ovarian cancers (N. Coleman et al. 2020; Nogales et al. 2015; Conteduca et al. 2020) (NCT03880019).

Multiple other trials utilising PARP inhibitors in are ongoing or recruiting based on these encouraging pre-clinical and initial clinical findings, including a phase 2/3 trial which has recently been approved to assess the efficacy of olaparib and temozolomide combination treatment in unresectable or advanced uterine LMS following progression on chemotherapy. This trial will compare the efficacy of this combination to standard of care second-line therapies for LMS including pazopanib and trabectedin (NCT05432791). Additionally a phase 2 trial has also recently been approved to assess niraparib monotherapy in advanced or metastatic LMS (NCT05174455) which, if shown to be efficacious, will be a much needed addition to the first-line treatment regimen of LMS and may provide an alternative to first line treatments which show a high degree of toxicity such as doxorubicin (L. Zhao and Zhang 2017)

1.5 Preclinical models for sarcoma research

The advancement of molecular profiling techniques has revealed distinct molecular subsets of STS tumours within individual histological subtypes that may benefit from targeted therapies. However, the standard of care treatment remains cytotoxic therapies and has seen few novel treatment options approved in the past decade despite the limitations of cytotoxicity and modest response rates (Grünewald et al. 2020). Investigation into novel treatment strategies is urgently needed to improve STS patient outcomes, although due to the rarity of such cancers, recruitment for innovative clinical trials is challenging and often underpowered, potentially not encapsulating the wide molecular heterogeneity of subtypes such as LMS which is particularly important when considering targeted therapies (Yuan, Li, and Yu 2021). Pre-clinical modelling is therefore vital for the assessment of novel treatment options in rarer cancers in order to guide clinical trial design. Several different types of pre-clinical models are routinely used in cancer research, including LMS, such as patient derived xenografts (PDXs), patient-derived *in vitro* monolayer cultures and organoids and immortalised cell lines. Each of these pre-clinical models have their own advantages and disadvantages.

Pre-clinical model	Advantages	Disadvantages
In vitro cultures	Low cost	Not always biologically relevant
	Ease of handling	Induced changes in gene expression
	Highly reproducible	Sub clonal selection pressure
	Amenable for high throughput screening	Low establishment rate
	Short experiment timescales	
In vivo xenografts	Mimics tumour growth kinetics	High cost
	Mimics pharmacokinetics of human tumours	Labour intensive
	Retains tumour heterogeneity and histology	Long experiment timescales
	Higher establishment rate	Not amenable for high throughput screening
	Can model tumour microenvironment	Variable tumour sizes and growth

Table 1.3. Summary of advantages and disadvantages of *in vitro* and *in vivo* xenograft models for pre-clinical modelling.

1.5.1 Current cell lines in STS research

In comparison to other cancer types there is a severe lack of STS cell lines readily available for research. In a review of the status of human sarcoma cell lines, 819 WHO classified cell lines classed under connective and soft-tissue neoplasms were identified in the Cellosaurus database and spanned 45 subtypes (Bairoch 2018). Given that the current WHO classification lists over 150 distinct histopathological subtypes, the number of subtypes represented in pre-clinical research is therefore lacking. In addition, multiple cell lines are only available for 36 histopathological subtypes and are most commonly established from Ewing's sarcoma, (156 cell lines), osteosarcoma (148 cell lines) and UPS (43 cell lines) (Hattori, Oyama, and Kondo 2019).

Furthermore, among the 819 cell lines identified in the 2019 review only 139 were available from public cell banks. In public cell banks there are only seven cell lines representing LMS (SK-UT-1, SK-UT-1b, SK-LMS-1, TYLMS-1, SKN, RKN, HS5.T) which does not fully capture the intra-subtype and intra-tumour heterogeneity observed in these cancers (Hattori, Oyama, and Kondo 2019). For example, the widely used LMS cell lines SK-UT-1 and SK-UT-1b were both established in 1972 from a patient with grade III uterine LMS and show stark differences in morphology, tumour suppressor aberrations and *in vivo* histology (Fogh, Fogh, and Orfeo 1977; Ganiatsas et al. 2001; T. R. Chen 1988). Only using the limited publicly available models for pre-clinical drug assessment might therefore fail to represent subsets of patients who might respond to certain molecular guided therapies or conversely miss tumour populations which might be more resistant to such therapies.

1.5.2 Established cell lines versus primary *in vitro* models

Established 2D cell cultures remain the most common *in vitro* model for cancer therapeutic drug screening and pre-clinical research due to low costs, ease of use and reproducibility. However, forcing cancer cells to grow in 2D for an extended period of time induces cytoskeletal rearrangement and leads to altered gene expression whilst exerting a clonal selection pressure (Kenny et al. 2007). These phenotypic differences can alter therapeutic response and often results in a poor correlation between cell lines and *in vivo* tumours (Cree, Glaysher, and Harvey 2010). Furthermore, most commercially available cell lines have undergone spontaneous genetic alterations to enable indefinite culture and have acquired genetic changes over years of continuous culture, thereby posing questions as to the relevance of these cells in accurate modelling of disease. For example, transcriptomic analysis of LMS cell lines frequently used in pre-clinical research, such as SK-UT-1 and SK-UT-1b has shown that these no longer resemble

expression profiles from LMS tumours, both in terms of global transcriptome or LMS specific transcriptional programs (Hemming et al. 2020).

To address these issues, primary cell line cultures can be generated which more closely resemble the genomic and phenotypic profiles of parent tumours from which they were derived and can capture disease heterogeneity (Salawu et al. 2016). An analysis of chondrosarcoma patient derived cells grown over 30 passages *in vitro* showed that these lower passage cell lines acquired some initial mutations upon *in vitro* growth but retained the most relevant mutations present in respective patient tumours (Rey et al. 2019). Although, it is important to note that even primary patient-derived cells grown in 2D will induce phenotypic and genetic changes in long-term cultures (Kato et al. 2008) and therefore, low passage *in vitro* cultures should be primarily used in order to maintain clinical relevance. However, the establishment of sarcoma primary culture panels is challenging due the rarity of this disease and additionally several studies have reported widely varying success rates.

The difficulty in generating sarcoma cell lines from tumour samples was described in 1985 whereby cell expansion from direct monolayer cultures was only successful in one out of eight samples (12.5%) (Bruland, Fodstad, and Pihl 1985). By plating these samples instead as single cell suspensions, allowing for aggregation, spheroids were established in eight out of 17 samples (47%) which then were able to grow long term in monolayer format, also retaining tumourigenicity shown by the formation of tumours *in vivo* (Bruland, Fodstad, and Pihl 1985).

Low passage (<10 passages) STS cell lines were established from mechanical and enzymatically dissociated surgical resections in a 2002 study, of which two were derived from primary tumour resections and nine were derived from metastatic resections (M. Hu et al. 2002). It was shown that six out of 11 cultures readily formed tumours *in vivo,* all of which were derived from metastatic samples and a further five formed spontaneous lung metastases, indicating the maintenance of metastatic potential (M. Hu et al. 2002).

Another study reported the establishment and characterisation of seven self-immortalised STS cell lines directly from patient resections with a range of subtypes such as LMS, UPS, DDLPS and myxofibrosarcoma (Salawu et al. 2016). Resections included metastases, recurrent tumours and tumours which had received neoadjuvant radiotherapy or chemotherapy. In total 47 resections were mechanically dissociated and cultured on plastic as monolayers. Out of 47, 14 failed to grow, giving an initial success rate of 70.2%. Of the established primary cultures, ten showed early onset senescence, nine with senescence around passage five and seven cultures showed senescence

around passage 10. The remaining seven cultures continued to expand and produce long-term immortalised cultures, able to proliferate for over 60 passages or at least three years in culture. It is possible that around passages five and ten, *in vitro* cell cultures experience a senescent selection pressure whereby only some tumour cells are able to overcome this crisis period and continue to divide. Interestingly, five of the seven long term cell cultures were established from grade III tumours and two from grade II tumours, suggesting that primary cultures might select for higher grade aggressive tumour types. However, long term cultures were established from both cases where tumours were treated neoadjuvant chemotherapy where a reduction in tumour quality was expected (Salawu et al. 2016). Furthermore, two morphologically distinct clones were established from the same LMS and myxofibrosarcoma resection samples via differential attachment under the same growth conditions, demonstrating the cellular heterogeneity of such tumours and how in this case selection of certain clones can occur due to handling i.e., attachment times and stochastic presence of different clones in the cultured flask, rather than selection based on cell fitness. Viability of clones should therefore be closely monitored during the establishment of cultures in order to retain all viable cell types. While primary LMS cells maintained a high similarity of copy number variations compared to the patient sample, one high passage (over passage 40) line began to show a loss of heterozygosity in STR profiling loci and some changes in copy number variations were noted in the established cell cultures compared to the tumour of origin (Salawu et al. 2016). Due to the high genomic instability of tumours such as LMS is it expected that continuous culture will introduce genetic drift therefore genomic comparison over time in patient-derived models is necessary to confirm disease relevance (Seligson et al. 2022; Anderson et al. 2021; Chudasama et al. 2018).

Recently, a biobank of primary RMS cells was established from PDX models, showing preserved phenotypic and molecular characteristics when compared to the respective PDX model and patient biopsies. Some focal differences were observed in DNA copy number between certain PDXs and respective cell cultures which was more prominent in clones expanded in Dulbecco's Modified Eagle Medium (DMEM) media. All somatic mutations from the PDX models were represented in each PDX cell culture covering the mutational spectrum observed in RMS. Additionally, similar or slight variations in methylation profiles were found between the PDXs and cell cultures whereas RMS commercially available cell lines showed far higher DNA methylation levels at multiple sites compared to the primary cultures (Manzella et al. 2020).

1.5.3 Modelling sarcoma in 3D

While primary monolayer cultures can recapitulate STS genetics and aspects of tumour phenotype, they are not suited to model microenvironmental cues including cell-cell and ECM interactions. 3D cultures such as spheroids or organoids, are therefore an attractive model for cancer research as they have been previously shown to closely mimic *in vivo* gene expression, growth kinetics, nutrient gradients and ECM production for a variety of cancer types (**Table 1.4**) (Nunes et al. 2019). However, compared to monolayer culture, 3D cultures are more laborious to generate, maintain and analyse, and on top of this spheroid or organoid sizes can vary within and between assays, reducing reproducibility (**Table 1.4**) (Adjei and Blanka 2015).

Culture format	Advantages	Disadvantages
2D	Cost effective	Reduced cell-cell interactions
	Ease of handling	Reduced cell-ECM interactions
	Highly reproducible	Induces altered gene expression
	Standardised assays	High clonal selection pressure
3D	Can model cell-cell interactions	High cost
	Can model cell-ECM interactions	Difficult to establish and maintain
	Mimics gene expression profile of tumours	Size variability reduces reproducibility
	Mimics nutrient gradients and hypoxia	Endpoint assays vary depending on culture technique
	Mimics drug penetration gradients	
	Lower clonal selection pressure	

Table 1.4. Overview of advantages and disadvantages of 2D and 3D *in vitro* culture format for cancer research. ECM; extracellular matrix.

Spheroids can be formed via the culture of cells in suspension using a non-adherent surface, leading to spontaneous aggregation where cell-cell or cell-ECM interactions predominate instead of cell-surface adherence (Kunz-Schughart, Kreutz, and Knuechel 1998). In 2009, three commercially available human sarcoma cell lines representing osteosarcoma (MG63), Ewing's sarcoma (HTB116) and fibrosarcoma (HT1080) were shown to readily form spheroids in suspension culture and had an elevated expression of stem cell associated genes such as *Nanog,* octamer-binding transcription factor 3/4 (*OCT3/4)* and *SOX2* compared to monolayer culture. When exposed to doxorubicin or cisplatin, spheroid cultured lines displayed a higher cell viability than monolayer cells (H.

Fujii et al. 2009). Another study analysed the effect of 3D culture of the fibrosarcoma line HT1080, SW872 (fibrosarcoma cell line) and RD (RMS cell line), showing that the expression of ECM genes was significantly upregulated compared to the respective monolayer cultures while a PDX derived cell line, HOSS1 (osteosarcoma cell line), also displayed an increased expression of gap junctions. The 3D cultured cell lines showed an increased chemo resistant phenotype, with lower early apoptosis events detected in doxorubicin, gemcitabine and docetaxel treated 3D cells compared to monolayer. This chemoresistance was hypothesised to be due to the increase in gap junction expression in addition to the mechanical barrier produced by upregulated ECM production (C. Bai et al. 2015).

The phenotypic changes induced by direct establishment of 2D primary cultures from tissue samples can be lessened with the use of primary 3D cultures (Imamura et al. 2015). Salerno and co-workers generated a panel of primary STS and bone sarcoma spheroids from biopsy samples via mechanical and enzymatic digestion followed by non-adherent, basic fibroblast growth factor (bFGF) and EGF supplemented culture. Mechanical dissociation of spheroids was used in order to expand cultures. Using this method, primary spheroid cultures were established in only five out of 49 biopsy samples (10.2%). This low success rate compared to other studies establishing sarcoma primary cultures could potentially be due to the deliberate lack of serum in culture media and also because biopsy rather than resection samples were used as a source of primary cells (Salerno et al. 2013). Cell viability, density and overall tissue quality can vary quite drastically from core needle biopsies (Ferry-Galow et al. 2018), although a subtype specific success rate of 50% (1 out of 2) was noted for Ewing's sarcoma and RMS compared to osteosarcoma, chondrosarcoma, LPS and unclassified sarcoma (9, 11, 6, and 0% respectively), suggesting that tumour subtype might also be a major factor in the success rate of spheroid establishment (Salerno et al. 2013). Monolayer cultures were also established in parallel to spheroids from the Ewing's sarcoma and RMS biopsy samples and it was shown that stem cell markers including OCT3/4, Nanog and SOX2 were elevated in spheroids compared to the respective monolayer cultures. The established spheroid cultures also maintained tumourigenicity *in vivo,* producing tumours with a histology comparable to the patient sample and matching subtype specific biomarker expression. Furthermore, the sarcoma spheroids increased in cell number and size during hypoxic induction, a condition frequently observed in the sarcoma microenvironment (Salerno et al. 2013). However RMS PDX cells, when cultured in 3D, showed no significant differences in drug response profiles when compared to 2D monolayer cultures, suggesting that in some models, format of culture does not impact

drug responses and the impact of 3D vs 2D culture on drug action might depend on subtype and tumour grade (Manzella et al. 2020).

In the body, tumours are surrounded by a complex microenvironment including the ECM, which has been shown in several cancer types including sarcoma to have profound effects on tumour growth, invasion and metastasis (Pickup, Mouw, and Weaver 2014). In order to model this *in vitro* and mimic tissue architecture, 3D cultures can be suspended in synthetic hydrogels containing common ECM components such as collagen, laminin and fibronectin or alternatively cultures can be suspended in naturally produced hydrogels such as matrigel which is produced by murine Engelbreth-Holm-Swarm (EHS) sarcoma tumours (Duval et al. 2017; Kleinman and Martin 2005). Matrigel can support cell survival and growth of cancer cells while preventing differentiation, although the composition of matrigel and therefore the mechanistic effect on cell cultures is poorly defined (Hughes, Postovit, and Lajoie 2010). While the ECM components of several cancer types have been well studied, allowing for the creation of cancer specific hydrogels with a defined, reproducible composition, in STS the ECM is poorly characterised and therefore the majority of hydrogel-based 3D sarcoma cultures rely on the use of matrigel and other biologically produced hydrogels (LeSavage et al. 2022).

Adult organoid cultures can be generated by the suspension of dissociated tissue in a hydrogel, surrounded by organ specific media that promotes stem cell self-renewal, allowing organoid cultures to be expanded and maintained almost indefinitely whilst reproducing complex *in vivo* tissue architecture due to the maintenance of cancer stem cell populations (Sachs et al. 2018). Cancer organoids can be defined as '3D self-organised assemblies of neoplastic cells derived from patient-specific tissue samples that mimic key histopathological, genetic and phenotypic features of the parent tumour' although a standardised definition has yet to be established (LeSavage et al. 2022). Patient-derived cancer organoids have become widely used pre-clinical models for carcinoma cancer types such as breast, colorectal, pancreatic, ovarian and lung cancer, as they have shown to be able to recapitulate the tumour architecture, sub clonal populations and niche-specific paracrine and autocrine signalling factors (Drost and Clevers 2018; LeSavage et al. 2022).

The success rate of organoid establishment for epithelial malignancies is often reported at around 60-80% (Tiriac et al. 2018; Kopper et al. 2019; Neal et al. 2018; Schütte et al. 2017; Sachs et al. 2018). This improves vastly from the establishment rate of conventional epithelial cancer cell lines (~ 20-30%), suggesting less strain is placed on

the dissociated tumour cells in an organoid format and the selection pressure for certain subclones is not as high (Kodack et al. 2017).

Molecular profiling of patient derived colorectal cancer organoids and PDXs (established both with a ~60% success rate) involving whole genome sequencing (WGS), whole exome sequencing (WES) and RNA sequencing (RNAseq) revealed a high similarity between patient-matched PDXs and organoid cultures, and furthermore showed a high concordance of drug response, indicating that organoid models are able to reflect *in vivo* drug response phenotypes but with the addition of high-throughput drug screening capabilities (Schütte et al. 2017). A similar study was also conducted on a panel of breast cancer organoids, where a success rate of >80% was reported from primary or metastatic tissues. This organoid panel recapitulated the molecular heterogeneity observed in the clinic and also showed consistent drug response profiles compared to *in vivo* xenografts as well as patient response (Sachs et al. 2018).

Organoid cultures can also be used for the *in vivo* growth of adult multi-cellular normal tissue with maintained histology in order to assess, in parallel, the effects that certain therapies might have on tumour cells vs surrounding non-transformed tissue, thus predicting potential toxicity of novel therapies (Driehuis, Kretzschmar, and Clevers 2020).

Patient-derived organoid culture represents an attractive model for drug screening and to elucidate mechanisms of therapy response in STS due to the potential to capture the extreme inter and intra-tumour heterogeneity. However, progress in this field has lagged quite substantially behind carcinoma organoid modelling and studies utilising STS patient-derived, hydrogel-based, organoid cultures in sarcoma research have only recently been reported (Meister et al. 2022; Gaebler et al. 2019; Al Shihabi et al. 2022; Loskutov et al. 2021). The translation of epithelial cancer organoid protocols and techniques to sarcoma has faced several challenges. Firstly, the cell of origin for carcinomas are often clearly defined, meaning that the culture media requirements can be shared or at least based on the requirements for the growth of respective epithelial cell types and stem cell niche, which have been well documented (M. Fujii and Sato 2020; Sato et al. 2009). For example, the majority of epithelial normal and cancer organoids are cultured with R-spondin which supports epithelial stem cell homeostasis and self-renewal by potentiating the wingless-related integration site (Wnt) pathway (Clevers 2016). In the context of sarcomas, the cell of origin is often not clear and, where known, the factors essential for connective or soft-tissue specific tissue niches are poorly defined. Secondly the tissue availability of sarcoma is considerably lower than that of

carcinomas due to disease rarity. On top of this, protocols for the collection, processing and banking of sarcoma tissue is not standardised and often only available for direct culture from sarcoma specialist centres, limiting the amount of research institutes which are able to work with fresh sarcoma samples.

Despite these limitations, Meister and co-workers have recently established and characterised a panel of rhabdomyosarcoma organoid models (one of the first patient-derived organoid panels described for sarcomas) reporting a success rate of 41%. These models were established from biopsy samples from both alveolar and embryonal rhabdomyosarcoma subgroups as well as different molecular subgroups with a range of fusions and fusion negative tumours (Meister et al. 2022). Organoid establishment was achieved through the culture of mechanically dissociated biopsies in Basement Membrane Extract (BME) hydrogels surrounded with media supplemented with growth factors including EGF, bFGF and IGF as well as the Rho associated protein kinase (ROCK) inhibitor Y-27632 and TFG-β inhibitor A83-01. Success rate of establishment was found to be higher in the more aggressive fusion positive rhabdomyosarcoma samples compared to fusion negative tumours (83 and 16% respectively) and additionally relapsed tumours showed a higher rate of establishment compared to primary tumours (61 and 30% respectively), suggesting that future panels of patient-derived sarcoma organoids might be enriched for particularly aggressive subtypes and advanced disease (Meister et al. 2022). The rhabdomyosarcoma organoids recapitulated the histology of the patient tumours as well as IHC markers while maintaining the molecular and genetic characteristics of the patient tumours, observed through copy number variation analysis and RNAseq. In addition, through single cell RNAseq, the authors showed that rhabdomyosarcoma organoids retain intra-tumoural genetic and molecular heterogeneity, with several subclones displaying differing expression of rhabdomyosarcoma classical biomarkers. Furthermore, genetic stability for up to six months of continuous culture was reported and drug screening revealed a similar distribution of response phenotypes as observed in the clinic (Meister et al. 2022).

1.5.4 Patient-derived models for adaptive personalised medicine

Generating novel patient-derived pre-clinical models of STS not only expands the currently limited arsenal of STS cell lines available for fundamental and translational research but can be a powerful tool for personalised medicine. *In vitro* analysis of tumour cells response provides an insight into how the patient will respond to certain therapies and treatment can be adjusted accordingly (Kodack et al. 2017).

For STS patients, personalised medicine is especially important in order to move away from the 'one size fits all' paradigm of treatment regimens due to the heterogeneity of these malignancies. The generation of primary cell cultures for high-throughput drug response analysis was shown to be feasible from resected tumours directly from rhabdomyosarcoma patients, allowing for the comparison of drug response profiles in the same patient from different metastases at different timepoints (Manzella et al. 2020).

The main technical issue, however, facing the development of precision medicine into clinical practice is the timescale from receiving tissue to establishing models amenable for drug response profiling and limited size or low quality tissue samples. The generation of rhabdomyosarcoma patient-derived organoids from patient biopsies was reported to take 27-42 days and were eligible for drug screening as early as 27 days after acquiring tumour samples, although the median time from sample acquisition to drug screening was 81 days, showing that fast assessment of patient-specific drug responses is feasible but the timescale from receiving tissue to generating response data can vary from patient to patient (Meister et al. 2022). In another study, success rate of culturing patient-derived SS monolayer cells *in vitro* directly from biopsies was noted as 58%, where several healthy, mesenchymal tissue-derived cells were also cultured in parallel (Brodin et al. 2019). These patient-derived models demonstrated drug sensitivities or resistances which correlated with the patient response to such therapies and highlighted drug sensitivities specific to tumour cells with minimal impact on the cell cultures derived from normal non-tumour tissue (Brodin et al. 2019). This study shows that culture establishment and drug response profiling is possible from STS biopsy tissue instead of resection tissue which is especially beneficial for precision medicine as it would potentially allow for the generation of a patient matched model from an early biopsy, although the successful growth of each model was dependant on the size and quality of the biopsy (e.g. cell density and viability). Additionally, proliferating cultures were established within a timescale of 2 days to 18 weeks (Brodin et al. 2019). Optimising the establishment of patient-derived models for fast, high-throughput drug screening could lead to informed primary treatment regimens based off *in vitro* data and/or informed adjuvant therapy upon surgical resection.

1.5.5 Patient-derived xenografts in LMS research

Currently, the gold-standard method for accurate pre-clinical modelling of solid cancers is patient-derived xenografts (PDXs), whereby patient tumour tissue is transplanted into immunocompromised mice, usually subcutaneously. The benefit of PDX use is the

heterogeneity that can be observed between models, with each representing an individual patient. Additionally PDX tumours retain the histology, biomarker expression, morphology and growth kinetics of the patient tumour and allows for the study of pharmacodynamics of drug treatment (Risbridger, Lawrence, and Taylor 2020). PDX modelling of cancer is limited by long establishment and growth times, cost, difficulty in handling and often less than optimal reproducibility especially in regard to low passage PDXs. (Risbridger, Lawrence, and Taylor 2020)

Recently, Hemming and co-workers established a panel of 17 subcutaneous leiomyosarcoma PDX models from surgical resection tissue, noting a success rate of 35% for engraftment and propagation for at least three passages. The study reported a higher success rate in high grade tumour samples compared to low or intermediate grade samples (42 and 22% respectively) and a higher percentage of the established PDXs were from uterine LMS patients (65%). Where possible engraftments that previously failed to propagate were repeated with successive resection tissue but also failed to establish PDX models, reducing the likelihood that failure of establishment was due to handling and suggesting that some LMS tumours are not compatible with PDX establishment due to poor tissue quality. Additionally, engraftment of tumours that were exposed to pre-operative radiotherapy were not successful which could potentially be explained by radiotherapy induced necrosis, leading to non-viable tumour tissue. Early (passage 0) and later (up to passage 17) *in vivo* passages retained the histology of the parent tumours including aspects such as cytomorphology, cellularity and abundance of mitotic bodies as well as LMS biomarker staining such as α-SMA or desmin in addition to maintenance of genome wide copy number alterations (Hemming et al. 2022).

The panel of LMS PDX models displayed a range of alterations in tumour suppressor genes frequently observed in LMS tumours such as *TP53, RB1* and *PTEN*. Via transcriptomic analysis, the panel of LMS PDX models were shown to retain the transcriptional programme of the parental tumour and even represent the three molecular classifications of LMS tumours, cLMS, iLMS and uLMS previously identified (Hemming et al. 2020). cLMS clustered PDX models had high expression of synemin (*SYNM)* and adipogenesis Regulatory Factor (*ADIRF),* while iLMS associated or uLMS PDX models were enriched for *PDGFRA* and Decorin (*DCN)* or estrogen receptor 1 (*ESR1)* and chordin like 2 (*CHRDL2)* respectively. While elevated expression of IGF1R is observed in a subset of cLMS tumours, treatment of a LMS PDXs with high IGF1R expression with the IGF1R inhibitors, linsitinib or berzosertib, failed to perturb tumour growth, highlighting the importance of functional assessment of therapeutic activity following pre-clinical target identification (Hemming et al. 2020; 2022). In order to test anti-tumour activity for

a range of therapies, LMS PDX models have been utilised in ex vivo drug screening, with one study able to test 35 compounds in order to ultimately identify transcriptional Cyclin-Dependent Kinases (CDK) inhibitors as therapeutically active and comparable to doxorubicin activity (Hemming et al. 2022).

A recent ongoing study aimed to generate a panel of STS PDX models (XenoSarc) and has so far reported a subcutaneous PDX establishment rate of 32% in total, spanning a total of 33 subtypes, in addition to undifferentiated sarcomas 'not otherwise specified'. Tissue was acquired from surgical excisions as well as biopsies, with surgical tissue showing a slightly higher but not statistically significant rate of PDX establishment (34% compared to 22%). Metastatic samples showed a higher rate of establishment compared to non-metastatic samples (40% vs 27%) but was not found to be significant and histological subtype had no impact on rate of establishment, although LMS tumours showed a success rate of 41%. Patients whose tumour was successfully established as a PDX had a significantly shorter OS compared to those whose tumour did not engraft successfully, showing a median OS of 77 months compared to 259 months. The study found that the established PDX models retained histological, copy number and gene expression features of the corresponding tumour samples and was maintained over repeat passages (up to passage 35) (Cornillie et al. 2019).

1.6 Hypothesis and aims

The mechanisms of drug response in STS remains poorly understood and the lack of models which closely represent patient tumours restricts our ability to develop effective treatment strategies for advanced sarcoma that can be translated into clinical benefit.

The hypothesis of this project is that patient tumours respond to chemotherapy or molecular targeted therapy via different mechanisms to that observed in established cell lines, and patient-derived models can more accurately model tumour responses. This hypothesis will be addressed via three main aims:

Aim 1: Derive and characterise novel LMS models. Establish a patient-derived model pipeline which I seek to implement in order to generate and characterise a panel of LMS PDXs and PDX-derived *in vitro* 2D and 3D cultures.

Aim 2: Define chemosensitivity in LMS models and signalling alterations associated with chemoresistance. Assess the sensitivity of PDX-derived LMS cells to standard of care chemotherapies and investigate cell-intrinsic signalling alterations associated with chemoresistance.

Aim 3: Identify candidate molecular targeted therapies for LMS. Conduct small molecule drug screening on LMS models to identify shared and patient-specific signalling pathway dependencies.

By achieving these aims, I seek to address the gap in the current knowledge of chemotherapy or targeted therapy response in LMS and add to the current limited arsenal of STS patient-derived models which will inform future clinical trials utilising novel candidate therapies.

Chapter 2 - Methods

2.1 In vivo techniques

2.1.1 Tissue collection and PDX establishment

Xenografts were generated from percutaneous needle biopsies from patients at the Royal Marsden Hospital. Biopsies were placed in Dulbecco's modified Eagle medium (DMEM) with 10 µM Y-27632 (LC Laboratories) immediately after collection prior to PDX establishment (within 24 hours). If immediate implantation was not possible, biopsies were frozen in DMEM with 10% dimethyl sulfoxide (DMSO) (Sigma Aldrich), 10% foetal bovine serum (FBS) (Gibco) and 10 µM Y-27632. PDX models were established by subcutaneous implantation of biopsy tissue into the flank of NOD scid gamma (NSG) immunocompromised mice. J000104314, TM01244, TM00199 and TM00219 PDX were purchased from Jackson Laboratory and passaged to NSG mice at the ICR to continue growth. Xenograft models were passaged, sacrificed and tumour samples harvested by Dr Amanda Swain and Dr Jian Ning. Tumour growth was monitored twice weekly with calipers and tumour volume was calculated with the following formula: (($width^2$ x length) / 2). Xenograft tumours were grown no larger than 1000 mm^3 and once harvested, tumour tissue was stored via snap freezing and slow freezing in DMEM with 10% DMSO (Sigma Aldrich), 10% FBS (Gibco) and 10 µM Y-27632. Where possible, tumours were also fixed in 10% formalin (Sigma Aldrich) and embedded in paraffin to generate formalin fixed paraffin embedded (FFPE) blocks.

2.1.2 PDX tissue dissociation

To dissociate single cells, tumour tissues were minced and digested in dissociation media (DMEM/Ham's F12 1:1 + 15 mM 4-(2-hydroxyethyl)-1-piperazineethanesulfonic acid (HEPES), 0.5 mg/mL collagenase (Sigma Aldrich), 0.1 mg/mL DNase I (Sigma Aldrich), 10 ng/mL epidermal growth factor (EGF) (Peprotech), 0.1x insulin-transferrin-selenium A (Gibco), 10 µg/mL hydrocortisone (Sigma Aldrich), 10 µM Y-27632, 0.1 mg/mL hyaluronidase (Sigma Aldrich), 5% FBS, and 0.5% penicillin/streptomycin) at 37 ⁰C for 2 hours on a rotor at 100 rpm. The dissociated tissue was centrifuged at 1400 rpm for 5 minutes and then washed in phosphate buffered saline (PBS) supplemented with 10 µM Y-27632. Red blood cells (RBCs) were lysed with RBC lysis buffer (Invitrogen) for 1 minute, after which remaining cells were washed with PBS supplemented with 10 µM Y-27632, centrifuged at 1400 rpm for 5 minutes and incubated in 0.05% trypsin-ethylenediamine tetraacetic acid (EDTA) (Gibco) with 10 µM Y-27632 at 37 ⁰C for 8

minutes. Cells were then incubated in a 1:1 mix of DNAse solution (1 mg/mL DNase I and 10 µM Y-27632 in PBS) and Y-media (DMEM:Ham's F12 1:1 + 15 mM HEPES, 1% L-glutamine, 5 µg/mL insulin (Sigma Aldrich), 0.4 µg/mL hydrocortisone, 10 ng/mL EGF, 250 ng/mL amphotericin (ThermoFisher Scientific), 9.62 ng/mL cholera toxin (Sigma Aldrich), 5 µM Y-27632, 10% FBS, and 0.5% penicillin/streptomycin). Cell suspensions were pelleted by centrifuging at 1400 rpm for 5 minutes then washed in PBS with 10 µM Y-27632 followed by resuspension in Y-media. Cells were then passed through a 70 µm strainer, counted and either cryopreserved in 10% DMSO in FBS and 10 µM Y-27632 or mouse cell depleted.

Mouse cell depletion was achieved by suspending cell pellets in 1x magnetic-activated cell sorting (MACS) buffer, diluted in PBS from a stock solution (20x MACS buffer; 5 g bovine serum albumin (BSA) (Sigma Aldrich), 4 mL 0.5 M EDTA (Sigma Aldrich) in 50 mL PBS), supplemented with 10 µM Y-27632. Mouse cells were labelled in MACS buffer by adding magnetic microbead conjugated antibodies via a Mouse Cell Depletion Kit (Miltenyi Biotec 130-104-694) according to manufacturer's instructions. The cell solution was incubated on ice for 15 minutes after which the solution was passed through a Quadro MACS magnet LS column (Miltenyi Biotec). The column was washed twice with 1x MACS buffer and the column was then discarded. The resulting flow through contained human enriched cells and were pelleted then resuspended in Y-media for cell counting and subsequent cell culture.

2.2 Histology

2.2.1 FFPE embedding and H&E stains

PDX tissues were fixed in 10% neutral buffered formalin (Sigma Aldrich) for 24 hours before storing in PBS at 4 °C for no longer than one week. To fix organoid cultures, Cultrex harvesting solution (R & D Systems) was first added to matrigel domes and plates were incubated at 4 °C for 1 hour. Released organoids were collected, spun at 300 xg for 5 minutes then washed with PBS. Pelleted organoids were resuspended in 10% formalin for 60 minutes at room temperature before formalin was removed and organoids were washed three times. Fixed organoids were then suspended in molten X12 HistoGel specimen processing gel (Thermo Fisher Scientific) and heated at 65 °C for 5 minutes. Organoid-histogel suspensions were then incubated on ice for 10 minutes and once set, was layered with PBS and stored at 4 °C for no longer than one week.

Fixed PDX tissues or histogel embedded organoids were embedded in paraffin by the ICR histopathology core facility to generate FFPE blocks.

Hematoxylin and eosin (H&E) stains were generated by slicing 4 μm sections from FFPE blocks onto charged slides. Sections were stained with haematoxylin and eosin followed by mounting with coverslips by the ICR hisopathology core facility. H&E slides were digitally scanned using Hamamatsu Nanozoomer-XR slide scanner and digital scans were analysed via Hamamatsu Nanozoomer software.

2.2.2 IHC staining

Unstained FFPE sections of 4 μm thickness were cut via a microtome onto charged slides. Slides were heated at 60 °C for 15 minutes and then left to cool briefly at room temperature before placing in xylene (Sigma Aldrich) twice each for 10 minutes. The slides were then placed into decreasing concentrations of ethanol (Sigma Aldrich); 100%, 96% and 80% each for 5 minutes and were then placed in water for 5 minutes. Antigen retrieval was conducted by boiling slides in 1x sodium citrate buffer with 0.05% Tween 20 (Sigma Aldrich) for 5 minutes followed by cooling at room temperature. Tissue sections were placed in 1x tris-buffered saline (TBS) for 5 minutes, then twice in 1x TBS with 0.025% Tween 20 (TBST) for 5 minutes at room temperature. Using a hydrophobic marker, a barrier was drawn around tissues allowing for the addition of blocking buffer: 3% BSA (Sigma Aldrich) in TBST to tissue samples. Samples were left in blocking buffer for 90 minutes before primary antibody was added diluted in blocking buffer and left at 4 °C overnight in a humidified chamber. Primary and secondary antibody used are described in **Table 2.1**. Primary antibody concentration was chosen after titrating 1:50, 1:100, 1:500 concentrations. IHC staining for Ki-67, carbonic anhydrase IX and cleaved caspase 3 were conducted by the ICR histopathology core facility along with positive control tissues for each antibody, where concentration parameters were already established.

Antibody	Dilution	Supplier
Primary antibodies		
Anti-Actin, α-Smooth Muscle antibody 1A4 (Mouse)	1:100	Sigma Aldrich (#A5228)
Secondary antibodies		
Anti-Mouse HRP linked antibody	1:100	SignalChem (#G32-62G-1000)

Table 2.1 Table of antibodies used for IHC staining. HRP; horseradish-perosidase.

Primary antibodies were removed from the tissue sections and slides were then washed in TBS, and twice in TBST for 5 minutes each. DAKO Peroxidase blocking solution (Agilent) was added to each slide and incubated for 60 minutes at room temperature before slides were washed in TBS, and twice in TBST for 5 minutes each. Horseradish peroxidase (HRP)-conjugated secondary antibodies were then added to tissue sections diluted 1:100 in blocking buffer and slides were incubated at room temperature for 60 minutes in a humidified chamber. Secondary antibodies were then removed from slides before washing in TBS, and twice in TBS. Dako 3,3′-Diaminobenzidine (DAB) substrate chromogen system (Agilent) stain was applied to tissue sections for a length of time optimised from the staining of positive tissue controls. Slides were then counterstained with haematoxylin solution (Abcam) for 20 seconds before washing under running water and dehydrating with 3 minutes in water followed by 3 minutes each in 80%, 96% and 100% ethanol. Dehydrated slides were then placed in xylene for 5 minutes before mounting with Pertex mounting medium (Pioneer Research Chemicals LTD) and covering with glass coverslips. Slides were left to dry for 24 hours before digital imaging using Hamamatsu Nanozoomer-XR slide scanner. Digital scans were analysed via Hamamatsu Nanozoomer software.

2.3 In vitro culture

2.3.1 Primary monolayer culture

The ICR-SS-1 cell model was generated from the PDX model obtained from the Jackson Laboratory, J000104314, which was established from a synovial sarcoma patient. All other primary monolayer cell cultures were derived from PDX models generated in this study.

Primary cell monolayer cultures were seeded with a range of conditions to optimise conditions for establishment. Mouse cell depleted PDX-dissociated cells were seeded into matrigel coated or non-coated tissue culture flasks at a density of 30,000 viable cells per cm^2 in either Y-media or Y-media supplemented with 10 ng/ml PDGF$\alpha\beta$ (PeproTech) and 20 ng/ml bFGF (PeproTech). All cells were cultured in 95% air:5% CO2 at 37 °C in humidified incubators. Matrigel coated flasks were generated by adding 2.5% Growth Factor Reduced Matrigel (Corning) in cold DMEM/Ham's F12 1:1 to flasks which were

then incubated at 37 ºC for 1 hour before excess Matrigel solution was removed. Coated flasks were then used immediately for cell culture.

After 4-5 days from cell seeding, cultures were visually inspected for cell adhesion using Evos m5000 microscope and an equal volume of Y-media to the seeding volume was added. Hereafter, twice a week half of the culture media was removed and replaced with fresh Y-media (with or without PDGF and bFGF). Viability of non-adhered cells in the removed media was assessed via staining with 0.4% trypan blue (ThermoFisher Scientific) and if cell viability exceeded 20%, removed media was centrifuged at 300 xg for 5 minutes, resuspended in fresh Y-media (with or without PDGF an bFGF) and added back into the culture flasks. Once cell cultures reached approximately 80% confluence, cells were trypsinised using TrypLE™ Express Enzyme (1X), phenol red (Gibco) until detachment and subcultured at a 1:2 ratio. During passaging, removed media was saved and added back to the subcultures at a 1:1 ratio with fresh media. This protocol was repeated until cells had been subcultured 10 times at which cells were considered to be established cell lines. From this point onwards, media was replaced by full fresh media twice a week. Primary cells were tested for mycoplasma with Mycoalert™ Mycoplasma Detection Kit (Lonza). following manufacturer's instructions.

2.3.2 Cell line maintenance and acquired resistant sublines

HS-SY-II (from RIKEN BioResource Centre, Kyoto, Japan), SYO-1 (obtained from Dr Chris Lord, Institute of Cancer Research, London, UK), MRC-5 (obtained from Dr Janet Shipley, Institute of Cancer Research, London, UK), NIH-3T3 (obtained from Dr Matilda Katan, University College London, London, UK) and PC9 (obtained from Dr Matilda Katan, University College London, London, UK) cells were cultured in DMEM supplemented with 1× penicillin/streptomycin and 10% FBS. SK-UT-1 and SK-UT-1b cells (obtained from Dr Priya Chudasama, German Cancer Research Centre, Heidelberg, Germany) were cultured in MEM (Gibco) supplemented with 1× penicillin/streptomycin and 10% FBS. Sheff-LMS-01 W1 and Sheff-LMS-01 WS (obtained from Dr Karen Sisley, University of Sheffield, Sheffield, UK) were cultured in RPMI-1640 supplemented with 1x penicillin/streptomycin and 10% FBS. ICR-SS-1, ICR-LMS-1, ICR-LMS-4 and ICR-LMS-6 and SARC-393 cells were cultured in Y-media and SARC-323 cells were cultured on matrigel coated flasks in Y-media supplemented with 10 ng/ml PDGF and 20 ng/ml bFGF. Cells were grown at 95% air:5% CO_2 at 37 °C. Medium was replenished twice weekly and cells were cryopreserved in 10% DMSO in

FBS. STR profiling was conducted on all cell lines used and were compared to the CLASTR Cellosaurus STR database to confirm cell identity.

Doxorubicin (Sigma Aldrich) was used to derive acquired resistance in SK-UT-1, SK-UT-1b and ICR-LMS-1 cell lines. Cells were cultured in media initially at the inhibitory constant (IC50) value which was determined from colony formation or cell viability assays. Doxorubicin concentration was doubled once cell growth exceeded cell death, from 10 nM to 20 nM, 40 nM and finally resistant cells were maintained with 80 nM doxorubicin, replacing media and drug twice a week. Resistance was confirmed via cell viability assays.

2.3.3 Spheroid and organoid cultures

Spheroids were grown by seeding cells in 96 well ultra-low attachment U-bottom plates (Corning) at indicated densities in 100 µl of Y-media then spinning at 1000 rpm for 10 minutes. Plates were incubated for 3 days, after which 100 µl of Y-media was added and 100 µl replaced every 3-4 days thereafter. Spheroids were imaged and measured using EVOS m5000 microscope (Thermo Fisher Scientific).

TM1244, TM219 and TM199 organoid cultures were generated from TM01244, TM00199 and TM00219 PDX models respectively which were purchased from the Jackson Laboratory. All other organoids were generated from PDX-models established in this study. For organoid cultures, cells pellets were taken directly after PDX tissue dissociation and suspended in Growth Factor Reduced Matrigel on ice. Single 40 µl droplets of the Matrigel-cell suspension were seeded onto 24 well plates and allowed to polymerise, inverted, at 37 ºC for 15-20 minutes. Once polymerised, droplets were surrounded with 500 µl of Y-media (with or without PDGF and bFGF) or lung organoid media (**Table 2.2**) and incubated at 37 ºC, replacing organoid media twice a week. Organoid cultures were imaged using EVOS m5000 microscope. Organoid cultures were cultured for 4 weeks initially and then subcultured 1:2-1:4 every 2 weeks by enzymatic and mechanical dissociation. To passage organoids, media was removed from Matrigel domes and PBS was added to wash. Matrigel domes were then dislodged from plates using a policeman cell scraper, collected and centrifuged at 300 xg for 5 minutes. PBS was removed and Matrigel-organoid pellets were resuspended in TrypLE™ Express Enzyme (1X), phenol red before incubating at 37 ºC for 10-20 minutes. Suspensions were visually inspected for dissociation of organoids as well as digestion of Matrigel and remaining cell clumps were dislodged via pipetting. Trypsin was inactivated by the addition of Y-media, followed by centrifuging at 300 xg for 5 minutes. Cell pellets were

resuspended in ice-cold Matrigel and Matrigel-cell suspensions were then seeded as domes onto 24 well plates to polymerise again.

Media component	Supplier	Final concentration
R-Spondin 1	Peprotech	500 ng/ml
FGF 7	Peprotech	25 ng/ml
FGF 10	Peprotech	100 ng/ml
Noggin	Peprotech	100 ng/ml
A83-01	Tocris	500 nM
Y-27632	LC laboratories	5 µM
SB202190	Sigma	500 nM
B27 supplement	Gibco	1x
N-Acetylcysteine	Sigma	1.25 mM
Nicotinamide	Sigma	5 mM
GlutaMax 100x	Invitrogen	1x
Hepes	Invitrogen	10 mM
Penicillin / Streptomycin	ICR	1x
Amphoceterin B	ThermoFisher Scientific	250ng/ml
Advanced DMEM/F12	ThermoFisher Scientific	1x

Table 2.2. NSCLC organoid media components. Media components with supplier and concentration. DMEM; Dulbecco's modified Eagle medium FGF; fibroblast growth factor.

2.4 Molecular biology

2.4.1 *SS18::SSX1* fusion PCR

ICR-SS-1 and HS-SY-II cells were seeded into 6 well plates at a density of 350,000 cells/well and incubated for 24 hours prior to RNA extraction. RNA was extracted from J000104314 PDX tissue, ICR-SS-1 and HS-SY-II cells using RNeasy mini and QIAshredder kits (Qiagen) following manufacturers instructions. DNA was degraded by RQ1 DNAse solution (Promega) before complementary DNA (cDNA) was synthesised using Superscript III kit (Invitrogen). HS-SY-II was used as a positive control for the *SS18:SSX1* fusion (Sonobe et al. 1992). Polymerase chain reaction (PCR) mixtures were made with GoTaq DNA polymerase (Promega) containing either the common *SS18* forward primer (Sigma Aldrich) or one of *SSX1, SSX2* or *SSX4* reverse primers (Sigma Aldrich). β-actin (*ACTB)* primers were used as a positive control of cDNA synthesis. Primer sequences are provided in **Table 2.3**. .

PCR amplicon	Forward Primer	Reverse Primer
SS18::SSX1	5′-AGACCAACACAGCCTGGACCAC-3′	5′-ACACTCCCTTCGAATCATTTTCG-3′
SS18::SSX2	5′-AGACCAACACAGCCTGGACCAC-3′	5′-GCACTTCCTCCGAATCATTTC-3′
SS18::SSX4	5′-AGACCAACACAGCCTGGACCAC-3′	5′-GCACTTCCTTCAAACCATTTTCT-3′
ACTB	5′-GACAGGATGCAGAAGGAGATCAC-3′	5′-TGATCCACATCTGCTGGAAGGT-3′

Table 2.3. Primer sequences for amplification of *SS18::SSX1*, *SS18::SSX2* or *SS18::SSX4* translocations as well as β-actin (*ACTB*). Forward and reverse primers from 5' to 3'.

Thermocycler conditions for the amplification of *SS18::SSX* or *ACTB* are described in **Table 2.4**-**Table 2.5**. PCR products were loaded onto 2% agarose (Invitrogen) gel stained with SYBR safe DNA gel stain (Invitrogen) or ethidium bromide (Sigma Aldrich) and digitally imaged using G-Box Chemi-XX6 (Syngene). PCR products of the predicted amplicon size of 108 bp were considered positive for the gene fusion.

SS18::SSX			
PCR Step	**Time**	**Temperature**	**Comments**
Denaturation	7 min	95 °C	
Touchdown Amplification	45 s	94 °C	10 cycles, reducing annealing temperature by 1 each cycle, from 66 to 57
	45 s	66 °C	
	1 min 30 s	72 °C	
Amplification	45 s	94 °C	30 cycles
	45 s	56 °C	
	1 min 30 s	72 °C	
Final Extension	5 min	72 °C	

Table 2.4. Thermocycler conditions for *SS18:SSX1/2/4* amplification. Conditions listed for denaturation, touchdown amplification, amplification and final extension.

ATCB			
PCR Step	**Time**	**Temperature**	**Comments**
Denaturation	2 min	95 °C	
Amplification	15 s	95 °C	
	15 s	60 °C	40 cycles
	1 min	72 °C	
Final Extension	5 min	72 °C	

Table 2.5. Thermocycler conditions for *ACTB* amplification. Conditions listed for denaturation, touchdown amplification, amplification and final extension of β-actin (*ACTB).*

2.4.2 Human vs mouse PCR

DNA was extracted from ICR-SS-1, NIH-3T3, SK-UT-1, ICR-LMS-1, ICR-LMS-3, ICR-LMS-4, ICR-LMS-5, ICR-LMS-6, SARC-323 and SARC-393 using DNease blood and tissue kit (Qiagen) following manufacturer's instructions. NIH-3T3 was used as a mouse positive control and SK-UT-1 was used as a human positive control. PCR mixtures were made with GoTaq DNA polymerase (Promega) containing a human or mouse specific Prostaglandin E receptor 2 (*PTGER2)* forward primer (Sigma Aldrich) with a common reverse *PTGER2* primer (Sigma Aldrich). Primer sequences are described in **Table 2.6.**

PCR Amplicon	**Forward Primer**	**Reverse Primer**
Human *PTGER2*	5′-GCTGCTTCTCATTGTCTCGG-3′	5′-GCCAGGAGAATGAGGTGGTC-3′
Mouse *PTGER2*	5′-CCTGCTGCTTATCGTGGCTG-3′	5′-GCCAGGAGAATGAGGTGGTC-3′

Table 2.6. Primer sequences for amplification of human and murine *PTGER2*. Forward and reverse primers from 5' to 3'. *PTGER2;* Prostaglandin E Receptor 2.

Thermocycler conditions used for both human and mouse *PTGER2* amplification are described in **Table 2.7**. PCR products were loaded onto 1.5% agarose (Invitrogen) gel stained with SYBR safe DNA gel stain (Invitrogen) and digitally imaged using G-Box Chemi-XX6 (Syngene). PCR products of the predicted amplicon size of 189 bp were considered positive for human or mouse DNA depending on the primers used.

PTGER2			
PCR Step	Time	Temperature	Comments
Denaturation	5 min	98 °C	
Amplification	5 s	98 °C	
	5 s	60 °C	40 cycles
	20 s	72 °C	
Final Extension	1 min	72 °C	

Table 2.7. Thermocycler conditions for *PTGER2* amplification. Conditions listed for denaturation, touchdown amplification, amplification and final extension of Prostaglandin E Receptor 2 (*PTGER2).*

2.4.3 Short tandem repeat profiling

DNA was extracted from frozen PDX tissue or cell cultures using DNeasy blood and tissue kits (Qiagen), following the manufacturer's instruction. Human Cell Line Authentication via short tandem repeat profiling was undertaken using the Eurofins Genomics cell cine authentication service. Percentage matches were calculated between PDX and cell cultures using the following equation: percentage match = number shared alleles/total number of alleles in the questioned profile. STR profiles of cell cultures were also used to calculate percentage matches to a database of cell line STR profiles via the CLASTR Cellosaurus STR similarity search tool (Robin, Capes-Davis, and Bairoch 2020).

2.5 Cell viability assay

For a 72 hour assay, cells were seeded in 96 well plates either at 2000 cells/well (SK-UT-1, SK-UT-1 doxoR, SK-UT-1b, SK-UT-1b doxoR, SYO-1, HS-SY-II, ICR-LMS-1, ICR-LMS-1 doxoR, ICR-LMS-4, ICR-LMS-6, SARC-323 and SARC-393) or 3000 cells/well (ICR-SS-1) for 24 hours prior to drug addition at indicated concentrations in triplicate. For cell viability assays, cells were seeded and drug were added in their respective growth media, described in section **2.3.2**. After incubation for 72 hours cell viability was determined using CellTitre-Glo (Promega) following manufacturer's instructions and data was generated with Victor X5 plate reader (PerkinElmer) or Spark plate reader (Tecan). Dose response curves were fitted with Graphpad-Prism software using four-parameter variable slope linear regression and IC50 values calculated based on the generated

response curve. Alternatively, for a 6 day treatment assay cells were seeded in 96 well plates at 1000 cells/well and incubated for 24 hours prior to drug treatment. Cells were then incubated for 72 hours after which media with respective drugs were replaced and incubated for a further 72 hours before cell viability assessment as above.

For 3D Matrigel embedded cell viability assays, cells were dissociated from Matrigel droplets and passed through a 70 μm filter before resuspending in Matrigel and seeding at a density of 1000 cells per 10 ul Matrigel droplets per well. Plates were inverted and incubated at 37 °C for 20 minutes to allow Matrigel to solidify. Once solidified, Y-media was added on top of Matrigel domes and cells were cultured for 7 days before culture media was removed and Y-media with doxorubicin doses were added. After incubating for another 72 hours, cell viability was assessed as above.

2.6 Small-molecule inhibitor screen

For a 72 hours screen, cells were seeded in 96 well plates either at 2000 cells/well (SK-UT-1, SK-UT-1 doxoR, SK-UT-1b, SK-UT-1b doxoR, SYO-1, HS-SY-II, ICR-LMS-1, ICR-LMS-1 doxoR, ICR-LMS-4, ICR-LMS-6, SARC-323 and SARC-393) or 3000 cells/well (ICR-SS-1) for 24 hours prior to drug addition at 0.5 μM. Components of the small molecule inhibitor screen are listed in **Table 2.8**. After incubation for 72 hours cell viability was determined using CellTitre-Glo (Promega) following manufacturer's instructions and data was generated with Victor X5 plate reader (PerkinElmer) or Spark plate reader (Tecan). Alternatively for a 6 day drug screen, cells were seeded in 96 well plates at a density of 1000 cells/well for 24 hours prior to drug addition at 0.5 μM. After incubation for 72 hours, media was removed and fresh media with small molecule inhibitors at 0.5 μM were added prior to incubation for another 72 hours. Cell viability was then assessed as above. Data was clustered using Perseus software (version 1.6.13) (Tyanova et al. 2016) with two-way Euclidean distance hierarchical clustering.

Inhibitor	Primary Target	Supplier
Lenvatinib	Broad Spectrum: RTKs	LC Labs
Sunitinib	Broad Spectrum: RTKs	LC Labs
Pazopanib	Broad Spectrum; RTKs	LC Labs
Ponatinib	Broad spectrum; RTKs	LC Labs
Regorafenib	Broad Spectrum: RTKs	LC Labs
Bosutinib	Src, Abl	LC Labs
Dasatinib	Abl, Src, c-Kit	LC Labs
Saracatinib	Src	Selleck Chemicals
Ceritinib	ALK	LC Labs
Crizotinib	c-Met, ALK	LC Labs
NVP-TAE684	ALK	Selleck Chemicals
AZD9291	EGFR	Selleck Chemicals
EAI045	EGFR	Selleck Chemicals
Erlotinib	EGFR	LC Labs
Gefitinib	EGFR	LC Labs
Lapatinib	EGFR, ErbB2	Selleck Chemicals
Neratinib	HER2, EGFR	LC Labs
BGJ398	FGFR1/2/3	Selleck Chemicals
Linsitinib	IGF1R	LC Labs
NVP-AEW541	IGF1R, InsR	Selleck Chemicals
Imatinib	v-Abl, c-Kit, PDGFRα	LC Labs
Cediranib	VEGFR	LC Labs
Foretinib	HGFR, VEGFR	LC Labs
Sorafenib	Raf-1, B-Raf, VEGFR2	LC Labs
Vandetanib	VEGFR2	LC Labs
BI-2536	Plk1	Selleck Chemicals
BX-795	PDK1	Sigma Aldrich
BEZ235	PI3K, mTOR	LC Labs
Rapamycin	mTOR	LC Labs
Binimetinib	MEK1/2	LC Labs
Trametinib	MEK1/2	LC Labs
Dabrafenib	BRAFV600	Selleck Chemicals
SB203580	p38 MAPK	LC Labs
SP600125	JNK	LC Labs
NVP-AUY922	HSP90	LC Labs
AZD5363	Akt1/2/3	Selleck Chemicals
MK2206	Akt1/2/3	Selleck Chemicals
Momelotinib	JAK1/2	Selleck Chemicals
Niclosamide	STAT3	Selleck Chemicals
SH-4-54	STAT	Selleck Chemicals
Cilengitide Trifluoroacetate	Integrin	Selleck Chemicals
Navitoclax	Bcl-xL, Bcl-2, Bcl-w	Selleck Chemicals
Galunisertib	TGFβ-R1	Selleck Chemicals
Entrectinib	TrkA/B/C, ROS1, ALK	Selleck Chemicals
GW441756	TrkA	Selleck Chemicals
BMS345541	IKK-1/2	Selleck Chemicals
GSK126	EZH2 Methyltransferase	Selleck Chemicals
XAV-939	Tankyrase-1/2	Selleck Chemicals
PF562271	FAK	Selleck Chemicals
TAE226	FAK	Selleck Chemicals
Alisertib	Aurora A	Selleck Chemicals
JQ1	BET Bromodomain	Selleck Chemicals
LY2603618	Chk1	Selleck Chemicals
MK-8776	Chk1	Selleck Chemicals
Palbociclib	CDK4/6	LC Labs
Silmitasertib	CK2	Selleck Chemicals
Rucaparib	PARP	LC Labs
Talazoparib	PARP	Selleck Chemicals

Table 2.8. Small molecule inhibitor screen components. List of small molecule inhibitors, targets and suppliers. ADP; Adenosine diphosphate, ALK; Anaplastic lymphoma kinase, Bcl-2/x; B-cell lymphoma

2/extra large protein; Bcl-w; Bcl-2-like protein 2, Bcr; Breakpoint cluster region protein, BET; Bromo- and extra-terminal domain, CDK4/6; Cyclin-dependent kinase 4/6; Chk1; Checkpoint kinase 1, CK2; Casein kinase 2, EGFR; Epidermal growth factor, EZH2; Enhancer of zeste homolog 2, FAK; Focal adhesion kinase, FGFR(1/2/3); Fibroblast growth factor receptor (1/2/3), HER2; Human epidermal growth factor receptor 2, HGFR; Hepatocyte growth factor receptor, Hsp90; Heat shock protein 90, IGF1R; Insulin-like growth factor 1 receptor, IKK(1/2); IκB kinase (1/2), InsR; Insulin receptor, JAK(1/2); Janus kinase (1/2), JNK(1/2/3); c-Jun N-terminal kinase (1/2/3), MAPK; Mitogen-activated protein kinase, MEK; Mitogen-activated protein kinase kinase, mTOR; Mechanistic target of rapamycin, N-terminal; Amino-terminal, NTRK(1/2/3); Neurotrophic tyrosine kinase receptor (1/2/3) PARP; Poly (ADP-ribose) polymerase, PDPK1; Phosphoinositide-dependent protein kinase 1, PI3K; Phosphoinositide 3-kinase, PLK1; Polo-like kinase 1, (B/C)-Raf; Rapidly accelerated fibrosarcoma, RTK; Receptor tyrosine kinase, STAT(3); Signal transducer and activator of transcription (3), TGFβR1; Transforming growth factor β receptor 1.

2.7 Proliferation assay

Cells were seeded into 8 black-walled 96 well plates (Greiner Bio-One) at a density of 1000 cells/well. After 24 hours, one plate (day 1) was fixed by replacing the media with 10% neutral-buffered formalin solution (Sigma Aldrich) and incubating at room temperature for 15 minutes. Fixed cells were washed three times with PBS and then stored at 4 °C in PBS. This protocol was repeated on consecutive plates at day 3, 4, 7, 8, 10, 11 and 14. Media was replaced on plates twice a week. Fixed cells were stained with Hoescht 33342 (R&D Systems) for 10 minutes at 37 °C and were then washed three times with PBS. Stained cells were counted using Celigo Imaging Cell Cytometer (Nexcelcom BioScience). Cell count fold change was fitted to a Malthusian exponential growth curve to calculate doubling time using GraphPad Prism software (GraphPad).

2.8 Colony formation assay

Cells were seeded into 6 well plates at a density of 1000 cells/well (SK-UT-1), 2000 cells/well (SK-UT-1b) or 10,000 cells/well (ICR-LMS-1 and ICR-LMS-4). After 24 hours cells were treated with compounds at the indicated concentrations for 10 days (SK-UT-1 and SK-UT-1b) or 14 days (ICR-LMS-1 and ICR-LMS-4). Media with compounds were replaced twice a week and after 10 or 14 days, cells were fixed with Carnoy's solution (1:3 acetic acid:methanol) for 5 minutes. Fixed cells were stained with 1% crystal violet solution for 5 minutes before washing under running water. Plates were imaged using G-Box Chemi-XX6 (Syngene). Colony density was quantified using ImageJ software (National Institutes of Health).

2.9 Immunoblotting

To prepare lysates, indicated cells were seeded in 6-well plates at a density to reach ~80% confluence after 24 hours. Drugs were added to the cells at defined timepoints or left untreated. 24 hours after seeding, cells were lysed in radioimmunoprecipitation assay (RIPA) lysis buffer (50 mM Tris.Cl pH 7.6, 150 mM NaCl, 1% IGEPAL CA-630 (NP-40) (Sigma Aldrich), 0.1% sodium dodecyl sulfate (SDS) (Sigma Aldrich), and 0.5% sodium deoxycholate (Sigma Aldrich)), supplemented with HaltTM protease and phosphatase inhibitors and EDTA #78442 (ThermoFisher Scientific) on ice. Lysates were then centrifuged at 15000 xg for 10 minutes at 4 ºC to remove cell debris. Protein concentration was determined using Pierce™ Bicinchoninic acid (BCA) Protein Assay Kit (ThermoFisher Scientific) following manufacturer's instructions. Lysate samples were loaded onto NuPage Novel 4-12% Bis-Tris gels (Invitrogen), followed by dry transfer to iBlot polyvinylidene fluoride (PVDF) membranes (Invitrogen) following using the iBlot transfer system. Membranes were blocked for 1 hour with 5% dried skimmed milk (Marvel) for pan-protein blots or 5% BSA (Sigma Aldrich) for phosphoprotein blots in 1x tris-buffered saline (TBS) with 0.1% Tween 20 (TBST) (Sigma Aldrich). Primary antibodies were added to membranes diluted in respective blocking buffers and left at 4 °C overnight under constant agitation. Primary antibodies were then removed and membranes were washed three times for 10 minutes each with TBST. Secondary horseradish peroxidase-conjugated antibodies diluted in 5% dried skimmed milk in TBST were then added to membranes and incubated for 1 hour in the dark at room temperature while under constant agitation. Antibodies were removed and the membranes were washed again three times for 10 minutes each with TBST. Primary and secondary antibodies used are described in (**Table 2.9**). Parameters for antibody concentrations were already established in the research team. Membranes were treated with SuperSignal West Pico PLUS chemiluminescence substrate (Thermo Fisher Scientific) for 5 minutes and then were imaged using G-Box Chemi-XX6 (Syngene).

Antibody	Dilution	Supplier
Primary antibodies		
Anti-pSTAT3 (Y705) D3A7 (Rabbit)	1:1000	Cell Signalling Technology (#9145)
Anti-STAT3α D1A5 (Rabbit)	1:1000	Cell Signalling Technology (#8768)
Anti-phospho-Src family (Y416) (Rabbit)	1:1000	Cell Signalling Technology (#2101)
Anti-Src (Rabbit)	1:1000	Cell Signalling Technology (#2108)
Anti-phospho-Akt (S473) 193H12 (Rabbit)	1:1000	Cell Signalling Technology (#4058)
Anti-Akt (pan) C67E7 (Rabbit)	1:1000	Cell Signalling Technology (#4691)
Anti-phospho-p44/42 MAPK (ERK1/2) (T202/Y204) D13.14.4E (Rabbit)	1:1000	Cell Signalling Technology (#4370)
Anti-p44/42 MAPK (ERK1/2) 137F5 (Rabbit)	1:1000	Cell Signalling Technology (#4695)
Anti-PTEN 138G6 (Rabbit)	1:1000	Cell Signalling Technology (#9559)
Anti-phospho-p70 S6 Kinase (T389) (Rabbit)	1:250	Cell Signalling Technology (#9205)
Anti-p70 S6 Kinase (Rabbit)	1:1000	Cell Signalling Technology (#9202)
Anti-Actin, α-Smooth Muscle antibody 1A4 (Mouse)	1:1000	Sigma Aldrich (#A5228)
Anti-α-tubulin (Mouse)	1:5000	Sigma Aldrich (#T5168)
Secondary antibodies		
Anti-Rabbit HRP-linked antibody	Total protein 1:5000	Cell Signalling Technology (#7074)
	Phosphoprotein 1:2000	
Anti-Mouse HRP-linked antibody	1:5000	SignalChem (#G32-62G-1000)

Table 2.9. Primary and secondary antibodies used for immunoblotting. List of antibodies with dilution used and supplier. ERK1/2; extracellular signal-regulated kinase 1/2, HRP; horseradish peroxidase, MAPK; mitogen-activated protein kinase, PTEN; phosphatase and tensin homolog, p70S6K; P70 ribosomal protein S6 kinase, STAT3; Signal transducers and activators of transcription 3.

2.10 Mass spectrometry proteomics

2.10.1   FFPE protein extraction

First, a H&E stain was generated for each FFPE block and slides were marked up by clinical fellows in the lab. Blocks with <75% tumour content were macrodisected. 20 μm tissue sections were cut from FFPE blocks and sections were deparaffinised by washing three times in xylene. Samples were rehydrated by washing in decreasing ethanol concentration gradients (100%, 96%, 70%) and left to air-dry. Dried samples were then homogenised in lysis buffer (0.1M Tris-HCL pH 8.8, 0.5% (w/v) sodium deoxycholate,

0.35% (w/v) sodium lauryl sulphate) (Sigma Aldrich) using a LabGen700 homogeniser (ColeParmer) with three 30 second pulses, followed sonicating on ice for 10 minutes and heading at 95 °C for 1 hour in order to reverse formalin crosslinks. Lysis was conducted by shaking at 750 rpm at 80 °C for 2 hours. Samples were then centrifuged at 14,000 rpm at 4 °C and the supernatants were collected. Protein concentration was measured by BCA assay (Pierce). Detergent removal was conducted by filter-aided sample preparation (FASP) with multiple washes with 8 M urea in Amicon-Ultra 4 (Merk) centrifugal flter units. Samples were transferred to Amicon-Ultra 0.5 (Merk) filters and reduced with 10 mM dithiothreitol and alkylated with 55 mM iodoacetamide. Samples were then washed with 100nM ammonium bicarbonate and were then digested with trypsin (Promega) (1 µg per 100 µg starting material) overnight at 37 °C. Samples were centriguged three times with 100mM ammonium bicarbonate and desalted in C18 SepPak columns (Waters) and then dried in a SpeedVac (Thermo Fischer Scientific).

2.10.2   Cell lysate protein extraction

ICR-SS-1, HS-SY-II, SYO-1, SARC-369, ICR-LMS-1, ICR-LMS-1 doxoR, SARC-323, ICR-LMS-3, SARC-401, ICR-LMS-4, SARC-409, ICR-LMS-6, SARC-393, SK-UT-1, SK-UT-1 doxoR, SK-UT-1b, SK-UT-1b doxoR, Sheffield LMS-01 WS and Sheffield LMS-01 W1 were seeded into T25 or T75 culture flasks and incubated for 72 hours to reach 80% confluence. Cells were lysed with 8 M urea (Sigma Aldrich) on ice. Protein quantification was conducted using Pierce BCA assay kit (Thermo Fisher Scientific) following manufacturer's instructions. For each sample 40 µg of total protein was treated with 10 mM of dithiothreitol and incubated at 56 °C for 40 minutes. Samples were treated with 55 mM idoacetamide and incubated at 25 °C for 30 min in the dark. After diluting to a final concentration of 2M urea and 0.1 ammonium bicarbonate, samples were treated with 0.4 g trypsin and incubated at 37 °C overnight. The digest was acidified to a pH of <4 with trifluoroacetic acid, desalted using Sep-Pak C18 Plus cartridge. Peptide estimation was undertaken using Pierce BCA assay kit with digested BSA as the standard curve. Samples were then dried in a SpeedVac.

2.10.3   SWATH mass spectrometry

Dried samples prepared in section **2.10.1** and **2.10.2** were later resuspended in buffer A (2% acetonitrile (Thermo Fisher Scientific) and 0.1% formic acid (Thermo Fisher Scientific)) supplemented with iRT peptides (Biognosys AG) and were then analysed in

an Agilent 1260 HPLC system coupled to a TripleTOF 5600+ mass spectrometer with NanoSource III (SCIEX). Sequential window acquisition of all theoretical mass spectra (SWATH) mass spectrometry data was acquired using a total of 2 µg of peptide per sample which was loaded onto a trap column packed with ReproSil Pur C18 AQ (120 Å, 3 µM) beads. A linear gradient of 2-40% of buffer B (98% acetonitrile and 0.1% formic acid) over 90 minutes and a flow rate of 250nl/minute was used. MS1 scans were acquired with a mass range of m/z 100-1500 (50 ms accumulation time) in positive ion mode. Per elution peak, 8 points were used to calculate the isolation windows for 58 precursor isolation windows, each with a fixed mass range of m/z 380-110 with a 1 Da overlap. MS2 scans were acquired with a mass range of m/z 100-1500 (50 ms accumulation time).

All SWATH data were analysed against a publicly available pan-human library using DIA-NN (version 1.8) (Demichev et al. 2020; Rosenberger et al. 2014). Raw data was processed using "robust LC (high precision)" mode with enabled "RT-dependent" cross-run normalisation. Mass accuracy of MS1, MS2 as well as scan window radius were all set to an average value for comparability. The spectral library was refined using the dataset with 1% FDR in order to generate an *in-silico* library, which was used to reanalyse the data. The subsequent report was filtered at a q-value of 0.01 for both precursor and proteins

Quantified protein data was log2 transformed, proteins with <70% values in analysed dataset were removed and missing values were imputed using default settings. Data was median normalised using Perseus software (version 1.6.13) (Tyanova et al. 2016). The processed dataset was visualised using two-way unsupervised clustering based on Pearson's correlation coefficient. Log2 transformed, normalised datasets from patient tissues versus PDX models, PDX models versus PDX-derived cell cultures, PDX-derived cell cultures versus LMS cell lines and parental vs doxoR cells were analysed by significant analysis of microarrays (SAM) using the samR package (Tusher, Tibshirani, and Chu 2001). The resulting dataset was processed by samR using a delta score threshold of 0.77 to reach 1% FDR. Positively and negatively regulated proteins were then subjected to over-representation analysis using the online tool g:Profiler using Benjamini–Hochberg FDR method with 0.1 FDR threshold and Hallmark gene set databases were downloaded from MSigDB (Raudvere et al. 2019; Liberzon et al. 2015).

Chapter 3 - Establishment of a panel of LMS PDX models

3.1 Introduction

The most common patient-derived model used in pre-clinical studies is the mouse xenograft due to their ability to mimic patient tumours in terms of histology as well as genetics and are often used to verify that candidate therapies are active *in vivo* before clinical assessment (Koga and Ochiai 2019; Risbridger, Lawrence, and Taylor 2020; Abdolahi et al. 2022). Additionally, patient-derived xenografts (PDX) models are able to recapitulate both inter-tumoural and intra-tumoural heterogeneity, thus establishing a well characterised panel of PDX models is a vital part of pre-clinical modelling of any solid cancer type in order to accurately capture the diversity of the disease (Sun et al. 2021). Due to the extreme rarity and heterogeneity of STS, recruiting enough patients for large-scale, subtype-specific clinical trials is challenging, placing further importance on robust pre-clinical models in order to more accurately identify potential drug candidates.

Unfortunately, there is a lack of PDX models derived from STS due to the rarity of the disease, restricting the diversity of models which can be utilised for drug testing, and research into mechanisms of drug response or resistance. The Jackson laboratory, a repository of commercially available PDX models lists only 44 STS PDX models in total spanning 14 subtypes and including sarcomas not otherwise specified. Only 3 non-uterine and one uterine LMS PDX models are listed,, which cannot fully capture the wide variety of anatomical location, histological variant, and molecular heterogeneity of the disease, highlighting the necessity to generate and characterise further LMS PDX models (The Jackson Laboratory 2022).

While several studies have recently reported the successful establishment of LMS PDX models, the majority of these have done so via inoculation of surgical resection tissue samples and it remains to be seen if LMS biopsy samples, which often have lower amount or quality of tissue can generate PDX models with the same efficiency (Cornillie et al. 2019; Hemming et al. 2022; Zhiying Zhang et al. 2019; Schoffski et al. 2019; Choi et al. 2021). The benefits of using biopsy samples for a patient derived model pipeline is that biopsy samples are routinely collected from patients, while not all patients undergo surgical excision (A. Gronchi et al. 2021). Thus, biopsy samples are more frequently available and additionally biopsies can be taken at multiple timepoints from a patient, for example during a clinical trial before and after treatment and this can be done far more frequently than surgical excision. Therefore, generating patient derived models from biopsies has the potential to create multiple different patient matched models each

representing a patient's cancer at a different stages of progression or therapy treatment (Guillen et al. 2022)

To that end, this chapter describes the generation of 18 PDX models including 13 LMS models from patient biopsy samples in order to expand the current repertoire of clinically relevant pre-clinical models for STS. Once generated these models were characterised by histological, short tandem repeat (STR) and proteomic analysis, comparing these to 1. the parental tumours of origin to confirm these models retain their clinical relevance and 2. between initial and subsequent passages to elucidate the degree of which these models can maintain tumour phenotype over time and to check if clonal selection or genetic drift is occurring in these models.

3.2 Patient cohort and tumour engraftment

Two clinical trial studies had given me a unique opportunity to develop new STS PDX models from paired pre- and post/on-treatment biopsy tissue. GEMMK is a phase I/II study, observing the safety, tolerability and preliminary response of gemcitabine and pembrolizumab combination treatment for advanced LMS or UPS (NCT03123276). APPLE is a phase I trial combining avelumab and radiotherapy on metastatic STS patients (NCT03602833). In order to establish and characterise PDX models from the patient biopsy samples, a pipeline was created and implemented on these GEMMK and APPLE biopsy samples, a schematic of which is presented in **Figure 3.1.**
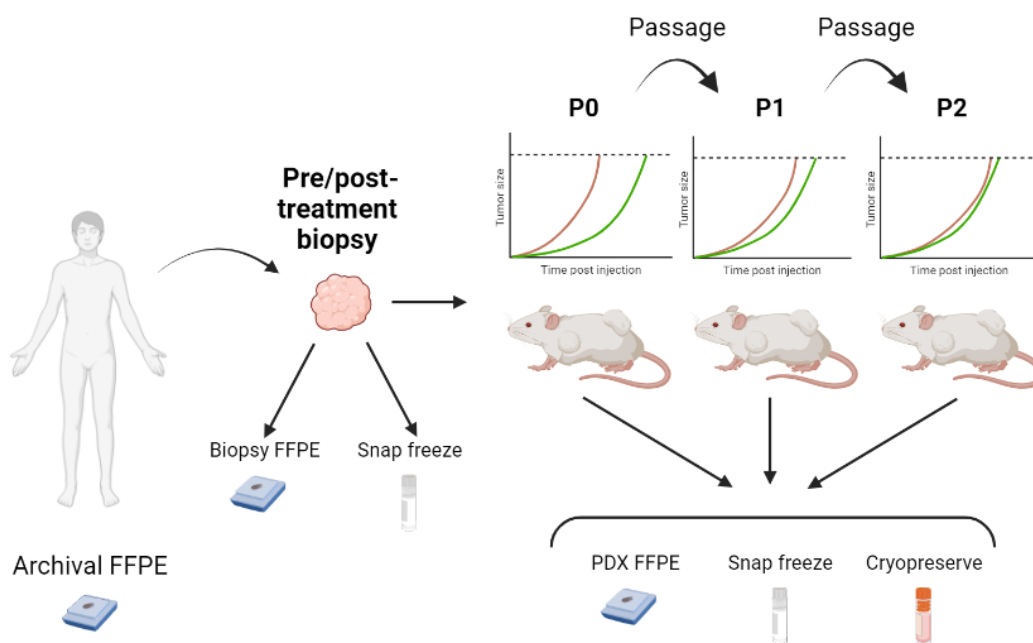
Figure 3.1. PDX establishment pipeline. Pre- and post-treatment biopsies from the GEMMK or APPLE clinical trial were engrafted into P0 immunocompromised mice which were subsequently passaged to P1 and P2 mice in order to establish the PDX model. Growth rates were measured to assess model stability with green and red representing different tumour growth rates and FFPE, snap frozen and cryopreserved tissue was stored for each tumour passage. Figure was created using BioRender. FFPE; formalin fixed paraffin embedded, P0; passage 0, P1; passage 1, P2; passage 2.

Over the course of three years, 43 biopsy samples in total were collected at baseline timepoints from both trials and at post-cycle 3 from GEMMK or post-radiotherapy (RT) from APPLE spanning 6 subtypes (**Table 3.1**). From GEMMK, 18 biopsies were taken at baseline and 12 were post- or on-treatment biopsies while for APPLE 7 biopsies were taken at baseline and 5 were taken post-treatment. The majority of biopsy samples were LMS in subtype (24/43) followed by UPS (12/43), ASPS (2/43), epithelioid sarcoma (ES) (2/43) clear cell sarcoma (CCS) (1/43), spindle cell sarcoma (SCS) (1/43) and non-tumour (1/43) (**Table 3.1Table 3.2**). Additionally, 30 of these biopsies were patient matched, making 15 pairs of pre- or post-treatment samples. Upon collection, each biopsy tissue was engrafted subcutaneously into immunocompromised mice immediately or was viably frozen if immediate engraftment was not possible. One biopsy was engrafted but subsequent histopathological analysis of the biopsy tissue revealed that no tumour was detectable in the sample and therefore 42 tumour-containing biopsy samples were engrafted in total.

Characteristic	Samples (n)	% of total
Total	42	
Sex		
Female	30	71%
Male	12	29%
Age		
<60	32	76%
≥60	10	24%
Trial		
GEMMK	30	71%
APPLE	12	29%
Subtypes		
LMS	24	57%
UPS	12	29%
ES	2	5%
ASPS	2	5%
CCS	1	2%
SCS	1	2%
Anatomical location		
Peritoneum	4	10%
Gluteus	1	2%
Occipital node	1	2%
Neck	1	2%
Lung	16	38%
Pelvis	2	5%
Abdominal wall	2	5%
Retroperitoneum	2	5%
Chest wall	1	2%
Leg	2	5%
Uterus	1	2%
Liver	4	10%
Axilla	1	2%
Arm	4	10%
Treatment history		
Treatment naive	13	31%
Treated	29	69%
Trial timepoint		
Pre-treatment	24	57%
Post/on-treatment	18	43%

Table 3.1. Patient biopsy demographics. Overview of patient specimen characteristics used in this study including sex, age, subtype, anatomical location of biopsy, treatment history and trial timepoint. ASPS; Alveolar Soft Part Sarcoma, CCS; Clear Cell Sarcoma, ES; Epithelioid Sarcoma, LMS; Leiomyosarcoma, ns; not significant, SCS; Spindle Cell Sarcoma, UPS; Undifferentiated Pleomorphic Sarcoma.

PDX engraft ID	Timepoint	Diagnosis	Site of biopsy/resection	Biopsy Grade	Primary site if known	Treatment history	Trial
SARC-298	Baseline biopsy	uLMS	Peritoneum	N/A	Uterus	None prior to biopsy	GEMMK
SARC-314	Post-cycle 3 biopsy	uLMS	Peritoneum	G3	Uterus	First-line GEMMK	
SARC-323	Baseline biopsy	LMS	Left gluteus	G3	Breast	Epirubicin+Cyclophosphamide in the adjuvant setting after surgery to the primary tumour; no treatment from diagnosis of metastatic disease to trial entry	
SARC-322	Baseline biopsy	LMS	Left occipital node	N/A	IVC	Dox-Ifosfamide started; due to renal impairment Dox single agent from cycle 3 to 6	
SARC-356	Post-cycle 3 biopsy	LMS	Neck	N/A	IVC	Second-line GEMMK	
SARC-355	Post-cycle 3 biopsy	UPS	Left lung	N/A	Heart	Caelyx + Ifosfamide in the adjuvant setting in; no treatment from diagnosis of metastatic disease to trial entry; on first-line GEMMK at the time of biopsy	
SARC-369	Baseline biopsy	uLMS	Pelvic	G3	Uterus	Doxorubicin (3 cycles)	
SARC-383	Post-cycle 3 biopsy	uLMS	Pelvic	N/A	Uterus	Second-line GEMMK	
SARC-376	Baseline biopsy	uLMS	Abdominal wall	G2	Uterus	Doxorubicin (3 cycles)	
SARC-384	Post-cycle 3 biopsy	uLMS	Abdominal wall	G2	Uterus	Second-line GEMMK	
SARC-385	Baseline biopsy	UPS	Right lung	N/A	Hamstring	Doxorubicin-Ifosfamide (2 cycles) followed by single agent Doxorubicin (2 cycles)	
SARC-389	Baseline biopsy	LMS	RP	G2	RP	Doxorubicin (2 cycles)	
SARC-400	Post-cycle 3 biopsy	LMS	RP	N/A	RP	Second-line GEMMK	
SARC-387	Baseline biopsy	UPS	Left anterior chest wall	G3	Posterior chest wall	Liposomal doxorucibin (5 cycles)	
SARC-395	Baseline biopsy	UPS	Upper leg	G3	Thigh	Liposomal doxorucibin (3 cycles)	
SARC-418	Post-cycle 3 biopsy	UPS	Upper leg	G3	Thigh	Second-line GEMMK	
SARC-397	Baseline biopsy	uLMS	Uterus	G3	Uterus	No prior treatments	
SARC-396	Baseline biopsy	LMS	Liver	N/A	RP	No prior treatments	
SARC-411	Post-cycle 3 biopsy	LMS	Left axilla	G1	RP	First-line GEMMK	
SARC-401	Baseline biopsy	uLMS	Liver	G3	Uterus	No prior treatments	
SARC-403	Biopsy - no tumour		Liver				
SARC-404	Baseline biopsy	LMS	Liver	N/A	Not clear	Doxorubicin first-line	
SARC-406	Baseline biopsy	UPS	Lung	N/A	Lower leg	No prior treatments	
SARC-420	Post-cycle 3 biopsy	UPS	Lung	N/A	Lower leg	First-line GEMMK	
SARC-407	Baseline biopsy	LMS	Peritoneum	N/A	Stomach	No prior treatments	
SARC-409	Post-cycle 3 biopsy	LMS	Peritoneum	N/A	Stomach	First-line GEMMK	
SARC-414	Baseline biopsy	LMS	Right forearm	N/A	IVC	No prior treatments	
SARC-416	Post-cycle 3 biopsy	LMS	Right forearm	N/A	IVC	First-line GEMMK	
SARC-417	Baseline biopsy	LMS	Liver	N/A	IVC	Cyclophosphamide	
SARC-419	Baseline biopsy	UPS	Right arm	G3	Forearm	No prior treatments	
SARC-426	Post-cycle 3 biopsy	UPS	Right arm	G3	Forearm	First-line GEMMK	

SARC-258	Week 7 biopsy	UPS	Lung	G3	Lower lip	No prior treatments	
SARC-280	Baseline biopsy	CCS	Lung	N/A	Right knee	Pazopanib, gemcitabine-docetaxel	
SARC-289	Baseline biopsy	UPS	Lung	N/A	Right shoulder	Treatment naïve	
SARC-304	Post-RT biopsy		Lung	N/A		Post-RT	
SARC-340	Baseline biopsy	ES	Lung	G2	Left foot	Treatment naïve	
SARC-359	Post-RT biopsy		Lung	G1		Post-RT	APPLE
SARC-393	Post-RT biopsy	uLMS	Lung	N/A	Uterus	Post-RT	
SARC-391	Baseline biopsy	uLMS	Lung	N/A	Uterus	Treatment naïve	
SARC-402	Post-RT biopsy		Lung	N/A		Post-RT	
SARC-405	Baseline biopsy	ASPS	Lung	N/A	Left thigh	Cediranib	
SARC-421	Post-RT biopsy		Lung	N/A		Post-RT	
SARC-431	Baseline biopsy	SCS	Lung	G3	Left thigh	Treatment naïve	

Table 3.2. Biopsy tissue and clinical information. All biopsy tissues which were engrafted to attempt PDX establishment from GEMMK or APPLE clinical trials including background information on trial timepoint, diagnosis, biopsy site, biopsy grade, primary tumour site if known, prior treatment history and trial enrolment. ASPS; Alveolar Soft Part Sarcoma, CCS; Clear Cell Sarcoma, ES; Epithelioid Sarcoma, G1; Grade 1, G2; Grade 2, G3; Grade 3, LMS; Leiomyosarcoma, N/A; Not Available, RP; Retroperitoneum, RT; Radiotherapy, IVC; Inferior Vena Cava, SCS; Spindle Cell Sarcoma, uLMS; uterine Leiomyosarcoma, UPS; Undifferentiated Pleomorphic Sarcoma.

3.3 PDX model establishment

From specimens from these two trials, PDX tumour growth was observed in 18 out of 42 engrafted biopsies, giving a biopsy take rate of 43% (**Table 3.3**). Biopsy take rates were calculated based on the number of biopsies which began to show exponential growth, thus biopsy samples which demonstrated initial tumour growth in mice followed by regression or showed inconsistent growth patterns were not considered to have taken. Out of 18 successfully engrafted biopsies 13 were from LMS patients, 4 were from UPS patients and 1 was from a SCS patient giving a subtype specific establishment rate of 54%, 33% and 100% for LMS, UPS and SCS biopsies respectively (**Table 3.3**). As the lung is a common site of metastasis, a large proportion of biopsies (37%) were taken from the lung although only 25% of these biopsies demonstrated successful engraftment. Meanwhile both biopsies taken from retroperitoneal tumours were successfully engrafted. When taking into account treatment history a successful engraftment rate of 38% was observed from biopsies of treatment naïve patients while 45% of biopsies taken from previously treated patients showed growth *in vivo*. When considering trial timepoint at which biopsy was obtained, 50% of baseline biopsies and 33% of post- or on-treatment biopsies were successfully engrafted. However, Chi-squared and Fisher's exact testing of these variables showed that sex, age, subtype, anatomical location, treatment history as well as trial timepoint had no statistically significant impact on biopsy engraftment success rate (**Table 3.3**). To assess whether these PDX models are suitable for biobanking, tissue from each model was cryopreserved for later thawing and engrafting. All 18 models demonstrated the ability to continue *in vivo* growth from cryopreserved tissue and therefore can be considered as a biobank of viable PDX tumours.

Characteristic	Samples (n)	Engraftment rate	P-value (significance)
Total	42	43% (18)	
Sex			
Female	30	47% (14)	0.5059 (ns)
Male	12	33% (4)	
Age			
<60	32	41% (13)	0.7201 (ns)
≥60	10	50% (5)	
Subtype			
LMS	24	54% (13)	0.2374 (ns)
UPS	12	33% (4)	
ES	2	0%	
ASPS	2	0%	
CCS	1	0%	
SCS	1	100% (1)	
Anatomical location of biopsy			
Peritoneum	4	50% (2)	0.4955 (ns)
Gluteus	1	100% (1)	
Occipital node	1	100% (1)	
Neck	1	100% (1)	
Lung	16	25% (4)	
Pelvis	2	50% (1)	
Abdominal wall	2	50% (1)	
Retroperitoneum	2	100% (2)	
Chest wall	1	100% (1)	
Leg	2	50% (1)	
Uterus	1	0% (0)	
Liver	4	25% (1)	
Axilla	1	0% (0)	
Arm	4	50% (2)	
Treatment history			
Treatment naive	13	38% (5)	0.7482 (ns)
Treated	29	45% (13)	
Trial timepoint			
Pre-treatment	24	50% (12)	0.3530 (ns)
Post/on-treatment	18	33% (6)	

Table 3.3. Tumour biopsy engraftment success rate. Number of biopsy samples which were successfully engrafted (i.e. demonstrated at least initial *in vivo* growth) considering sex, age, subtype, anatomical location of biopsy, treatment history and trial timepoint. p-values were calculated using Chi-squared or Fisher's exact test where P-value < 0.05 indicates significance. ASPS; Alveolar Soft Part Sarcoma, CCS; Clear Cell Sarcoma, ES; Epithelioid Sarcoma, LMS; Leiomyosarcoma, ns; not significant, SCS; Spindle Cell Sarcoma, UPS; Undifferentiated Pleomorphic Sarcoma.

Due to the large window of time for patient enrolment as well as variability of PDX tumour lag phase and growth rates, not all PDX models were able to be passaged twice at the time of this report, however failure of a PDX tumour to continue growing after passaging into the next generation was only observed in two of the models, indicating that once biopsy engraftment is successful these PDX models maintain tumour growth (**Figure 3.2**). Out of 18 PDX models, 12 had to be passaged via inoculation of dissociated cells from PDX tissue at least once instead of direct passage of tumour pieces due to measures put in place by the Biological Services Unit in order to minimise risk of C.Bovis infection which was detected in several mice in the unit (**Figure 3.2**). C.Bovis does not infect human cells and therefore dissociated cell inoculation was used to continue the growth of the patient-derived tumour cells while removing potentially contaminated stroma. Of the 12 inoculated PDX lines 10 were able to re-establish tumours after inoculation with cells while only two models showed no tumour growth after inoculation of PDX cells. One of these was from a passage 0 (P0) PDX tumour and the other was from a passage 1 (P1) PDX tumour but both were LMS models (SARC-376 and SARC-389 respectively). Taking both tumour passage and cell inoculation into account 94% (17/18) of PDXs were successfully passaged from P0 to P1 and 92% of PDX models passaged from P1 to passage 2 (P2) continued to grow (12/13). Therefore, in total 12 PDX models were grown to P2 and can be considered fully established, giving a full establishment rate from the total number of biopsies at 29% (12/42). Fully established PDX models included seven LMS PDX models (two of which are uterine LMS), four UPS models and one SCS model (**Table 3.4**).

14 of the successfully engrafted STS models were from patients within the GEMMK trial, and four derived from the APPLE trial (**Table 3.4**). Five patient matched pre- and post-treatment biopsy pairs were successfully engrafted: SARC-322 & SARC-356, SARC-389 & SARC-400, SARC-407 & SARC-409, SARC-414 and SARC-416 and SARC-289 & SARC-304. Of the successfully engrafted biopsies, 12 were from baseline biopsies while the remaining 6 were from post-cycle 3 or post-RT biopsies (SARC-356, SARC-400, SARC-409, SARC-416, SARC-304 and SARC-393). Only one PDX model was generated from a post-treatment biopsy where the corresponding baseline biopsy did not establish a tumour (SARC-393).
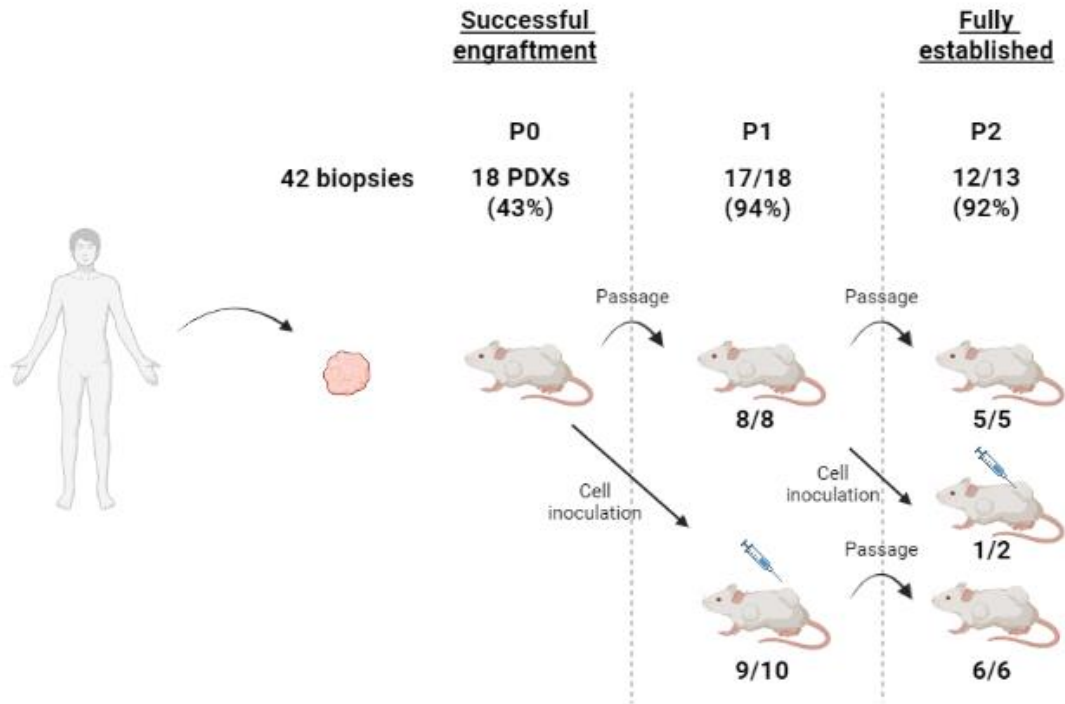
Figure 3.2. Overview of PDX engraftment rates for each passage. 42 tumour containing biopsies were engrafted in total of which a total of 18 were considered successful (i.e. showed in vivo growth). Tumours were passaged once to P1 either by direct engraftment or by dissociated cell inoculation. P1 tumours were then passaged again to P2 either by direct engraftment or by dissociated cell inoculation. x/n indicates the number n of PDX lines which were passaged via each method and the number x which successfully grew after passaging. 12 PDXs which continued to grow at P2 were considered fully established. Figure was created using BioRender. PDX; Patient-Derived Xenografts, P0; Passage 0, P1; Passage 1, P2; Passage 2.

The growth of these PDX models were monitored closely in order to determine growth kinetics and these tumour measurements were fitted to an exponential growth equation in order to determine the variation of doubling time both between passages of the same model and between different models (**Table 3.4**) (**Figure 3.3**-**Figure 3.4**). **Figure 3.3** shows the growth curves of PDX models which were passaged only via serial tumour engraftment. For instance, SARC-369 displayed a mean tumour doubling time of approximately 18 days upon initial engraftment (P0) which was also consistent with P2 tumour growth rates, although P1 SARC-369 tumours displayed a higher doubling time (**Figure 3.3**). Other established PDX lines which were passaged only via engraftment (SARC-409, SARC-414, SARC-416 and SARC-431) showed similar doubling times across passages or decreasing doubling times with each successive passage indicating stabilisation of growth kinetics and adaption to *in vivo* growth (**Figure 3.3**).

PDX engraft ID	Timepoint	Subtype	Site of biopsy/resection	Biopsy grade	Primary site if known	Treatment history	Passage limit	Tumour doubling time (days)
GEMMK								
SARC-323	Baseline biopsy	LMS	Left gluteus	G3	Breast	Epirubicin+Cyclophosphamide in the adjuvant setting after surgery to the primary tumour; no treatment from diagnosis of metastatic disease to trial entry	>P2	23.00
SARC-322	Baseline biopsy	LMS	Left occipital node	N/A	IVC	Dox-Ifosfamide started; due to renal impairment Dox single agent from cycle 3 to 6	>P2	18.07
SARC-356	Post-cycle 3 biopsy		Neck	N/A		Second-line GEMMK	>P1	
SARC-369	Baseline biopsy	uLMS	Pelvic	G3	Uterus	Doxorubicin (3 cycles)	>P3	17.80
SARC-376	Baseline biopsy	uLMS	Abdominal wall	G2	Uterus	Doxorubicin (3 cycles)	P1	
SARC-389	Baseline biopsy	LMS	RP	G2	RP	Doxorubicin (2 cycles)	P0	
SARC-400	Post-cycle 3 biopsy		RP	N/A		Second-line GEMMK	>P1	
SARC-387	Baseline biopsy	UPS	Left anterior chest wall	G3	Posterior chest wall	Liposomal doxorucibin (5 cycles)	>P2	6.55
SARC-395	Baseline biopsy	UPS	Upper leg	G3	Thigh	Liposomal doxorucibin (3 cycles)	>P2	30.10
SARC-401	Baseline biopsy	uLMS	Liver	G3	Uterus	No prior treatments	>P2	9.85
SARC-407	Baseline biopsy	LMS	Peritoneum	N/A	Stomach	No prior treatments	>P1	
SARC-409	Post-cycle 3 biopsy		Peritoneum	N/A		First-line GEMMK	>P2	33.49
SARC-414	Baseline biopsy	LMS	Right forearm	N/A	IVC	No prior treatments	>P2	17.50
SARC-416	Post-cycle 3 biopsy		Right forearm	N/A		First-line GEMMK	>P2	17.18
APPLE								
SARC-289	Baseline biopsy	UPS	Lung	N/A	Right shoulder	Treatment naïve	>P2	16.18
SARC-304	Post-RT biopsy		Lung	N/A		Post-RT	>P2	13.22
SARC-393	Post-RT biopsy	uLMS	Lung	N/A	Uterus	Post-RT	>P1	
SARC-431	Baseline biopsy	SCS	Lung	G3	Left thigh	Treatment naïve	>P2	9.02

Table 3.4. Overview of successfully engrafted biopsies. All PDX models which were successfully engrafted (i.e. demonstrated initial growth in vivo) with respective biopsy information including trial timepoint , subtype, anatomical location, tumour grade at biopsy, primary site, treatment history. The highest reached PDX passage number and mean doubling times of P2 models are included. G2; Grade 2, G3; Grade 3, LMS; Leiomyosarcoma, N/A; Not Available, P0; Passage 0, P1; Passage 1, P2; Passage 2, RP; Retroperitoneum, RT; Radiotherapy, IVC; Inferior Vena Cava, SCS; Spindle Cell Sarcoma, uLMS; uterine Leiomyosarcoma, UPS; Undifferentiated Pleomorphic Sarcoma
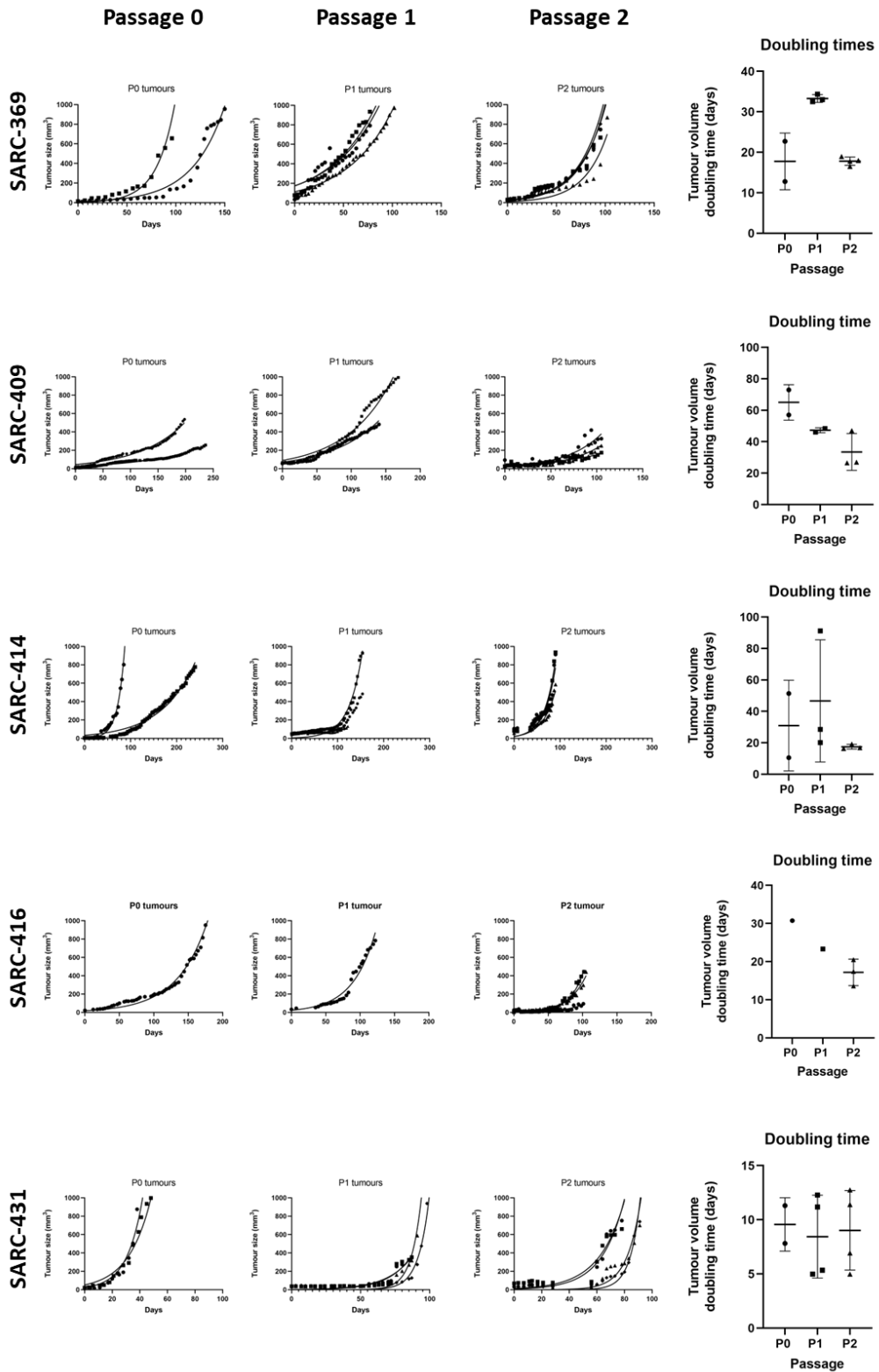
Figure 3.3. Growth curves and doubling times of established PDXs passaged via serial tumour engraftment only. Tumour growth of PDXs throughout P0-P2 passages via tissue engraftment. The first day after which a tumour was consistently detected was recorded as day 1. Growth measurements were fitted to a Malthusian growth curve equation to give doubling times. Error bars represent standard deviation. LMS; Leiomyosarcoma, P0; Passage 0, P1; Passage 1, P2; Passage 2, SCS; Spindle Cell Sarcoma.
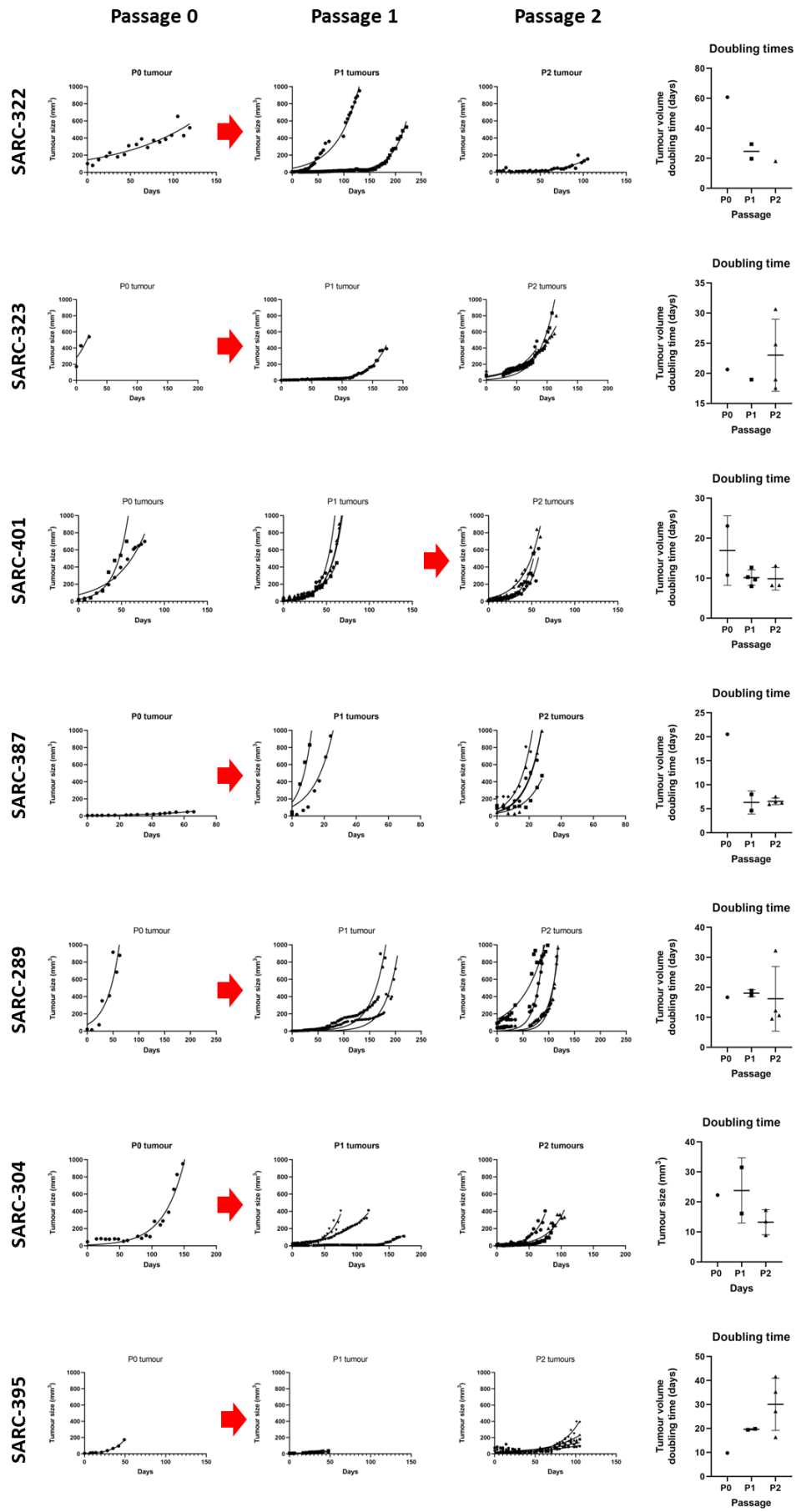
Figure 3.4. Growth curves and doubling times of established PDXs passaged via cell inoculation. Tumour growth of PDXs throughout P0-P2 passages which were passaged at least once via cell inoculation.. Red arrows indicate passaging via cell inoculation instead of tissue engraftment. The first day after which a tumour was consistently detected was recorded as day 1. Growth measurements were fitted to a Malthusian growth curve equation to give doubling times. Error bars represent standard deviation. LMS; Leiomyosarcoma, P0; Passage 0, P1; Passage 1, P2; Passage 2, UPS; Undifferentiated Pleomorphic Sarcoma.

The growth curves of established PDX models which were passaged at least once via dissociated cell inoculation are presented in **Figure 3.4**. SARC-401, SARC-387 and SARC-304 PDX models demonstrated a lower mean doubling time with lower variability at P2 passages compared to the respective P0 tumours indicating stabilisation of growth and adaption to *in vivo* growth despite undergoing injection of dissociated tissue for passaging. This data suggests that inoculation with dissociated PDX tissue can be used to continue the growth of certain PDX lines and is a feasible method of passaging these models where direct engraftment of tissue is not possible. However, SARC-395 showed an increase in doubling time upon successive passaging while SARC-289 and SARC-323 demonstrated a variable doubling time at P2, suggesting these models might require further passaging of select tumours to stabilise growth rates.

The panel of established PDXs demonstrated a range of growth rates upon reaching passage 2, with doubling time ranging from 6.5 to 33.5 days (**Table 3.4**). Additionally, patient matched models SARC-414 & SARC-416 and SARC-289 & SARC-304 showed similar growth kinetics (17.8 vs 17.5 days and 16.2 vs 13.2 days respectively) (**Table 3.4**). Therefore this panel of PDX model represents a range of tumour growth kinetics and also suggests that PDX growth is patient specific. The subtype of PDX models had no significant impact on tumour growth rate (p=0.4892), nor did anatomical location of biopsy sample (p=0.1372), trial timepoint (p=0.4412) or prior treatment status (p=0.1803).

3.4 PDX tumours retain histology of patient tumours

In order to examine the histology of each PDX model upon successful engraftment, P0 tumour samples were fixed, embedded in paraffin and stained with haematoxylin and eosin (H&E). PDX H&E slides were then compared with archival patient tissue where possible to assess whether the PDX models recapitulated patient histology including whether PDXs can capture intra-tumoral heterogeneity frequently observed in histology specimens from LMS patients. The uterine LMS models SARC-369 and SARC-401 displayed similar histological features consistent with uterine LMS including spindle shaped cells with hyperchromatic, polymorphic nuclei, some areas of eosinophilic cytoplasm, and some areas of fascicular bundles which were consistent with tumour samples from the corresponding patients (**Figure 3.5A & B**). The uterine LMS PDX model SARC-376 showed smaller, dense spindle cells arranged in fascicular bundles with hyperchromatic but relatively uniform nuclei (**Figure 3.5C**). Meanwhile the uterine LMS PDX model SARC-393 displayed a morphology consistent with de-differentiated LMS with less dense spindle cells, loosely arranged in fascicles, with polymorphic nuclei and the presence of occasional hyperchromatic nuclei and giant cells (**Figure 3.5D**).

Two patient matched PDX pairs SARC-322 & SARC-356 and SARC-414 & SARC-416 were engrafted from patients with LMS originating in the inferior vena cava (IVC) and all showed a similar well-differentiated histology, with spindle cells arranged in prominent fascicular structures and relatively uniform nuclei (**Figure 3.5E & F**). The other matched PDX pair SARC-407 and SARC-409 were engrafted from a patient with LMS originating in the stomach and displayed smaller cells with uniform nuclei, consistent with the histology of the patient tumour (**Figure 3.5G**). SARC-323 and SARC-323 PDX models were engrafted from two patients with LMS originating in the breast and stomach respectively, and each displayed a de-differentiated histology, with polymorphic nuclei, giant cells and loose fascicular bundles (**Figure 3.5H & I**). All of the LMS PDX models showed a histology which were consistent with the LMS subtype and to the corresponding patient tumour tissue, while patient matched models recapitulated patient specific histological features.

	Patient tissue	Baseline PDX	Post-treatment PDX
A		SARC-369	
B		SARC-401	
C		SARC-376	
D			SARC-393
E		SARC-322	SARC-356
F		SARC-414	SARC-416
G		SARC-407	SARC-409
H		SARC-323	
I		SARC-389	
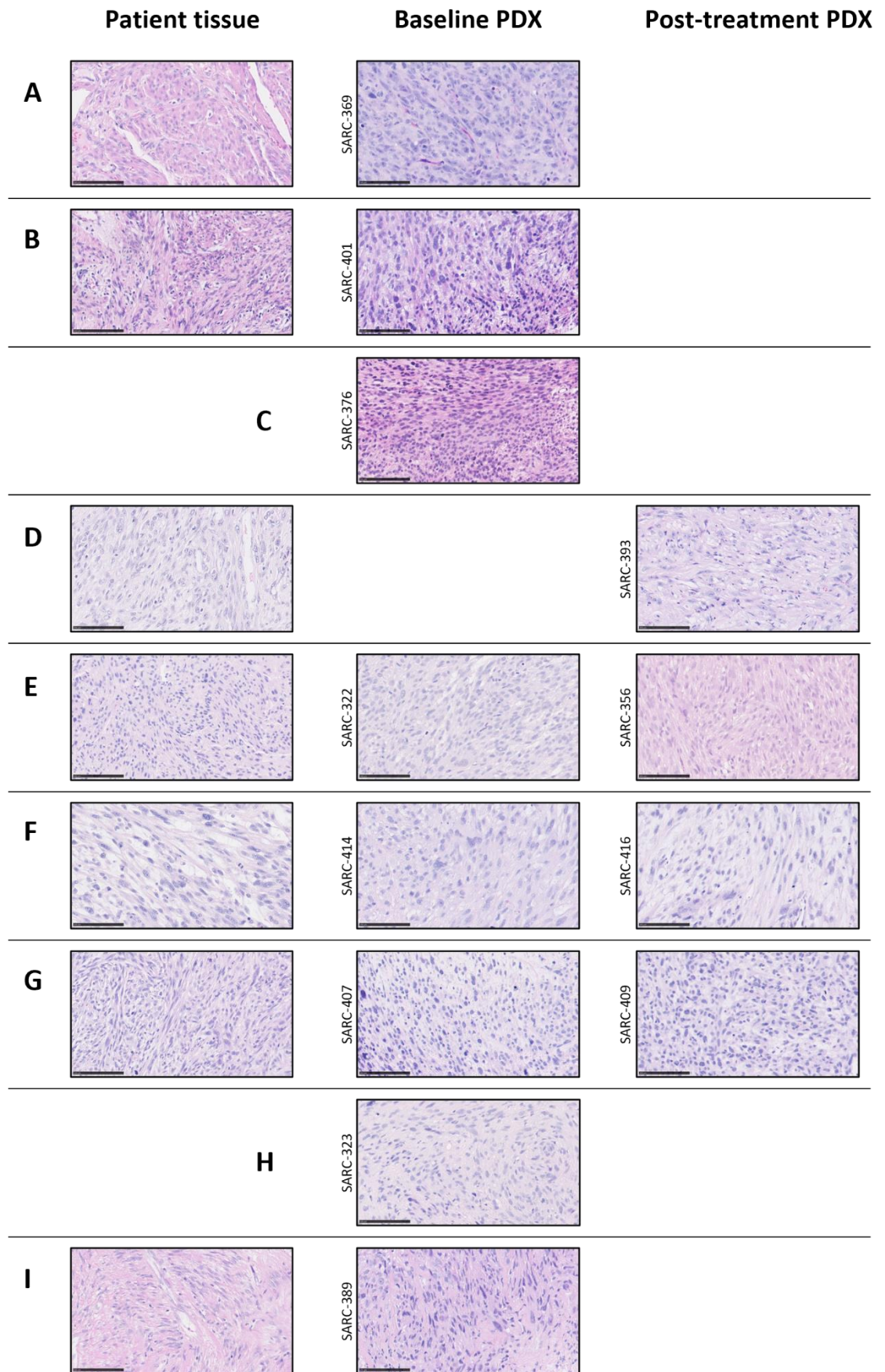
Figure 3.5. Histology of engrafted LMS PDX models from pre or post-treatment biopsies with respective patient tumour tissue. H&E stains of tissue slices from engrafted PDX models derived from post or pre-treatment biopsies compared to respective patient archival tissue. (A) SARC-322 and SARC-356. (B) SARC- 369. (C) SARC-393. (D) SARC-389. (E) SARC-401. (F) SARC-407 and SARC-409. (G) SARC-414 and SARC-416. (H) SARC-323. (I) SARC-376. Scale bar = 100 μm. Magnification 40x. PDX; patient-derived xenograft.

Histological features of the non-LMS models were also assessed for similarities to patient tumour tissues. The UPS PDX model SARC-387 displayed small round cells with hyperchromatic nuclei meanwhile SARC-395 showed a histology more consistent with UPS including extreme nuclear polymorphism and the presence of giant cells which matched the respective patient tumours (**Figure 3.6A & B**). The patient matched UPS PDX models SARC-289 and SARC-304 showed a matching histology which also corresponded to the patient tissue, with dense cells and polymorphic nuclei (**Figure 3.6C**). SARC-431 was engrafted from a biopsy of a SCS patient and displayed highly compact spindle cells, with uniform nuclei arranged in prominent fascicular structures (**Figure 3.6D**).

| | Patient tissue | Baseline PDX | Post-treatment PDX |
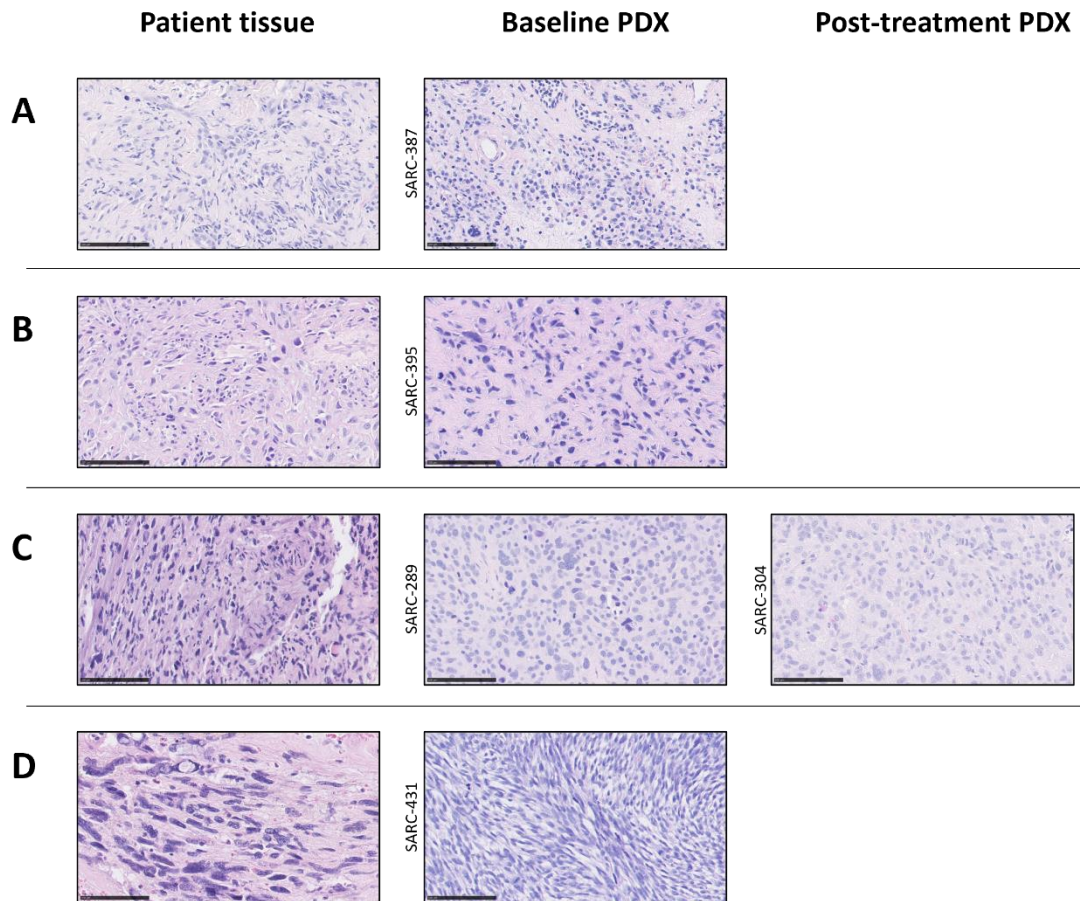
Figure 3.6. Histology of engrafted non-LMS PDX models from pre or post-treatment biopsies with respective patient tumour tissue. H&E stains of tissue slices from engrafted PDX models derived from post or pre-treatment biopsies compared to respective patient archival tissue. (A) SARC-387. (B) SARC-395. (C) SARC-289 and SARC-304. (D) SARC-431. Scale bar = 100 μm. Magnification 40x. PDX; patient-derived xenograft

H&E images from an initial P0 PDX tumour and successive P1 and P2 passages were compared for models where all of these stains were available, in order to identify any changes in histology which might occur upon continuous growth after passaging *in vivo*. Additionally it was important to check if passaging via dissociated cell inoculation had altered tumour histology in any way and if these models still represented the patient tumours. Assessing SARC-369, SARC-414 and SARC-431, each successive passage clearly retains the histological characteristics of the original P0 PDX tumour such as cellularity, spindle cell morphology, fascicular structures, while each model retains its distinct histological appearance. (**Figure 3.7A-C**). P0 tumours from SARC-323 and SARC-289 PDX models were dissociated and inoculated into mice in order to passage as a substitute for direct tissue passage. However, the inoculated tumour showed almost

identical histological features compared to the P0 tumour, each retaining the heterogeneous cell morphology found in the P0 tumour (**Figure 3.7D & E**). Additionally, successive passage to P2 via tissue engraftment was also able to maintain the histological features of the P0 tumours, indicating that passaging PDX tissue via dissociated cell inoculation does not alter patient-specific histology.
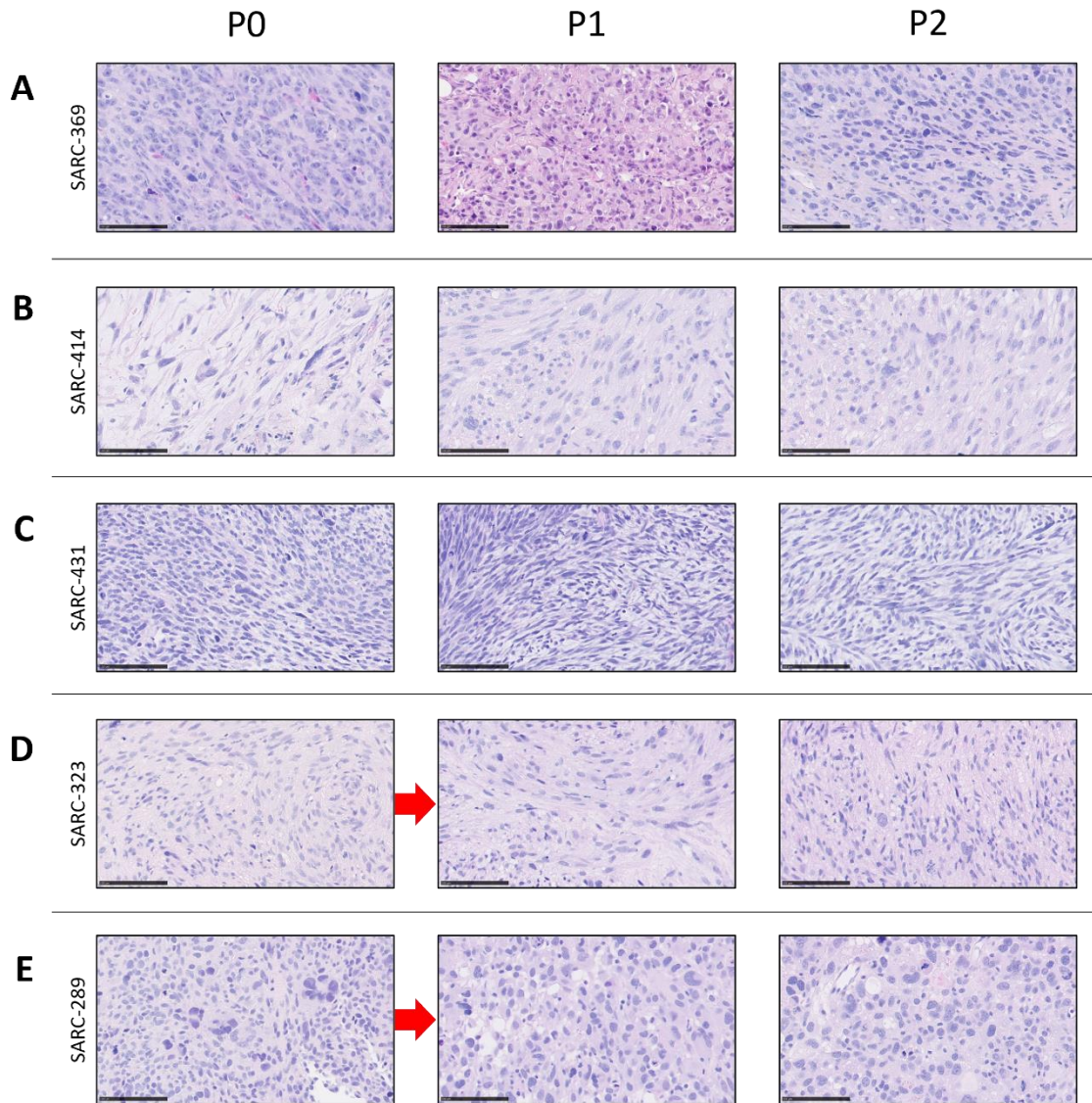
Figure 3.7 Histology of PDX models across successive *in vivo* passages. H&E stains of tissue slices from initial engrafted PDX models (P0) and successive passages (P1 and P2). (A) SARC-369. (B) SARC-414. (C) SARC-431. (D) SARC-323. (E) SARC-289. Red arrows indicate passaging via dissociated cell inoculation. 40x magnification.

3.5 Proteomic profiling of LMS PDX models

Next, to molecularly characterise the successfully engrafted LMS PDX models, tumour samples were subject to SWATH-mass spectrometry by two PhD students in our lab: Yuen Bun Tam and Madhumeeta Chadha. Mass spectrometry data was used to assess the differences between archival patient tumours and corresponding PDX models established from pre- or post-treatment biopsies. Additionally, these proteomic profiles were also compared to a historical proteomic dataset of STS patients including DDLPS, LMS, UPS and SS which was previously generated in the lab in order to observe if the PDX models retain their proteomic signatures associated with sarcoma histological subtypes (Milighetti et al. 2021). After hierarchical clustering of proteomic profiles, the LMS PDX models clustered together as one distinct group and clustered separately from all patient specimens, although the PDX models were clustered next to the LMS patient specimens versus other histological subtypes, indicating that these PDX models have distinct proteomes from patient tumours but most closely resemble the LMS subtype (**Figure 3.8**)
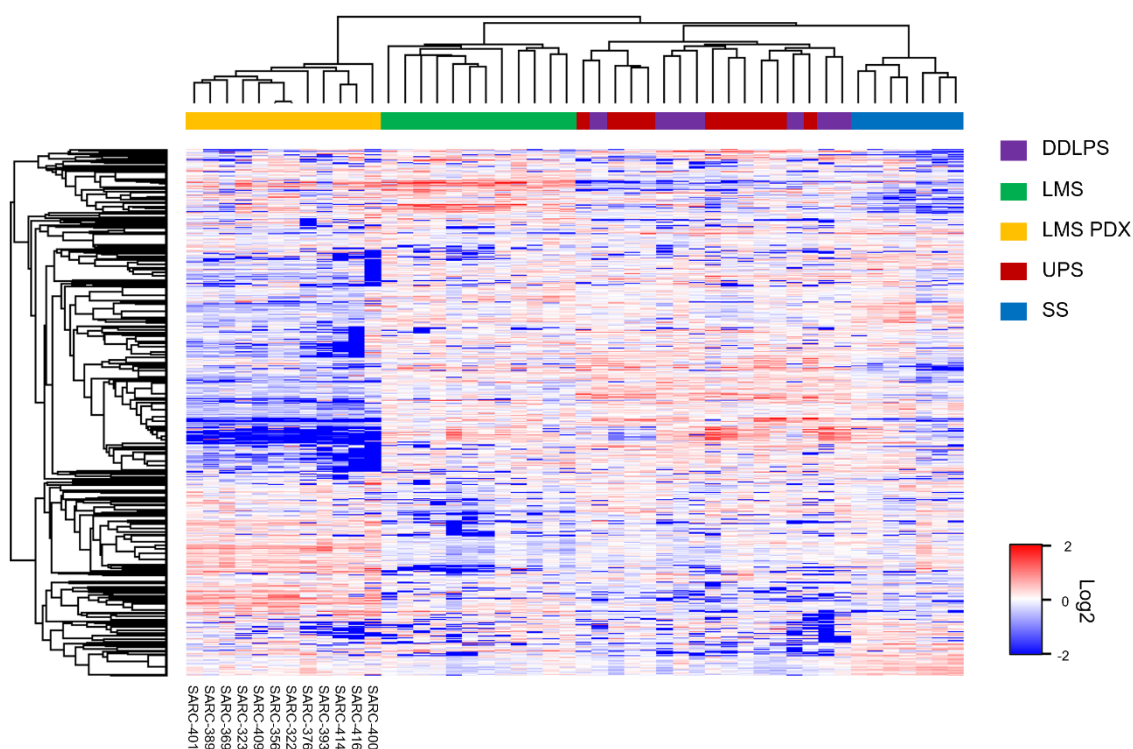
Figure 3.8. Proteomic analysis of LMS PDX models compared to DDLPS, LMS, UPS and SS tissue.
Heatmap showing hierarchical clustering of proteomic profiles of LMS PDX models in addition to profiles of

DDLPS (dedifferentiated liposarcoma), LMS (leiomyosarcoma), UPS (undifferentiated pleomorphic sarcoma) and SS (synovial sarcoma) tumour tissue. Profiles were clustered via two-way unsupervised clustering based on Pearson's correlation co-efficient. Mass spectrometry data was acquired and processed via DIA-NN by Yuen Bun Tam, Madhumeeta Chadha and Martina Milighetti. DIA-NN output data was further processed by myself to generate a heatmap of normalised proteomic profiles.

In order to assess the extent of which the engrafted LMS PDX models retain their LMS subtype identity, the abundance of smooth muscle associated proteins such as caldesmon, desmin, vinculin and vimentin were compared to LMS patient tumour specimens. These four markers were identified in every patient tissue and each LMS PDX model and for each of these markers, there was no significant difference in abundance between patient tissue and PDX tumours, showing that these models retain smooth muscle identity indicative of LMS (**Figure 3.9A**). Next, to further assess the biological differences between patient tumours and the engrafted PDX models, a SAM analysis was conducted to identify the proteins which show a significant difference in abundance between these two groups. Analysis of hallmark gene sets enriched in PDX models or patient tissue via g:Profiler over-representation analysis found that PDX tumours have elevated levels of proteins associated with E2F targets, G2M checkpoint and mTORC1 signalling (**Figure 3.9B**). Patient tissue instead showed elevated proteins especially associated with xenobiotic metabolism, the reactive oxygen species pathway, peroxisomes, adipogenesis and the complement pathway (**Figure 3.9B**)
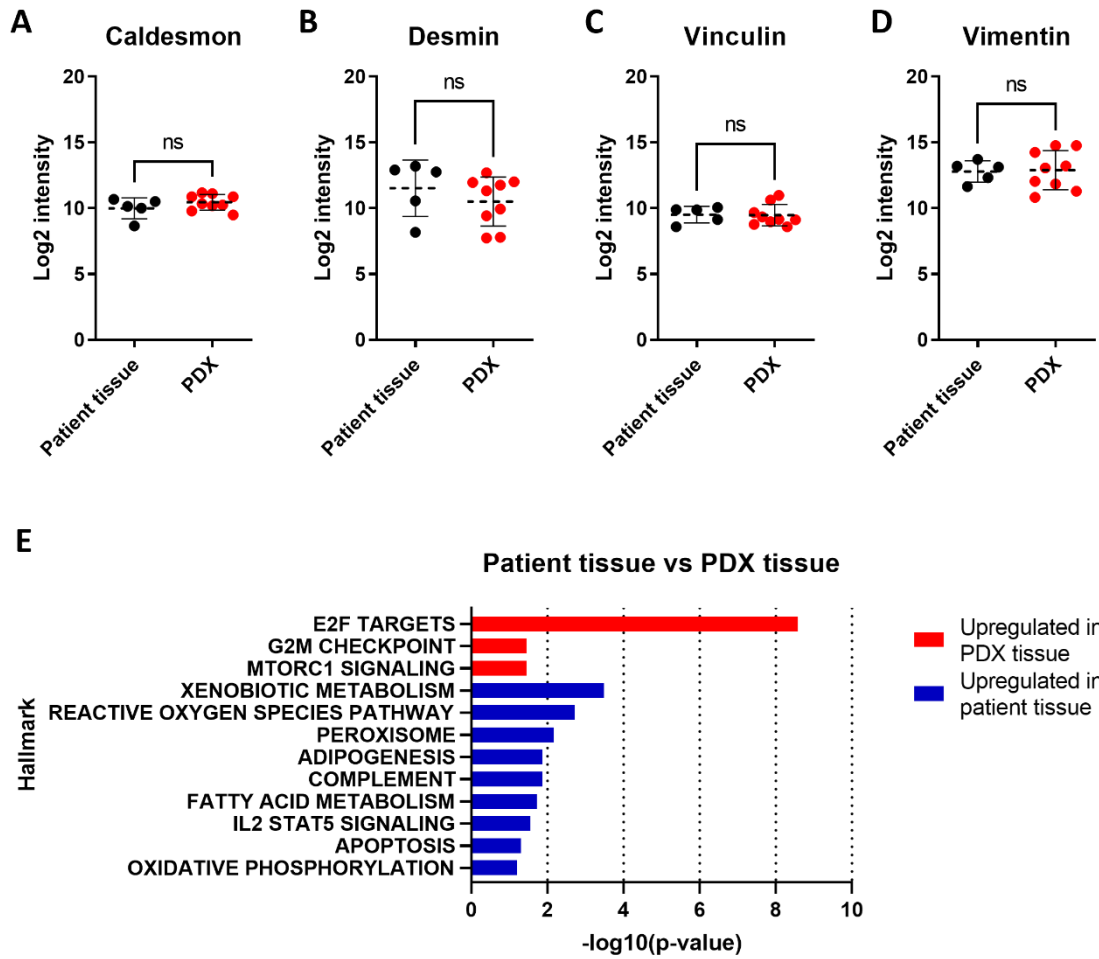
Figure 3.9. Proteomic comparison of LMS patient tumour and PDX model FFPE tissue. Log2 intensity values of smooth muscle associated proteins (A) caldesmon, (B) desmin, (C) vinculin and (D) vimentin in patient or PDX FFPE tissues. (E) Over-representation analysis plot showing hallmark pathways upregulated in PDX tissue (red) and in patient tissue (blue) after mutual comparison. Mass spectrometry data was acquired and processed via DIA-NN by Yuen Bun Tam, Madhumeeta Chadha. DIA-NN output data was further processed by myself to assess log2 protein abundance. SAM and enrichment analysis was conducted by myself.

3.6 Discussion

Chapter 3 Describes the successful engraftment of 18 biopsy samples from advanced metastatic STS patients as part of the GEMMK and APPLE clinical trials. Of these 18 successfully engrafted biopsies, 12 resulted in fully established PDX models, with maintained growth over at least two passages at the time of this report. Some PDX models have not yet been passaged twice and are therefore not included as part of the established PDX number reported, but do show continuous growth. Accounting for this, an establishment rate of 32% for all subtypes included in this study or 35% for LMS specifically was reported which is very similar to previous studies which have generated PDX models from patient resection tissue (Hemming et al. 2022; Cornillie et al. 2019). Therefore , the data presented in this chapter demonstrates that biopsy tissue engraftment is a viable and equally effective method for STS PDX generation compared to surgical tissue engraftment, expanding on the amount of source material which can be used for PDX pipelines. Additionally, two pairs of patient matched PDXs were fully established in this study from pre- and post-/on treatment biopsies demonstrating that the generation of patient matched STS models at multiple timepoints is also feasible. Previous studies have reported lower establishment rates of PDX models from treated patients compared to treatment naïve patients however the results in this chapter show no significant correlation between treatment history and PDX establishment rate (Cornillie et al. 2019; Hajdu et al. 1981).

Several studies have used PDX models of STS for pre-clinical drug testing and also as patient-specific avatars to inform treatment which has led to direct clinical benefit in an LMS patient (Stebbing et al. 2014; Schoffski et al. 2019). However, by demonstrating that STS PDX generation from biopsy samples is feasible with comparative rates of establishment to surgical tissue and no significant impact of treatment on take rates, this study encourages future work to generate patient matched PDX models at various clinical stages of treatment pathway. These models would allow for analysis of changing drug response phenotypes and molecular characteristic of tumours at each of these disease timepoints Although, a caveat to this is that patient response data is not yet available for the biopsy tissues presented in this chapter. Therefore, PDXs generated from pre- or on-treatment biopsies may enrich for tumours showing poor response to treatment.

As PDX models are more likely to be established from patients with higher grade tumours or from patients who develop metastases, PDX panels are often enriched for models of more aggressive tumours (Cornillie et al. 2019; Stebbing et al. 2014; Hemming et al.

2022). Many of these studies report subcutaneous PDX generation, which might explain why aggressive tumours are more easily able to adjust to this heterotopic environment compared to lower grade tumours. Future work on this chapter could therefore consider PDX generation via orthotopic implantation in order to potentially allow for the growth of less aggressive tumour models. Orthotopic LMS PDXs could also be utilised to model mechanisms of metastatic transformation or local invasion (Zhiying Zhang et al. 2019).

The panel of PDX models shown in this chapter reveals a range of growth rates with tumour doubling times ranging from approximately 6 to 33 days, or 10 to 33 days for LMS models in particular, which is comparable to growth rates of previously reported PDX LMS models established from patient resections (Cornillie et al. 2019; Hemming et al. 2022; Cuppens, Depreeuw, et al. 2017). Additionally, several of these PDX models with variable growth rates were established from grade 3 biopsies, while patient matched PDXs demonstrated similar doubling times, suggesting these PDX models represent patient to patient growth kinetics, not necessarily dependent on tumour grade. A wide variation of PDX growth rates between different models is important when conducting pre-clinical assessment of drug response in cancers which can demonstrate varying tumour growth characteristics such as LMS, due to the differential targeting of fast or slow cycling cancer cells with certain anti-cancer agents (Anderson et al. 2021; Bathan et al. 2013; Abdolahi et al. 2022; Brownhill, Cohen, and Burchill 2014; Bonetti et al. 1996).

Unfortunately, further passaging beyond P2 was not possible at the time of this report although future work should assess the growth and histology of higher passages as shown in other PDX LMS models in order to determine feasibility for *in vivo* drug treatment experiments which require many PDX tumours with exact growth rates (Cornillie et al. 2019). Histological characterisation of the engrafted PDX models showed that these models clearly retain patient-specific histological identity while representing different extent of smooth muscle differentiation ranging from PDXs with well differentiated histology to LMS PDXs with poorly differentiated and de-differentiated histology. This range of histology is commonly seen in LMS tumours and therefore demonstrates that the panel of engrafted PDX models captures the histological variation of LMS (Demicco et al. 2015; E. Chen, O'Connell, and Fletcher 2011).

One drawback of this study was that some PDX models had to be passaged via dissociated cell inoculation instead of tumour passage which was predicted to cause some loss of intra-tumoural heterogeneity via clone selection *ex vivo*. However, upon inoculation, some of the PDX models were able to show similar growth rates to prior passages which suggests that these particular models have stabilised, robust growth

rates. Additionally, inoculated PDX models demonstrated an almost identical histology to the initial PDXs which was also retained upon a successive tumour passage, showing that inoculation of dissociated PDX tissue does not alter the histology of PDX tissues and can still lead to fully established PDX models which represent patient tumours. However, future work for this chapter should investigate any possible loss of intra-tumoural heterogeneity in terms of biomarker expression and also investigate any genetic drift or changes in proteomic profiles which may have occurred. One caveat for the characterisation of the PDX models presented in this chapter is that the patient tumours were archival samples and not taken at the same timepoint when the biopsy for PDX establishment was taken. This may explain the stark histological difference between SARC-431 and the respective patient tissue sample. Therefore, to more accurately compare patient tumour to PDX model in the future, the biopsy samples at the same timepoints will also undergo molecular profiling and histological assessment.

Proteomic analysis of the LMS PDX models compared to a previously generated dataset showed that PDX models have a distinct proteome compared to STS patient samples including LMS patient specimens, although, LMS PDX models are most similar to LMS patient specimens and not other STS subtypes, indicating that the PDX models have not undergone substantial changes in subtype identity. When comparing LMS PDX models and the patient tumours from which they were derived from, a high fidelity of biomarker expression was seen. Caldesmon and desmin are diagnostic LMS markers, however there is no one LMS specific marker, therefore diagnosis usually consists of IHC staining for several markers which are known to be enriched in smooth muscle (Demicco et al. 2015; Oliva 2015; K. Watanabe et al. 2000). Vimentin is a marker of mesenchymal tissue while vinculin has also demonstrated expression in LMS in previous profiling studies (Tian et al. 2013; Kirik et al. 2014). Based on the similarity of these markers and histology shown in this chapter, the PDXs derived from LMS patients can be considered as models of the LMS subtype. However, LMS PDX models did show elevated levels of proteins associated with E2F targets which are mainly involved in DNA replication as well as proteins associated with G2M checkpoint (Oshi et al. 2020; H. Wang et al. 2020). Together this indicates that PDX models are undergoing enhanced proliferation compared to patient tissue. In contrast, patient LMS tissue was enriched in proteins associated with metabolic hallmarks including reactive oxygen species, fatty acid metabolism and oxidative phosphorylation which is consistent with previous reports showing that xenograft models can display differing metabolomic profiles compared to patient tissue (Z. Chen et al. 2021; Forrester et al. 2018; Jun et al. 2018). Additionally, patient tissue showed an enrichment for proteins associated with the complement

pathway and interleukin-2 (IL2)- Signal transducer and activator of transcription 5 (STAT5) signalling which are immune based pathways, therefore the loss of these pathways is consistent with the use of immunodeficient mouse models for PDX growth (D. M. Jones, Read, and Oestreich 2020; M. K. Verma et al. 2017).

In summary, this chapter describes the successful engraftment and establishment of a panel of LMS PDX models from pre- and post-treatment biopsy tissue which showed high histological and proteomic fidelity to patient tissues, also encapsulating patient to patient histological variability within the LMS subtype. WES is currently being conducted in order to assess if genome wide copy number alterations are maintained in the PDX models compared to the patient tumours and if these PDX models undergo genetic drift after successive passaging. Whole exome sequencing will also be conducted to reveal the distribution of frequently altered genes in LMS, such as *PTEN, TP53* and *RB1*, showing whether these can be maintained in PDX models and what, if any mutations are consistently lost or gained in PDX LMS models compared to patient tissue.

Chapter 4 - Establishment and characterisation of PDX-derived LMS in vitro cultures

4.1 Introduction

The assessment of candidate targets via high-throughput drug screening or large-scale functional genetic screens is often the first stage of cancer drug discovery, followed by phenotypic and biochemical assessment of drug response before validation *in vivo,* leading into clinical trials (Honkala et al. 2021)**.** Commercially available, immortalised cancer cell lines are widely used pre-clinical models to identify candidate targets due to the low cost, ease of procurement and handling, as well as high reproducibility (Capes-Davis et al. 2010; Kaur and Dufour 2012). However, the long-term growth of cell lines *in vitro* induces altered gene expression while selecting for sub clonal populations, therefore leading to altered therapeutic responses with a poor correlation to molecular phenotypes of patient tumours (Cree, Glaysher, and Harvey 2010; Rey et al. 2019). Additionally, most commercially available cell lines have undergone spontaneous or engineered genetic alterations to enable indefinite culture and further genetic drift can occur over years of continuous culture, therefore such cell cultures might not be an accurate representation of the disease they originally derived from (Kaur and Dufour 2012). For LMS, as with the majority of STS subtypes, there are few commercially available cell lines and due to the inter-patient heterogeneity within subtypes such as LMS, leads to the underrepresentation of patient-to-patient variability (Hattori, Oyama, and Kondo 2019). Therefore, there is an urgent need to establish more STS pre-clinical models which can represent a range of patient tumour characteristics.

Several studies have reported the successful establishment of primary cell lines directly from STS patient resection tissue which maintains the cellular and molecular heterogeneity of the patient tumour (M. Hu et al. 2002; Salawu et al. 2016)**.** However, the generation of cultures from biopsy tissue is challenging due to small sample size. Therefore, the initial generation of PDX models from biopsy samples allows for tissue expansion prior to culture of PDX-derived cells**.** In contrast to immortalised cell lines, PDX-derived cell cultures are more clinically relevant models. Such models have been shown to recapitulate the cellular and molecular heterogeneity of the patient tumour and subsequent PDX (Manzella et al. 2020). Establishing PDX-derived cultures creates patient-specific models often accompanied by clinical information each of which should be considered when observing and comparing molecular profiles (Brodin et al. 2019)**.**

In order to establish primary cell cultures, assessing the optimal growth conditions is important so as not to influence the results of *in vitro* assays. A panel of rhabdomyosarcoma PDX models were dissociated and cultured in a variety of different conditions including differing media with or without growth factors such as EGF or bFGF

which have previously been shown to allow for tumour stem cell cultures which closely mirror the phenotype of primary tumours (J. Lee et al. 2006). Interestingly, subgroups of RMS cultures were identified to have their own optimal culture condition, assessed by proliferation, viability and degree of differentiation. Growth factor addition induced an increase or decrease in proliferation depending on the cell model culture, and a higher proportion of contaminating mouse cell expansion was observed in DMEM supported cultures, highlighting the importance of cell culture media optimisation for the cell type of interest. Furthermore, for difficult to culture PDX cells, the use of DMEM/F12 medium containing the ROCK inhibitor Y-27632 was sufficient to allow for proliferation and establishment of primary cell lines (Manzella et al. 2020).

ROCK inhibitors such as Y-27632 have been shown previously to aid in the plating efficiency of induced pluripotent and embryonic stem cells, maintaining stem cell markers compared to culture without ROCK inhibitors. Y-27632 supplemented media also decreased apoptosis during cell passaging via the reduction of anoikis (detachment induced apoptosis) (Vernardis et al. 2017; Kiichi Watanabe et al. 2007). Y-27632 has since been used to establish and expand primary cultures for several cancer types such as glioblastoma and colorectal cancer while maintaining cell populations expressing cancer stem cell markers (Tilson et al. 2015; Miyoshi et al. 2018). Additionally, ROCK inhibitor treatment with fibroblast feeder cells is used frequently for conditional reprogramming of epithelial cells, inducing indefinite proliferation *in vitro* of both tumour and normal epithelial cells. Importantly, this conditional reprogramming does not induce immortalisation via transformation as normal cells expanded by this method retain a normal karyotype (X. Liu et al. 2012).

In this chapter, a PDX-derived cell culture pipeline was initially optimised and then implemented using LMS PDX tumour tissue described in **chapter 3** in order to expand the number of clinically relevant, novel, LMS pre-clinical models. Three long-term PDX-derived LMS cultures were established as well as 2 short-term cultures. These cultures were phenotypically characterised and molecular profiles were compared to the patient tumour and subsequent PDX of origin.

4.2 Optimising a PDX derived in vitro culture pipeline from a synovial sarcoma model

In order to generate primary STS cell lines I began with optimising a pipeline for the culture of PDX-derived cells to show a proof-of-principle. This was done using a synovial sarcoma PDX model J000104314 which was acquired from The Jackson Laboratory (http://tumor.informatics.jax.org/mtbwi/pdxDetails.do?modelID=J000104314). PDX growth in NGS mice was assessed after an initial passage from the mouse received from The Jackson Laboratory and showed a doubling time of 14.06 days, as fitted to an exponential growth equation (**Figure 4.1A**)**.** This PDX showed a histology consistent with monophasic synovial sarcoma, presenting with hypercellular fascicular of spindle cells with little stroma and monotonous nuclei (**Figure 4.1B**)**.** Once tumours reached 1000mm^3 in size, they were harvested and dissociated by mincing followed by incubation in collagenase containing media. Dissociated cells were mouse cell depleted and then cultured as monolayer cells in Y-media, which contains the ROCK inhibitor Y-27632 or DMEM based media. Y-media was included due to the successful establishment of other PDX-derived cell cultures which have been reported at the ICR using this media. Upon initiation of primary culture, DMEM cultured cells showed adherence and initially proliferated but entered senescence soon after (data not shown) while Y-media allowed the outgrowth of proliferative cells. Therefore, Y-media based cultures were pursued further**.** Dissociated J000104314 cells proliferated in 2D culture with a spindle cell morphology for at least 18 passages over 4 months (**Figure 4.1C**) and could also aggregate to form spheroids after 3 days in low attachment wells (**Figure 4.1D**). Once cultures were passaged over 10 times, these monolayer cells were named ICR-SS-1. To begin characterisation, I evaluated the growth rate of ICR-SS-S over 14 days which showed an exponential growth pattern and a doubling time of 92 hours (**Figure 4.1E**)
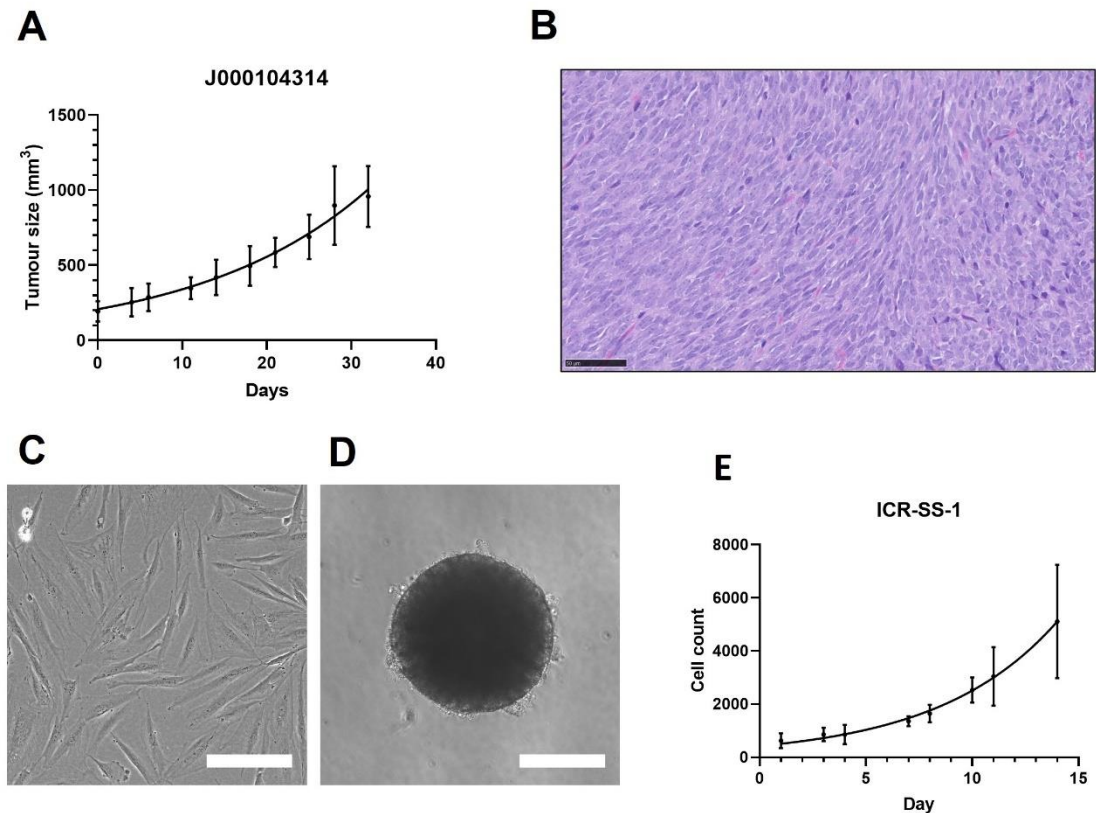
Figure 4.1 Synovial sarcoma PDX and established PDX-derived cell line. (A) Tumour growth of J000104314 PDX model. N=5. (B) H&E stain of J000104314 PDX tumour. Scale bar = 50 µm. 20x magnification. (C) Phase contrast image of ICR-SS-1 cells in monolayer culture. Scale bar = 200 µm. (D) Brightfield image of ICR-SS-1 spheroid. Scale bar = 200 µm. (E) Cell count of ICR-SS-1 cells over a period of 14 days. N=3.

Almost all synovial sarcomas harbour the pathognomonic translocation t(X;18)(p11;q11) which causes the fusion of *SS18* on chromosome 18 to either *SSX1*, *SSX2* or *SSX4* on chromosome X (Jungbluth et al. 2001). The PDX J000104314 was reported to harbour the specific translocation *SS18:SSX1*, therefore PCR was used to confirm the presence of this specific translocation in PDX tissue and subsequent PDX derived cell line. To do this a common forward primer within the *SS18* gene and reverse primers within the *SSX1, SSX2* and *SSX4* genes were used to amplify cDNA from the PDX tumour, ICR-SS-1 and also HS-SY-II which acts as a positive control of the SS18:SSX1 translocation. *Actin* was also amplified to confirm if cDNA synthesis occurred correctly. If a translocation is present between *SS18* and *SSX1, SSX2* or *SSX4*, a PCR transcript of 108bp will be produced. Following gel electrophoresis, a band of 108bp can be seen from HS-SY-II template cDNA reaction containing *SS18* and *SSX1* primers (**Figure 4.2A**)

as well as the PCR reactions containing ICR-SS-1 or J000104314 tumour cDNA. No bands were observed in the PCR reactions where SS18 and SSX2 or SSX4 primers were used for any of the cDNA samples confirming that the ICR-SS-1 retains the characteristic synovial sarcoma translocation found in the PDX tumour.

Early contamination of the primary cultures with fast growing fibroblasts was observed upon culturing J000104314 cells which were removed via differential trypsinisation and repeated EDTA washes. Mouse fibroblast contamination has been frequently noted in studies culturing primary cells from PDX models (Manzella et al. 2020; Domenici et al. 2021). However, differentiating between these fibroblasts and the synovial sarcoma cells was challenging due to the mesenchymal, spindle-like morphology of both cell types. To confirm that the ICR-SS-1 PDX-derived cell line did not contain any contaminating mouse fibroblasts, a PCR protocol was used to amplify the *PTGER2* gene with human or mouse specific primers (Alcoser et al. 2011). The human LMS cell line SK-UT-1 was used as a positive control for human DNA and a negative control of mouse DNA and vice versa for the murine line NIH-3T3. Gel electrophoresis of the PCR products shows a clear band from ICR-SS-1 DNA with human primers but no band when murine specific primers are used instead, indicating this established cell line does not contain murine fibroblast contamination (**Figure 4.2B**).
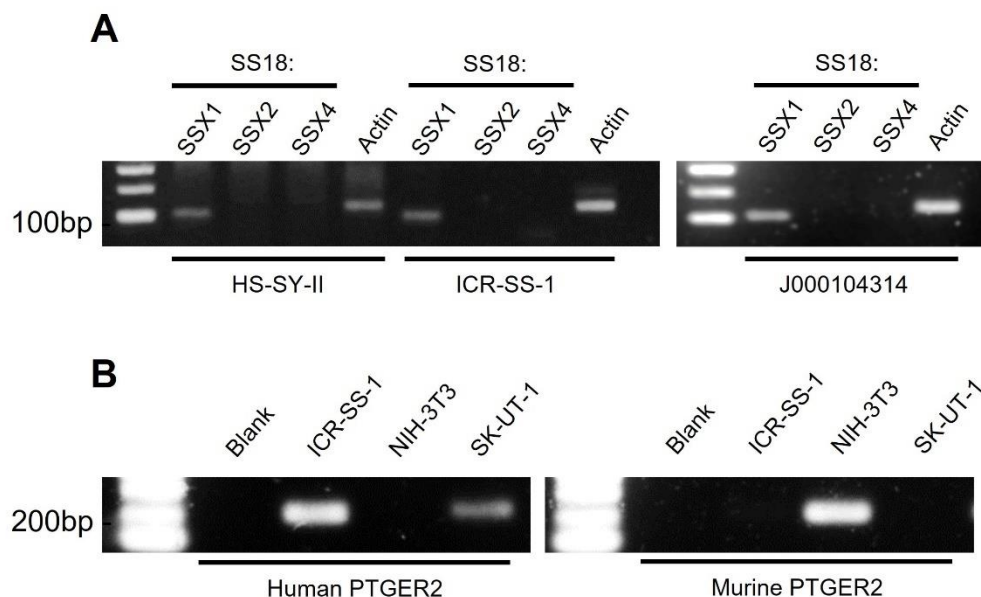
Figure 4.2. Validation of ICR-SS-1 gene fusion and human origin. (A) PCR analysis of SS18::SSX1, SSX2 or SSX4 gene fusions in ICR-SS-1 and respective PDX tissue from J000104314. HS-SY-II is a positive control of SS18::SSX1 fusion. (B) PCR analysis of human and murine PTGER2 in ICR-SS-1 compared to murine positive control NIH-3T3 and human positive control SK-UT-1.

Next, short-tandem repeat (STR) profiling was conducted in order to compare with the tissue of origin and rule out contamination with other human cell lines while checking genetic similarity. Indeed, DNA extracted from J000104314 and ICR-SS-1 have an identical STR profile, confirming that ICR-SS-1 is a biological derivative of J000104314 and has not undergone substantial genetic drift (**Table 4.1**)

Locus	J000104314	ICR-SS-1
D8S1179	13, 13	13, 13
D21S11	29, 31.2	29, 31.2
D7S820	7, 8	7, 8
CSF1PO	10, 12	10, 12
D3S1358	17, 17	17, 17
TH01	6, 9.3	6, 9.3
D13S317	12, 14	12, 14
D16S539	9, 12	9, 12
D2S1338	20, 23	20, 23
D19S433	13, 15	13, 15
vWA	16, 16	16, 16
TPOX	8, 9	8, 9
D18S51	12, 15	12, 15
AMEL	X, Y	X, Y
D5S818	11, 13	11, 13
FGA	24, 24	24, 24
% Similarity	100%	

Table 4.1. STR profiling of J000104314 PDX tumour and PDX-derived ICR-SS-1 culture. STR loci of J000104314 PDX tumour and ICR-SS-1 cell culture. STR; Short Tandem Repeat.

We have previously conducted proteomic profiling of FFPE tumour specimens from a cohort of STS patients (n=36) consisting of four histological subtypes, including synovial sarcoma, LMS, UPS and DDLPS which revealed that different STS subtypes can have distinct proteomic profiles (Milighetti et al. 2021). In order to assess if ICR-SS-1 can recapitulate the molecular profile of human synovial sarcoma tissues, the PDX-derived cell line as well as SYO-1 and HS-SY-II was subjected to proteomic analysis via sequential window of acquisition of all theoretical fragment ion spectra (SWATH) mass spectrometry by a post-doctoral fellow in the lab, Lukas Krasny. These profiles were

integrated with the cohort of 36 patients across 4,336 proteins and subjected to hierarchical clustering, revealing that the synovial sarcoma cell lines, including ICR-SS-1, clustered closely with synovial sarcoma patient tissue but were separate from LMS, UPS and DDLPS patient tissue. This result suggests that ICR-SS-1 can faithfully capitulate the molecular features of synovial sarcoma found in patient samples and is distinct from other STS subtypes (**Figure 4.3**).
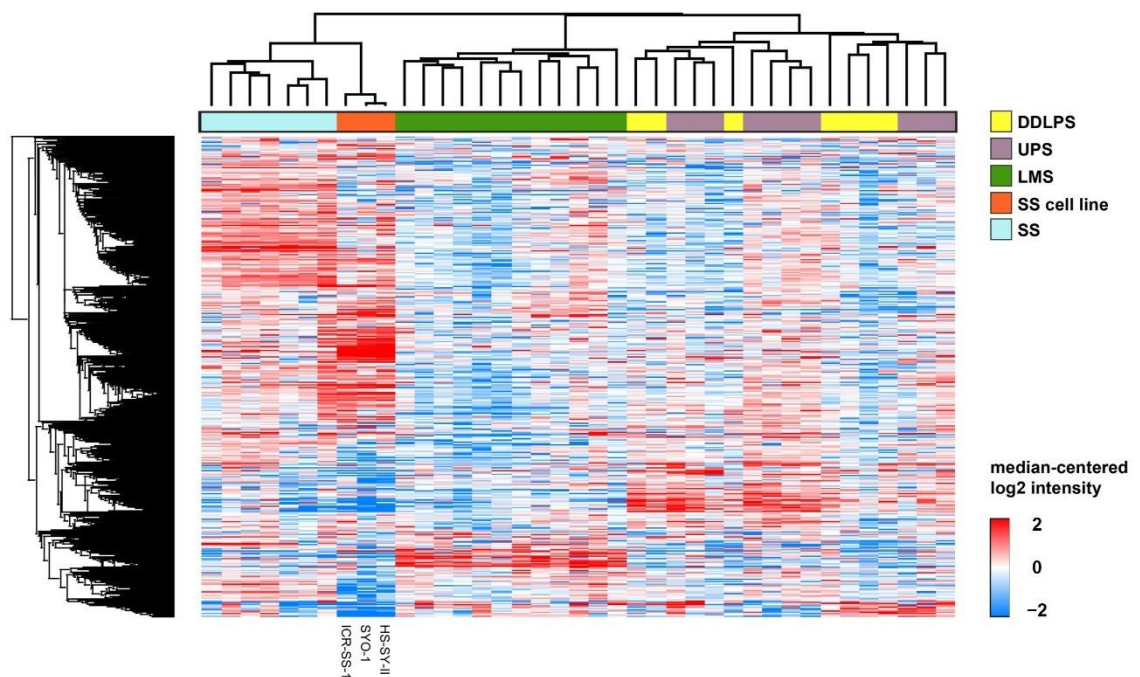
Figure 4.3. Proteomic profiles of ICR-SS-1, synovial cell lines and STS tumours. Heatmap showing hierarchical clustering of proteomic data from synovial sarcoma cell lines, patient tissue from DDLPS (dedifferentiated liposarcoma), UPS (undifferentiated pleomorphic sarcoma), LMS (Leiomyosarcoma) and SS (synovial sarcoma) subtypes. Clustering was achieved by two-way unsupervised clustering based on Pearson's correlation coefficient. Mass spectrometry data was acquired and processed via DIA-NN by Lukas Krasny and Martina Milighetti. DIA-NN output data was further processed by myself to generate a heatmap of normalised proteomic profiles.A

Some differences were observed in the proteomic profiles of the synovial sarcoma cells and patient samples (**Figure 4.3**). To identify the proteins which show a significant difference between the synovial sarcoma cell lines and patient tissue SAM analysis was conducted followed by over-representation analysis via g:Profiler. This analysis revealed that protein translation, biosynthesis and metabolism processes were significantly enriched in synovial sarcoma patient tissue compared to the cell lines which included "cytoplasmic translation", "peptide biosynthetic", "peptide metabolic" and "amide

biosynthesis" labelled ontologies (**Figure 4.4A**). Meanwhile, biological processes enriched in cell lines included lipoprotein particle clearance and RNA splicing.

To understand the differences between the PDX-derived cell line ICR-SS-1 and the commercially available synovial cell lines SYO-1 and HS-SY-II, a SAM analysis was performed to identify the proteins showing a significant difference between the two. Over-representation analysis was then used to show that ICR-SS-1 cells were enriched for proteins involved in mesenchymal to epithelial transition, while the commercially available synovial lines were enriched in proteins associated with E2F targets, demonstrating that ICR-SS-1 and synovial sarcoma cell lines have distinct biological processes (**Figure 4.4B**).
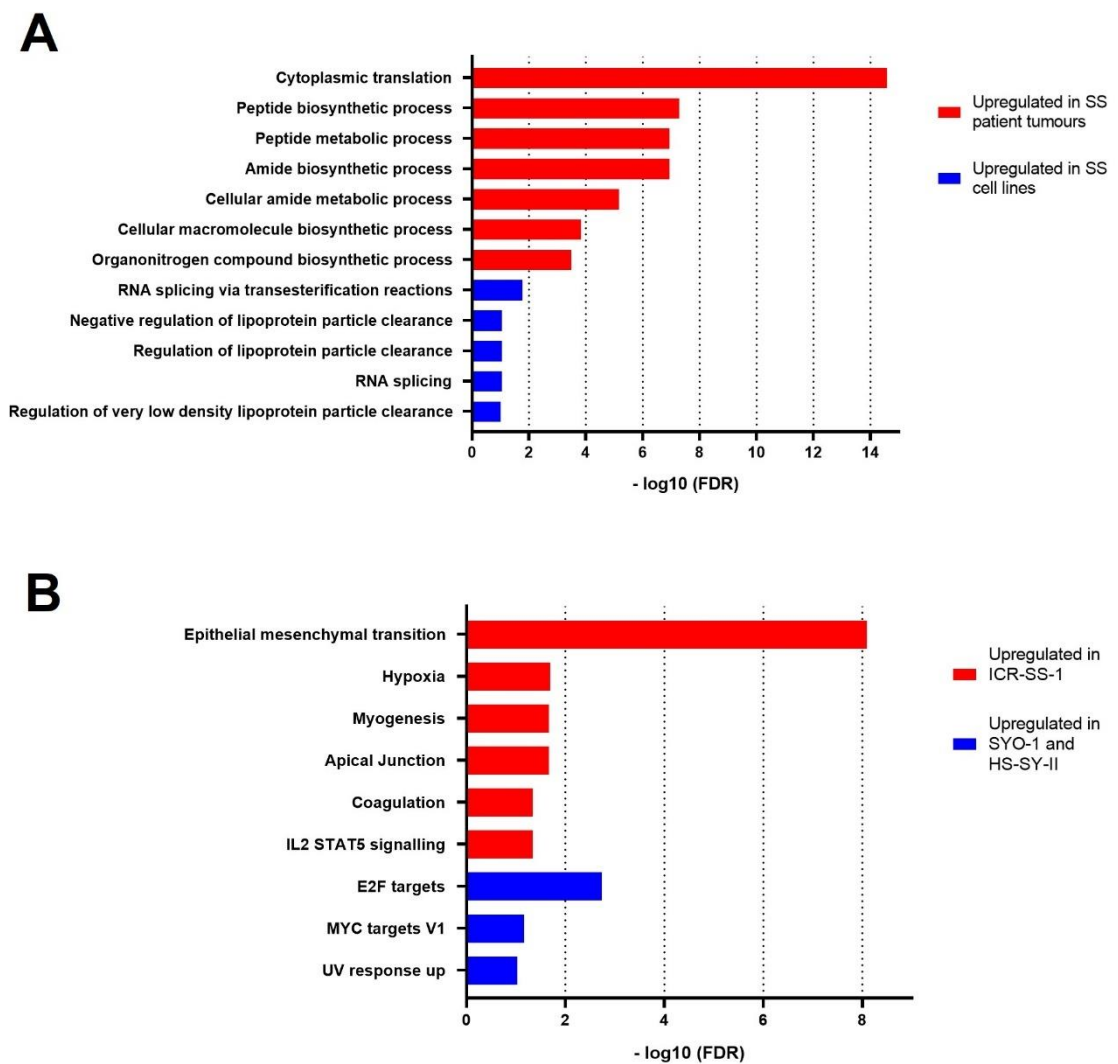
Figure 4.4. Proteomic comparison of ICR-SS-1, synovial sarcoma cell lines, and patient samples. (A) Over-representation analysis plot of specific biological processes which show upregulation in synovial

sarcoma patient tumours (red) or cell lines (blue) following a mutual comparison. (B) Over-representation analysis plot of hallmark pathways which show upregulation in ICR-SS-1 (red) and those upregulated in synovial sarcoma cell lines SYO-1 and HS-SY-II (blue). FDR; False Discovery Rate, SS; Synovial sarcoma. Mass spectrometry data was acquired and processed via DIA-NN by Lukas Krasny and Martina Milighetti. DIA-NN output data was further processed by myself to assess log2 protein abundance. SAM and enrichment analysis was conducted by myself.

Following proteomic characterisation of ICR-SS-1, I sought to assess the response of this cell line to the anthracycline doxorubicin, which is a first line standard of care chemotherapy for the vast majority of STS, including synovial sarcoma. ICR-SS-1 was significantly more resistant to doxorubicin (ICR-SS-1 IC50=613 ±299nM) compared to SYO-1 and HS-SY-II (SYO-1 IC50 = 13 ± 1nM, HS-SY-II IC50 = 31 ±14) (p<0.01) (**Figure 4.5A**). Response to pazopanib was also assessed in these cell models as this is the only approved tyrosine kinase inhibitor (TKI) approved for use in synovial sarcoma patients following progression on first line chemotherapy. All three tested cell lines were resistant to this therapy, showing an IC50 value > 5µM (**Figure 4.5B**). In order to identify therapeutic vulnerabilities ICR-SS-1, SYO-1 and HS-SY-II were all exposed to a small molecule inhibitor screen consisting of 58 small molecules, designed in house to target a range of oncogenic signalling pathways **(methods section)**. Overall, ICR-SS-1 shows a distinct drug response profile compared to SYO-1 and HS-SY-II and is more resistant to the majority of the small molecule inhibitors tested (**Figure 4.5C**). Assessment of shared vulnerabilities from the drug screen identified three compounds: the dual PI3K and mTOR inhibitor NVP-BEZ235, the polo-like kinase 1 (PLK1) inhibitor BI 2536 and the Bromo- and extra-terminal domain (BET) bromodomain inhibitor JQ1 (**Figure 4.5D**), suggesting that targeting these pathways might lead to a therapeutic benefit in synovial sarcoma.
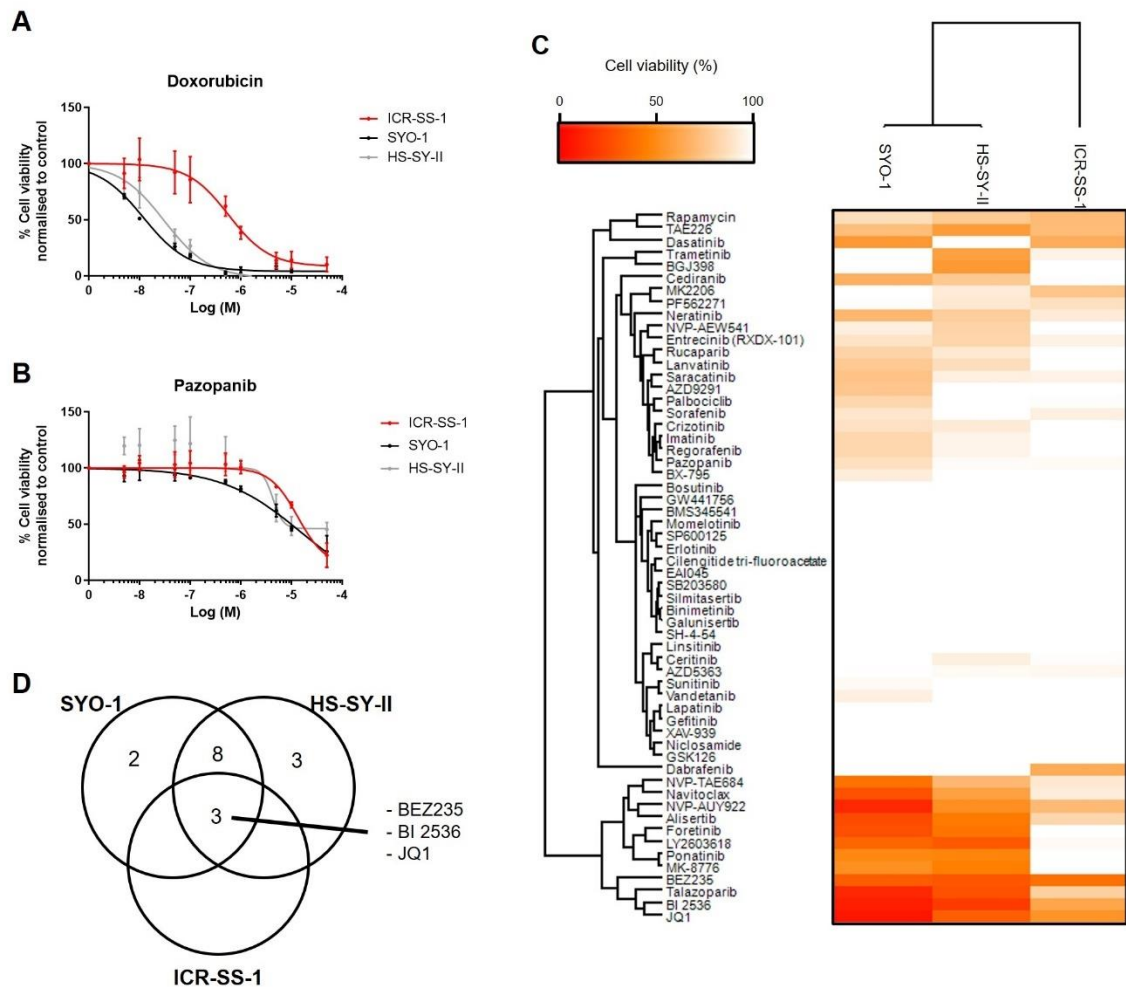
Figure 4.5. Drug response phenotypes of ICR-SS-1 compared to SYO-1 and HS-SY-II. (A) Dose response curves of ICR-SS-1, SYO-1 and HS-SY-II cells treated with increasing doses of doxorubicin. N=3. (B) Dose response curves ICR-SS-1, SYO-1 and HS-SY-II cells treated with increasing doses of pazopanib. N=3. (C) Cell viability heatmap of ICR-SS-1, SYO-1 and HS-SY-II cells treated with a targeted panel of 58 small molecule inhibitors at a concentration of 500 nM or 50 nM for NVP-AUY922. N=3. (D) Venn diagram of shared and distinct targeted inhibitor sensitivities when a cut-off of 65% is applied to ICR-SS-1, SYO-1 and HS-SY-II cells.

4.3 Establishing PDX derived LMS in vitro cultures

Following the successful implementation of a primary cell culture pipeline from a synovial sarcoma PDX model, I then sought to implement this workflow with the novel LMS PDX models generated in **Chapter 3** in order to establish and characterise a panel of LMS PDX-derived cell lines which will be used for assessing drug targets, biochemical analysis of response and resistance mechanisms (**Figure 4.6**).
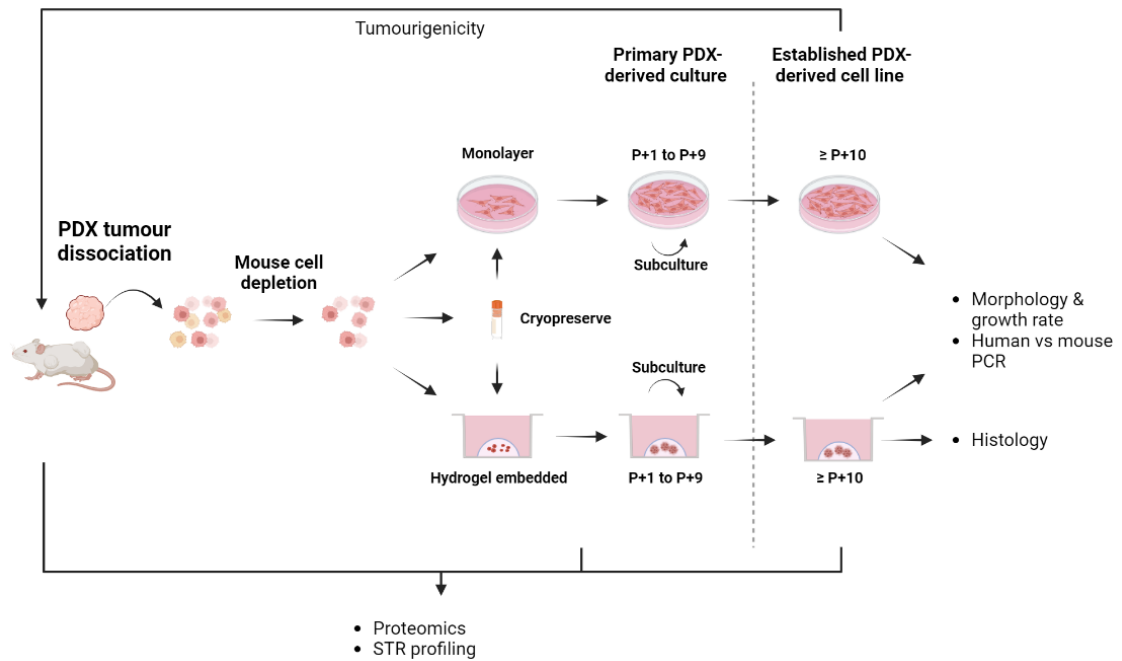
Figure 4.6. PDX-derived in vitro culture pipeline overview. PDX tumours were dissociated and mouse cells depleted to enrich for human cells. Dissociated cells were cultured in monolayer or hydrogel embedded conditions and were also cryopreserved. Following growth in vitro, subcultures from P+1 to P+9 were considered primary cultures and cells continuing to grow over P+10 were considered established PDX-derived cell lines. These lines were used for morphological, histological and growth rate characterisation as well as human cell authentication and were inoculated into immunocompromised mice to test tumorigenicity. Proteomic and STR profiling was conducted on PDX tissue, respective primary cultures and established cell lines. PCR; Polymerase Chain Reaction, PDX; Patient-Derived Xenograft, P+1; Passage 1, P+9; Passage 9, P+10; Passage 10, STR; Short Tandem Repeat.

Cell culture was attempted from a total of 12 dissociated LMS PDX lines after mouse cell depletion via magnetic bead separation and, where necessary, mouse cell depletion of cultures was repeated to ensure the absence of contaminating mouse stromal cells (**Figure 4.7**). To identify the optimal culture conditions supporting cell proliferation, dissociated cells were cultured initially in several different conditions including Matrigel coated flasks or non-coated flasks, in Y-media, with or without the addition of PDGF and bFGF. Matrigel coating has been shown to support the growth of primary cell cultures for several cancer types (Kleinman and Martin 2005) while PDGF and bFGF growth factors can stimulate the growth of fibroblasts and mesenchymal derived cells *in vivo* (Ng et al. 2008)**,** thus both were chosen as conditions to assess in addition to monolayer culture without coating and with base Y-media. 3D matrigel embedded organoid-like cultures were also attempted with dissociated cells (**Figure 4.6-Figure 4.7**). Following dissociation of PDX tissue, cells were either used fresh for culture or viably frozen and

thawed at a later date for establishing cultures (**Figure 4.6**). Cultures which demonstrated outgrowth of cells which continued upon subculture were considered as proliferative primary cells. Some PDX tissue showed proliferative colonies in multiple conditions although some conditions lead to faster growth or showed cell outgrowth earlier (**Figure 4.7**). A total of 5 LMS PDX models were able to grow *in vitro* as monolayer cultures and one LMS PDX model was also able to expand in 3D matrigel embedded organoid-like condition and are listed in **Table 4.2**.

| Model | 2D | | | | 3D | |
| | Uncoated | | Coated | | | |
	Y	Y & GF	Y	Y & GF	Y	Y & GF
SARC-322	Red	Red	Red	Red	Red	Red
SARC-323	Red	Red	Red	Dark green	Red	Red
SARC-356	Red	Red	Red	Red	Red	Red
SARC-369	Dark green	Dark green	Light green	Light green	Dark green	Dark green
SARC-376	Red	Red	Red	Red	Red	Red
SARC-389	Red	Red	Red	Red	Grey	Grey
SARC-393	Dark green	Light green	Light green	Light green	Grey	Grey
SARC-400	Red	Blue	Red	Blue	Red	Blue
SARC-401	Dark green	Dark green	Light green	Light green	Red	Red
SARC-409	Dark green	Dark green	Light green	Light green	Grey	Grey
SARC-414	Red	Red	Red	Red	Red	Red
SARC-416	Red	Red	Red	Red	Red	Red

Legend:
- Green (dark) / Green (light): *In vitro* proliferation
- Red: No *in vitro* proliferation
- Blue: Mouse cell contaminants

Figure 4.7. In vitro growth condition screen of primary PDX-derived LMS cells. Outcomes of primary culture with dissociated LMS PDX tumours, indicating proliferation, no proliferation or proliferation that was later revealed to be mouse cell contaminants. Light green indicates cell cultures which underwent proliferation but were slower growing or took longer before outgrowth was observed compared to cultures in dark green. Cells were cultured in 2D with or without Matrigel coating. Matrigel coated, uncoated and Matrigel embedded (3D) conditions were attempted in Y-media or Y-media supplemented with PDGF and bFGF. GF; Growth factors (PDGF and bFGF), Y; Y-media. Grey denotes conditions which were not assessed.

		In vitro culture information				Respective PDX information						
Tissue ID	PDX tumour passage	Culture condition	Maximum *in vitro* passage reached	Cell line ID	Cell line doubling time (days)	Timepoint	Biopsy grade	Subtype	Site of biopsy/resection	Primary site if known	Treatment history	Trial
SARC-323	P0	2D, Y-media with PDGF & bFGF Coated	P+8			Baseline biopsy	G3	LMS	Left gluteus	Breast	Epirubicin+Cyclophosphamide in the adjuvant setting after surgery to the primary tumour; no treatment from diagnosis of metastatic disease to trial entry	GEMMK
SARC-369	P0	2D, Y-media Uncoated	≥ P+35	**ICR-LMS-1**	4.4 days	Baseline biopsy	G3	uLMS	Pelvic	Uterus	Doxorubicin (3 cycles)	
		Matrigel embedded, Y-media	≥ P+6	**ICR-LMS-3**								
SARC-400	P0	2D, Y-media with PDGF & bFGF Uncoated	P+5			Post-cycle 3 biopsy	N/A	LMS	RP	RP	Doxorubicin (2 cycles). Second-line GEMMK (Gemcitabine & pembrolizumab)	
		Matrigel embedded, Y-media with PDGF & bFGF	P+7	**ICR-LMS-5**								
SARC-401	P0	2D, Y-media Uncoated	≥ P+38	**ICR-LMS-4**	3.2 days	Baseline biopsy	G3	uLMS	Liver	Uterus	No prior treatments	
SARC-409	P0	2D, Y-media Uncoated	≥ P+16	**ICR-LMS-6**	4.2 days	Post-cycle 3 biopsy	N/A	LMS	Peritoneum	Stomach	No prior treatments. First-line GEMMK (Gemcitabine & pembrolizumab)	
SARC-393	P1	2D, Y-media Uncoated	≥ P+10			Post-RT biopsy	N/A	uLMS	Lung	Uterus	Post-RT	APPLE

Table 4.2. Primary and established PDX-derived LMS cell cultures. Overview of PDX-derived culture characteristics including PDX model information, culture condition used and maximum passage reached. Once monolayer cultures reached P+10 they were considered established cell lines and given a cell line ID. Matrigel embedded cultures were given cell line IDs at P+5. Otherwise primary cell cultures were labelled with the PDX ID from which they were derived. bFGF; Basic Fibroblast Growth Factor, G2; Grade 2, G3; Grade 3, LMS; Leiomyosarcoma, N/A; Not Available, PDGF; Platelet-Derived Growth Factor, PDX; Patient-Derived Xenograft, RP; Retroperitoneum, RT; Radiotherapy, uLMS; uterine Leiomyosarcoma.
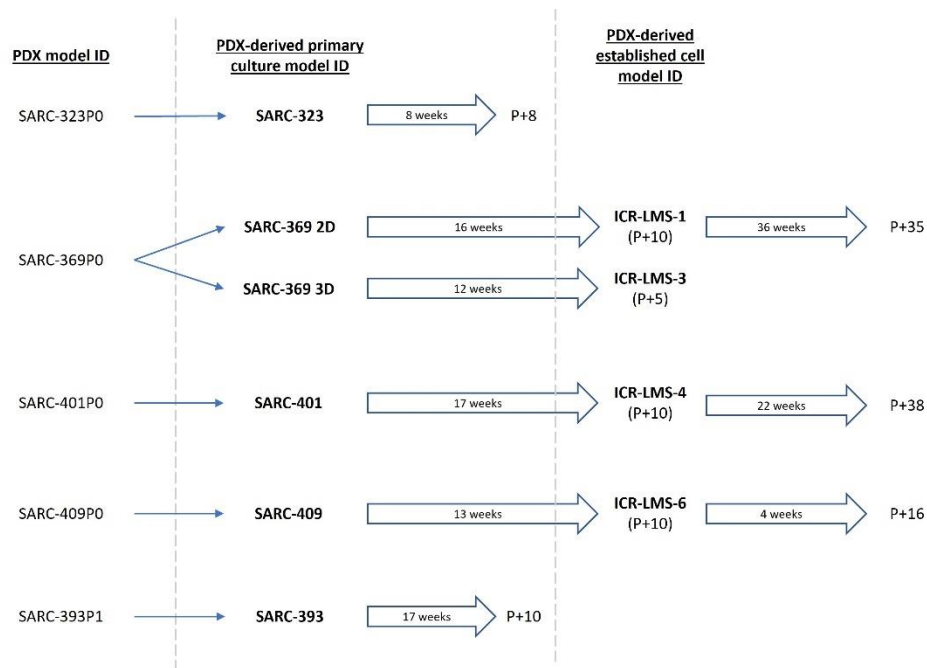
Figure 4.8. Schematic of PDX-derived cell culture models. PDXs which gave rise to short-term primary cultures or long-term established cell models showing timescales to reach highest *in vitro* passage. P0; *in vivo* passage 0, P1; *in vivo* passage 1, P+X; *in vitro passage* X.

4.3.1 ICR-LMS-1

ICR-LMS-1 was established from a P0 tumour of the uterine LMS PDX model SARC-369 (**Table 4.2)**. Dissociated, mouse cell depleted cells from this PDX were cultured for a period of five weeks under Y-media test conditions as well as DMEM based media. Adherence of the majority of cells occurred after 5 days and proliferative colonies were observed in non-coated flasks with Y-media without the addition of PDGF and bFGF after approximately 30 days (**Figure 4.9A**). Initial primary cultures of SARC-369 showed morphological heterogeneity, with proliferative spindle cells which arranged in fascicles in (**Figure 4.9A bottom**) addition to senescent, enlarged cells (**Figure 4.9A top left**) which were observed throughout the first 10 passages. Other tightly clustered colonies were observed which did not show a spindle cell morphology (**Figure 4.9A top right**). Proliferative cells were eventually observed under other tested monolayer conditions tested although growth was notably slower and cell viability assays showed DMEM cultured SARC-369 cells had lower viability compared to Y-media cultured cells (data not shown). Thus, SARC-369 cells were maintained and expanded in Y-media on non-coated flasks, cryopreserving at regular intervals.

SARC-369 cells were passaged 10 times in continuous culture for a period of approximately 16 weeks, at which point these cells were labelled ICR-LMS-1 (**Figure 4.8**). For use in subsequent assays, only cells beyond this population were labelled as ICR-LMS-1 for reproducibility. ICR-LMS-1 continued to proliferate for at least 9 months in culture, maintaining elongated spindle cell morphology of the primary cultures (**Figure 4.9B**) and have reached at least 35 passages (P+35). ICR-LMS-1 cells were able to proliferate in an exponential growth pattern, showing a doubling time of 4.4 days (**Figure 4.9C**). Additionally after viably freezing ICR-LMS-1 cells were still able to proliferate upon thawing.

Figure 4.9. Morphology and growth rate of ICR-LMS-1 cell line. (A) Phase contrast images of SARC-369 primary cell culture with 4 fields of view at *in vitro* passage 0 (P+0) after 30 days in culture, scale bar = 300

µm. (B) Phase contrast images of ICR-LMS-1 established cell line with 4 points of view at *in vitro* passage 18 (P+18), scale bar = 300 µm. (C) Cell count fold change of ICR-LMS-1 cells at *in vitro* passage 15 (P+15) over 14 days normalised to day 1, n=3, fold change measurements were fitted to a Malthusian exponential growth curve equation via GraphPad Prism. Red arrows denote areas of interest.

4.3.2 ICR-LMS-4

ICR-LMS-4 was established from a P0 tumour of the uterine LMS PDX model SARC-401 (**Table 4.2**). Dissociated, mouse cell depleted cells from this PDX were cultured for a period of five weeks in Y-media monolayer test conditions. After five days, the majority of cells adhered to the flasks in all conditions. Proliferative colonies were seen after approximately 23 days in non-coated conditions without PDGF and bFGF and showed morphological heterogeneity in terms of cell shape and also cell size (**Figure 4.10A**). The majority of cells demonstrated spindle cell morphology and were loosely clustered (**Figure 4.10A top right, bottom left**). However, there were also some tightly clustered colonies arranged in fascicular bundles (**Figure 4.10A top left**) as well as enlarged cells with elongated lamellipodia (**Figure 4.10A bottom right**) which were observed in culture throughout passages 1 to 8. Proliferative colonies were also noted in cultures with PDGF and bFGF at the same timepoint and demonstrated matching morphology to cultures without PDGF and bFGF. Cultures on Matrigel coated flasks eventually showed proliferative colonies at a later timepoint. Non-coated monolayer SARC-401 cells in Y-media without PDGF and bFGF were therefore chosen for further expansion.

Once over passage 10, after approximately 17 weeks in culture, cells were termed ICR-LMS-4 and continued to proliferate for another 22 weeks at least, reaching up to passage 38 with a total culture time of at least 8 months (**Figure 4.8**). During expansion as established cells no reduction in growth rate was observed. ICR-LMS-4 cells showed a more homogenous morphology compared to SARC-401 primary cultures although two distinct morphologies could still be observed; elongated spindle cells (**Figure 4.10B top right & bottom**) and rounded cells with visible nuclei (**Figure 4.10B top left & bottom**). ICR-LMS-4 showed exponential growth with a doubling time of 3.2 days (**Figure 4.10C**). Additionally, ICR-LMS-4 cells could be cryopreserved and thawed to continue growth *in vitro*.
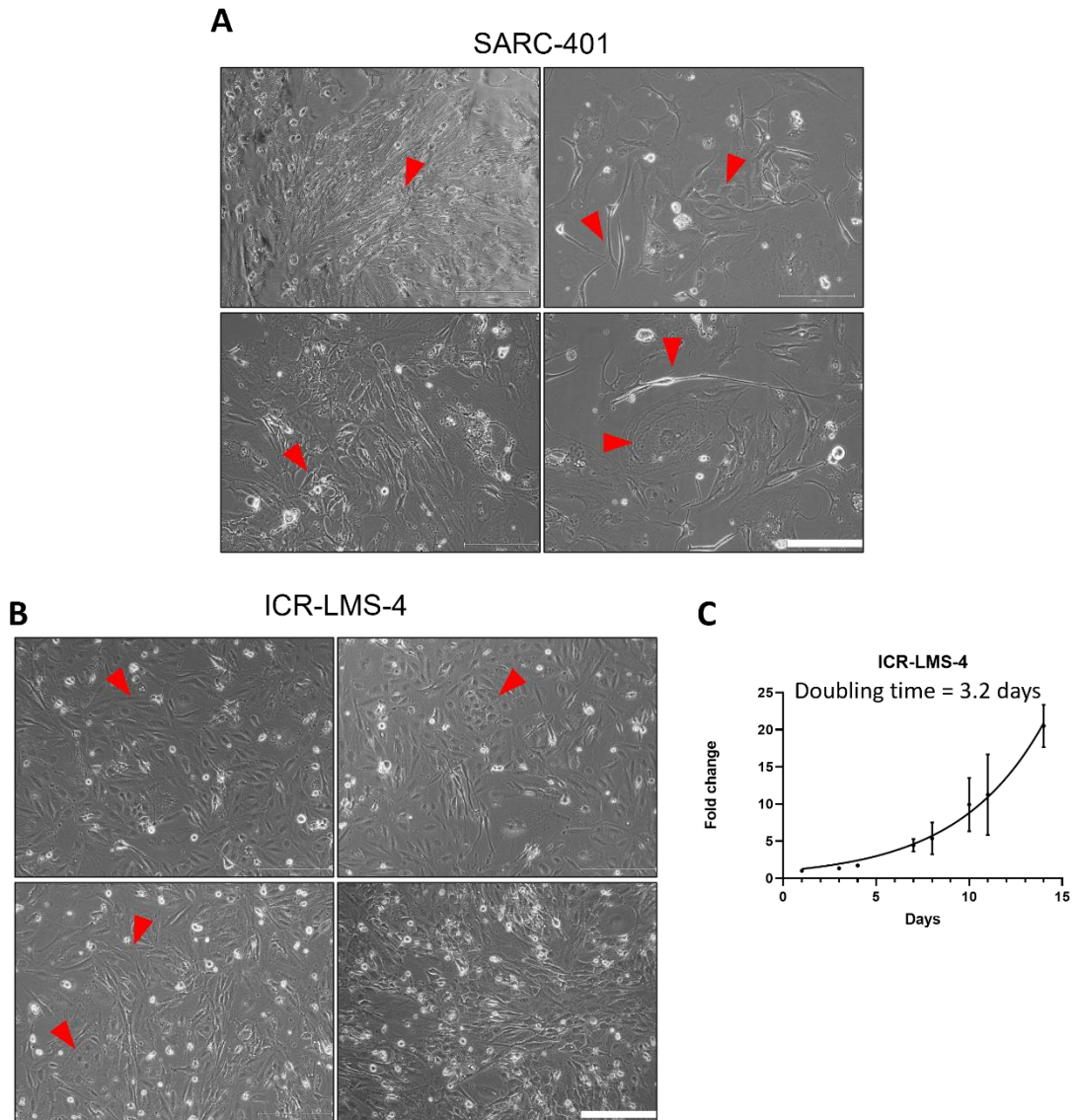
Figure 4.10. Morphology and growth rate of ICR-LMS-4 cell line. (A) Phase contrast images of SARC-401 primary cell culture with 4 fields of view at *in vitro* passage 0 (P+0), scale bar = 300 µm. (B) Phase contrast images of ICR-LMS-4 established cell line with 4 points of view at *in vitro* passage 16 (P+16), scale bar = 300 µm. (C) Cell count fold change of ICR-LMS-4 cells at P+16 over 14 days normalised to day 1, n=3, fold change measurements were fitted to a Malthusian exponential growth curve equation via GraphPad Prism. Red arrows denote areas of interest.

4.3.3 ICR-LMS-6

ICR-LMS-6 cells were established from a P0 tumour of the LMS PDX model SARC-409 (**Table 4.2**). Mouse cell depleted cells from SARC-409 were cultured in monolayer test conditions for a period of five weeks and similar to other lines, cells showed adherence after 5 days in all conditions. After 4 weeks in culture, proliferative colonies were

observed in cultures grown on non-coated flasks in Y-media without PDGF and bFGF, showing a heterogenous morphology with some rounded, slightly spindle shaped cells (**Figure 4.11A top left)**, some tightly packed, elongated spindle cells (**Figure 4.11A bottom left**), other loose elongated spindle cells (**Figure 4.11A top right**) and enlarged cells with elongated lamellipodia and stress fibres (**Figure 4.11A bottom right**). Proliferation at a similar timepoint was also observed in SARC-409 cultures grown in Y-media with PDGF and bFGF and also demonstrated matching morphologies while Matrigel coated cultures only later produced proliferative but slower growing colonies. For this reason, cells growing on non-coated flasks in Y-media without PDGF and bFGF were chosen for further expansion.

After approximately 13 weeks, SARC-409 cells were passaged 10 times at which these cells were labelled as ICR-LMS-6 and continued to proliferate for a further 4 weeks reaching at least passage 16 with a total culture time of approximately 5 months (**Figure 4.8**). Once generated ICR-LMS-6 cells showed no reduction in growth rate upon successive passaging. ICR-LMS-6 cells showed less morphological heterogeneity compared to primary SARC-409 cells, with the majority of cells showing a spindle cell, slightly elongated morphology which do not cluster into colonies (**Figure 4.11B**). ICR-LMS-6 showed exponential growth with a doubling time of 4.2 days and could be cryopreserved and thawed to continue cultures (**Figure 4.11C**).
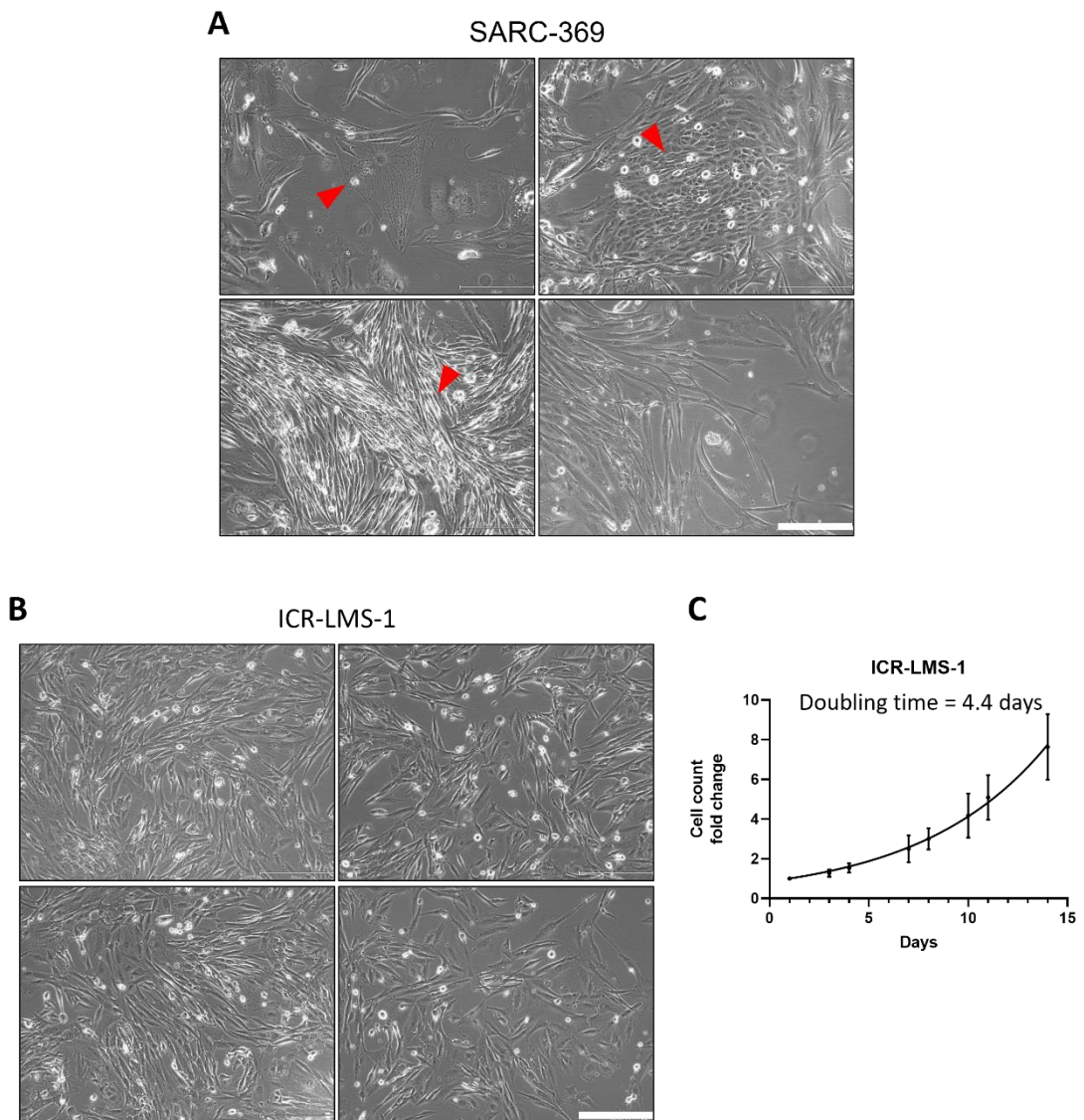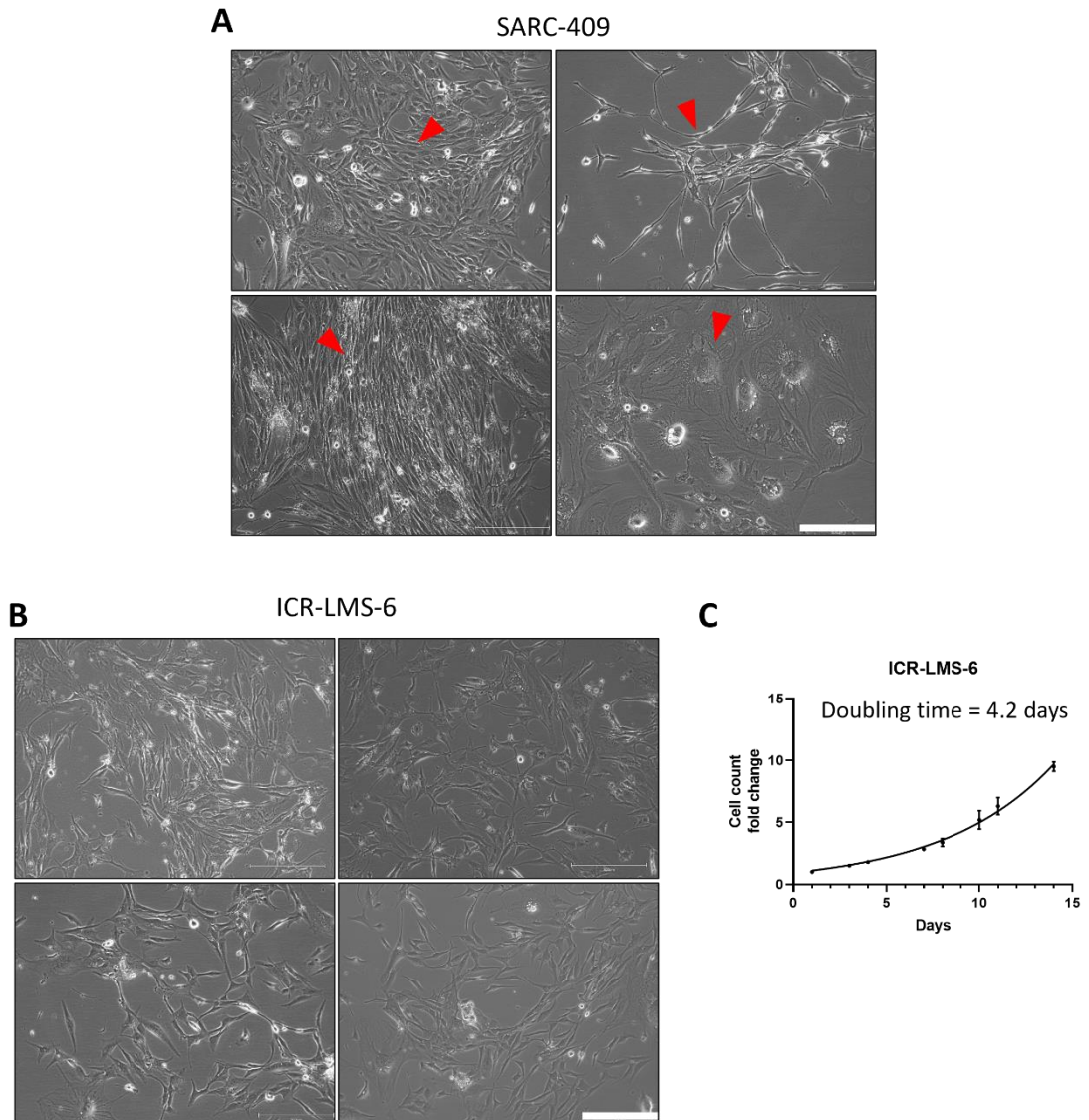
Figure 4.11. Morphology and growth rate of ICR-LMS-6 cell line. (A) Phase contrast images of SARC-409 primary cell culture with 4 fields of view at *in vitro* passage 0 (P+0), scale bar = 300 μm. (B) Phase contrast images of ICR-LMS-6 established cell line with 4 points of view at *in vitro* passage 13 (P+13), scale bar = 300 μm. (C) Cell count fold change of ICR-LMS-6 cells at P+13 over 14 days normalised to day 1, n=3, fold change measurements were fitted to a Malthusian exponential growth curve equation via GraphPad Prism. Red arrows denote areas of interest.

4.3.4 3D matrigel embedded cultures ICR-LMS-3 and ICR-LMS-5

In addition to monolayer cultures, dissociated mouse cell depleted cells from the uterine LMS PDX model SARC-369 were also cultured in a hydrogel embedded format in order to establish a 3D, patient-matched model to ICR-LMS-1 (**Table 4.2**). 3D cancer organoid models usually utilise hydrogel scaffolds such as Matrigel with a media supplemented

with growth factors specific to resident adult stem cells (LeSavage et al. 2022). Recently, a report outlined the specific media components which supported the growth of lung adenocarcinoma organoids in Matrigel domes (Sachs et al. 2019)**.** To first assess whether the process of PDX tissue dissociation and mouse cell depletion will still yield viable organoid cultures, I implemented this protocol with three NSCLC PDX models TM1244, TM199 and TM219 acquired from the Jackson Laboratory (http://tumor.informatics.jax.org/mtbwi/pdxDetails.do?modelID=TM01244) (http://tumor.informatics.jax.org/mtbwi/pdxDetails.do?modelID=TM00199) (http://tumor.informatics.jax.org/mtbwi/pdxDetails.do?modelID=TM00219). Organoid cultures were successfully established from all three PDX models after 21 days (**Figure 4.12**), highlighting that PDX tissue is still a viable source of tissue to generate 3D organoids.
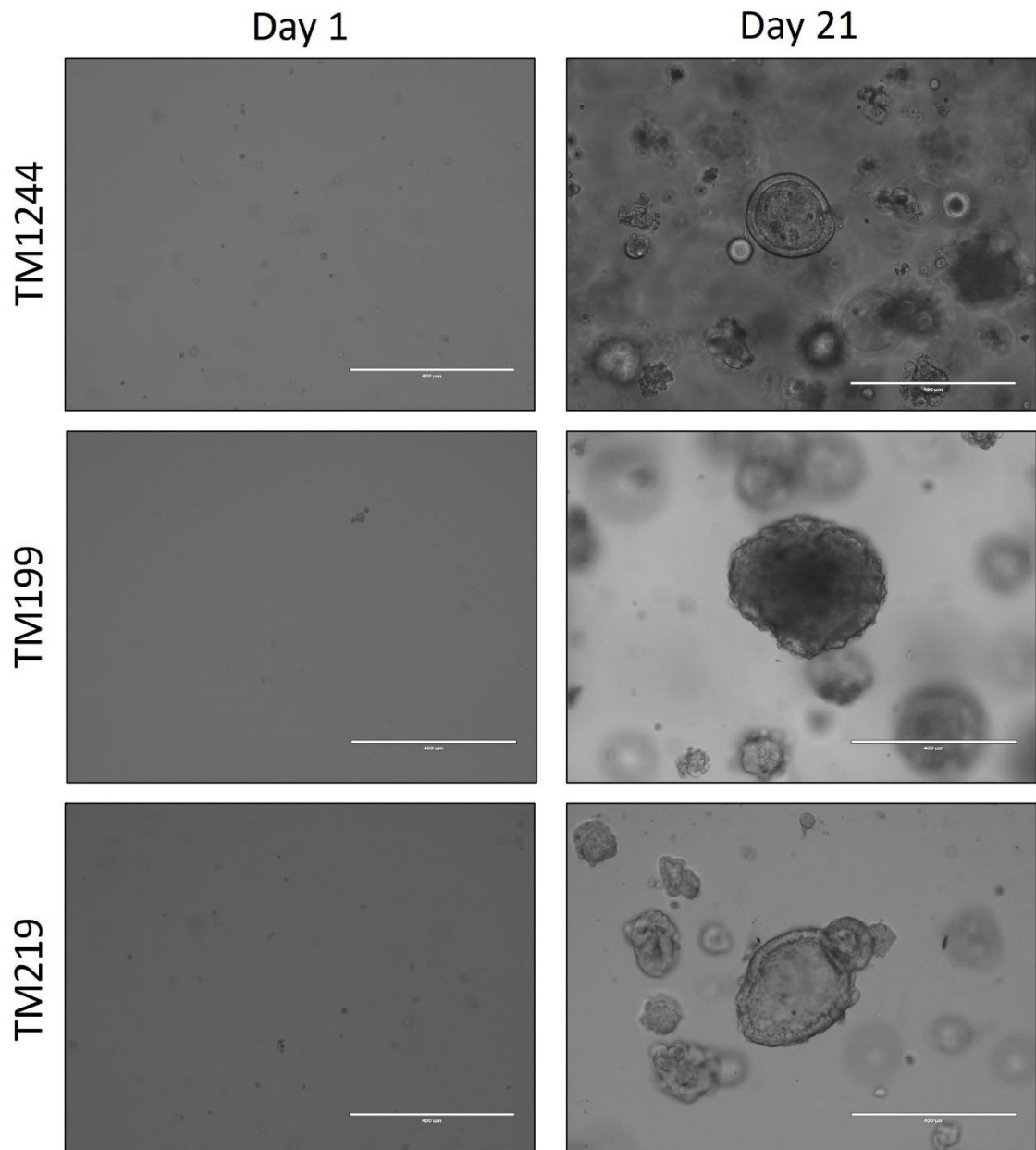
Figure 4.12. PDX-derived NSCLC organoid culture morphology. Brightfield images of dissociated NSCLC cells from PDX models cultured in matrigel and surrounded with NSCLC media. Images were taken at day 1 and at day 21. Scale bars = 400 μm

Little is known about the stem cell niches from which sarcomas arise, although due to the fact that STS including LMS often metastasise to the lungs it was hypothesised that similar culture conditions may support the growth of LMS organoids representing advanced disease. Therefore dissociated mouse cell depleted SARC-369 cells were cultured in matrigel domes surrounded by either the NSCLC organoid media or Y-media (**Figure 4.13**). After 21 days, expanding spheres were observed in cultures containing

Y-media but no growth was observed in cultures containing NSCLC organoid media (**Figure 4.13**), which were maintained for a further 30 days before discarding due to lack of growth. Cells were also cultured in matrigel domes surrounded with PDGF and bFGF supplemented Y-media, although no difference time until growth or growth rate was observed (data not shown).
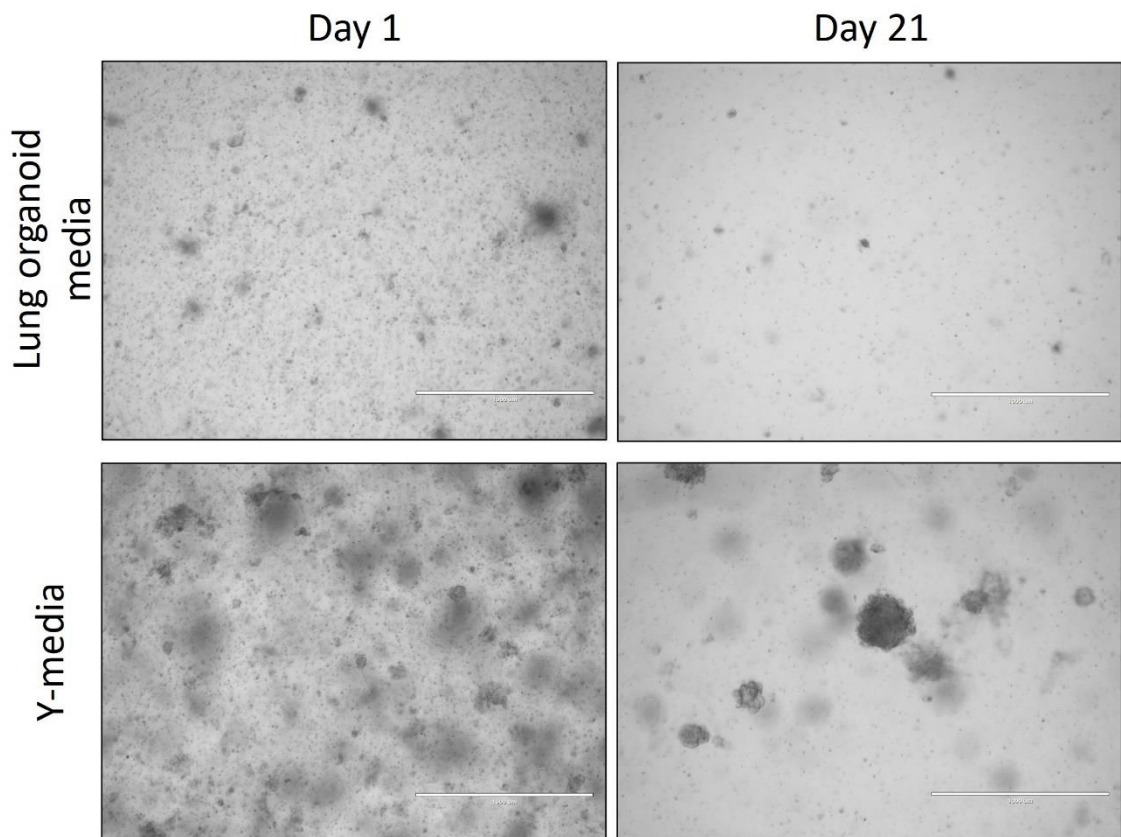
Figure 4.13. SARC-369 hydrogel embedded culture optimisation. Dissociated cells from SARC-369 PDX tumour were seeded into Matrigel and surrounded by lung organoid media or Y-media. Brightfield images were taken at day 1 and at day 21. Scale bar = 400 μm.

SARC-369 cells began to grow in undiluted Matrigel droplets in loose spheres which were mechanically and enzymatically dissociated after 1 month and then again every two weeks in order to expand cultures or for routine passaging. Spheroids were cryopreserved at low passages (P0-5). After 5 passages 3D SARC-369 cultures were termed ICR-LMS-3 which still formed spherical structures (**Figure 4.14A**). To assess the extent of which the organoid-like cultures can recapitulate the histology of the PDX tumour of origin, sections were stained with haematoxylin and eosin (H&E). Similar to

the PDX tumour, ICR-LMS-3 shows pleomorphic, hyperpigmented nuclei with some areas of scant cytoplasm particularly in the centre of the spheroid and other areas of multinucleated cells (**Figure 4.14B**). ICR-LMS-3 spheroids do not have well defined edges and instead show cellular blebbing at the boarders of the spheroid.
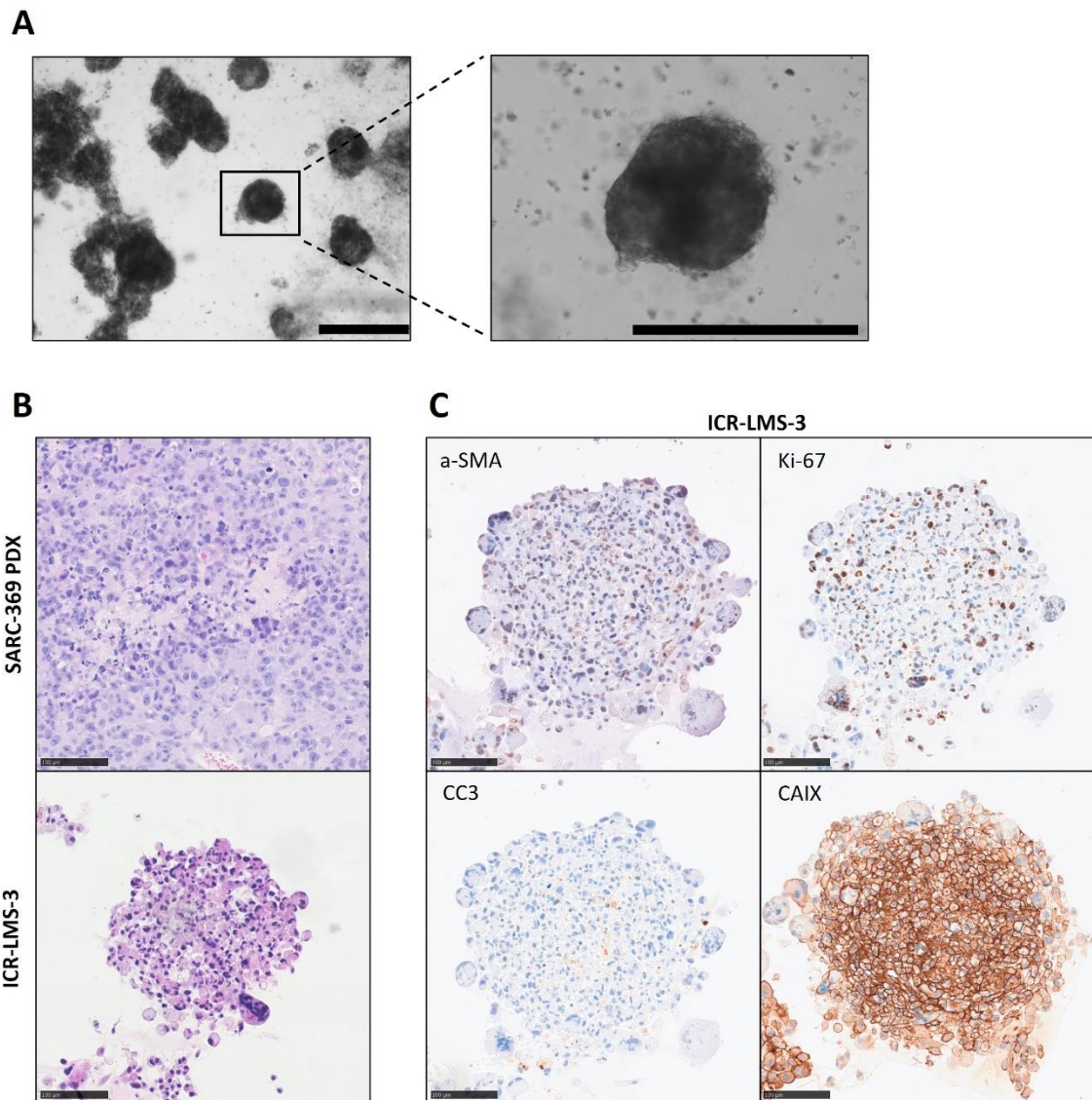
Figure 4.14. ICR-LMS-3 morphology and histology. (A) Brightfield images of ICR-LMS-3 established Matrigel embedded 3D culture 2 weeks after seeding. Scale bar = 750 μm. (B) H&E staining of ICR-LMS-3 and SARC-369 PDX tumour from which ICR-LMS-3 was derived. Scale bar = 100 μm. (C) IHC staining of ICR-LMS-3 for a-SMA, Ki-67, CC3 and CAIX. Scale bar = 100 μm. α-SMA, Alpha Smooth Muscle Actin, CAIX; Carbonic Anhydrase IX, CC3; Cleaved Caspase 3, PDX; Patient-Derived Xenograft.

A prominent feature of spheroid cultures is the ability to mimic spatial compartments and nutrient gradients. In order to observe the spatial characteristics of ICR-LMS-3, IHC staining was conducted for biomarkers of smooth muscle (α-SMA) to confirm these cells

retain LMS smooth muscle lineage, as well biomarkers of proliferation (Ki-67), apoptosis (cleaved caspase 3 (CC3)) and hypoxia (Carbonic anhydrase IX (CAIX)). While not homogenously expressed, α-SMA expression can be seen throughout the spheroids, without localisation (**Figure 4.14C**). Ki-67 can also be observed throughout the organoid, highlighting the proliferative capacity of ICR-LMS-3, although strong Ki-67 staining is not observed in the centre of the spheroids. Low expression of CC3 is seen and largely localised to the centre of the spheroid, whilst the spheroid shows a high expression of the hypoxic marker CAIX, which is only lessened at the outer edge of the spheroid. Therefore, ICR-LMS-3 spheroids have a steep hypoxic gradient but with proliferative cells throughout, mimicking the hypoxic environment characteristic of tumour tissue *in vivo.* ICR-LMS-3 could therefore be used to assess the impact of hypoxia on drug response and biochemical processes which might contribute to LMS progression.

In addition to ICR-LMS-3, dissociated cells from a non-uterine LMS PDX model, SARC-400 were cultured in matrigel domes, establishing expanding spheroid structures when cultured with PDGF and bFGF, with well-defined edges which were termed ICR-LMS-5 upon undergoing subculture every two weeks for at least 5 passages (**Table 4.2**) (**Figure 4.15A**). Examination of sections stained with H&E shows that ICR-LMS-5 spheroids have well defined edges with dense cellular areas and monotonous nuclei (**Figure 4.15B**). Additionally, some lumens within the spheroids can be observed suggesting some degree of self-organisation (**Figure 4.15B**).

A

B
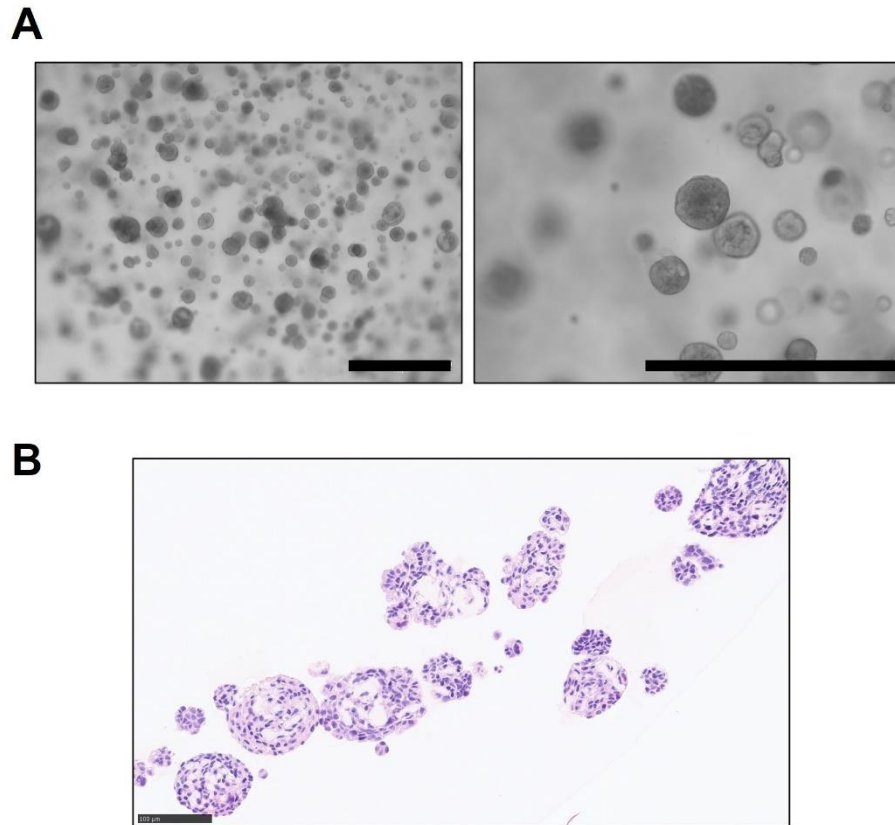
Figure 4.15. ICR-LMS-5 morphology and histology. (A) Brightfield images of ICR-LMS-5 Matrigel embedded 3D cultures. Scale bar = 750 μm. (B) H&E stain of ICR-LMS-5 cultures. Scale bar = 100 μm.

4.3.5 ICR-LMS-1 and ICR-LMS-3 form tumours in mice

An important factor to consider when using any cell line is whether the model is able to form tumours *in vivo* and if such tumours recapitulate the disease from which the cell line was derived from. To explore this, and to test whether the tumourigenic capacity of cell lines might be affected by culture format, PDX matched cell lines ICR-LMS-1 (2D) and ICR-LMS-3 (3D) were dissociated into single cell suspensions, suspended in Matrigel and the same number of cells were injected into mice. Tumours were observed as early as 25 days after injection with ICR-LMS-3 cells and showed a similar growth rate to the PDX of origin SARC-369 while tumours were only observed in ICR-LMS-1 injected xenografts 71 days after inoculation (**Figure 4.16A**). Once established however, ICR-LMS-1 xenografts showed a similar growth rate to ICR-LMS-3 xenografts and SARC-369 PDX.

Once tumours reached approximately 1000mm3 in size, they were harvested and sections of the tumours were stained with H&E to assess histological similarities or

discrepancies to the PDX of origin (SARC-369P0). Compared to SARC-369, ICR-LMS-3 xenografts showed a similar histology with dense cellular areas and pleomorphic, occasionally hyperpigmented nuclei (**Figure 4.16B**). ICR-LMS-1 xenografts showed two distinct histological regions, the first containing hypercellular regions, interspersed with spindle cells with enlarged nuclei (**Figure 4.16C top**)and the second containing spindle cells with elongated nuclei, arranged in fascicle structures (**Figure 4.16C bottom**). ICR-LMS-3 was able to establish *in vivo* tumours quickly compared to ICR-LMS-1, which also matched SARC-369 histology suggesting that 3D cultures are better able to adapt to *in vivo* growth and maintains tissue architecture. While ICR-LMS-1 are able to establish tumours which is consistent with LMS based on histology, this xenograft does show a distinct region of histology, suggesting that a clone might have been selectively enriched during 2D culture.
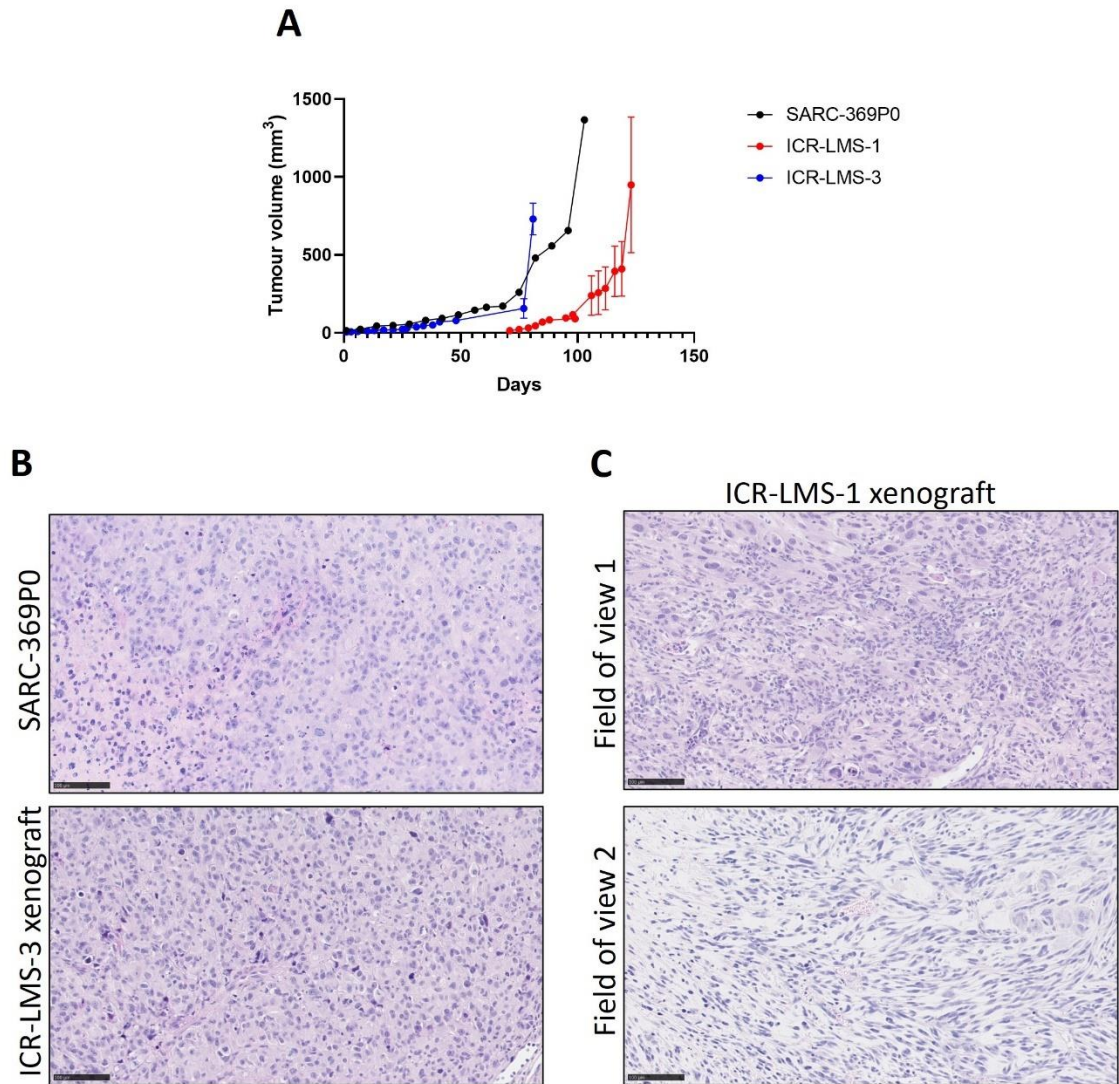
Figure 4.16. In vivo tumourigenicity of ICR-LMS-1 and ICR-LMS-3 cell lines. (A) Tumour volume of SARC-369, ICR-LMS-1 or ICR-LMS-3 xenografts. Day 1 denotes the first day that SARC-369 presented with growing tumour or the day of ICR-LMS-1/ICR-LMS-3 inoculation. (B) H&E stains of both SARC-369 original PDX and ICR-LMS-3 xenograft. Scale bar = 100 μm. *20x magnification.* (C) H&E stains of ICR-LMS-1 xenograft representing two points of view of the same tumour sample. Scale bar = 100 μm. *20x magnification.*

4.3.6 Short-term primary cultures

Upon culturing dissociated, mouse depleted cells from the non-uterine LMS PDX model SARC-323 in 2D, SARC-323 cells adhered but did not proliferate, even when maintaining cultures for 2 months. However, if SARC-323 cells were plated on Matrigel coated flasks and with Y-media supplemented with PDGF and bFGF, cells adhered and underwent proliferation which was observed after 2 weeks in culture. SARC-323 cells showed an

154

elongated spindle cell morphology (**Figure 4.17A**) and were continually cultured for a further 6 weeks during which no significant change in morphology occurred until the onset of senescence after 8 passages (**Figure 4.8**) (**Table 4.2**). Additionally, *in vitro* 2D cultures were successfully established from the uterine LMS PDX model SARC-393, showing proliferative cells on non-coated flasks without the addition of PDGF or bFGF after 3 weeks in culture (**Figure 4.17B**). SARC-393 showed an irregular morphology made up of large cells with spindle projections (**Figure 4.17B**). SARC-393 continued to grow for at least 4 months in culture but has not yet been passaged more than 10 times and therefore has been designated as a primary short term culture for this thesis (**Figure 4.8**) (**Table 4.2**). Unfortunately, while SARC-322, SARC-356, SARC-376, SARC-414 and SARC-416 dissociated cells all adhered to plastic following culture in monolayer conditions, they did not proliferate and were eventually discarded due to eventual cell detachment.
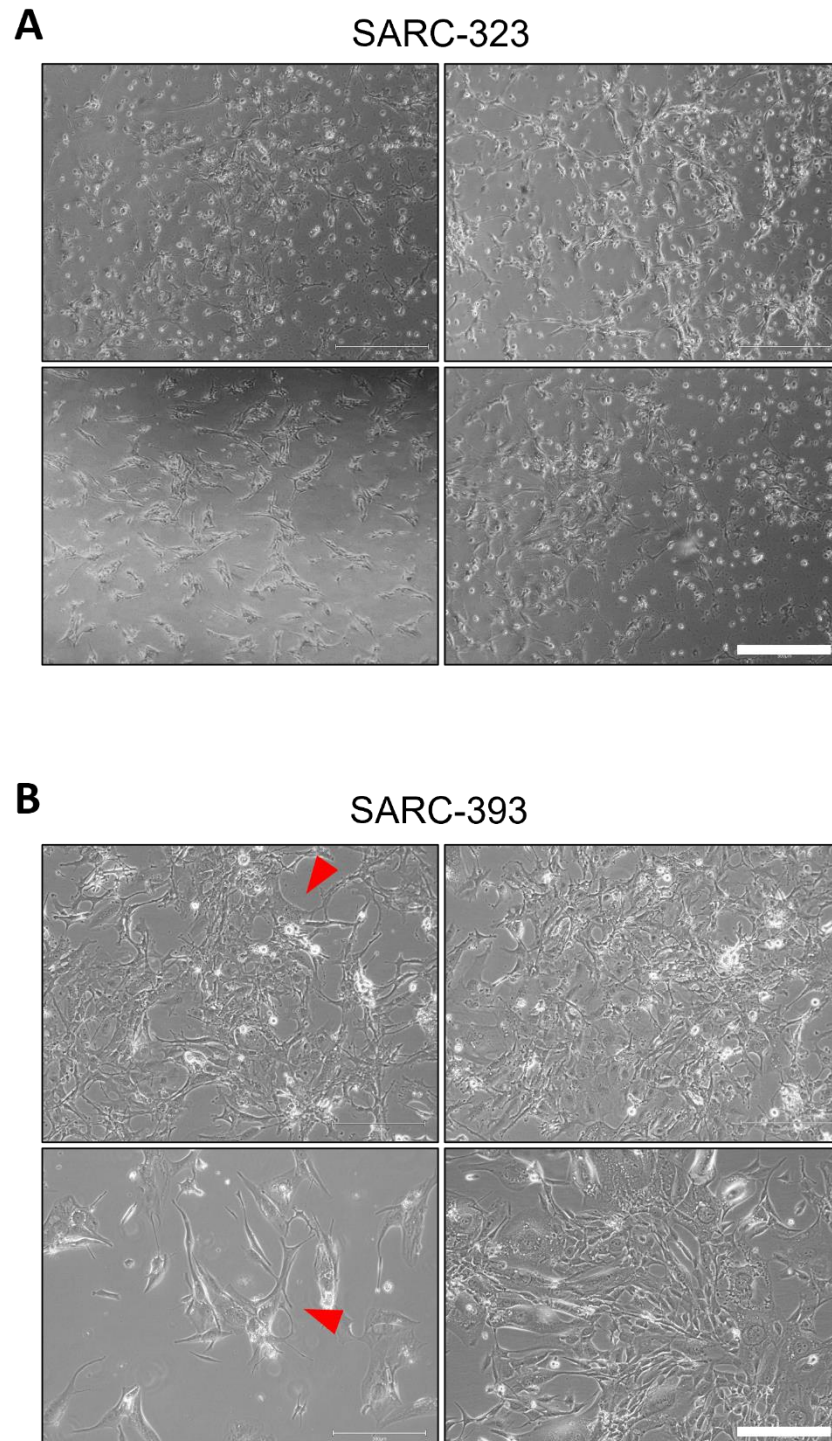
A SARC-323

B SARC-393

Figure 4.17. Morphology of SARC-323 and SARC-393 primary cultures. (A) Phase contrast images of 4 points of view for SARC-323 cells at P+0. Scale bar = 300 μm. (B) Phase contrast images of 4 points of view for SARC-393 cells at P+0. Scale bar = 300 μm. Red arrows denote areas of interest.

4.4 Verification of PDX-derived LMS cells

Upon the establishment of a panel of PDX-derived LMS cells, both long term and short term lines were tested for the presence of contaminating murine fibroblasts which might eventually overgrow the tumour cell population and are especially difficult to identify in 3D conditions. In order to detect mouse DNA, a PCR reaction was performed with primers specific to human or murine *PTGER2*. DNA was collected from SK-UT-1 cells as a positive control for human DNA and negative control for murine DNA and vice versa for NIH-3T3 cells. Following PCR amplification, the PCR products were separated via electrophoresis. The presence of a clear band in human PTGER2 amplifying conditions for ICR-LMS-1, SARC-323 cell culture, ICR-LMS-3, ICR-LMS-4, ICR-LMS-6 and SARC-393 cell culture, with no band under murine PTGER2 amplifying conditions indicates that these cultures do not contain murine cells and are human in origin (**Figure 4.18A**). Meanwhile, the LMS PDX-derived 3D culture ICR-LMS-5 showed a clear band when murine PTGER2 was amplified and no band when human specific primers were used indicating that this line is murine in origin and not composed of human tumour cells (**Figure 4.18A**). Therefore ICR-LMS-5 was discarded and was not characterised further or used for subsequent assays.
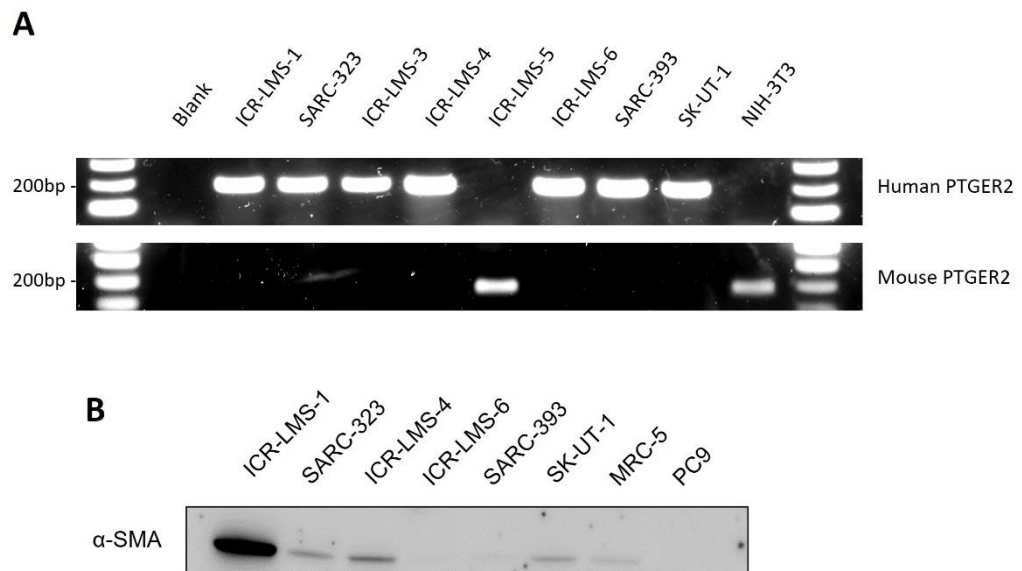
Figure 4.18. Identification of mouse contaminants in PDX-derived LMS cultures and a-SMA expression. (A) PCR amplification of human or murine *PTGER2* with DNA isolated from ICR-LMS-1, SARC-323 cell culture, ICR-LMS-3, ICR-LMS-4, ICR-LMS-5, ICR-LMS-6, SARC-393 cell culture, SK-UT-1 and NIH-3T3 cells. A band of 189bp indicates amplification of target. (B) Immunoblot of ICR-LMS1, SARC-323, ICR-

LMS-4, ICR-LMS-6, SARC-393, SK-UT-1, MRC-5 and PC-9 against α-SMA. α-SMA; Alpha Smooth Muscle Actin, PTGER2; Prostaglandin E Receptor 2

Next, in order to determine to what extent the 2D LMS cell cultures express smooth muscle specific markers, western blotting was performed for α-SMA on lysates from ICR-LMS-1, SARC-323, ICR-LMS-4, ICR-LMS-6 and SARC-393. Here PC9, a NSCLC immortalised line, was used as a negative control while the LMS cell line SK-UT-1 and fibroblast cell line MRC-5 were used as positive controls of α-SMA expression, although only moderate expression of α-SMA has been reported in MRC-5. ICR-LMS-1 had the highest intensity of α-SMA in comparison to other samples tested and SARC-323 and ICR-LMS-4 also showed a noticeable band for α-SMA, indicating that these cell cultures retain smooth-muscle identity (**Figure 4.18B**). ICR-LMS-6 and SARC-323 however only showed a weak band at higher exposures indicating these cultures do not express α-SMA to the same extent.

Further characterisation of the established LMS PDX-derived cell cultures was achieved via STR and proteomic profiling. To start with, STR analysis was conducted in order to check the similarity between the PDX tissue of origin and the respective cell culture and rule out the possibility of other human cell line contamination. ICR-LMS-1 and ICR-LMS-3 maintained identical loci compared to the PDX tissue of origin, SARC-369, as did ICR-LMS-6 and SARC-393 cell culture compared to their respective PDX models of origin (**Table 4.3**). Therefore, these cultures are comprised of cells from the PDX tissue and have not undergone any substantial genetic drift which might show a change in STR loci. However, SARC-323 cell culture as well as ICR-LMS-4 were not identical to the STR loci of their respective PDX of origin. ICR-LMS-4 shows a loss of heterozygosity at two loci while SARC-323 shows a gain of heterozygosity at four loci, although the percentage of similarity between the PDX and cell line profiles is over 80% (87.5 and 93.75% respectively for SARC-323 and ICR-LMS-4 cultures) and therefore can be considered as biological derivatives (Capes-Davis et al. 2013). STR profiles from all LMS PDX-derived cell cultures were compared to a database of cell lines via the CLASTR Cellosaurus STR similarity search tool and showed no matches exceeding 76% (Robin, Capes-Davis, and Bairoch 2020). All cell line database matches above 70% have not been used in the laboratory and are therefore unlikely to be contaminants.

	SARC-369P0 PDX	ICR-LMS-1	ICR-LMS-3	SARC-323P0 PDX	SARC-323 cell culture	SARC-401P0 PDX	ICR-LMS-4	SARC-409P0 PDX	ICR-LMS-6	SARC-393P1 PDX	SARC-393 cell culture
D8S1179	12,13	12,13	12,13	12,14	12,14	11,12	11,12	10,10	10,10	13,15	13,15
D21S11	32.2,33.2	32.2,33.2	32.2,33.2	28,29	28,29	27,29	27,29	28,31.2	28,31.2	29,30	29,30
D7S820	9,10	9,10	9,10	13,13	10,13	10,11	10,11	8,8	8,8	11,11	11,11
CSF1PO	12,12	12,12	12,12	10,11	10,11	10,11	10,11	10,12	10,12	11,11	11,11
D3S1358	15,16	15,16	15,16	15,18	15,18	15,15	15,15	15,17	15,17	14,19	14,19
TH01	9.3,9.3	9.3,9.3	9.3,9.3	9,9	7,9	7,9.3	9.3,9.3	9,9	9,9	9.3,9.3	9.3,9.3
D13S317	11,11	11,11	11,11	12,13	12,13	10,12	10,12	11,11	11,11	11,11	11,11
D16S539	11,11	11,11	11,11	11,12	11,12	11,13	11,13	12,12	12,12	14,14	14,14
D2S1338	20,20	20,20	20,20	21,21	21,23	17,17	17,17	16,16	16,16	18,18	18,18
D19S433	13,13	13,13	13,13	14,14	14,14	15,15	15,15	13,13	13,13	13,15	13,15
vWA	18,18	18,18	18,18	16,16	16,16	15,19	15,19	17,17	17,17	17,17	17,17
TPOX	11,11	11,11	11,11	8,8	8,8	9,9	9,9	8,8	8,8	8,8	8,8
D18S51	13,15	13,15	13,15	16,19	16,19	14,16	14,14	13,15	13,15	14,14	14,14
AMEL	X,X	X,X	X,X	X,X	X,X	X,X	X,X	X,X	X,X	X,X	X,X
D5S818	12,12	12,12	12,12	9,11	9,11	12,13	12,13	12,13	12,13	11,11	11,11
FGA	18,18	18,18	18,18	22,22	20,22	22,22	22,22	18,18	18,18	25,25	25,25
% Similarity	100%			87.5%		93.75		100%		100%	

Table 4.3. STR profiling of PDX tumours and PDX-derived in vitro cultures. STR loci of PDX tumours and respective PDX-derived short or long term in vitro cultures including SARC-369 PDX, ICR-LMS-1, ICR-LMS-3, SARC-323 PDX and cell culture, SARC-401 PDX, ICR-LMS-4, SARC-409 PDX, ICR-LMS-6, SARC-393 PDX and cell culture. Loci in red indicate discrepancies between PDX tissue and respective cell culture. PDX; Patient-Derived Xenograft, STR; Short Tandem Repeat.

To assess if PDX-derived LMS primary cultures grown *in vitro* (below passage 10, P <10) or established PDX-derived LMS cells (beyond passage 10, P ≥ 10) retain the LMS identity of the PDX models, proteomic profiling by two PhD students in our lab: Yuen Bun Tam and Madhumeeta Chadha, was conducted on all LMS cell cultures which were generated in this chapter. PDX-derived LMS cells were not assessed beyond passage 20. Proteomic profiling was also conducted on the immortalised LMS cell lines SK-UT-1, SK-UT-1b, and the patient-derived cell lines Shef-LMS 01 W_1 and Shef-LMS 01 W_S (Salawu et al. 2016) to assess the similarities and differences between LMS cell lines and the patient-derived models in this chapter. First, proteins associated with expression in smooth muscle tissue including caldesmin, desmin, vinculin and vimentin were present in all PDX tissue, PDX-derived cell lines as well as SK-UT-1 and SK-UT-1b cells but desmin was not detected in the patient-derived Shef-LMS 01 W_1 and Shef-LMS 01 W_S cell lines. When compared, no significant difference was observed in caldesmon, desmin, vinculin or vimentin abundance (**Figure 4.19A-D**). SK-UT-1 and SK-UT-1b cells specifically displayed a slightly lower abundance of caldesmon compared to all other samples and was lower than Shef-LMS 01 W_1 and Shef-LMS 01 W_S (**Figure 4.19A**). Additionally, while not significant, the abundance of desmin was slightly higher in PDX tissue compared to PDX-derived cells as well as SK-UT-1 and SK-UT-1b cells (**Figure 4.19B**). Together these results indicate that the LMS PDX-derived cell lines established in this chapter retain the LMS subtype characteristics of PDX models tissue and are also comparable to established LMS cell lines.

Next, to identify the biological differences between PDX tissue and PDX-derived cell cultures and also the differences between PDX-derived cell cultures and LMS cell lines, a SAM analysis was conducted to identify proteins which have a significant enrichment in either group. These significant proteins were then analysed via g:Profiler over-representation analysis and showed that proteins associated with mTORC1 signalling and mitotic spindle were enriched in LMS PDX-derived cells compared to LMS PDX models, however no specific hallmarks were found to be significantly enriched in PDX tissue compared to the derived *in vitro* cells (**Figure 4.19E**). Proteins associated with mTORC1, epithelial to mesenchymal transition, hypoxia and metabolic pathways such as glycolysis and oxidative phosphorylation were enriched in PDX derived cells compared to LMS cell lines, meanwhile no genes were found to be significantly elevated in LMS cell lines (**Figure 4.19F**). Together these results demonstrate that there are distinct biological pathways operating in PDX-derived LMS cultures established in this chapter versus LMS cell lines including the patient derived lines Shef-LMS 01 W_1 and Shef-LMS 01 W_S.
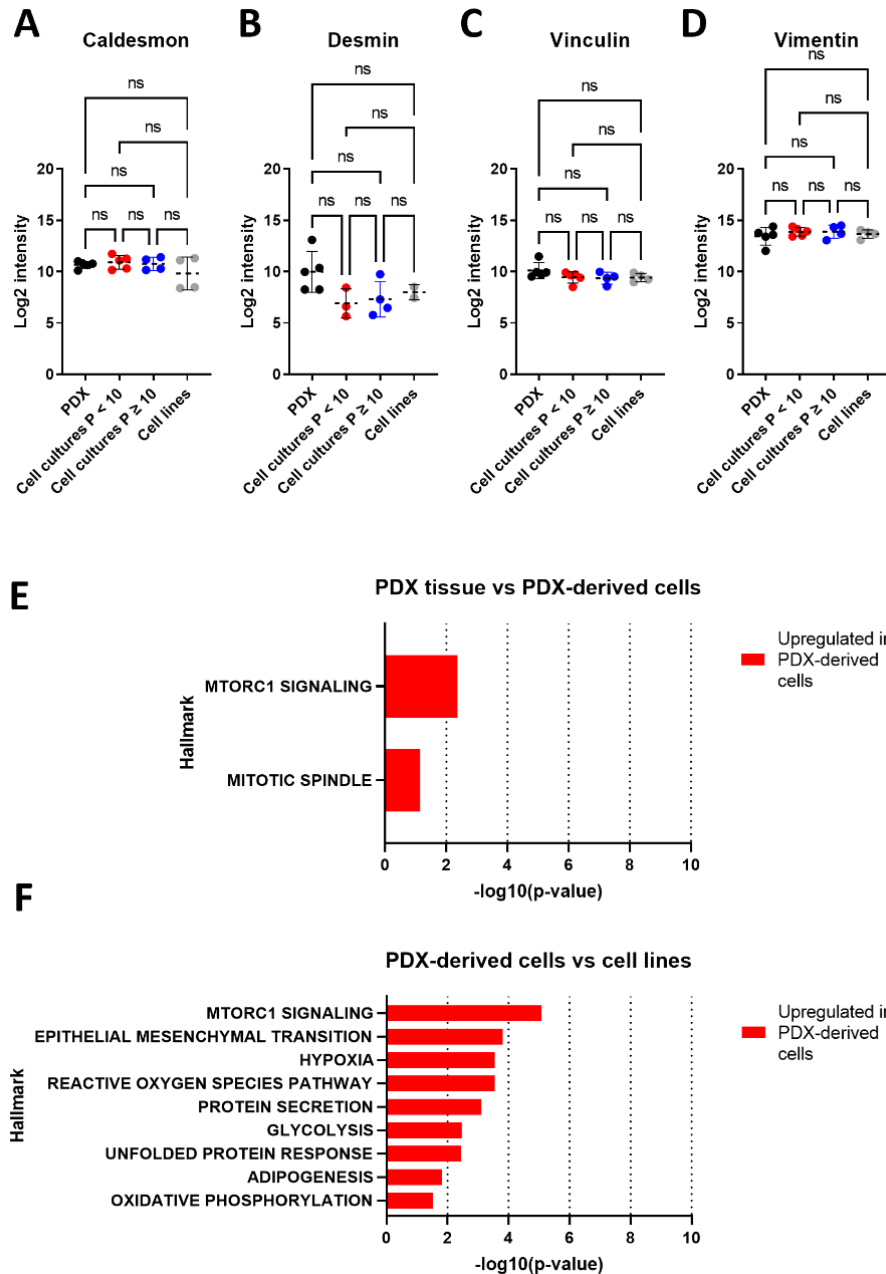
Figure 4.19. Proteomic comparison of LMS PDX model tissue, PDX-derived cells and LMS cell lines. Log2 intensity values of smooth muscle associated proteins (A) caldesmon, (B) desmin, (C) vinculin and (D) vimentin in PDX FFPE tissue, PDX-derived cells below passage 10, PDX-derived cells beyond passage 10 and LMS cell lines invluding SK-UT-1, SK-UT-1b, Shef-LMS01 W1 and Shef-LMS-1 Ws. (E) Over-representation analysis plot showing hallmark pathways upregulated in PDX-derived cells compared to PDX tissue after mutual comparison. (F) Over-representation analysis plot showing hallmark pathways upregulated in LMS PDX-derived cells compared to LMS cell lines SK-UT-1, SK-UT-1b, Shef-LMS 01 W_1 and Shef-LMS-1 W_s after mutual comparison. Cell lysate samples were prepared for mass spectrometry analysis by myself. Mass spectrometry data was acquired and processed via DIA-NN by Yuen Bun Tam, Madhumeeta Chadha. DIA-NN output data was further processed by myself to assess log2 protein abundance. SAM and enrichment analysis was conducted by myself.

4.5 Discussion

In this chapter, a PDX-derived *in vitro* pipeline was optimised using a synovial sarcoma PDX model which was then applied to a total of 12 LMS PDX tumours from different models. These LMS PDX tumours were dissociated and cultured as monolayers *in vitro* with a success rate of initial, short-term culture (<10 passages) of 42% (5 of 12 PDX samples). Of these short-term cultures, 4 out of 5 were able to continue proliferating to or past 10 passages without the onset of senescence giving a long term culture establishment rate of 33% (4 out of 12 PDX samples). These success rates improve upon previously reported studies in generating sarcoma and other cancer lines directly in monolayer from tissue resections which demonstrated success rates of 6-15% and is comparable to the success rate of long term LMS cultures reported by Salawu and co-workers (Bruland, Fodstad, and Pihl 1985; Giard et al. 1973; Salawu et al. 2016). Cell line establishment rates are often higher when derived from metastatic tumours in comparison to primary tumours so this may partially explain the lower rates reported in previous studies when culturing directly as monolayers compared to this study which used samples representing metastatic disease (Bruland, Fodstad, and Pihl 1985; Giard et al. 1973). The *in vitro* establishment rates in this study are lower than reported in a recent study which demonstrated a 58% culture rate from a range of translocation associated sarcomas, although the reported rate represents the number of proliferating primary cultures after initial seeding and therefore does not reflect the rate of long-term culture establishment (Brodin et al. 2019).

Within this study, information regarding tumour grade of biopsies was not available for all samples. However it is noted that out of five generated LMS *in vitro* cultures, three of these were derived from PDXs of grade 3 tumour biopsies and the grade of the other two models is not available. While the amount of confirmed grade 2 and grade 1 patient biopsies used in this study was lower than the number of confirmed grade 3 biopsies, it is possible that *in vitro* cultures enrich for samples which represent aggressive disease. Salawu and colleagues previously reported that of seven STS cell lines, five were established from grade 3 tumours and two were established from grade 2 tumours (Salawu et al. 2016). Tumour grading of the remaining biopsy samples presented in this study should be done in order to support analysis of the effect of tumour grade on *in vitro* establishment rate.

ICR-LMS-1 and ICR-LMS-4 represent uterine LMS cell line models which were derived from PDXs of baseline trial biopsies, both of which were grade 3 tumours. Additionally the patient specimen from which ICR-LMS-4 was ultimately derived from was treatment

naïve while the patient specimen which ultimately gave rise to ICR-LMS-1 had undergone three cycles of doxorubicin treatment prior to biopsy. Therefore these models represent tumours different stages of LMS treatment pathways. Meanwhile, ICR-LMS-6 was ultimately derived from a non-uterine stomach originating LMS patient after three cycles of gemcitabine and pembrolizumab treatment during the GEMMK trial although the patient had received no other treatment prior to trial enrolment. Therefore the three long term LMS cell lines in this study represent two anatomical subgroups of LMS (gynaecological and digestive) which were previously shown via transcriptomic profiling to also cluster into separate molecular subgroups, therefore it would be particularly important to assess differences in these two groups regarding drug response (Anderson et al. 2021). Unfortunately, no PDXs which were derived from vascular LMS patients were able to proliferate in culture (SARC-322, SARC-356, SARC-414 and SARC-416) which suggests that these LMS cells may require distinct culture conditions to allow for expansion.

The cell lines described in this study have a doubling time of 3.2 to 4.4 days which is markedly slower than a previous study of STS cell lines established from patient tissue which reported a doubling time of 27.44 and 44.62 hours for LMS cell lines and 27.44-63.97 hours across all cell lines described (Salawu et al. 2016). The reason behind this slow proliferation may be due to cell extrinsic factors such as culture media, growth factors composition and culture format or could be due to cell intrinsic factors such as maintenance of slowly proliferating subclones. Cancer cell lines have significantly enhanced proliferation rates compared to primary cells or tumour doubling times due to increased nutrient availability and selection for fast growing subclones (Kaur and Dufour 2012; Nakamura et al. 2011; Rööser, Pettersson, and Alvegård 1987). Therefore, the slower growth rates of the PDX-derived LMS cells presented in this study may represent more clinically relevant models of tumour growth kinetics. This would additionally impact phenotypic responses to chemotherapy agents as these preferentially kill actively proliferating cells, which may explain the enhanced sensitivity of the synovial sarcoma cells lines SYO-1 and HS-SY-II to doxorubicin compared to the PDX-derived synovial sarcoma line ICR-SS-1. It remains to be seen if prolonged culture of the established PDX-derived lines will shorten doubling time by clonal selection although passages no higher than 20 were deliberately used for experimental assays in order to minimise this possibility.

Following the results of this study, the impact of several different culture media components and growth factors on proteomic profiles should be explored to determine whether certain conditions are better able to maintain tumour characteristics rather than

relying on effect on cell proliferation rate alone to inform culture conditions. The detection of smooth muscle markers in PDX-derived primary LMS culture condition screens could be employed here similar to a recent study which assessed differentiation status of PDX-derived RMS primary cells which was a consideration in choosing appropriate cell culture conditions (Manzella et al. 2020).

To determine growth conditions in organoid-like matrigel embedded cultures, a NSCLC organoid media was utilised in parallel to Y-media on dissociated SARC-369 cells and showed spheroid growth only in Y-media cultures. The observation that NSCLC specific organoid media did not permit for spheroid growth is consistent with the current consensus that epithelial cancer organoid conditions are distinct from mesenchymal cell niches, thus leading to difficulty in translating organoid technology to sarcoma modelling (Colella et al. 2018; LeSavage et al. 2022; Gaebler et al. 2019; Meister et al. 2022). The long-term 3D LMS model presented in this chapter ICR-LMS-3 demonstrated a similar histology to the PDX of origin, consistent with studies establishing organoid cultures from PDX models in other cancer (L. Huang et al. 2020; Pham et al. 2021; Guillen et al. 2022). Additionally, ICR-LMS-3 showed spatial arrangement of biological process, such as strong hypoxic activation of CAIX within spheroids and an outer layer of slight hypoxia, with an inner core lacking proliferative cells. This result demonstrates that ICR-LMS-3 can model nutrient gradients and hypoxic conditions which are often observed in solid tumours (Cairns, Harris, and Mak 2011).

Both the patient and PDX matched cell cultures ICR-LMS-1 and ICR-LMS-4 demonstrated tumourigenicity *in vivo*, both establishing tumours when injected as cell suspensions. Interestingly the 3D model ICR-LMS-3 was able to establish tumours faster than ICR-LMS-1 suggesting that the 3D model is better able to adapt to *in vivo* growth compared to monolayer cells. ICR-LMS-3 xenografts displayed a similar histology to the PDX of origin which is commonly reported in studies utilising organoid derived xenografts (Jian et al. 2020; Calandrini et al. 2021). However ICR-LMS-1 cell xenografts showed some areas of distinct histology not observed in the original PDX or the ICR-LMS-3 xenograft, which suggests that *in vitro* culture may induce phenotypic changes or select for the outgrowth of a cell population which is not predominant *in vivo*.

Determining the outgrowth of cells in 3D culture was difficult due to the inability to distinguish between murine fibroblasts and human cells as well as live and dead cells (other than observing proliferation). Some cultures showed spindle cells invading through the Matrigel and forming sheets but did not grow as cellular aggregates and thus were not continued for study. Potentially to improve on the establishment rate reported

in this study, early 3D cultures showing outgrowth of cells with no structure could be removed from Matrigel and cultured as monolayers in a similar system to Bruland and colleagues which greatly improved establishment rates compared to direct monolayer culture (Bruland, Fodstad, and Pihl 1985). Additionally, these cultures should be tested for the presence of murine cells as the 3D conditions used in this study were shown to support murine spheroid growth. Following PCR based identification of human or murine DNA, ICR-LMS-5 was shown to be heavily contaminated with mouse cells. In fact, no human DNA could be detected in this PCR assay, highlighting the importance of this test to prevent the erroneous labelling of such cultures as PDX-derived LMS cells.

Through the process of cell line establishment, cultures can become contaminated with stromal cells such as fibroblasts which might eventually become the dominant population in the cell line. Additionally, cultures can be cross contaminated with frequently used cell lines, other primary cells or even directly mislabelled and if not detected early, can lead to highly misleading potentially erroneous results (Alston-Roberts et al. 2010). For example, HeLa cells, one of the most widely used human cervical cancer cell line has previously been detected in over 116 individual cell lines (J. Lin et al. 2019; Gartler 1968). To avoid this issue, STR profiling is recommended in order to authenticate cell lines by comparison to a STR profile database or by the comparison to a reference sample of origin such as patient tissue (Souren et al. 2022; Almeida, Cole, and Plant 2016). In a study of 2,279 STR profiles from cell lines, calculating the percentage match (the number of shared alleles divided by the total number of alleles in the STR profile for the sample in question) was able to distinguish related samples at ≥80% and unrelated samples at <50% STR profile matches, while a small overlap of related and unrelated samples was noted at STR matches between 50-79%, concluding that STR profiles which are ≥80% matching can be considered as related (Capes-Davis et al. 2013). All short and long-term cell lines in this study showed a STR profile match of >80% compared to each PDX tissue of origin, bar ICR-LMS-5, which was not tested. Limitations of comparing STR profiles for cell line authentication has limitations in that even primary short-term cultures can display some genetic drift or selection for genetically distinct subclones, which can be especially prevalent in cancer types characterised by high genomic instability.

In this study two PDX-derived cell lines displayed slightly different STR profiles to the PDX-tissue. LMS tumours display a high loss of heterozygosity, comparable to ovarian and breast cancers which can be associated with homologous recombination DNA repair (Seligson et al. 2022). ICR-LMS-4 shows a loss of heterozygosity at two loci which could be explained by the genetic instability of the disease. In contrast, the short-term culture SARC-323 shows a gain of heterozygosity at four loci. This could also be explained

because of inherent genetic instability but also raises the possibility that this culture is composed of non-transformed patient-cells which could also be present in the PDX tumour. It is also difficult to say whether the genetic changes occurring in the cell lines are a consequence of in vitro culture or whether this would also be observed in the patient as sequencing of patient tumours at differing timepoint has not yet been conducted.

Detection of cancer biomarkers is an important step of characterisation for novel cell lines in order to assess disease relevance and similarity to the tumour of origin. Well differentiated LMS tumours display smooth-muscle differentiation, therefore common biomarkers for the detection of smooth-muscle tumours includes α-SMA, desmin and H-caldesmon and combined are relatively specific for LMS tumours. However, poorly differentiated LMS tumours are more difficult to classify and the expression of these myogenic markers may have been lost (Demicco et al. 2015). Of the 5 LMS PDX-derived cell lines established, three showed expression of a-SMA which is the most commonly observed smooth muscle marker in LMS (Demicco et al. 2015). However ICR-LMS-6 and SARC-393 cell culture displayed a lower expression of a-SMA than the other models and even SK-UT-1, which has been previously reported to have lost myogenic markers (Hemming et al. 2020). Interestingly ICR-LMS-6 displays a similar morphology in culture to ICR-LMS-1 which had the highest expression of a-SMA, showing elongated spindle cells growing in fascicles structures, characteristic of smooth muscle cells. Therefore, the expression of other smooth muscle cell markers was further assessed via proteomic profiles in these two cell lines in particular.

The differences in smooth muscle associated proteins in PDX-models, PDX-derived cells lines, both early and later passages, and LMS cell lines showed no significant difference in protein abundance. Caldesmon, desmin, vinculin and vimentin which are proteins associated with smooth muscle were detected in all PDX-derived LMS models and respective PDX tissue indicating that these cultures retain the smooth muscle characteristics of LMS seen in the PDX models and can therefore be considered as LMS cell cultures (Demicco et al. 2015). SK-UT-1 and SK-UT-1b cells did display a slight loss of desmin abundance which is consistent with the loss of myogenic markers shown in these cells shown in a previous study (Hemming et al. 2020). Analysis of differing biological pathways active in PDX tumours, PDX-derived cells and LMS cell lines showed upregulated mTORC1 signalling. mTORC1 is a sensor of nutrient availability and a major component of mechanisms of amino acid, glucose, reactive oxygen species detection, leading to increased cell survival and proliferation in response to these signals (Tan and Miyamoto 2016). This suggests that mTORC1 activation is a consequence of improved nutrient availability of cells grown *in vitro* compared to *in vivo*. Upregulated mTORC1

signalling is also seen in PDX-derived cells compared to LMS cell lines also indicating higher nutrient availability. PDX-cell lines showed an enrichment of proteins associated with metabolic pathways such as glycolysis and oxidative phosphorylation which was a similar observation made in **chapter 3** when comparing patient tissue to PDX tumour tissue. This result suggests that PDX-derived cell lines are still able to demonstrate an enhanced metabolic state associated with patient tissue compared to LMS cell lines, which is consistent with a previous study specifically analysing metabolic differences in primary low passage cells and longer term cell lines via proteomics (Pan et al. 2009).

In summary, **chapter 4** describes the optimisation of a patient-derived model pipeline from PDX tissue which was used to establish a panel of robust PDX-derived LMS cell cultures which can be grown longer term to show differing growth rates and a range of distinct cell morphologies. These models were further characterised via STR profiling and proteomics showing that these models recapitulate associated PDX genetics, LMS associated markers and biological hallmarks with high fidelity. PDX-derived LMS cultures also showed several enriched hallmark pathways which were not seen in LMS cell lines suggesting that PDX-derived cells may be better able to capture biological processes of LMS as seen in patient tumours.

Chapter 5 - Investigating chemotherapeutic response in LMS patient derived models

5.1 Introduction

Cytotoxic chemotherapeutic drugs such as anthracyclines and alkylating agents have remained the cornerstone of advanced STS treatment for decades due to the significant reduction of tumour burden observed in responding patients (Bramwell, Anderson, and Charette 2000; Linch et al. 2014). However, response rates to commonly used chemotherapies are low in first line advanced STS patients, recorded at 12-24% (Judson et al. 2014; Tap et al. 2020; D'Ambrosio et al. 2020). Additionally, the degree of sensitivity to such agents varies depending on STS subtype and histological variant. For example, well-differentiated liposarcomas demonstrate general chemoresistance while the myxoid variant is particularly sensitive to anthracyclines and trabectedin, while LMS displays varying levels of chemosensitivity between patients (Kasper et al. 2021; Scurr 2011). Therefore, assessment of chemotherapy responses in patient-derived models provides an opportunity to identify biomarkers predictive of chemotherapy response. The acquisition of multi-drug resistance remains a major problem in STS treatment, requiring higher doses to maintain efficacy which can lead to serious toxicity (R. L. Jones 2014). For this reason ultimately the majority of STS patients will fail on chemotherapeutic regiments, shown by a short progression free survival ranging from 2-8 months (Verschoor et al. 2020; Tap et al. 2016; D'Ambrosio et al. 2020; Judson et al. 2014).

Modelling the response of STS to certain chemotherapies is challenging due to the lack of cell lines and patient-derived models available, but additionally, commercially available cell lines can display exceedingly high sensitivity to cytotoxic agents due to enhanced proliferation compared to the disease of origin (Kato et al. 2008; Mitra, Mishra, and Li 2013; Pan et al. 2009). Doxorubicin, as with many other widely used chemotherapeutic agents show enhanced cytotoxic activity against actively dividing cells due to the stalling of DNA replication (J. Zhao 2016). Furthermore, when assessing targeted therapy efficacy in pre-clinical models, the impact of prior chemotherapy treatment and resistance should be assessed, due to the fact that targeted therapy is currently only recommended as a second line or later regimen (Gamboa, Gronchi, and Cardona 2020).

One of the most well reported mechanisms of multi-drug resistance in STS and other cancer types is the upregulation of ABC transporter proteins such as P-glycoprotein (P-gp) which actively transports toxic molecules out of the cell (Abolhoda et al. 1999; Longley and Johnston 2005; Coley et al. 2000; Plaat et al. 2000). However, additional mechanisms of doxorubicin induced drug resistance have since been reported including the activation of the MAPK or JAK/STAT3 pathway, upregulation of anti-apoptotic BCL-

2 family proteins as well as alterations in DNA damage response and repair pathways (Christowitz et al. 2019; Zhiwei Zhang et al. 2020; De Graaff et al. 2016; Longley and Johnston 2005; Das, Jain, and Mallick 2021). Similar alterations in drug efflux, anti-apoptotic, and DNA damage response and repair pathways were additionally noted via proteomic analysis of matched sensitive and resistant uterine sarcoma cell lines (S. T. Lin et al. 2012). Despite these reports, few studies have observed the specific molecular and drug response profile changes which occur following chemotherapy exposure and resistance in patient-derived STS samples with direct comparison between sensitive and resistant primary cells. Such studies could give valuable insights into potential combinatorial therapies to prolong progression free survival in first line advanced STS and to suggest subsequent therapies which chemo-refractory tumours might still respond to.

This chapter will assess the response of the PDX-derived LMS cell cultures established in **chapter 4** to standard of care chemotherapies for advanced STS, correlating these responses with patient treatment history. Additionally, acquired doxorubicin resistant *in vitro* LMS models were generated and used to identify the molecular mechanisms of doxorubicin resistance via proteomic profiling and small molecule inhibitor screening. This experimental work was conducted while continuing with the generation and characterisation of further LMS PDX and PDX-derived cell models in **chapter 3 & 4** in addition to assessment of targeted therapy responses described later in **chapter 6** (**Figure 5.1**).
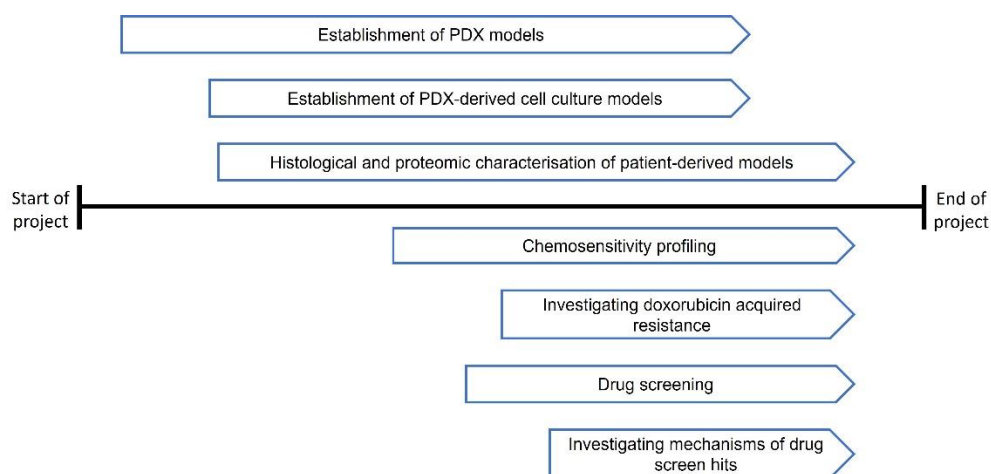
Figure 5.1. Timeframe of experimental approaches described in chapters 3-6.

5.2 LMS PDX-derived cells display varying sensitivity to chemotherapy

Initially I sought to characterise the chemotherapy response profiles of the five 2D PDX-derived LMS cell lines by exposing them to increasing doses of standard of care chemotherapies often used in the first line treatment of advanced LMS, including doxorubicin, gemcitabine and docetaxel. Each model was treated with doses ranging from 5nM to 50uM for a period of 72 hours after which cell viability was assessed. The dose response profiles generated show varying sensitivity and resistance to the three tested chemotherapies across each of the models (**Figure 5.2A-E).** ICR-LMS-1 is the most sensitive of the five models, particularly to doxorubicin and gemcitabine **(Figure 5.2A),** while ICR-LMS-6 demonstrates the most chemo resistant phenotype with neither doxorubicin, gemcitabine or docetaxel able to reduce viability beyond 50% at the highest tested dose of 50 µM (**Figure 5.2C**). Bar ICR-LMS-1 cells treated with doxorubicin, almost all of the chemotherapies tested show a dose response curve which plateaus before reaching 0% viability, suggesting the presence of viable cells able to withstand high concentrations of chemotherapy treatment.

Comparing the IC50 values of doxorubicin in each cell line shows a significantly variable response rate ranging from ICR-LMS-1 as the most sensitive to doxorubicin (IC50=248nM) to the most doxorubicin resistant model, ICR-LMS-6 (IC50 > 50µM) (**Table 5.1**) (**Figure 5.2F&G**). Gemcitabine demonstrates a potent effect on ICR-LMS-1 cell viability (IC50 = 23.2nM) although shows an IC50 value of >20 µM in the remaining culture models (**Figure 5.2G**). In contrast a resistant dose response phenotype to docetaxel was observed in all models with IC50 values higher 50µM (**Figure 5.2G**).
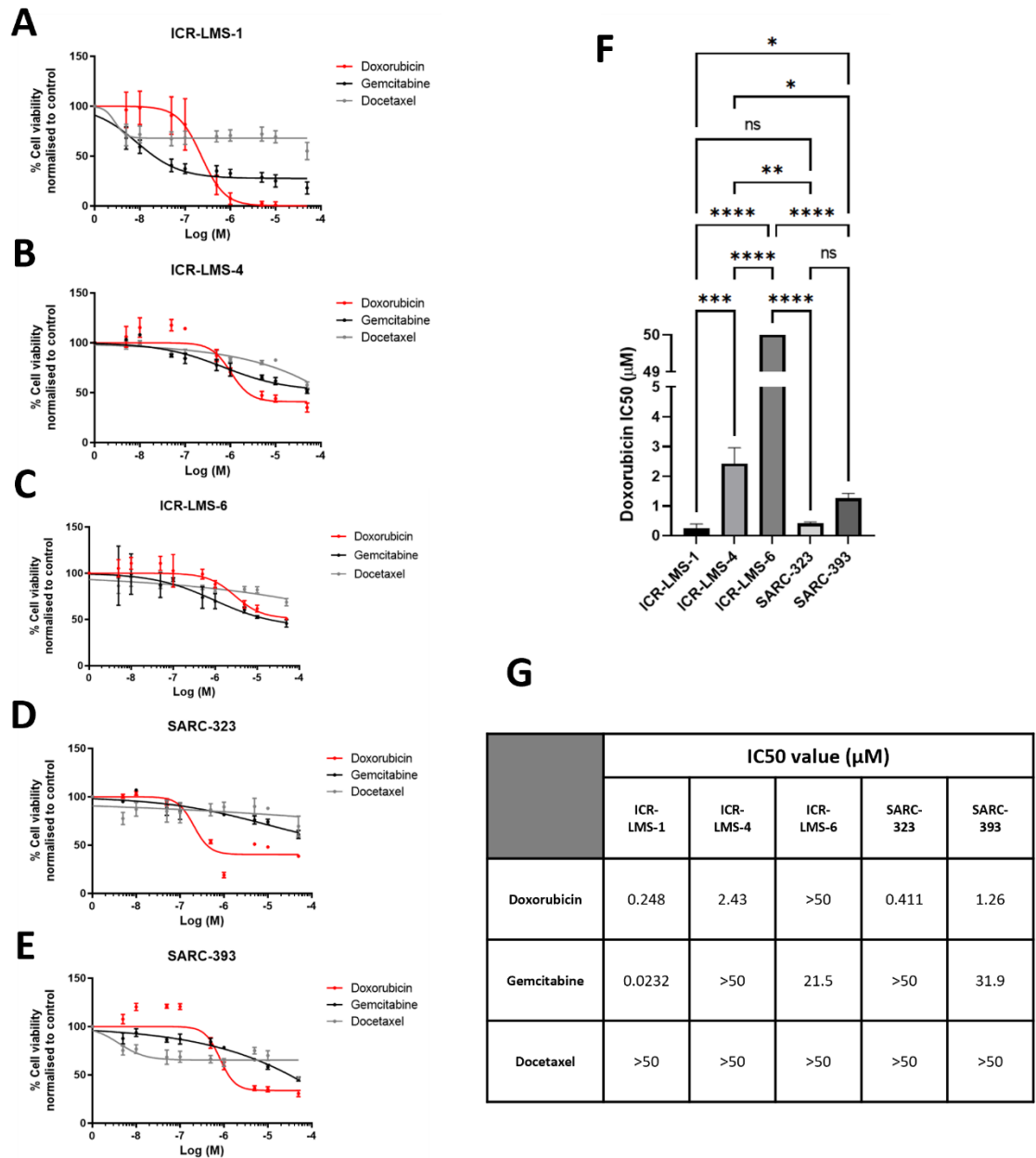
Figure 5.2. Standard of care chemotherapy response profiles of PDX-derived LMS cultures. (A-E) Dose response curves showing cell viability of ICR-LMS-1, ICR-LMS-4, ICR-LMS-6, SARC-323 cell culture and SARC-393 cell culture after 72 hours of doxorubicin, gemcitabine or docetaxel treatment at doses ranging from 5 nM to 50 µM. Viability measurements were fitted to non-linear variable slope four parameter curve. Error bars represent standard deviation. N=3. (F) Mean doxorubicin half-maximal inhibitory concentration (IC50) values for ICR-LMS-1, ICR-LMS-4, ICR-LMS-6, SARC-323 and SARC-393 cells based on fitted dose response curves. Error bars indicate standard deviation. Significance values were calculated via one-way ANOVA with multiple comparisons. ns; not significant ($p > 0.05$), *; $P < 0.05$, **; $P \leq 0.01$, ***; $P \leq 0.001$, ****; $P \leq 0.0001$). (G) Mean doxorubicin, gemcitabine and docetaxel IC50 values for ICR-LMS-1, ICR-LMS-4, ICR-LMS-6, SARC-323 and SARC-393 cell based on fitted dose response curves.

Cell line ID	Subtype	Timepoint	Biopsy grade	Site of biopsy/resection	Primary site if known	Treatment history	Doxorubicin IC50 value (μM)
ICR-LMS-1	uLMS	Baseline biopsy	G3	Pelvic	Uterus	Doxorubicin (3 cycles)	0.248
ICR-LMS-3							0.426
ICR-LMS-4	uLMS	Baseline biopsy	G3	Liver	Uterus	No prior treatments	2.43
ICR-LMS-6	LMS	Post-cycle 3 biopsy	N/A	Peritoneum	Stomach	No prior treatments. First-line GEMMK (Gemcitabine & pembrolizumab)	>50
SARC-323	LMS	Baseline biopsy	G3	Left gluteus	Breast	Epirubicin+Cyclophosphamide in the adjuvant setting after surgery to the primary tumour; no treatment from diagnosis of metastatic disease to trial entry	0.411
SARC-393	uLMS	Post-RT biopsy	N/A	Lung	Uterus	Post-RT	1.26

Table 5.1. **Treatment history of patients from which PDX cell lines were derived and doxorubicin IC50 values.** Information of cell lines used for chemosensitivity testing including subtype, timepoint of biopsy used to establish PDX model, biopsy grade, site of biopsy, primary site of disease, treatment history and doxorubicin half-maximal inhibitory concentration (IC50) values. G3; Grade 3, LMS; Leiomyosarcoma, uLMS; uterine Leiomyosarcoma, N/A; Not Available, RT; RadioTherapy.

I next sought to assess the sensitivity of ICR-LMS-3, the PDX-matched 3D model corresponding to ICR-LMS-1 to doxorubicin in order to check for any differences in response which could be attributed to 3D culture. A cell viability assay was performed with ICR-LMS-3 in 3D, matrigel embedded conditions. Cells were dissociated from spheroids and passed through a filter before seeding to minimise the presence of cell clusters at the beginning of the assay which might affect the results. Cells were cultured for 7 days before doxorubicin doses were added in order to allow spheroids to form before doxorubicin treatment (**Figure 5.3A**). After 72 hours of doxorubicin treatment cell viability was assessed. Despite the differences in culture format, both for the assay itself and for expansion from PDX tissue, ICR-LMS-3 shows a similar dose response profile to doxorubicin, with a clear reduction in cell viability noted at 500 nm (**Figure 5.3B**). However, the dose response curve of ICR-LMS3 is slightly shifted to the right, indicating a slight loss of sensitivity. IC50 values were also elevated in ICR-LMS-3, increasing from 0.248 µM to 0.426 µM but were not found to be significantly different (**Figure 5.3C**).
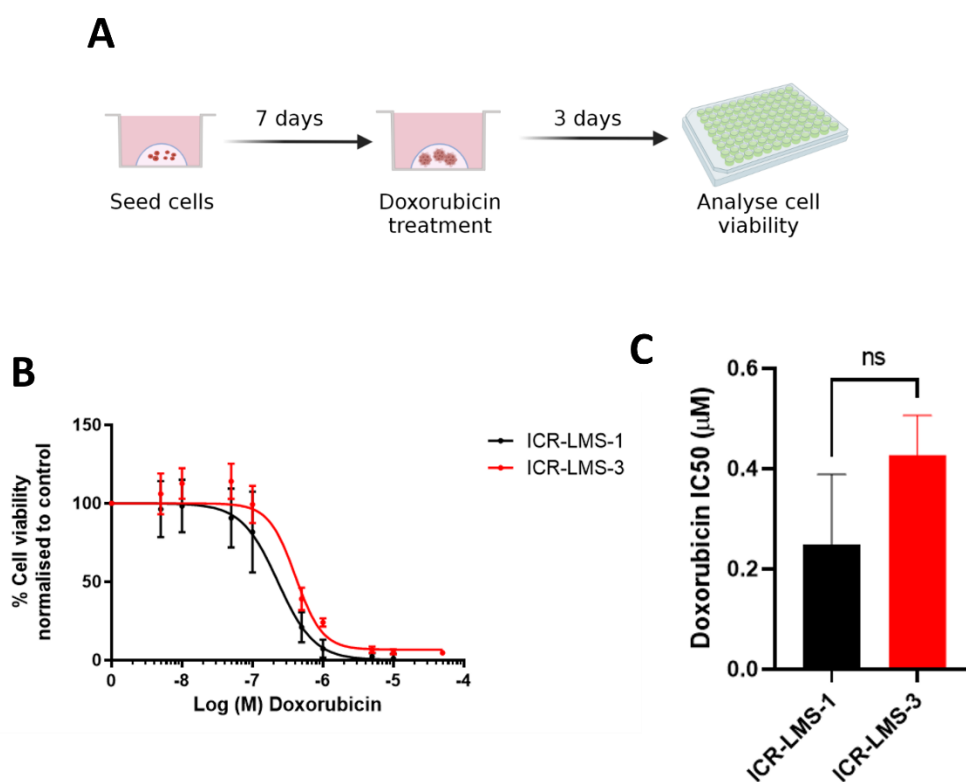
Figure 5.3. **Doxorubicin dose response assay with ICR-LMS-3 spheroids.** (A) Schematic of 3D dose response assay. Cells were cultured for 7 days before doxorubicin treatment for 3 days and cell viability analysis. Error bars represent standard deviation (B) Dose response curve of ICR-LMS-1 in monolayer and

ICR-LMS-3 cells in 3D treated with doxorubicin concentrations ranging from 5 nM to 50 µM. Viability measurements were fitted to non-linear variable slope four parameter curve. N=3. Error bars indicate standard deviation. (C) Mean doxorubicin half-maximal inhibitory concentration (IC50) values for ICR-LMS-1 and ICR-LMS-3 cells based on fitted dose response curves. Error bars indicate standard deviation. ns; not significant ($p > 0.05$).

To further explore the differing sensitivity of ICR-LMS-1 and ICR-LMS-4 to doxorubicin, low density colony formation assays were conducted first with a wide range of concentrations (from 100nM to 5uM) and then at low doses (5nM to 500nM) to observe the colony forming capacity of these PDX-derived cultures under doxorubicin treatment. After 2 weeks of treatment, qualitative analysis shows no visible ICR-LMS-1 colonies at a concentration of 50nMm while colonies can still be observed in ICR-LMS-4 cultures treated with 500nM doxorubicin (**Figure 5.4A**). Quantitative analysis of confluence shows that ICR-LMS-1 colony density is reduced by 60% at the lowest dose tested (5nM) compared to vehicle control and at this lowest dose ICR-LMS-4 showed a significantly higher density of colonies. ICR-LMS-4 continued to show a significant higher colony density at 10, 50 and 100nM of doxorubicin compared to ICR-LMS-1 (**Figure 5.4B**).
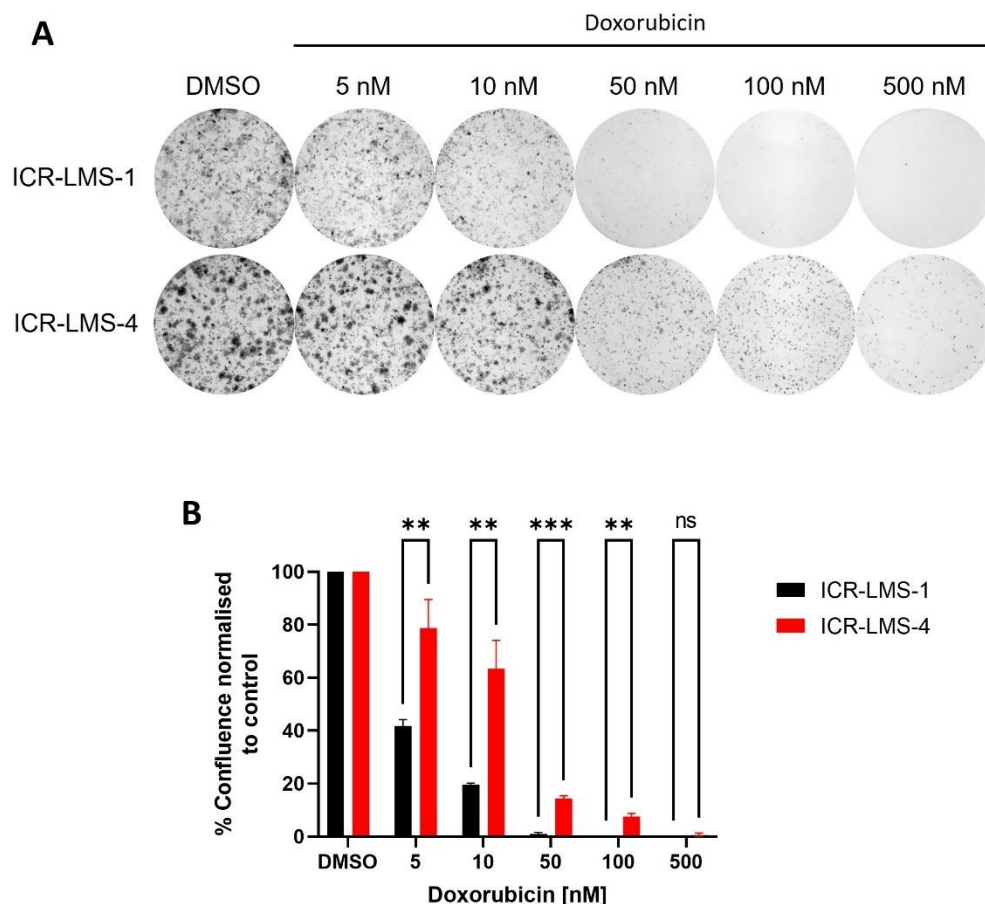
Figure 5.4. Colony formation assay of ICR-LMS-1 and ICR-LMS-4 with doxorubicin treatment. (A) Images of crystal violet stained wells after 2 weeks of ICR-LMS-1 or ICR-LMS-4 treatment with doxorubicin at 5 nM, 10 nM, 50 nM, 100 nM and 500 nM or DMSO vehicle control. (B) Mean % confluence of ICR-LMS-1 and 4 cells from colony formation images normalised to Dimethylsulfoxide (DMSO) vehicle control. Error bars indicate standard deviation. Significance is shown following a multiple unpaired t-test at each concentration. ns; not significant, *; $P < 0.05$, **; $P \leq 0.01$, ***; $P \leq 0.001$, ****; $P \leq 0.0001$.

5.3 Establishing acquired doxorubicin resistant LMS models

Following the observation that the panel of LMS PDX-derived cultures show a range of chemosensitivities, I sought to generate an acquired doxorubicin resistant model in order to study the molecular changes causing drug resistance between the matched sensitive and resistant cells. To achieve this, ICR-LMS-1 was selected for dose escalation as this was the PDX-derived cell line which demonstrated the highest sensitivity to doxorubicin. Dose escalation is a method to generate acquired resistant cell lines *in vitro* by gradually exposing cells to increasing doses of the compound (McDermott et al. 2014). Over a period of 6 months ICR-LMS-1 was exposed to doxorubicin increasing in a stepwise

manner (**Figure 5.5**). A starting dose of 10 nM was chosen as the previous colony formation assay showed this was the highest dose where adherent colonies could still be detected (**Figure 5.4**). Flasks were visually inspected and dose was doubled once cells displayed a similar growth pattern to parental cells for at least two passages. Eventually cells were able to proliferate continuously whilst treated with 80nM doxorubicin. At this point the cells were termed 'ICR-LMS-1 doxoR' and all subsequent assays with this cell line only used passages beyond this point for reproducibility (**Figure 5.5**). This dose escalation method was also conducted on SK-UT-1 and SK-UT-1b to generate SK-UT-1 doxoR and SK-UT-1b doxoR cell lines which also continuously proliferate in media containing 80nM doxorubicin. Alternative methods to generate resistant cells were attempted, including pulsed IC50 and IC90 value doses to mimic the transient high dose observed from intravenous administration of doxorubicin, however no outgrowth of resistant colonies was observed under these conditions after 1 month, at which point cultures were discarded due to lack of adherent cells.
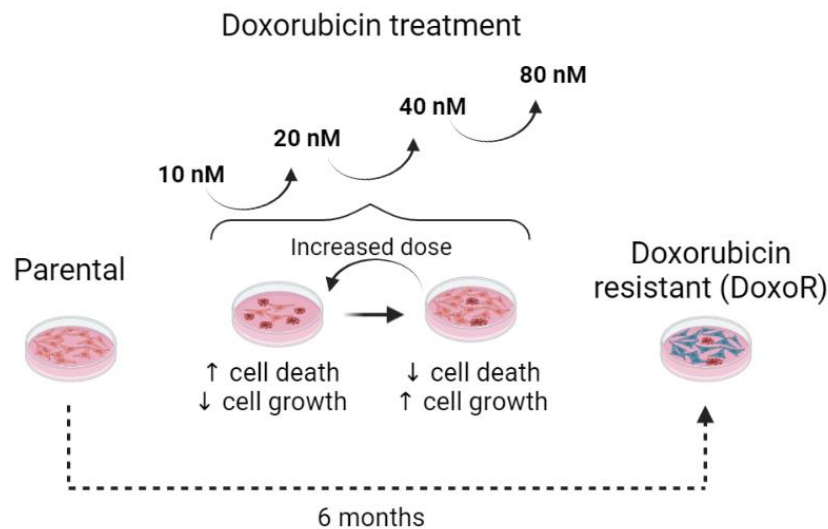
Figure 5.5. Schematic of doxorubicin dose escalation to generate doxorubicin resistant cells. Parental ICR-LMS-1, SK-UT-1 or SK-UT-1b were grown under stepwise increases in doxorubicin concentrations. Doses were doubled when cells displayed a similar growth pattern to parental cells for at least two passages and cell lines were termed doxorubicin resistant (doxoR) when this occurred during treatment with 80 nM doxorubicin. Figure created using BioRender

Due to the long period of continuous culture required to establish ICR-LMS-1, SK-UT-1 and SK-UT-1 doxoR cell lines, STR analysis was performed on both the parental and doxoR cells in order to check for 1) contamination of culture with other cell lines and 2) percentage similarity of the STR profiles between parental and doxoR samples. STR profiles of SK-UT-1 doxoR, SK-UT-1b doxoR and ICR-LMS-1 doxoR were compared to a database of cell lines via the CLASTR Cellosaurus STR similarity search tool. SK-UT-1 doxoR and SK-UT-1b doxoR showed highest matches to SK-UT-1 and SK-UT-1b database profiles respectively while other cell lines showing over 70% similarity to each doxoR lines included SK-UT-1b and SK-UT-1 respectively (each for the other respective variant) and cell lines which have not been grown in the laboratory, meaning that contamination with other cell lines is unlikely. ICR-LMS-1 doxoR showed no cell line matches above 73.68% on the CLASTR Cellosaurus database and any cell lines showing a match higher than 70% have not been used in the laboratory, making contamination of the patient derived doxoR line unlikely.

STR profiles were also compared between parental and doxoR cells, each showing over 90% similarity and therefore can be considered as biologically related with high certainty. However, none of the paired parental and doxoR cell lines displayed an identical STR profile, with SK-UT-1 and SK-UT-1b in particular showing multiple alleles for certain loci which are lost in the respective doxoR cell line, suggesting that slight changes in the genome have occurred during the process of generating doxorubicin resistant cells (**Table 5.2**).

	SK-UT-1	SK-UT-1 doxoR	SK-UT-1b	SK-UT-1b doxoR	ICR-LMS-1	ICR-LMS-1 doxoR
D8S1179	13,15,16	13,15	14,15,16	14,15,16	12,13	13,13
D21S11	29,30,31.2,32.2,33.2	29,32.2	29,30,32.2,33.2	29,32.2	32.2,33.2	32.2,33.2
D7S820	9,10,11	9,10	9,10	9,10	9,10	9,10
CSF1PO	10,11	10,11	10,11,12	10,11	12,12	12,12
D3S1358	15,16	15,16	15,16	15,16	15,16	15,16
TH01	7,7	7,7	7,7	7,7	9.3,9.3	9.3,9.3
D13S317	13,14	13,13	10,13	10,12,13	11,11	11,11
D16S539	13,14,15	13,14	12,13,14,15	12,13,14,15	11,11	11,11
D2S1338	19,21	19,21	18,19,20,21,22	18,22	20,20	20,20
D19S433	12,13	12,13	13,13	13,13	13,13	13,13
vWA	14,15,16,17	15,16,17	16,17	16,17	18,18	18,18
TPOX	8,8	8,8	8,8	8,8	11,11	11,11
D18S51	11,15,16	11,16	11,16,17	11,17	13,15	13,15
Amel	X,X	X,X	X,X	X,X	X,X	X,X
D5S818	10,11	10,11	10,11,12,13	10,12	12,12	12,12
FGA	22,23,24	22,24	22,23,24	22,23	18,18	18,19
% Similarity	96.96%		97.22%		93.75%	

Table 5.2. STR profiling of parental and doxorubicin resistant in vitro cultures. STR loci of ICR-LMS-1, SK-UT-1 and SK-UT-1b cell lines and respective doxorubicin resistant (doxoR) cells. Loci in red indicate discrepancies between parental and doxoR cells. STR; Short Tandem Repeat.

Both the parental and respective doxoR cell lines were cultured for 2 weeks either in the presence or absence of doxorubicin to observe changes in cell morphology and growth patterns. When cultured with doxorubicin at a concentration of 80 nM parental ICR-LMS-1, SK-UT-1 and SK-UT-1b cells all showed a clear reduction in cell number and proliferative colonies could not be observed compared to the untreated parental cells (**Figure 5.6A**). Any remaining parental cells treated with doxorubicin displayed a senescent morphology such as enlarged cell size and lack of proliferation (**Figure 5.6A).** However, when doxoR cell cultures were treated with doxorubicin no difference in morphology or confluence could be observed compared to untreated doxoR cells (**Figure 5.6B**). Morphological differences between the parental and the respective doxoR cultures when grown without doxorubicin were minor (**Figure 5.6A, B**).
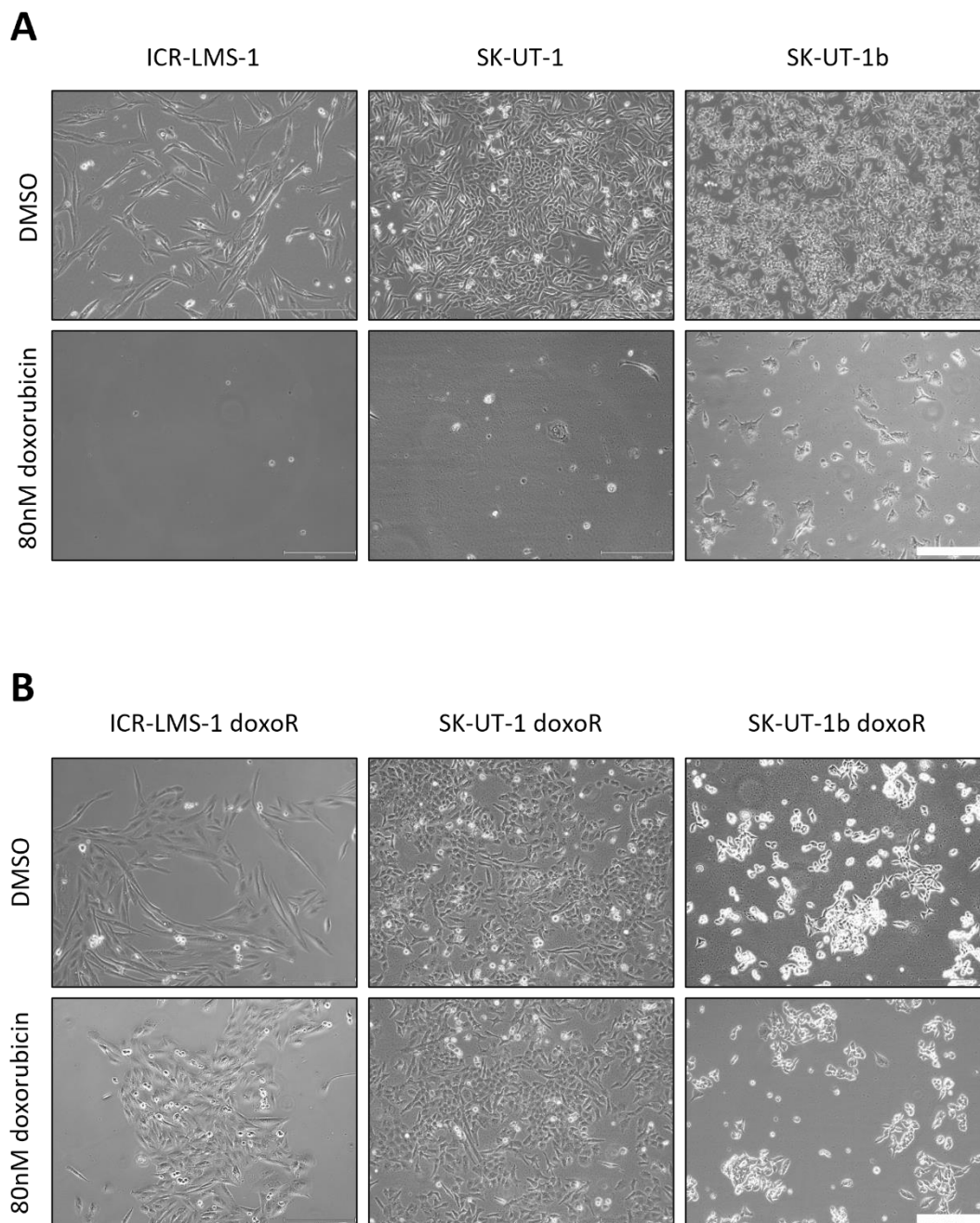
Figure 5.6. Morphology of ICR-LMS-1, SK-UT-1 and SK-UT-1b parental or doxoR cells treated with doxorubicin. (A) Phase contrast images of ICR-LMS-1, SK-UT-1 and SK-UT-1b cells when treated for 2 weeks with 80 nM doxorubicin or Dimethylsulfoxide (DMSO) vehicle control. Scale bar = 300 µm. (B) Phase contrast images of ICR-LMS-1 doxoR, SK-UT-1b doxoR and SK-UT-1b doxoR when treated for 1 week with 80 nM doxorubicin or DMSO vehicle control. Scale bar = 300 µm.

In order to confirm doxorubicin resistance in doxoR cell lines, a cell viability assay was conducted by treating cell lines for 72 hours with doxorubicin ranging from 5nM to 50 µM. ICR-LMS-1 doxoR, SK-UT-1 doxoR and SK-UT-1b doxoR each showed a dose response profile indicating reduced sensitivity to doxorubicin compared to the respective

parental line (**Figure 5.7A, C, E**). IC50 values were significantly higher in the doxoR cell lines, increasing by 6.65, 6.2 and 5.6 fold for ICR-LMS-1 doxoR, SK-UT-1 doxoR and SK-UT-1b doxoR respectively compared to their parental lines (**Figure 5.7B, D, F**), indicating that these lines have indeed acquired doxorubicin resistance.
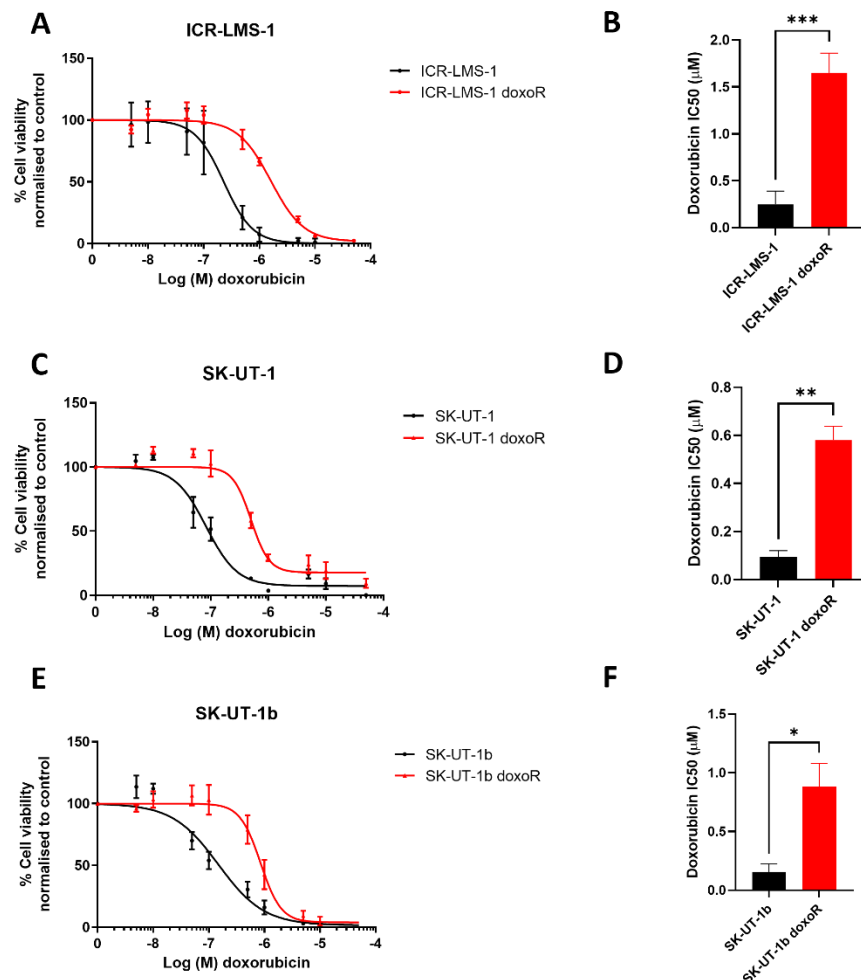
Figure 5.7. Doxorubicin dose response curves in parental and doxorubicin resistant cells. (A, C, E) Percentage cell viability of ICR-LMS-1, SK-UT-1 and SK-UT-1b parental or doxoR cells when treated with doxorubicin concentrations from 5 nM to 50 µM. Viability measurements were fitted to non-linear variable slope four parameter curve. N=3. Error bars indicate standard deviation. (B, D, F) Mean doxorubicin half-maximal inhibitory concentration (IC50) values for ICR-LMS-1, SK-UT-1 and SK-UT-1b parental or doxoR cells based on fitted dose response curves. Error bars indicate standard deviation. ns; not significant (P > 0.05). *; P < 0.05, **; P ≤ 0.01, ***; P ≤ 0.001.

Next, the extent of which doxoR ICR-LMS-1 cells can maintain their resistance to doxorubicin in the absence of drug was assessed by culturing the cell line without doxorubicin and conducting a dose response cell viability assay every two weeks.

Morphologically, after 2 week of drug withdrawal ICR-LMS-1 doxoR showed a similar morphology to parental ICR-LMS-1 cells, proliferating as spindle cells which was also observed in doxoR cells grown without doxorubicin for 8 weeks (**Figure 5.8A**). ICR-LMS-1 doxoR cells grown without drug for 4 weeks or longer showed similar doxorubicin dose response profiles to ICR-LMS-1 doxoR cells which were grown without doxorubicin only for 2 weeks. Although, a very slight shift in the response curve towards lower concentrations at week 6 and 8 could be observed but all timepoints displayed markedly resistant dose response curve compared to the ICR-LMS-1 parental line (**Figure 5.8B**). Additionally IC50 values were significantly higher in doxoR cells at all timepoints compared to the parental line with a small but significant decrease in IC50 value between 4 and 6 weeks and no significant change in IC50 values between week 6 and week 8 without drug (**Figure 5.8C**). Taken together this data indicates that a doxorubicin resistant phenotype is persistent in ICR-LMS-1 doxoR cells despite prolonged drug withdrawal.
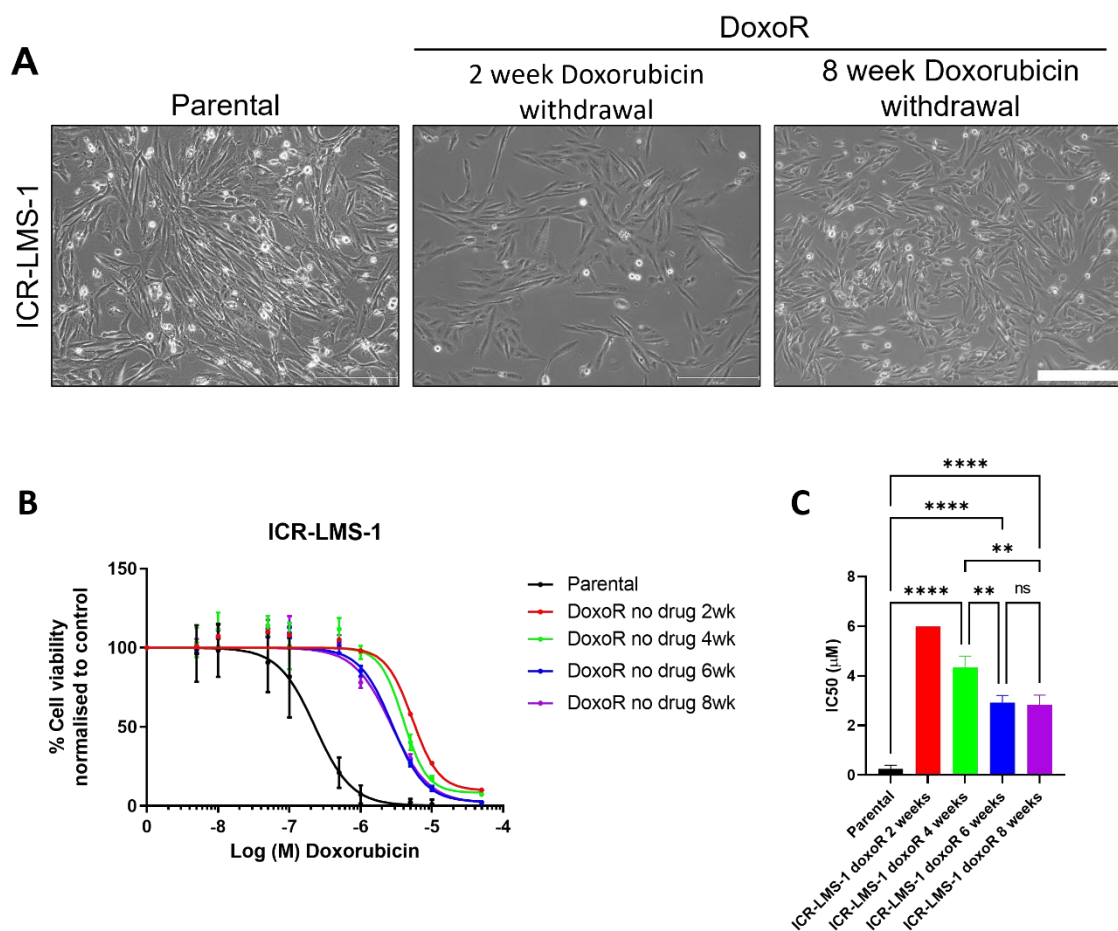
Figure 5.8. Doxorubicin drug withdrawal in ICR-LMS-1 doxoR cells. (A) Phase contrast images of ICR-LMS-1, ICR-LMS-1 doxoR cells grown in 80 nM doxorubicin or ICR-LMS-1 doxoR cells grown without doxorubicin for 8 weeks. Scale bar = 300 μm. (B) Cell viability assay of parental ICR-LMS-1 cells and ICR-

LMS-1 doxoR cells growth without doxorubicin for 2, 4, 6 and 8 weeks in response to doxorubicin treatment at concentrations of 5 nm to 50 μM for 72 hours. Viability measurements were fitted to a non-linear variable slope four parameter curve. N=3. N=1 for ICR-LMS-1 doxoR 2 week timepoint. Error bars indicate standard deviation. (C) Mean doxorubicin half-maximal inhibitory concentration (IC50) values for ICR-LMS-1 parental cells or ICR-LMS-1 doxoR cells grown without drug for 2, 4, 6 and 8 weeks based on fitted dose response curves. Error bars indicate standard deviation. ns; not significant ($p > 0.05$). *; $p < 0.05$, **; $p \leq 0.01$, ***; $p \leq 0.001$, ****; $p \leq 0.0001$.

5.4 Proteomic and drug response profiling of acquired doxorubicin resistant LMS cells

To determine if doxorubicin resistance is achieved via shared biological changes in different models, parental ICR-LMS-1, SK-UT-1 and SK-UT-1b cells as well as the respective doxorubicin resistant cell lines were subjected to SWATH-mass spectrometry by two PhD students in our lab: Yuen Bun Tam and Madhumeeta Chadha. Mass spectrometry profiles were median normalised and subsequent proteomic profiles were subjected to heirarchical clustering. ICR-LMS-1 parental and doxorubicin resistant cells clustered together and were separate from all SK-UT-1 and SK-UT-1b samples. Meanwhile, proteomic profiles of parental SK-UT-1 and SK-UT-1b cells clustered together while the doxorubicin resistant SK-UT-1 doxoR and SK-UT-1b doxoR cells also clustered together but separately from the parental lines (**Figure 5.9A**). This result suggests that there are shared proteomic changes which occurs in these immortalised cell lines upon doxorubicin resistance but these are distinct from proteomic changes associated with doxorubicin resistance in ICR-LMS-1 (**Figure 5.9A**). Next, SAM analysis was conducted on the grouped proteomic profiles of parental versus doxorubicin resistant cells. However, SAM analysis found no significantly upregulated or downregulated proteins between these two groups, indicating that the proteomic alterations associated with doxorubicin resistance do not overlap when considering all three LMS cell models (**Figure 5.9B**).
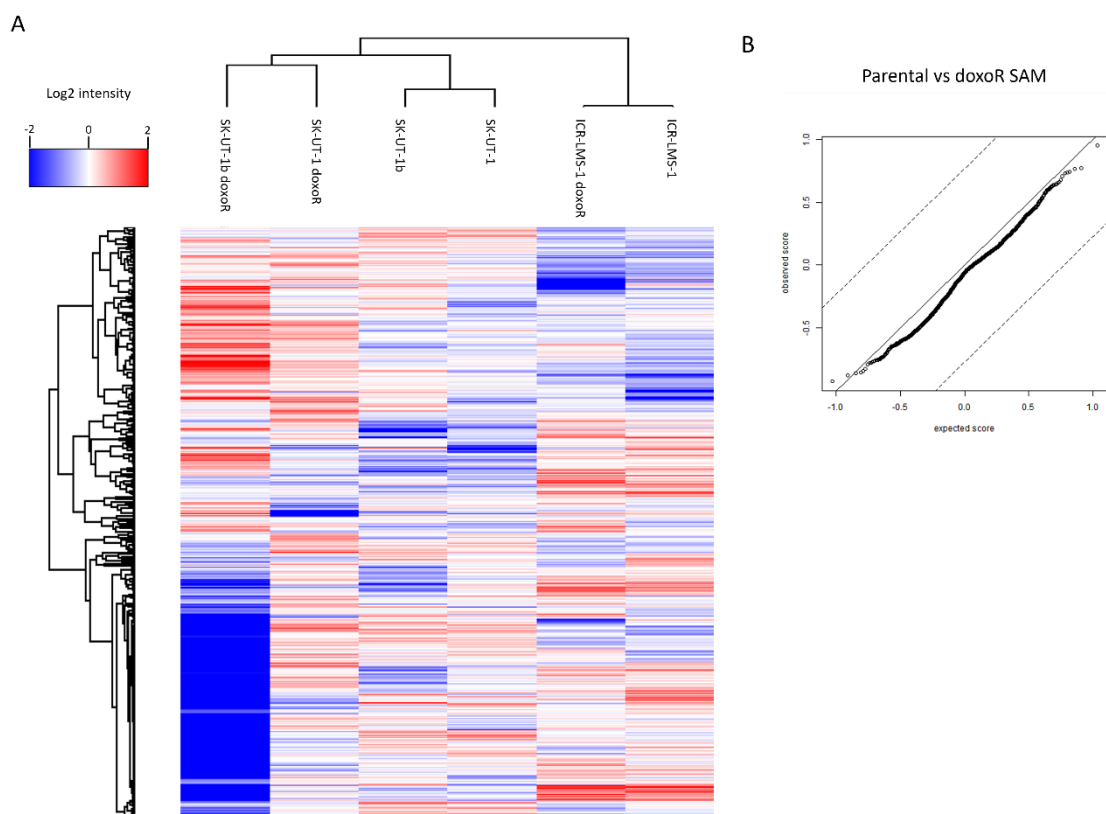
Figure 5.9. Proteomic analysis of parental and doxorubicin resistant ICR-LMS-1, SK-UT-1 and SK-UT-1b cells. (A) Heatmap showing hierarchical clustering of proteomic profiles of parental and doxorubicin resistant ICR-LMS-1, SK-UT-1 and SK-UT-1b cells via two-way unsupervised clustering based on Pearson's correlation coefficient. (B) Significant analysis of microarrays (SAM) plot of proteins showing that there were no significant proteins between parental and doxorubicin resistant cells. Cell lysate samples were prepared by myself for mass spectrometry. Mass spectrometry data was acquired and processed via DIA-NN by Yuen Bun Tam and Madhumeeta. DIA-NN output data was further processed by myself to generate a heatmap of normalised proteomic profiles.

To investigate any changes in the molecular pathways which might have occurred upon acquisition of resistance to doxorubicin, ICR-LMS-1 doxoR, SK-UT-1 doxoR and SK-UT-1b doxoR in addition to their respective parental lines were subjected to treatment with an panel of 58 small molecule inhibitors which was designed to target a range of key oncogenic signalling pathways (**see methods**). Heirarchical clustering of response profiles showed that each doxoR cell line clustered with their respective parental cell line, demonstrating that overall the doxoR lines have similar drug response profiles to their respective parental cells and drug response profiles do not cluster together based on parental and doxorubicin resistant groups (**Figure 5.10**). No compounds show a significant difference in viability between the parental and doxoR line for all three models. However SK-UT-1 and SK-UT-1b parental and doxoR cells showed a significant

difference in viability when treated with the polo-like kinase 1 (PLK-1) inhibitor BI 2536, with the reduction in cell viability significantly lessened in doxorubicin resistant cells (**Figure 5.10**) **(Table 5.3**). The lack of shared sensitivity changes in each parental and doxoR pair indicates that salvage therapies may need to be individualised to specific patients which have developed doxorubicin resistance and there isn't a particular drug which can be used for all doxorubicin resistant patients. However, not many compounds were less efficacious in doxoR cells, suggesting that doxorubicin resistance may not lead to substantial cross resistance to targeted molecular therapies.

ICR-LMS-1 doxoR cells showed an increased sensitivity to six inhibitors compared to parental ICR-LMS-1: the multi-target TKI ponatinib, the HER2 inhibitor neratinib, the Bcl-2 inhibitor navitoclax, the PARP inhibitor talazoparib, the dual PI3K/mTOR inhibitor NVP-BEZ235 and the Akt inhibitor MK-2206 indicating that doxorubicin resistant ICR-LMS-1 cells have an elevated dependency on these factors for growth and/or survival compared to parental cells and have gained a collateral sensitivity towards inhibitors of these factors (**Figure 5.10**) (**Table 5.3**).
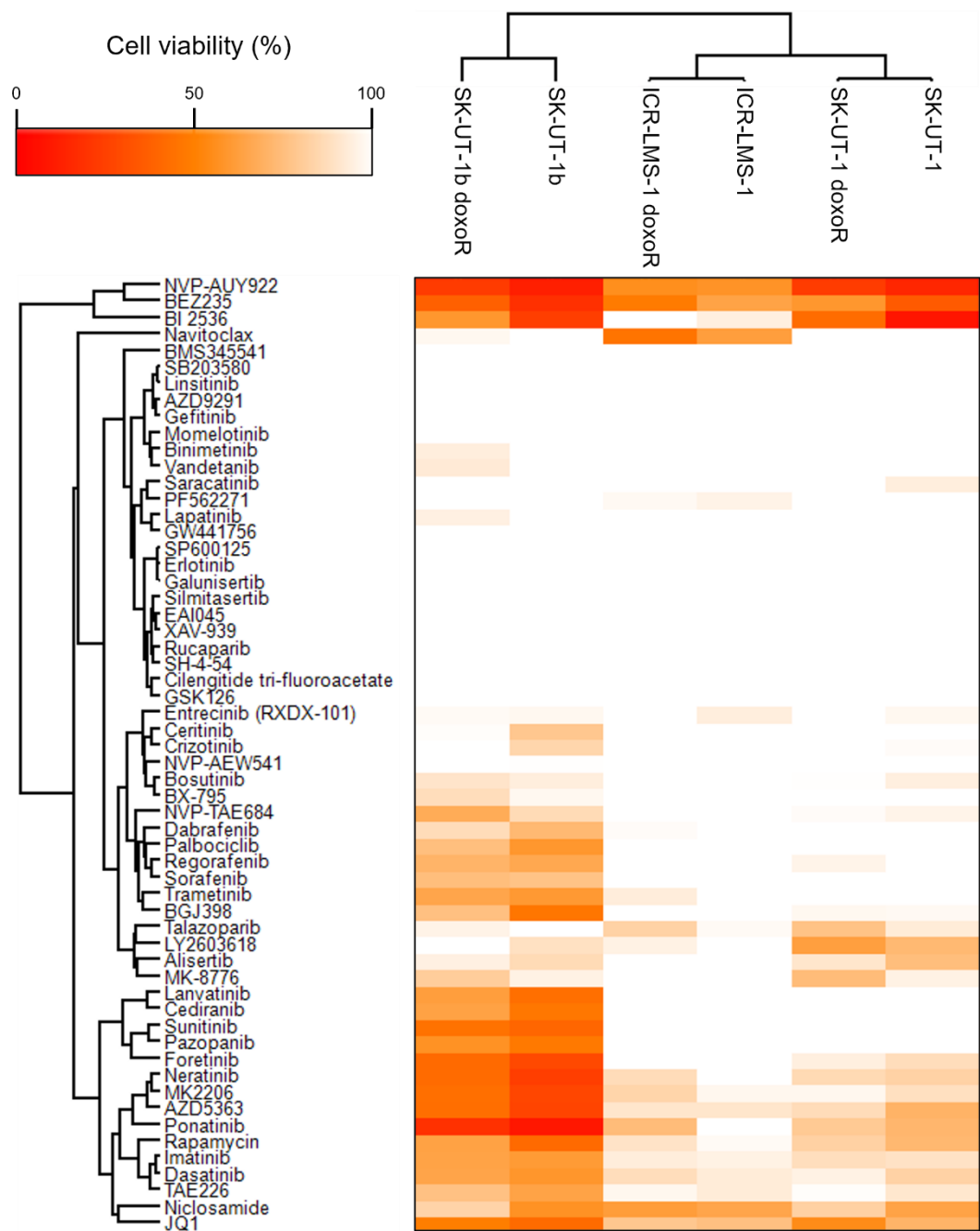
Figure 5.10. 3-day targeted drug screen of parental and doxorubicin resistant cells. Cell viability heatmap of SK-UT-1, SK-UT-1 doxoR, SK-UT-1b, SK-UT-1b doxoR, ICR-LMS-1, ICR-LMS-1 doxoR cells treated with a targeted panel of 58 small molecule inhibitors at a concentration of 500 nM (or 50 nM for NVP-AUY922) for 72 hours. N=3. Profiles underwent hierarchical clustering showing Euclidean distance.

SK-UT-1 vs SK-UT-1 doxoR					
Compound	P value	Mean of parental	Mean of doxoR	Difference	Target
BI 2536	0.000136	8.337	42.07	-33.73	Plk1
BEZ235	0.006672	35.21	58.82	-23.61	PI3K, mTOR
MK-8776	0.014253	94.7	73.43	21.27	Chk1
Niclosamide	0.037644	63.71	81.68	-17.97	STAT3
SK-UT-1b vs SK-UT-1b doxoR					
Compound	P value	Mean of parental	Mean of doxoR	Difference	Target
BI 2536	0.013604	24.02	58.8	-34.77	Plk1
BGJ398	0.037662	46.05	75.23	-29.18	FGFR1/2/3
ICR-LMS-1 vs ICR-LMS-1 doxoR					
Compound	P value	Mean of parental	Mean of doxoR	Difference	Target
Ponatinib	0.000001	103.9	73.73	30.19	Broad spectrum; RTKs
Neratinib	0.001271	105.6	86.08	19.57	HER2, EGFR
Navitoclax	0.004527	62	44.83	17.18	Bcl-xL, Bcl-2, Bcl-w
Talazoparib	0.009186	97.85	82.11	15.74	PARP
BEZ235	0.010682	63.34	47.93	15.41	PI3K, mTOR
MK2206	0.025165	96.44	82.96	13.49	Akt1/2/3

Table 5.3. Compounds showing a significant difference in viability between parental and doxorubicin resistant cells in a short term drug screen. Only compounds which produced a significantly different response in parental vs doxoR cells treated for 72 hours and lowered viability to <90% in either are listed. Significance analysis was performed via two way ANOVA with multiple comparisons. Mean of parental and doxoR cell viability is listed with differences and drug target. Bcl-w; B-cell lymphoma, Bcl-xl; B-cell lymphoma-extra large, Bcl-2; B-cell lymphoma 2, Chk1; checkpoint kinase 1, EGF; Epidermal growth factor receptor, FAK; Focal adhesion kinase, FGFR1/2/3; Fibroblast growth factor receptor 1/2/3, HER2; human epidermal growth factor receptor 2, mTOR; mammalian target of rapamycin, PARP; poly-ADP ribose polymerase, PI3K; phosphatidylinositol-3 kinase, Plk1; polo like kinase 1, STAT3; Signal transducers and activators of transcription 3.

As ICR-LMS-1 cells proliferate at a slower rate to SK-UT-1 and SK-UT-1b (doubling time of ICR-LMS-1 = 4.4 days compared to 1.1 and 1.3 days for SK-UT-1 and 1b, the drug screen was modified to extend treatment time to 6 days. A longer treatment time was used in order to highlight drugs which cause a cytostatic response and therefore might not have shown significant reduction in viability after 72 hours due to inherent slow cell growth. Cell viability after 6 days of drug treatment revealed more compounds which had a significantly different response in ICR-LMS-1 doxoR cells compared to parental cells (**Figure 5.11**) (**Table 5.4**).

Similar to the shorter treatment, doxorubicin resistance in ICR-LMS-1 cells induced further sensitivity to ponatinib and navitoclax following 6 days of treatment, however the longer treatment also highlighted several other small molecule inhibitors which doxorubicin resistant cells displayed an increased sensitivity towards compared to parental ICR-LMS-1 cells, particularly the anaplastic lymphoma kinase (ALK) inhibitor

NVP-TAE684, the focal adhesion kinase (FAK)/IGF-1R inhibitor TAE226, the Src inhibitor Dasatinib, and the mTOR inhibitor Rapamycin (**Figure 5.11**) (**Table 5.4**).

The PLK-1 inhibitor, BI 2536 is the only inhibitor which the doxoR line show a significantly lower sensitivity towards, which was also seen in both SK-UT-1 and SK-UT-1b doxoR cells in the shorter drug screen (**Table 5.3**) (**Table 5.4**).
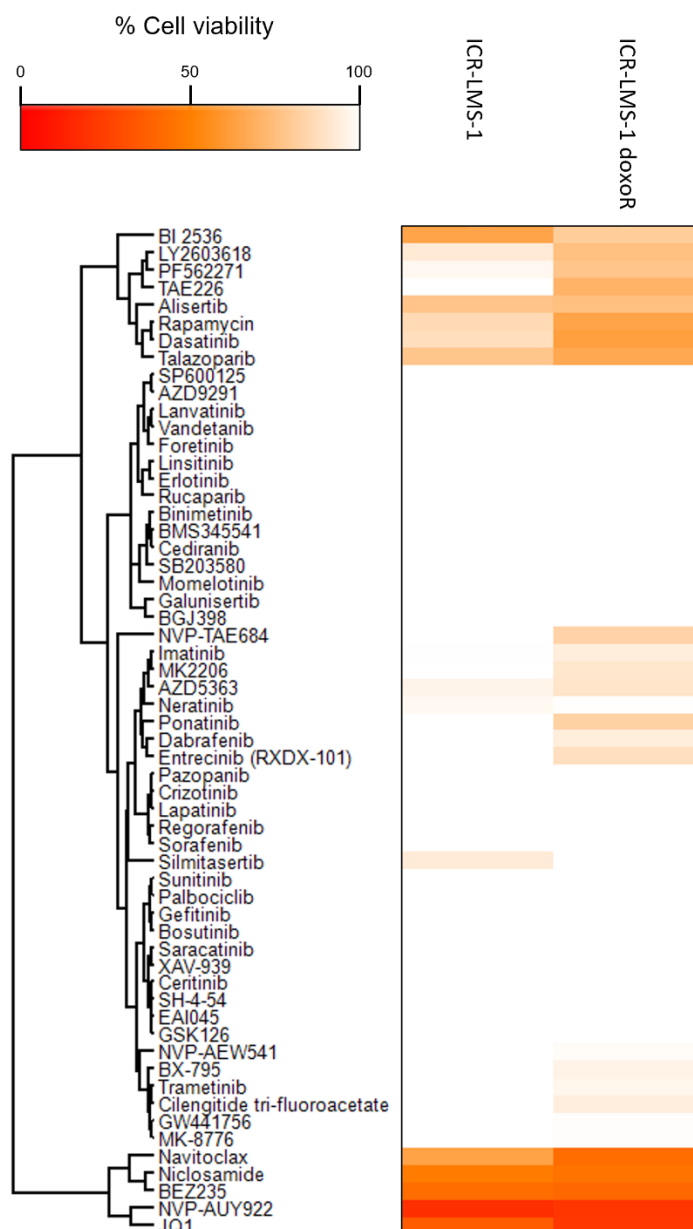
Figure 5.11. 6-day targeted drug screen of ICR-LMS-1 and ICR-LMS-1 doxoR cells. Cell viability heatmap of ICR-LMS-1, ICR-LMS-1 doxoR cells treated with a targeted panel of 58 small molecule inhibitors at a concentration of 500 nM or 50 nM for NVP-AUY922 for 6 days. N=3. Profiles were mapped with Euclidean hierarchical row clustering.

ICR-LMS-1 vs ICR-LMS-1 doxoR (6 day treatment)					
Compound	P value	Mean of parental	Mean of doxoR	Difference	Target
NVP-TAE684	<0.000001	127.2	82.68	44.54	ALK
NVP-TAE226	0.000171	100.8	70.2	30.64	FAK
Dasatinib	0.001922	87.17	62.05	25.12	Abl, Src, c-Kit
Rapamycin	0.008376	85.35	64.09	21.27	mTOR
Navitoclax	0.009988	63.52	42.75	20.77	Bcl-xL, Bcl-2, Bcl-w
Ponatinib	0.010423	102.8	82.15	20.65	Broad spectrum; RTKs
PF562271	0.013444	97.15	77.23	19.91	FAK
Entrectinib	0.015809	106.8	87.36	19.44	TrkA/B/C, ROS1, ALK
LY2603618	0.035998	91.81	74.96	16.85	Chk1
BI 2536	0.048814	64.27	80.09	-15.82	Plk1

Table 5.4. Compounds showing a significant difference in viability between ICR-LMS-1 and ICR-LMS-1 doxoR cells in a long term drug screen. Only compounds which produced a significantly different response in ICR-LMS-1 vs ICR-LMS-1 doxoR cells treated for 1 week and lowered viability to <90% in either are listed. Significance analysis was performed via two way ANOVA with multiple comparisons. Mean of parental and doxoR cell viability is listed with differences and drug target. ALK; anaplastic lymphoma kinase, Bcl-w; B-cell lymphoma, Bcl-xl; B-cell lymphoma-extra large, Bcl-2; B-cell lymphoma 2, Chk1; checkpoint kinase 1, FAK; Focal adhesion kinase, mTOR; mammalian target of rapamycin, Plk1; polo like kinase 1, ROS1; c-ros oncogene 1, RTK; receptor tyrosine kinase, Src; steroid receptor co-activator, TrkA/B/C; Tropomyosin-related kinase A/B/C.

5.5 Discussion

In this chapter, the response profiles of five PDX-derived LMS cell cultures to standard of care chemotherapies was analysed and the data showed a range of chemosensitivities. Similar variations in doxorubicin sensitivity have also been reported in patient-derived soft-tissue sarcoma cultures (Kirilin et al. 2022). However, assessing the clinical relevance of *in vitro* drug concentrations is particularly challenging due to widely varying and unique pharmacokinetic profiles of different anti-cancer agents (Liston and Davis 2017). Based off a recent meta-analysis of maximum plasma concentrations from common anti-cancer agents, the IC50 concentration of doxorubicin in ICR-LMS-1 cells presented in this chapter was within a clinically relevant range (Liston and Davis 2017). One out of the five established PDX-derived LMS models can therefore be considered as doxorubicin sensitive while the rest are chemo resistant, making these good models to further explore markers and mechanisms of both innate and acquired chemoresistance. Future characterisation could include the assessment of PDX chemosensitivity in order to verify if the *in vitro* cultures retain the response profiles of the corresponding *in vivo* tumours. Interestingly, the doxorubicin sensitive model ICR-LMS-1 was derived from a PDX model established from a patient who had received three cycles of doxorubicin treatment prior to biopsy, while the chemo resistant model ICR-LMS-4 was ultimately derived from a treatment naïve patient. Therefore ICR-LMS-4 can be considered as having innate chemoresistance. Unfortunately, patient outcomes are not available so it is not possible to firmly conclude that the patient from which ICR-LMS-1 was derived from maintained response to doxorubicin or whether treatment was stopped due to toxicity concerns.

In **chapter 4** the PDX-derived 3D LMS line ICR-LMS-3 demonstrated a high level of hypoxia and an inner core of non-proliferative cells. However, in this chapter ICR-LMS-3 showed a similar doxorubicin dose response profile to the corresponding 2D line ICR-LMS-1, indicating that the effect of doxorubicin on cell viability is not significantly impacted by 3D culture factors such as hypoxia, cell-cell interactions and drug penetration. Several studies have demonstrated that sarcoma spheroid cultures, have a reduced sensitivity to chemotherapeutic agents although these studies are so far limited to bone sarcomas such as chondrosarcoma, osteosarcoma and Ewing's sarcoma (Voissiere et al. 2017; Munoz-Garcia et al. 2021; Perut et al. 2018). The same is also observed in other cancer types (Gong et al. 2015; Filipiak-Duliban et al. 2022; Mellor and Callaghan 2011; Gobbo et al. 2022).

A study on chondrosarcoma cell lines grown in alginate scaffolds showed that two of three tested cell lines showed elevated doxorubicin resistance in 3D compared to monolayer cultures however one cell line instead showed elevated sensitivity to doxorubicin in 3D compared to monolayer, suggesting that 3D sarcoma cultures to not always lead to reduced chemotherapy response (Palubeckaitė et al. 2020). Additionally, scaffold-free chondrosarcoma spheroids showed different sensitivity to doxorubicin when response assays were conducted on 7 day or 14 day old spheroids, which had markedly different sizes and doxorubicin penetration, highlighting that spheroid size can greatly impacts drug response outcomes (Voissiere et al. 2017). Thus, further characterisation of ICR-LMS-3 should include the assessment of doxorubicin response at different stages of spheroid formation. In osteosarcoma, Ewing's sarcoma and fibrosarcoma spheroids this reduced doxorubicin sensitivity has also been attributed to the increased presence of cancer stem cells which confer a drug resistant phenotype (Bassi et al. 2020; Ozturk et al. 2020; H. Fujii et al. 2009; Honoki 2010; Honoki et al. 2010). However, studies assessing the effect of cancer stem cells on chemosensitivity in LMS 3D models are lacking, therefore future work for this chapter could include assessment of stem cell markers in ICR-LMS-3 compared to ICR-LMS-1.

Acquired doxorubicin resistant cells were generated in this chapter by utilising a long term dose escalation method which has been frequently used for studying acquired resistance in a variety of cancer types and therapies (McDermott et al. 2014). While pulsed, high dose doxorubicin treatment would best mimic the intravenous treatment cycle regimen in patients, in my hands, this selection strategy did not permit for outgrowth of resistant ICR-LMS-1 cells which could be attributed to the even exposure of monolayer cultures to cytotoxic agents compared to *in vivo* tumours with drug penetration gradients (Primeau et al. 2005; Grantab, Sivananthan, and Tannock 2006; Huxham et al. 2004; Kyle et al. 2007). In a 2012 study, Tegze and co-workers generated a panel of doxorubicin and paclitaxel resistant cell lines from two parental breast cancer cell lines (Tegze et al. 2012). The authors separated each cell line into 29 subcultures were all treated in parallel via constant dose escalation to generate distinct resistant lines originating from the same parental cell line in order to identify recurrent mechanisms of chemoresistance. The study went on to show few recurrent mechanisms of resistance in models originating from the same parental line, and additionally differing levels of cross-resistance were also observed in the resistant lines originating from the same parental line (Tegze et al. 2012). On top of investigating the mechanistic basis of the collateral sensitivities identified in this chapter, future work could also generate parallel doxorubicin resistant cultures both in monolayer and in 3D in order to assess the variability of

doxorubicin resistance mechanisms in STS and also highlight recurrent mechanisms of resistance which could be targeted. Alternatively resistance could be achieved *in vivo* in order to take into account tumour microenvironment based resistance mechanisms (Mañas et al. 2022).

Drug withdrawal studies have been conducted in other cancer types such as melanoma to show that chemotherapy treatment can lead to drug tolerant persister cells with transient alterations in metabolic pathways (Karki et al. 2022). The results from this chapter demonstrate that acquired doxorubicin resistant ICR-LMS-1 cells retain resistance even after withdrawal of doxorubicin treatment. A slight decrease in resistance was noted at 6 and 8 weeks after drug withdrawal compared to 4 weeks although differences in IC50 values were still significantly higher than the parental cells. This suggests that ICR-LMS-1 cells have acquired persistent doxorubicin resistance which is not transient and therefore can be considered as an *in vitro* model of chemo refractory LMS.

Clustering of proteomic profiles derived from SK-UT-1 and SK-UT-1b doxoR cells demonstrates that the resistant lines cluster together while the parental cells also both cluster together, suggesting that similar molecular changes have occurred in these two resistant models, although further work is needed to identify mechanisms of resistance in these two doxoR models. After assessing the signalling pathway dependencies in all three doxoR models via small molecule inhibitor perturbation, the only observable cross-resistance, whereby resistance to one compound also induces resistance to another compound, was to the PLK-1 inhibitor BI2536. PLK-1 plays an important role in cell cycle progression as a key regulator of multiple G2-M stages including checkpoint regulation, spindle assembly, centrosome maturation, chromatid separation and cytokinesis (Z. Liu, Sun, and Wang 2017; Schmucker and Sumara 2014; Jeong et al. 2018). Inhibitors of PLK-1 have been shown to cause mitotic arrest and subsequent apoptosis in MPNST, synovial sarcoma and LMS cell lines including SK-UT-1 and SK-UT-1b (Nair and Schwartz 2015).

Importantly, other than BI 2536, doxorubicin resistant cells showed no other shared significant loss of sensitivity to the tested inhibitors. In contrast, the remaining differences in viability between the parental and doxoR ICR-LMS-1 cells instead showed an increase in sensitivity to certain inhibitors. This result suggests that molecular targeted therapies which demonstrate anti-tumour efficacy in LMS may continue to be effective despite the acquisition of chemoresistance. For advanced LMS almost all patients will undergo first or even multiple lines of chemotherapy as a standard of care treatment (A. Gronchi et al.

2021). Therefore, this drug screening data suggests that novel therapies are still effective in a chemo refractory setting and could be candidate therapies to be used in the salvage setting following failure of doxorubicin.

Acquired doxorubicin resistant ICR-LMS-1 cells did display several collateral sensitivities compared to the parental line which were not seen in SK-UT-1 and SK-UT-1b doxorubicin resistant cells, such as inhibitors of FAK, Src, mTOR, Bcl, and CHK1. Two inhibitors of FAK, NVP-TAE226 and PF562271 separately lead to an enhanced response in doxorubicin resistant cells suggesting that FAK activity is important for growth or survival of chemotherapy resistant cells. FAK is a cytoplasmic tyrosine kinase, activated by growth factors or integrins, which is upregulated in many cancer types (Moritake et al. 2019; Y. Bai et al. 2012). Upregulation of FAK signalling promotes tumour progression and metastasis via kinase dependent interactions with downstream targets including Src as and PI3K/Akt pathway components as well as kinase independent interactions with p53 and MDM2 (Sulzmaier, Jean, and Schlaepfer 2014). In Ewing's sarcoma cells FAK inhibitors have previously been shown to synergise with chemotherapies including doxorubicin although the mechanisms behind this synergy has not been explored (Moritake et al. 2019). However, the role of FAK on doxorubicin sensitivity in LMS cells is less well studied although increased FAK expression and phosphorylation has been demonstrated in endometrial adenocarcinoma patients with *PTEN* mutations, which correlated to worse outcomes (Thanapprapasr et al. 2015). Additionally, FAK inhibition in orthotopic xenograft models of endometrial adenocarcinoma synergized with chemotherapy treatment (paclitaxel and topotecan) (Thanapprapasr et al. 2015).

In this chapter it was shown that ICR-LMS-1 doxorubicin resistant cells are significantly more sensitive to navitoclax, an inhibitor of antiapoptotic proteins, BCL-X$_L$, BCL-2 and BCL-w. This is consistent with a previous report demonstrating that doxorubicin resistant chondrosarcoma cell lines or primary cells were sensitised to BCL-2 inhibition and navitoclax also sensitises LMS cells to doxorubicin although the relationship between doxorubicin acquired resistance and BCL-2 addiction has not been explored in LMS (De Graaff et al. 2016; Van oosterwijk et al. 2012).

Based on the results in this chapter future work should focus on establishing the mechanistic basis behind sensitivity and resistance in each of the three paired parental and acquired doxoR models. Additionally future directions for this chapter could include investigation into the mechanisms behind the observed collateral sensitivities.

Chapter 6 - Evaluating molecular targeted therapeutic response in LMS patient derived models

6.1 Introduction

The treatment of advanced STS with chemotherapeutic agents is almost always with palliative intent and disease progression is often seen following several treatment regimens, at which point treatment options are extremely limited (Kasper et al. 2021; Verschoor et al. 2020). Additionally, cytotoxic chemotherapies such as doxorubicin are not suitable for maintenance therapy even in responding patients due to the toxicity associated with high cumulative doses (Volkova and Russell 2012). Therefore, novel treatment options are urgently needed for advanced STS patients which might prolong survival beyond that achieved with current therapeutic regimens.

Targetable candidate pathways in STS varies depending on subtype. For example, advancements in the molecular characterisation of GIST has led to the identification of distinct subgroups with recurrent oncogenic mutations and subsequently the approval of several targeted therapies including the c-KIT and PDGFRα inhibitor imatinib (Szucs et al. 2017). In advanced or metastatic GIST, imatinib shows an impressive 80% disease control rate and a mPFS of approximately 20 months (Verweij et al. 2004; Blanke et al. 2008). However, STS subtypes with complex karyotypes such as LMS often display many mutations contributing to pathogenesis, making the identification of targeted therapies challenging (Asano et al. 2022; Chudasama et al. 2018). Currently, only one molecular targeted therapy, the multi-target TKI pazopanib, is approved for use in STS such as LMS, although clinicopathological biomarkers of pazopanib response are not fully understood (A. T. J. Lee, Jones, and Huang 2019).

An increasing proportion of pre-clinical studies are focusing on the use of patient-derived *in vitro* cultures in order to highlight candidate therapies for *in vivo* assessment and subsequent clinical assessment. Compared to commercial cell lines, patient-derived cultures are able to recapitulate several aspects of the tumour of origin including molecular characteristics, histology (if 3D modelling), sub clonal heterogeneity and drug response phenotypes, making them better suited for pre-clinical studies (Kodack et al. 2017; Cree, Glaysher, and Harvey 2010; Imamura et al. 2015; Salawu et al. 2016). Several reports have conducted large scale drug screening on patient-derived STS models, mainly focusing on genetically simple STS subtypes such as RMS, synovial sarcoma and alveolar soft-part sarcoma (ASPS), identifying the Src inhibitor dasatinib as well as Akt inhibitors as candidate targeted therapies for these subtypes (Brodin et al. 2019; Manzella et al. 2020). One of these studies further utilised high throughput drug screening approaches to identify subsets of RMS patients with distinct drug response profiles which were compared with molecular profiles (translocation positive and

negative) (Manzella et al. 2020). However, large scale patient-derived cell screening studies focusing on LMS are limited (Babichev et al. 2016; Noguchi et al. 2020; Edris et al. 2012).

Molecular profiling studies of both uterine and non-uterine LMS tumours have identified a high frequency (54-57%), with a predominance in uterine LMS, of homologous repair deficiency (HRD) signatures including somatic loss of function or deletions in DNA damage repair associated genes (*PTEN, BRCA2, ATM, CHEK1, XRCC3, CHEK2, BRCA1, RAD51)* and genomic scarring suggesting that targeting the DNA damage response pathway might be a promising therapeutic strategy (H. Li et al. 2020). Indeed, uterine LMS cell lines demonstrate reduced HR capacity and sensitivity to PARP inhibitors as well as inhibitors of DDR components shown via HR reporter assays or quantification of Rad51 foci as a marker of HR (Chudasama et al. 2018; Anderson et al. 2021; H. Li et al. 2020). However, the specific mechanism by which PARP inhibitors exert an anti-tumour effect is currently unknown and is based on inferences of PARP inhibitor mechanism of action observed in other cancer types (Helleday 2011; Godon et al. 2008). Additionally, due to the fact that many chemotherapeutic agents are genotoxic, prior treatment and possible resistance of LMS tumours to chemotherapies may alter the DDR pathway and thus might effect the sensitivity of LMS tumours to DDR targeted therapies such as PARP inhibitors which has not been fully explored.

In order to highlight novel targeted therapies active in the LMS subtype, this chapter utilises the PDX-derived LMS cell lines previously established and characterise in **chapter 4**. LMS lines were subjected to small molecule inhibitor drug screening to identify shared and patient specific molecular dependencies in LMS. Response phenotypes and were further investigated in two uterine LMS cell lines, ICR-LMS-1 and ICR-LMS-4, which, based on the results from **chapter 5** represent a chemo-sensitive and resistant model respectively and building on these results, mechanisms of response to PI3K/mTOR inhibitors were assessed.

6.2 PDX-derived LMS cultures display both shared and distinct drug sensitivities

Each of the PDX-derived LMS cell cultures from **chapter 4** both established and primary, as well as the commercially available LMS cell lines SK-UT-1 and SK-UT-1b were exposed to a targeted panel of 58 small molecule inhibitors designed to target a range

of key oncogenic pathways (see **methods**). Initially, cells were exposed for 72 hours before cell viability was assessed. Here, the BET bromodomain inhibitor JQ1 and heat shock protein 90 (HSP90) inhibitor NVP-AUY-922 were considered as a positive control of reduced viability, as these compounds show broad anti-tumour activity (Jiang et al. 2020; Menezes et al. 2012). Hierarchical clustering of the resulting response profiles demonstrates that the commercially available uterine LMS cell line SK-UT-1b clusters separately to all other models, indicating that this model has distinct molecular dependencies from other LMS models (**Figure 6.1A**). The drug response profile of SK-UT-1 was more similar to the five PDX-derived LMS models compared to SK-UT-1b although distinct clustering is still observed. Out of the PDX-derived models, SARC-323 clustered separately, showing a reduction of cell viability in response to more small molecule inhibitors in general, while ICR-LMS-6 and ICR-LMS-4 were clustered together as pairs, as was SARC-393 and ICR-LMS-1 (**Figure 6.1A & B).** When observing the clustering of drugs used in this screen, The STAT3 inhibitor niclosamide and the dual PI3K inhibitor BEZ235 clustered together with the HSP90 inhibitor NVP-AUY-922, each causing a reduction in viability in all LMS cultures, suggesting that the targets of these inhibitors are necessary for survival or proliferation of LMS cells. JQ1 also reduced the viability of all LMS cultures but to a lesser extent (**Figure 6.1A**). However no compounds were able to reduce the viability of all PDX-derived LMS models below a cut-off of 70% (**Figure 6.1B**).
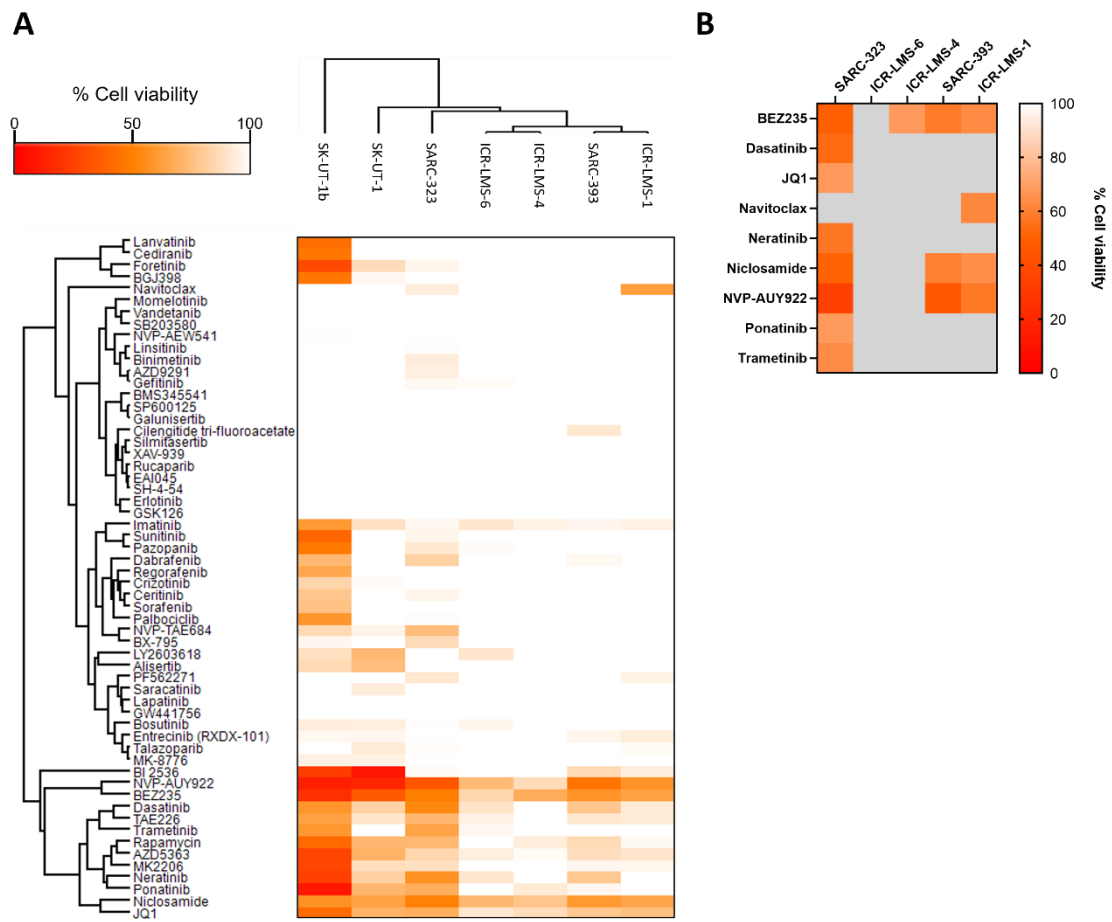
Figure 6.1. 3-day targeted drug screen of PDX-derived and immortalised LMS cells. (A) Cell viability heatmap of SK-UT-1b, SK-UT-1, SARC-323, ICR-LMS-6, ICR-LMS-4, SARC-393 and ICR-LMS-1 cells treated with a targeted panel of 58 small molecule inhibitors at a concentration of 500 nM or 50 nM for NVP-AUY922 for 72 hours. Viability is normalised to DMSO controls N=3. Profiles were mapped with two-way hierarchical clustering with Euclidean distance. (B) Heatmap of compounds causing <70% viability in SK-UT-1b, SK-UT-1, SARC-323, ICR-LMS-6, ICR-LMS-4, SARC-393 and ICR-LMS-1 cells from drug screening.

Due to the slow growth rates of the established PDX-derived cells included in this study, ranging from 3.2 to 4.4 days, four of the LMS cultures (ICR-LMS-1, 4, 6 and SARC-393) were exposed to the same concentration of drug screen for 6 days before cell viability was assessed. When the drug response profiles were compared, the uterine LMS model ICR-LMS-1 clustered separately to the remaining three models while the other two uterine LMS models ICR-LMS-4 and SARC-393 are clustered together, suggesting these models share similar pathway dependencies (**Figure 6.2A**). A cut-off of 70% was applied to the cell viability dataset to highlight the inhibitors which displayed a robust reduction of viability. BEZ235, niclosamide, NVP-AUY-922 and JQ1 were able to reduce viability of all four tested cell cultures to below 70% and also clustered together in dose response

profiles, suggesting the targets of these inhibitors are necessary for cell growth or survival of LMS cells and could be candidate targets for molecular therapy in LMS (**Figure 6.2A, B, C**).
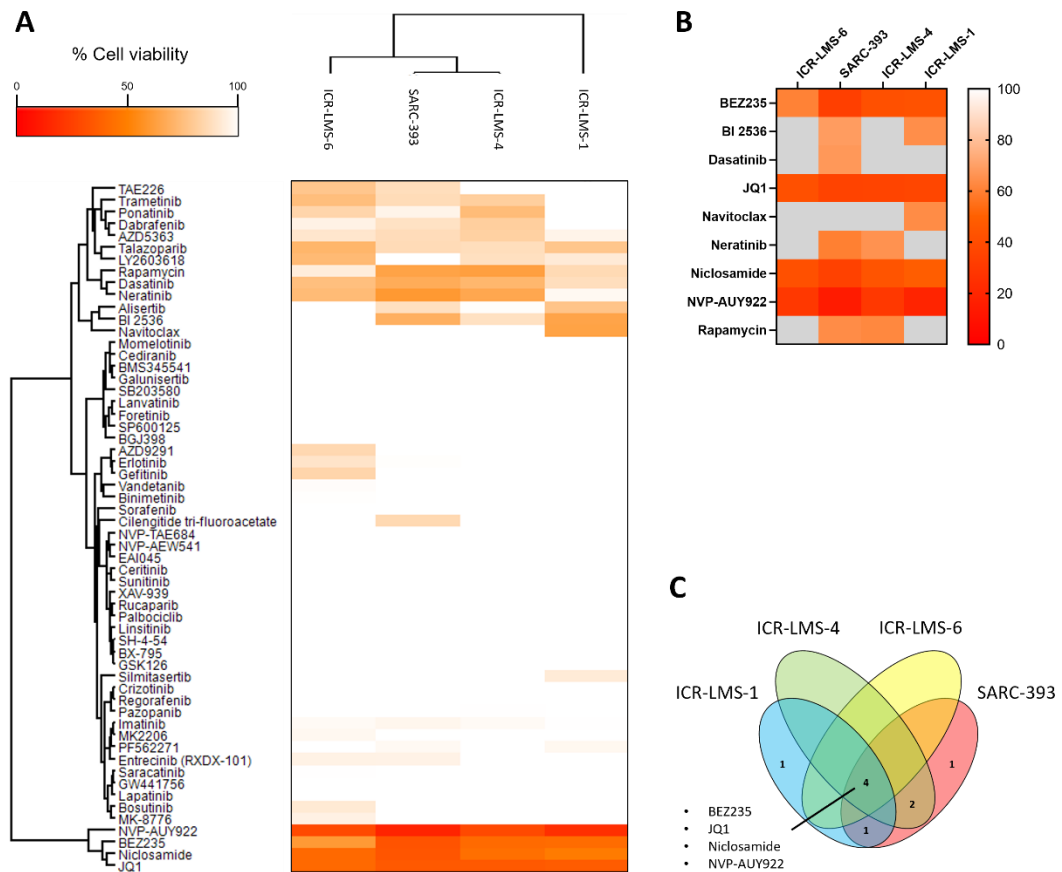
Figure 6.2. 6-day targeted drug screen of PDX-derived LMS cells. (A) Cell viability heatmap of ICR-LMS-6, SARC-393, ICR-LMS-4 and ICR-LMS-1 cells treated with a targeted panel of 58 small molecule inhibitors at a concentration of 500 nM or 50 nM for NVP-AUY922 for 6 days. Viability is normalised to DMSO controls N=3. Profiles were mapped with Euclidean hierarchical clustering. (B) Heatmap of compounds causing <70% viability in ICR-LMS-6, SARC-393, ICR-LMS-4 and ICR-LMS-1 cells from drug screening. (C) Venn diagram of shared and unique drug sensitivities able to reduce cell viability to below 70% based on screening data. Including BEZ235, BI 2536, dasatinib, JQ1, navitoclax, neratinib, niclosamide, NVP-AUY922 and rapamycin.

The non-uterine LMS PDX-derived line ICR-LMS-6 showed the most resistant drug response profile whereby only BEZ235, JQ1, niclosamide and NVP-AUY-922 were able to reduce viability beyond 70% (**Figure 6.2B & C**). In contrast, the uterine LMS culture SARC-393 displayed the highest number of drug sensitivities. In addition to the four inhibitors which reduced viability in all LMS cultures, SARC-393 also displayed sensitivity

towards the Src inhibitor dasatinib, the PLK-1 inhibitor BI2536, the HER2 inhibitor neratinib and the mTOR inhibitor rapamycin. On top of the four shared sensitivities, ICR-LMS-1 cells also demonstrated sensitivity to BI2536 and ICR-LMS-4 also showed sensitivity to neratinib and rapamycin (**Figure 6.2B & C**). ICR-LMS-1 cells displayed a unique sensitivity towards treatment with the BCL-2 inhibitor navitoclax which was not observed in ICR-LMS-4, ICR-LMS-6 or SARC-393 (**Figure 6.2B & C**). Taken together, this data shows that LMS cells can display both shared and distinct sensitivities to certain molecular targeted therapies and highlights that LMS cells are broadly sensitive towards BEZ-235 as well as niclosamide.

6.3 Targeting PI3K/mTOR pathway

Based on the observation that PDX-derived LMS cultures are sensitive to dual PI3K/mTOR inhibition or mTOR inhibition alone, I sought to determine the PTEN expression status of these models via western blot. SK-UT-1 and the NSCLC cell line PC-9 were used as controls of PTEN loss as both show low expression of this protein (Broad Institute 2021). The non-transformed fibroblast cell line MRC-5 was used as a positive control of PTEN expression (L. Liu et al. 2019). All PDX-derived cultures tested showed a reduction in PTEN levels compared to MRC-5, with no PTEN band observed in the three uterine LMS models ICR-LMS-1, 4 and SARC-393 models while non-uterine LMS cultures SARC-323 and ICR-LMS-6 both display weak PTEN expression (**Figure 6.3**).
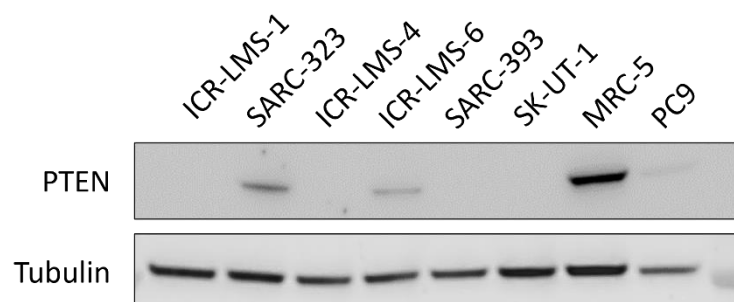
Figure 6.3. PTEN loss in PDX-derived LMS cells. Immunoblot of ICR-LMS-1, SARC-323, ICR-LMS-4, ICR-LMS-6, SARC-393, SK-UT-1, MRC-5 and PC9 against PTEN and tubulin as a loading control. PTEN; phosphatase and tensin homolog. MRC-5 is a positive control of PTEN expression.

The two established uterine LMS PDX-derived cells lines ICR-LMS-1 and ICR-LMS-4 were selected for further analysis of response to PI3K/mTOR pathway inhibition. As the Akt inhibitors included in the small molecule drug screen (AZD-5356 and MK2206) showed no impact or only a modest reduction on cell viability (**Figure 6.2A**) specific inhibition of Akt was not investigated further. Initially, to verify the results of the drug screen, dose response curves and colony formation assays were conducted for ICR-LMS-1 and ICR-LMS-4 treated with the PI3K/mTOR inhibitor BEZ235, the PI3Kα inhibitor alpelisib or the mTOR inhibitor rapamycin. All three compounds caused a dose dependent reduction in ICR-LMS-1 and ICR-LMS-4 cell viability, although both cell lines showed a higher sensitivity to BEZ235 and rapamycin compared to alpelisib (**Figure 6.4A & B**). For ICR-LMS-1 alpelisib caused a dose dependent reduction of colonies although BEZ235 and rapamycin treatment caused a significantly larger reduction of colony formation, with no observable colonies present after 2 weeks of treatment at concentrations of 100 nM (**Figure 6.4C & D**). This result was also observed in ICR-LMS-4 cells where BEZ235 and rapamycin had a significantly enhanced effect on colony formation compared to alpelisib treatment (**Figure 6.4E & F**). Together these results suggest that mTOR inhibition has a greater effect on LMS cell viability compared to PI3K inhibition.
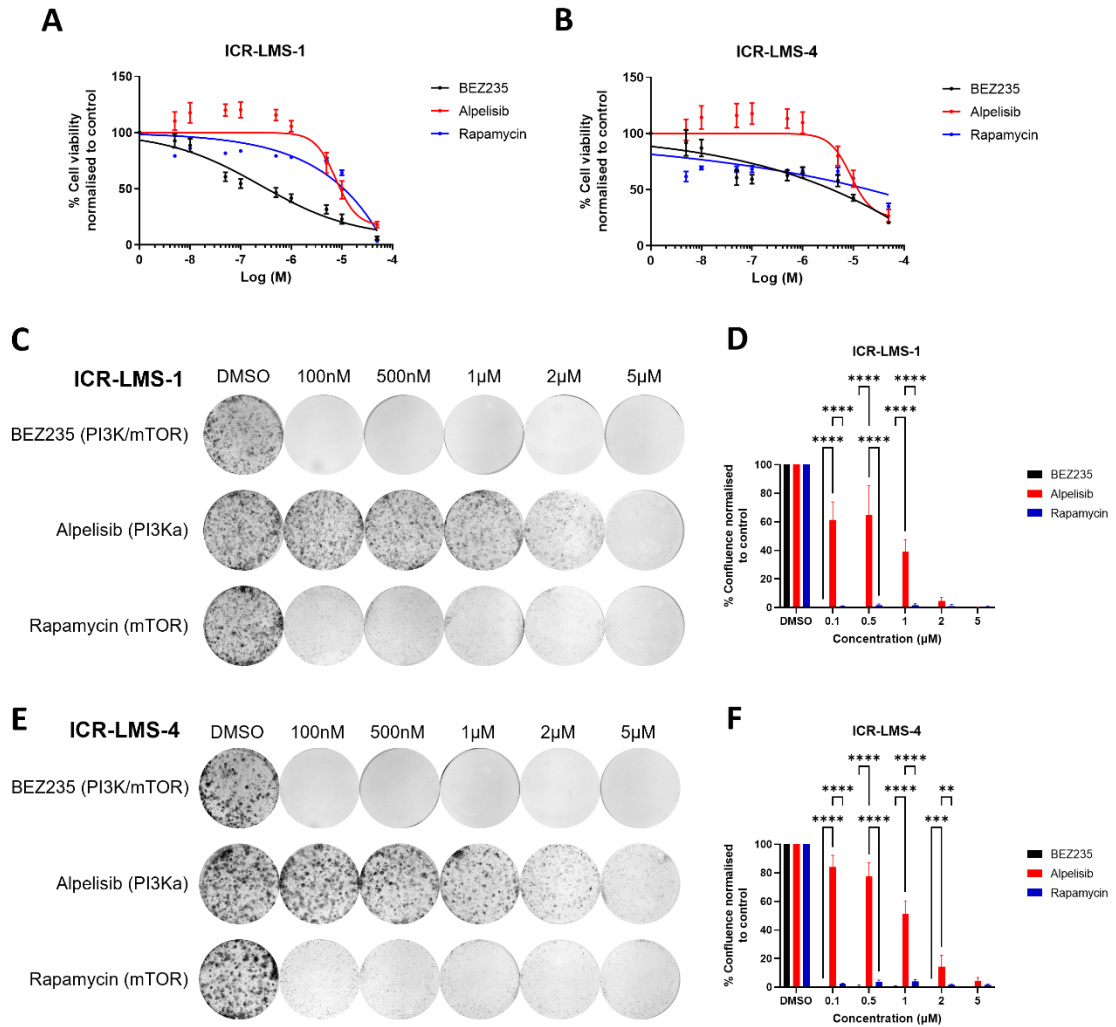
Figure 6.4. Response of ICR-LMS-1 and ICR-LMS-4 cells to PI3K and/or mTOR inhibition. (A, B) Cell viability dose response curve of ICR-LMS-1 or ICR-LMS-4 cells treated with BEZ235, alpelisib or rapamycin for 72 hours at concentrations ranging from 5 nM to 50 μM. N=2. Viability measurements were fitted to non-linear variable slope four parameter curve. Error bars indicate standard deviation. (C, E) Images of crystal violet stained wells after 2 weeks of ICR-LMS-1 or ICR-LMS-4 treatment with BEZ235, alpelisib or rapamycin at 100 nM, 500 nM, 1 μM, 2 μM and 5 μM or Dimethylsulfoxide (DMSO) vehicle control. (D, F) Mean % confluence of ICR-LMS-1 or ICR-LMS-4 cells from colony formation images normalised to DMSO vehicle control. Error bars indicate standard deviation. Significance is shown following a two-way ANOVA with multiple comparisons at each concentration. **; $p \leq 0.01$, ***; $P \leq 0.001$, ****; $P \leq 0.0001$.

In order to assess the effects of PI3K and/or mTOR inhibitors on cell signalling pathways in LMS, immunoblotting was conducted in ICR-LMS-1 and ICR-LMS-4 cells treated with a range of BEZ235, alpelisib or rapamycin concentrations for 6 hours. Upon BEZ235 treatment, a potent reduction of Akt Ser473 phosphorylation was observed in both ICR-

LMS-1 and 4 cells (**Figure 6.5**). With BEZ235 treatment, a reduction of Thr 389 phosphorylated p70S6K was only seen in ICR-LMS-4 cells, although for ICR-LMS-1 cells, BEZ235 treatment abolished the upper P-p70S6K band. BEZ235 also caused a reduction in STAT3 Tyr705 phosphorylation in both cell lines particularly at 5 µM while no effect on Src or ERK1/2 phosphorylation or total protein was observed (**Figure 6.5**).

Alpelisib cause only a minor reduction in phosphorylated Akt at 5 µM in both cell lines while rapamycin abolished the upper P-p70S6K band at 500 nM in both cell lines (**Figure 6.5**). Alpelisib or rapamycin showed no effect on pan or phosphorylated STAT3, Src or Erk at any concentration after treatment for 6 hours. Therefore BEZ235 displays a combined effect on Akt and p70S6K phosphorylation, and especially a more potent effect on Akt, compared to alpelisib or rapamycin which may explain the reduced effect of alpelisib and rapamycin on cell viability and colony formation inhibition compared to BEZ235. Furthermore, modulation of STAT3 signalling may also be a mechanism of BEZ235 action in addition to PI3K/mTOR inhibition and could contribute to enhanced potency.
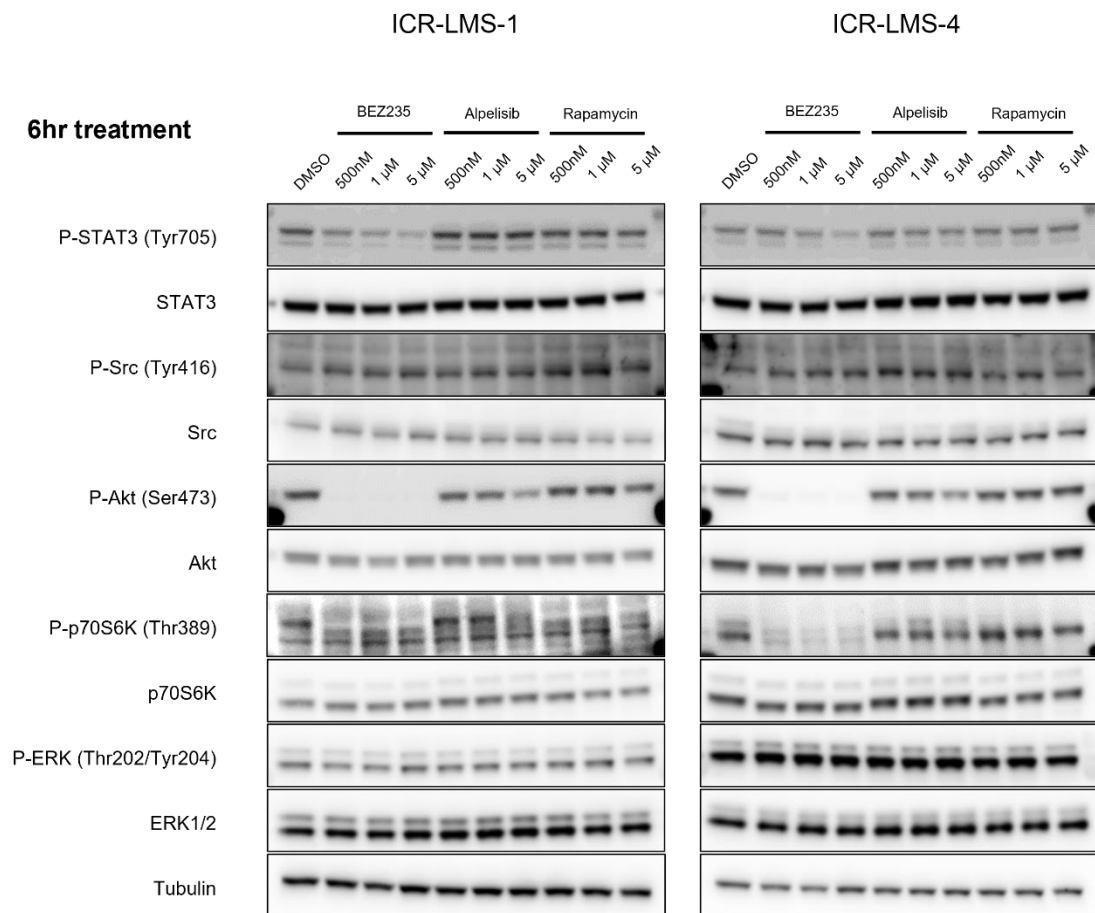
Figure 6.5. Immunoblot of ICR-LMS-1 and ICR-LMS-4 cells in response to BEZ235, alpelisib or rapamycin treatment. Immunoblot of ICR-LMS-1 or ICR-LMS-4 cells after 6 hours of treatment with 500 nM, 1 μM or 5 μM of BEZ235, alpelisib or rapamycin. ERK1/2; extracellular signal-regulated kinase, p70S6K; p70 ribosomal S6 kinase, Signal transducer and activator of transcription 3.

6.4 Targeting BRCAness

Following the small molecule drug screening of PDX-derived LMS cells, the PARP inhibitor talazoparib but not rucaparib was observed to cause a slight decrease in cell viability after 6 days and therefore PARP inhibition in PDX-derived LMS cells was further investigated (**Figure 6.2A**).

Within the previously shown drug screen, talazoparib only shows an impact on PDX-derived LMS cells after 6 days and had no effect on viability after 72 hours (**Figure 6.2A**). Therefore, colony formation assays were conducted with ICR-LMS-1 and ICR-LMS-4 cells alongside SK-UT-1 and SK-UT-1b cells which have previously been shown to be sensitive to PARP inhibition in this assay format (Chudasama et al. 2018). The cells were

exposed to three PARP inhibitors: talazoparib, olaparib and rucaparib which resulted in varying degrees of clonogenic growth inhibition. Talazoparib potently reduced the formation of colonies at 100 nM for ICR-LMS-1 and ICR-LMS-4 cells in addition to SK-UT-1 and SK-UT-1b colonies, although the presence of remaining colonies could be observed in ICR-LMS-4 even at 5 µM talazoparib (**Figure 6.6A**). When quantified, the only significant difference between cell lines at each talazoparib concentration was between SK-UT-1 and SK-UT-1b, showing that ICR-LMS-1 and ICR-LMS-4 cells have similar responses to talazoparib treatment compared to the immortalized LMS cell lines (**Figure 6.6B**). Olaparib and rucaparib reduced the formation of colonies in all four cell lines in a dose dependent manner though were considerably less potent compared to talazoparib (**Figure 6.6C & E**). ICR-LMS-1 showed a significantly lower colony density at olaparib concentrations of 100 nM, 500 nM and 1 µM compared to SK-UT-1 and SK-UT-1b while ICR-LMS-4 showed a significantly higher colony density compared to all other lines at 5 µM (**Figure 6.6D**). ICR-LMS-4 also demonstrated significantly higher density compared to other cell lines at 5 µM rucaparib (**Figure 6.6E & F**). Taken together, these results suggest that both ICR-LMS-1 and ICR-LMS-4 are sensitive to PARP inhibition although extent of response varies considerably with the specific compound used and ICR-LMS-4 cells are less sensitive to olaparib and rucaparib treatment compared to ICR-LMS-1.
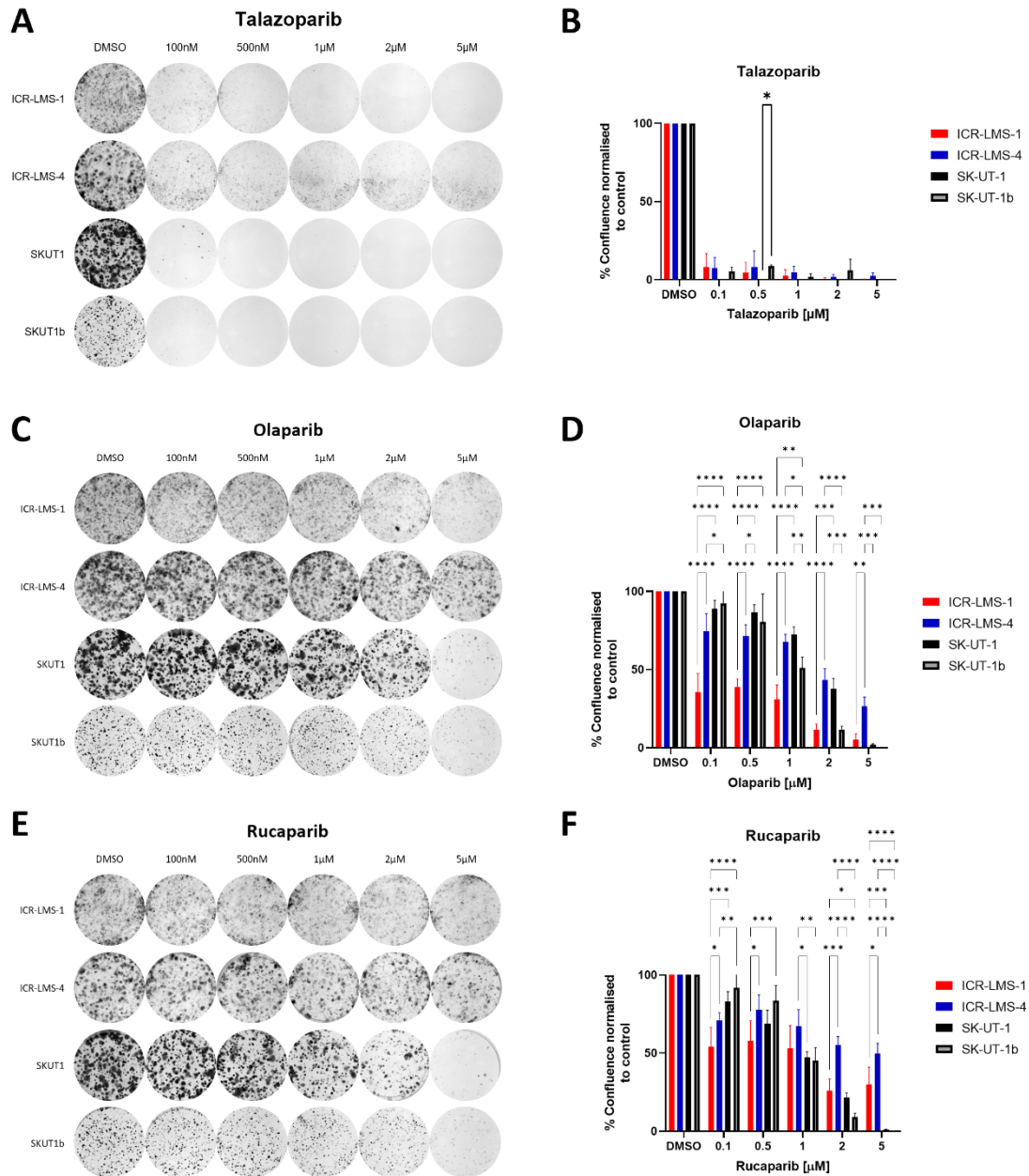
Figure 6.6. PARP inhibitor response in established and PDX-derived cells. (A, C, E) Images of crystal violet stained wells of ICR-LMS-1, ICR-LMS-4, SK-UT-1 or SK-UT-1b cells treated with talazoparib, olaparib or rucaparib at a concentration of 100 nM, 500 nM, 1 μM, 2 μM and 5 μM or Dimethylsulfoxide (DMSO) vehicle control for 2 weeks. (B, D, F) Mean % confluence of ICR-LMS-1, ICR-LMS-4, SK-UT-1 or SK-UT-1b cells from colony formation images normalised to DMSO vehicle control when treated with talazoparib, olaparib or rucaparib. N=3. Error bars indicate standard deviation. Significance is shown following a two-way ANOVA with multiple comparisons at each concentration. *; $p < 0.05$ **; $p \leq 0.01$, ***; $p \leq 0.001$, ****; $p \leq 0.0001$.

In order to determine if prior doxorubicin treatment may affect the sensitivity of LMS cells to PARP inhibition, ICR-LMS-1 doxoR cells previously established and characterised in **chapter 4** were exposed to talazoparib, olaparib or rapamycin at a range of concentrations for 6 days at which point cell viability was assessed. ICR-LMS-1 and ICR-LMS-1 doxoR cells both displayed similar PARP inhibitor dose response curves, with all three inhibitors able to reduce ICR-LMS-1 doxoR viability in a dose dependent manner (**Figure 6.7A, C & E**). Talazoparib and rucaparib IC50 values showed no significant difference between parental and doxoR ICR-LMS-1 cells although olaparib did show a significantly higher IC50 value in ICR-LMS-1 doxoR cells (**Figure 6.7B, D & F**). This result indicates that acquired doxorubicin resistant ICR-LMS-1 cells are still sensitive to PARP inhibition, although slight loss of response to olaparib can be observed.
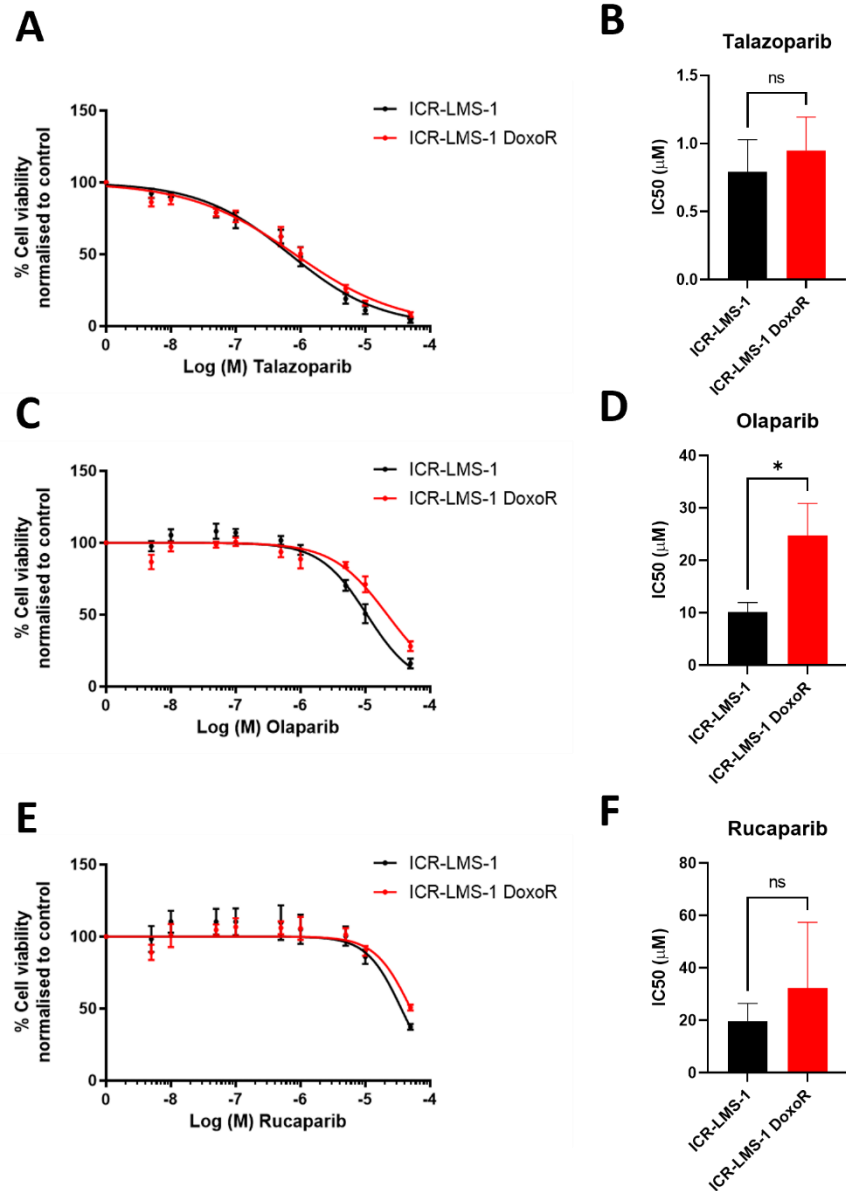
Figure 6.7. Cell viability of doxorubicin resistant cells in response to PARP inhibition. (A, C, E) Percentage cell viability of ICR-LMS-1 parental or doxoR cells when treated with talazoparib, Olaparib or rucaparib concentrations from 5 nM to 50 µM for 6 days. Viability measurements were fitted to non-linear variable slope four parameter curve. N=3. Error bars indicate standard deviation. (B, D, F) Mean talazoparib, Olaparib or rucaparib half-maximal inhibitory concentration (IC50) values for ICR-LMS-1 parental or doxoR cells based on fitted dose response curves. Error bars indicate standard deviation. ns; not significant (P> 0.05). *; p < 0.05.

6.5 Discussion

In this chapter, candidate signalling pathway dependencies were assessed in the PDX-derived LMS cultures established in **chapter 4** via small molecule inhibitor screening. Similar to other patient-derived model screening studies in subtypes such as RMS, variable responses to different inhibitors were observed in different models, while the presence of shared molecular dependencies was clear. After initial assessment of inhibitor response after 72 hours, a longer treatment time was able to better identify compounds which have anti-proliferative effects. Previous studies demonstrated that the doubling time of in vitro models is an important consideration when conducting oncogenic drug screening and to address this variability, the authors implemented an equation to calculate the effect of each drug on cell viability, taking into account individual growth rates (Hafner et al. 2016; Gupta et al. 2020). Implementing such an equation on the small molecule screening dataset presented in this study would further aid in identifying pathway dependencies of LMS cells.

An important result presented in this chapter was that none of the PDX-derived LMS models displayed a response to the multi-target TKI pazopanib, which is currently the only molecular targeted therapy approved for use in LMS patients. Indeed, none of the anti-angiogenic multi-TKI inhibitors included in the small molecule inhibitor screen were able to reduce the viability of any of the five PDX-derived LMS cell cultures. Pazopanib, along with other multi-TKI anti-angiogenic compounds have been shown to exert anti-tumour effects via two mechanisms of action: first by directly inhibiting proliferation of tumour cells and second by inhibiting angiogenesis (Podar et al. 2006; Gril, Palmieri, Qian, Smart, et al. 2011; Gril, Palmieri, Qian, Anwar, et al. 2011; Gril et al. 2013)**.** Therefore, it can be deduced from this study that the viability of patient derived LMS cells is not directly affected by pazopanib treatment and should be further assessed in corresponding PDX models generated in **chapter 3** to confirm whether pazopanib can lead to in vivo responses via angiogenesis inhibition.

Longer term treatment of ICR-LMS-1, ICR-LMS-4, ICR-LMS-6 and SARC-393 cell cultures empirically identified a shared sensitivity to niclosamide. Niclosamide is an FDA approved anthelminthic drug which exerts its effects via uncoupling oxidative phosphorylation and inhibiting glucose uptake and anaerobic metabolism, although it also known to modulate various signalling pathways including Wnt/β-catenin, Neurogenic locus notch homolog protein (Notch), mTOR, STAT3 and Nuclear factor κB (NF-kB) (A. Ibrahim et al. 2020; Sekulovski et al. 2021; Ahn et al. 2017; C. Wang et al. 2018). A number of pre-clinical studies have shown niclosamide also exerts anti-tumour

activity in multiple cancer types via varying mechanisms. For example in renal cancer cells, niclosamide reduced cell proliferation, cell migration and induce apoptosis by causing reduced expression of E2 promoter binding factor 1 (E2F1) and c-Myc while reducing PTEN expression leading to reduced PI3K signalling (Yu et al. 2018). Disruption of Wnt/β signalling has been demonstrated in oral squamous cell carcinoma, ovarian carcinoma and colon cancer cells, leading to cell cycle arrest, apoptosis and altered invasive potential (Ahn et al. 2017; L. H. Wang et al. 2018; King et al. 2015). Furthermore, niclosamide has demonstrated synergy with doxorubicin sequential or concurrent treatment in breast cancer cells by inhibiting Wnt signalling (Lohiya and Katti 2021). However other studies have shown that niclosamide inhibited proliferation and apoptosis in oesophageal squamous cell carcinoma or hepatocellular carcinoma cells via the inhibition of STAT3 signalling (C. Wang et al. 2018; M. C. Lee et al. 2020). The assessment of niclosamide in sarcoma is currently limited to bone sarcomas such as osteosarcoma where one study reported that niclosamide suppressed osteosarcoma cell migration and invasion via reducing the expression transforming growth factor β (TGF-β) and another showed the effects of niclosamide on osteosarcoma cell migration via Wnt/Zinc finger protein SNAI1 (SNAIL) axis modulation (Yeh et al. 2022; Yi et al. 2021). Further mechanistic investigation into the specific effects of niclosamide on LMS cells is warranted based off the findings in this chapter in order to suggest predictive biomarkers of response.

The repurposing of niclosamide as an anti-cancer drug demonstrated limited clinical success in prostate cancer due to low oral bioavailability and absorption rate, meaning that at standard dosing, plasma concentrations were not able to reach therapeutic ranges identified from prior *in vitro* studies (Schweizer et al. 2018). However, in metastatic colorectal cancers, initial results from a phase II trial has shown that similar doses of niclosamide can result in stable disease with a peak plasma concentration (Cmax) concentration corresponding to approximately 1.8 µM (Burock et al. 2018). In this chapter all PDX-LMS cells tested showed a reduction in viability at 500 nM niclosamide, indicating that LMS cells respond to this drug at clinically relevant concentrations.

This chapter also assessed the therapeutic potential of targeting the PI3K/Akt/mTOR pathway in PDX-derived LMS models. Aberrations in *PTEN* causing loss of expression is common in LMS, reported to be present in 41% of non-primary LMS tumours (Schaefer et al. 2021). The results within this chapter demonstrate that three of five LMS PDX-derived cell models have a loss of PTEN expression. The remaining two models, SARC-323 and ICR-LMS-6 (both of which were the only non-uterine LMS cells tested) showed a reduction of PTEN expression compared to normal fibroblasts but to a lesser extent.

This does conflict with previous results showing that a larger proportion of non-uterine LMS tumours have a complete loss of PTEN compared to uterine LMS tumours although this discrepancy could be attributed to the small sample size of preclinical models tested in this chapter (Schaefer et al. 2021). Whole exome sequencing profiling of the larger panel of LMS PDX models established in **chapter 3** will reveal if full PTEN loss is consistently not observed in the non-uterine LMS models. All five PDX-derived LMS models were sensitive to the dual PI3K and mTOR inhibitor BEZ235, therefore PTEN expression does not necessarily correlate with BEZ235 sensitivity. Further analysis of response in ICR-LMS-1 and ICR-LMS-4 revealed that the dual PI3K/mTOR inhibitor BEZ235 inhibited colony formation and reduced viability at lower doses compared to the PI3K inhibitor alpelisib. This is consistent with other reports which show dual PI3K/mTOR inhibition via BEZ235 has potent anti-tumour activity in LMS cells, and is superior to individual PI3K or mTOR inhibition alone (Fourneaux et al. 2016; Serra et al. 2008).

Fourneaux and co-workers demonstrated that treatment of three patient derived LMS cell lines with BEZ235 showed an increase in Erk activation after 3 days due to the inhibition of an mTORC2 mediated negative feedback loop (Fourneaux et al. 2016). The results in this chapter shows that following BEZ235 treatment for 6 hours, no effect on Erk signalling was observed in either ICR-LMS-1 or ICR-LMS-4 cells, indicating that feedback mechanisms are not activated in these models at this short timepoint. Long term treatment would be necessary further test if mTORC2 feedback loops are also active in the LMS models presented in this study or are only activated in a portion of LMS models reported in literature, suggesting that perhaps feedback mechanisms might be patient specific.

Inspecting the signalling pathways effected by PI3K and mTOR inhibitors shortly after treatment initiation revealed that BEZ235 and rapamycin reduced the phosphorylation of p70S6K, a downstream target of mTOR while BEZ235 also potently inhibited Akt phosphorylation at Ser473 which is an important phosphorylation site for activation downstream of PI3K. However, alpelisib demonstrated minimal effects on Akt, only slightly reducing activation at the highest dose tested. In previous studies, biochemical analysis demonstrated that alpelisib and BEZ235 have similar IC50 values towards PI3Kα isoform while BEZ235 can also inhibit PI3Kδ and γ isoforms at a similar concentration. Therefore, in ICR-LMS-1 and ICR-LMS-4 cells, inhibition of PI3Kα, δ and γ isoforms might be necessary to ameliorate Akt activation and reduce cell viability. Another observation following BEZ235 treatment was the reduction of STAT3^{Tyr705} phosphorylation and therefore activation in ICR-LMS-1 cells and to a lesser extent in ICR-LMS-4. However, a previous study reported that BEZ235 treatment at the same

concentration and timepoint to that presented in this chapter instead prompts STAT3^{Tyr705} phosphorylation in PTEN deficient breast cancer, renal cell carcinoma and melanoma cells as part of a negative feedback loop, which suggests that the mechanistic response of LMS cells to dual PI3K/mTOR inhibition may be distinct from that of other cancer types with PTEN deficiency (J. Wang et al. 2021). In this chapter, STAT3 inhibition is observed in response to BEZ235 which demonstrated activity in LMS cells, meanwhile LMS cells were also sensitive to niclosamide which has been previously shown to target STAT3 (C. Wang et al. 2018; M. C. Lee et al. 2020). STAT3 is an interferon gene known to be part of the interferon responsive DNA damage resistant signature and combined with the knowledge that LMS tumours often display high genomic instability, a model can be hypothesised that targeting STAT3 interferon signalling causes LMS cells to become sensitised to DNA damage, leading to reduced viability (Weichselbaum et al. 2008). Thus further investigation into mechanisms behind STAT3 pathway inhibition in these LMS cell models and possible cross-talk between DDR is warranted.

Clonogenic assays confirm that ICR-LMS-1 and ICR-LMS-4 are sensitive to PARP inhibition, most notably by talazoparib and is consistent with emerging reports that uterine LMS cell lines are sensitive to such inhibitors (Anderson et al. 2021; Chudasama et al. 2018; Vornicova et al. 2022). Talazoparib, olaparib and rucaparib have been previously shown to have similar potencies towards the catalytic inhibition of PARP, although talazoparib has an increased PARP trapping potency of approximately 100 fold compared to olaparib and rucaparib (Murai, Huang, et al. 2014). Therefore, the enhanced response of ICR-LMS-1 or ICR-LMS-4 cells to talazoparib indicates that PARP trapping might be the main pathway driving response as opposed to catalytic inhibition of PARP. Specific trapping versus inhibition studies should be therefore be conducted to confirm this finding (Hopkins et al. 2019). While the non-uterine LMS models SARC-323 and ICR-LMS-6 were not tested further for PARPi response, drug screening data suggests ICR-LMS-6 is also sensitive to talazoparib, highlighting that therapeutic targeting of the DDR pathway is not limited to uterine LMS. ICR-LMS-6 was found to be the most chemo resistant model in **chapter 5** and also shows resistance to multiple targeted agents, thus could be considered as a model of multi-drug resistance. Interestingly, despite this multi-drug resistant phenotype, ICR-LMS-6 still demonstrated sensitivity to talazoparib based of drug screening data, which suggests that PARP inhibition may be a candidate therapy for patients with multi-drug resistant phenotypes. Despite the lower efficacy of olaparib and rucaparib on cell viability compared to talazoparib, all three inhibitors were able to reduce clonogenic growth and viability of LMS cells at concentrations comparable to the recorded Cmax plasma concentration of breast and ovarian cancer patients receiving on

label PARP inhibitor therapy (Bruin et al. 2022). Additionally, IC50 values are similar to that recorded in immortalised LMS cell lines (Laroche et al. 2017; Anderson et al. 2021; Pignochino et al. 2017). Together this data shows that PARP inhibitors are active in PDX-derived LMS cells at clinically relevant doses.

Doxorubicin and most other chemotherapies approved for use in sarcoma mainly act by interacting with DNA (Pommier *et al.*, 2010). Therefore, it was hypothesised that tolerance to doxorubicin may also induce cross-resistance to small molecules targeting the DNA damage response and repair pathways such as PARP inhibitors. However, PARP inhibitors were still able to reduce viability of doxorubicin acquired resistant PDX-derived LMS cells, demonstrating similar dose response profiles. This result indicates that targeting PARP could be a viable treatment option for advanced LMS patients even after progression on prior doxorubicin treatment and thus, as a second line therapy would be a much needed addition to the currently limited treatment options. Doxorubicin resistant ICR-LMS-1 cells did show a significantly higher IC50 value for Olaparib and rucaparib IC50 value was also slightly higher in the resistant model. However talazoparib showed little difference in IC50 value towards doxorubicin resistance cells. As the PARP trapping ability of talazoparib is higher than that of olaparib and rucaparib, this result suggests that the effects of PARP trapping is unaffected by doxorubicin resistance (Murai et al. 2012).

Anderson et al. recently demonstrated that SK-UT-1 and SK-UT-1b had defective HR and also defective NHEJ specifically in SK-UT-1b by using a functional HR/NHEJ reporter assay (Anderson et al. 2021). In order to assess mechanism behind the apparent PARP inhibitor sensitivity in the PDX-derived LMS cell lines generated in this thesis, work is currently underway to determine first, the ability of ICR-LMS-1 and ICR-LMS-4 to undergo homologous repair following DNA damage via ionising radiation (IR) and second, the impact of PARP inhibition on DNA double strand break formation and repair mechanisms. For this, RPE-1 P53Δ and RPE-1 P53Δ BRCA1-/- isogenic cell lines will be used as positive and negative controls of HR capacity respectively. Following IR or PARP inhibitor treatment, cells will be scored as γ-H2AX and Rad51 positive or negative which are functional readouts of DNA double strand breaks and sites of HR respectively and will also be co-stained for geminin (Cruz et al. 2018). Geminin accumulates in the nucleus during S-G2 phases of the cell cycle and can be used as a marker to restrict the analysis of γ-H2AX and Rad51 foci to cells in the correct phase of the cell cycle for HR activity, reducing the likelihood of falsely reporting HR deficient cells (Cruz et al. 2018). Geminin staining is particularly important to account for slowly proliferating cells where a lower percentage of cells will actively be in S-G2 phase.

Additionally the effect of dual PI3K/mTOR inhibition on HR activity in these cell lines will be assessed as previous studies have shown that PI3K/mTOR inhibition can induce a transient HRD phenotype (Chang et al. 2014; De et al. 2014; Philip et al. 2017).

Other future work for this chapter could involve testing PARP inhibitors in the respective PDX models to verify the sensitivity observed *in vitro* and to also test other PDX models which were not able to grow *in vitro* and have therefore not yet been assessed for PARP inhibitor sensitivity. Due to the prevalence of PARP inhibitor acquired resistance in cancer types where this therapy is standard of care such as ovarian and breast cancer, potential mechanisms of PARP inhibitor acquired resistance in LMS should be investigated (K. K. Lin et al. 2019; Vidula et al. 2020). To achieve this, dose escalation to generate acquired resistant models is already underway. It would be interesting to evaluate if LMS cells are able to acquire stable or transient resistance to PARP inhibitors as a recent study reported that ovarian cancer cell lines exposed to escalating doses of olaparib did not cause PARP inhibitor resistance or cross-resistance to other chemotherapies (Fedier et al. 2022). Meanwhile in ovarian and breast cancer patients, certain mutations causing a BRCAness phenotype may be more likely to lead to PARP inhibitor resistance than others (Pettitt et al. 2020). Therefore future work assessing resistance mechanisms should check for a correlation with certain mutations in DDR components in order to potentially stratify LMS patients who are most suited to long term maintenance PARP inhibitor therapy.

Chapter 7 - Discussion

7.1 Future directions for pre-clinical modelling of LMS

7.1.1 Orthotopic xenografts

While the LMS PDX models presented in this thesis show high fidelity to patient tumours in terms of histology and proteomic profiles, subcutaneous models are limited in that they cannot fully mimic native tumour microenvironment and tumour invasion. Therefore, future *in vivo* models of LMS can be further improved by generating patient derived orthotopic xenografts (PDOX), where patient tumours are engrafted into immunocompromised mice in an anatomical location corresponding to the patient tumour site. PDOX are able to more accurately model patient tumours responses compared to subcutaneous PDX models and can also mimic patterns of invasion and metastasis (Russell et al. 2017). PDOX models of LMS have been established in a limited number of studies. One such study generated a LMS PDOX model 1.5 months after receiving the tumour resection sample via initial subcutaneous implantation followed by passaging into femoral murine muscle (Zhiying Zhang et al. 2019). The author noted that the LMS PDOX model showed a response to combined gemcitabine and docetaxel which was significantly more effective than doxorubicin (Zhiying Zhang et al. 2019). Additionally, this model was susceptible to trabectedin and temozolomide treatment while pazopanib and olaratumab showed no significant response (Zhiying Zhang et al. 2019). One of the main drawbacks of orthotopic models is the difficulty in non-invasive monitoring of tumour growth over time due to the often deep anatomical locations of engrafted tumours (Imle, Kommoss, and Banito 2021). However, another study generated a gastric LMS PDOX by initially implanting patient tissue subcutaneously into a mouse expressing the fluorophore red-fluorescent protein (RFP) to label the tumour stroma. The PDX tumour was then implanted orthotopically into the gastric wall of a non-transgenic mouse so that the impact of drug treatment on tumour invasion could be easily analysed over time via non-invasive fluorescent imaging (Kawaguchi et al. 2017).

As with most STS subtypes, LMS tumours metastasise most frequently to the lungs although the reason behind this is poorly understood and for this reason potential therapies which could specifically prevent metastatic spread in STS have yet to be investigated in detail (Gladdy et al. 2013; Gamboa, Gronchi, and Cardona 2020). In order to study site specific metastases, orthotopic implantation could be utilised with the PDX LMS models generated in **chapter 3** to identify the ability of these models to invade local tissue and metastasise. If spontaneous metastasis isn't observed following orthotopic PDX growth, then injection of the tumourigenic PDX-derived LMS cell cultures ICR-LMS-

1 or ICR-LMS-3 derived in **chapter 4** into murine tail veins could mimic metastatic spread. These metastatic models could then be used to assess if certain therapies can prevent the outgrowth of metastases similar to a previous study which used the fibrosarcoma cell line HT1080 (Miwa et al. 2014).

7.1.2 Genetically engineered mouse models (GEMMs)

Another method to model cancer *in vivo* is to use genetically engineered mouse models (GEMMs). These models can be either germline or somatic mutants and can also be inducible, which means they can potentially be used to investigate mechanisms of early tumourigenesis (Rao et al. 2014; Halaoui et al. 2017). Somatic GEMM generation has seen considerable advancements in the past decade due the widespread availability of targeted gene editing technologies such as Clustered Regularly Interspaced Short Palindromic Repeats (CRISPR) which improves on traditional cre-recombinase based GEMM establishment for ease and time of establishment (Dodd et al. 2015; J. Huang et al. 2017; Annunziato et al. 2016). The unique benefit of these models is that they can mimic invasive and metastatic behaviour of human tumours and are do not have to overcome *ex vivo* growth conditions (Imle, Kommoss, and Banito 2021). However the disadvantages of GEMM models is that cannot always capture the genetic complexity of human tumours and establishment relies on known driver mutations in order to cause transformation (Imle, Kommoss, and Banito 2021). Several reports have used GEMM models in other cancer types such as pancreatic and breast cancer to demonstrate mechanisms of tumour invasion and metastasis while identifying candidate drug targets to prevent this progression (Gopinathan et al. 2015; Annunziato et al. 2016; Ross et al. 2020).

Additionally, GEMMs are immunocompetent and therefore can model the immune microenvironment throughout different stages of cancer such as tumourigenesis, local invasion and metastasis (Nguyen and Spranger 2020). Because of the intact tumour microenvironment, these models are useful for assessing response to immunotherapies. Gutierrez and co-workers have recently derived GEMM models of UPS and RMS, comparing the immune landscape of each to syngeneic models, whereby GEMM tumours are cultured *in vitro* and then injected into immunocompetent mice of the same strain (W. R. Gutierrez et al. 2021). The study found that in both UPS and RMS models, tumours were infiltrated with a similar percentage of immune cells, with an especially high proportion of macroohages, although RMS models had higher proportion of CD8+ infiltrating T-cells while UPS had a higher proportion of CD4+ infiltrating T-cells which is

consistent with IHC immunoprofiling studies on human tumours (Dancsok et al. 2020; 2019; W. R. Gutierrez et al. 2021). Additionally, the authors demonstrated that the respective syngeneic models showed differing immune landscapes to the original GEMMs, making syngeneic models less robust for immuno-oncology studies (W. R. Gutierrez et al. 2021).

GEMM models of STS consist mainly of translocation associated sarcomas due to the well characterised pathognomonic gene fusions required for transformation while GEMM models representing sarcoma subtypes with complex karyotypes are difficult to generate due to the lack of well-defined defined driver mutations (Abeshouse et al. 2017; Imle, Kommoss, and Banito 2021).. However, GEMM establishment could be achieved by perturbing genes which show recurrent aberrations in large scale LMS sequencing studies such as *TP53*, *RB1, ATRX* and *PTEN* (Hensley et al. 2020). Recently, LMS GEMM models were generated via *PTEN* mutation and *KRAS* activation specifically in uterine smooth muscle cells which produced tumours with a histology consistent with uterine LMS and were utilised in a transposon genetic screen for candidate genes which contribute to metastasis (Kodama et al. 2021). This demonstrates that GEMM modelling of LMS tumours is feasible, therefore these could be utilised in future studies to assess candidate therapies to prevent metastasis. However the generation of GEMM models for other STS subtypes faces another challenge in that the cell of origin must be well characterised so that location specific promotors can be used to express the oncogenic genes of interest (W. R. Gutierrez et al. 2021).

7.1.3 Zebrafish models in STS research

In addition to mouse models, zebrafish are another common model organism used in pre-clinical cancer research. Zebrafish have several advantages over mouse models, such as lower cost, easier handling, shorter time to model establishment both for transgenic models and xenografts as well as transparency of zebrafish embryos, allowing for optical assessment of tumours in high-throughput time-lapse experiments (Kendall et al. 2018; Casey and Stewart 2020). Additionally, the conservation of multiple signalling pathways implicated in many cancer types as well as overall genetic conservation of human genes has highlighted zebrafish as excellent cancer models (Howe et al. 2013). Furthermore, zebrafish demonstrate a high penetrance of sarcoma development seen in studies producing transgenic STS subtypes such as RMS and LPS, which also demonstrated remarkably similar molecular and histological characteristics

compared to the respective human disease (A. Gutierrez et al. 2011; Kendall et al. 2018; Ignatius et al. 2012).

Zebrafish xenografts can also be established via cell inoculation, providing a means for high-throughput *in vivo* drug response profiling of patient-derived cells. (Yan et al. 2019; De Vita et al. 2021; Rebelo de Almeida et al. 2020; Siebert et al. 2023). For example, Yan and co-workers reported the establishment of two RMS zebrafish xenografts using patient-derived cell lines which showed distinct histology. Within these models the authors demonstrated intra-tumoural subpopulation of cells including migratory cells, proliferative cells and bystander cells that could each be visualised live at single cell resolution, going on to show sensitivity of RMS xenografts to combined olaparib and temozolomide treatment (Yan et al. 2019). The use of zebrafish xenografts for drug response assessment in LMS has yet to be described but is a promising avenue for future modelling of this disease.

7.1.4 Modelling the tumour microenvironment *in vitro*

One main drawback of my work is that I was not able to conduct high throughput culture condition screens in order to assess the effect of different media components and growth factors on cell growth and viability, although it was found that one non-uterine LMS cell culture in **chapter 4** required the addition of bFGF and PDGF for *in vitro* growth. In a recent study, Manzella et al. conducted screening of a panel of RMS primary PDX-derived cells with basal media, flask coating, media supplements and growth factor addition, analysing the impact of each on cell viability, extent of differentiation and growth rate (Manzella et al. 2020). The study reported that culture condition screening was able to identify subsets of RMS PDX-derived cells which required similar conditions for optimal growth (Manzella et al. 2020). Optimising culture conditions based on growth rates alone should be done with caution, as these conditions may not necessarily represent the tumour microenvironment from which the cells were derived. Perhaps in addition to screening, molecular profiling such as proteomics of each candidate condition should be conducted in order to also take into account the condition that causes the cell cultures to most closely resemble patient or PDX tumours. Additionally, due to the variety of cellular processes known to be modulated by hypoxia such as cell proliferation, survival, migration and metastasis, the degree of hypoxia should be optimised for 3D Matrigel embedded models in order to mimic respective *in vivo* tissue (Cairns, Harris, and Mak 2011). The effects of a hypoxic microenvironment on cell signalling and drug response could then be further explored in order to highlight therapies which may be able

to selectively target hypoxic tumour cells or to suggest possible combination treatment with anti-angiogenics.

As organoid culture protocols are adapted and applied to sarcoma research, the potential to model different aspects of the sarcoma microenvironment is expanding. In addition to the histological recapitulation of tumours in vivo, cancer organoid cultures can also include stromal cells such as cancer associated fibroblasts (CAF) which have been shown to contribute to therapy response in liver and pancreatic cancer organoids (Schuth et al. 2022; J. Liu et al. 2021). Studies of CAF-sarcoma cell interaction are extremely limited due to the original suggestion that sarcomas solely consisted of a single compartment of malignant cells (Tomlinson et al. 1999). On top of this both CAF and sarcoma cells are mesenchymal in origin, sharing similar morphologies and mesenchymal markers which makes the identification of these distinct groups difficult (Vokurka et al. 2022). Some studies have assessed the co-culture of CAFs with sarcoma cells but these mainly utilise separate culture inserts to assess migration or addition of pre-established sarcoma spheroids onto stromal cell monolayers (H. Yoon et al. 2021; D'Agostino et al. 2021). Additionally, sarcoma cells and CAFs were not always isolated from the same tumour sample (H. Yoon et al. 2021; D'Agostino et al. 2021). Furthermore, the assessment of LMS cell-CAF interaction has not yet been documented. Future directions of sarcoma modelling *in vitro* could involve the dissociation of patient samples and direct expansion of both stromal and malignant cells as mixed multi-cell type organoid cultures as achieved in other cancer types (Schuth et al. 2022; J. Liu et al. 2021; Ebbing et al. 2019). Modelling sarcomas in 3D mixed with stromal cells will reveal the crosstalk between malignant cells and microenvironment and potentially highlight candidate signalling pathways which could be targeted to prevent stromal mediated tumour progression and invasion.

In several epithelial tumours, studies have combined cancer organoids with immune cells such as tumour infiltrating lymphocytes (TIL) and tumour associated macrophages (TAMS) to further model the tumour microenvironment (Jenkins et al. 2018; Zumwalde et al. 2016; Neal et al. 2018). Neal and co-workers derived over 100 cancer organoids which retained both native CAF and TIL populations, showing that TILs populations also retained the T-cell receptor repertoire observed in the tumour sample, indicating that the immune landscape can be accurately modelled in patient-derived organoid cultures (Neal et al. 2018).

Due to initial PDX establishment in immune compromised mice in **chapter 3**, human infiltrating immune cells in the patient sample will no longer be present or viable in the

PDX tumour once dissociated. However current work is ongoing to isolate peripheral blood mononuclear cells (PBMCs) from patients with a matched PDX model or PDX-derived cell line. This will allow us to set up short term co-cultures to assess the immunomodulatory impact of certain therapies and also as a way of testing immunotherapies such as immune checkpoint inhibitors (ICI) in 3D cultures via T-cell cytotoxicity assays, similar to a previous study which utilised this approach on NSCLC patient tumours (Dijkstra et al. 2018).

7.1.5 Modelling tumour extracellular matrix

Another future direction for sarcoma organoid modelling is the use of more defined, disease relevant hydrogel scaffolds which can recapitulate native ECM composition. The role of the ECM in sarcoma is not well understood, although mounting evidence suggests that ECM-sarcoma cell interactions have significant effects on tumour growth, invasion and metastasis (Pankova et al. 2021). For example, collagen III expression can be seen in both LMS and benign leiomyoma tumours, collagen IV is less weakly expressed in LMS tumours and laminin is expressed in benign leiomyomas but only a subset of LMS tumours (D'Ardenne, Kirkpatrick, and Sykes 1984; Ogawa et al. 1986). Additionally, fibronectin expression is variable across STS subtypes but appears to correlate with cellular differentiation, where high expression is observed in areas of mesenchymal morphology while low expression is seen in areas of epithelioid morphology (Benassi et al. 1998). Interaction of collagen VI and the proteoglycan neuron-glial antigen 2 (NG2) was shown to contribute to cell adhesion in the LMS cell line SK-UT-1, where NG2 silencing reduced migration through collagen I and matrigel scaffolds when collagen VI was added but had no effect on migration through scaffolds without collagen VI (Cattaruzza et al. 2013). In a fibrosarcoma cell line, NG2-collagen VI interaction was shown to activate a range of intracellular signalling pathways involved in cell survival and migration which converged on PI3K (Cattaruzza et al. 2013). Therefore, PI3K represents a candidate target for preventing tumour cell invasion in collagen VI & NG2 enriched STS tumours.

Similar studies should now be conducted in patient-derived LMS models to identify recurrent ECM interactions in LMS cells which contribute to invasion. Emphasis should be placed on deep molecular characterisation of ECM composition, for example via proteomic analysis, in order to identify candidate ECM components which correlate with patient outcomes for functional investigation. Another emerging technology which will support the study of sarcoma ECM is the generation of tumour-derived hydrogels, which

is achieved via tissue decellularisation followed by ECM scaffold digestion to form a solution that can polymerise under certain conditions (Romero-López et al. 2017). These patient-derived hydrogels could be used in conjunction with patient-derived organoid cultures such as ICR-LMS-3 generated in **chapter 4** in order to further mimic the tumour microenvironment and highlight certain drugs which can modulate STS growth and migration in native ECM (Jia et al. 2022). Additionally, tumour ECM could be included as a condition for *in vitro* condition screening to assess if using native ECM coating can enhance monolayer culture establishment rates.

7.1.6 *Ex-vivo* tumour cultures

The tissue architecture maintained in PDX models and high throughput capabilities of *in vitro* culture can be combined with the use of *ex vivo* tissue cultures, whereby tissue is cultured for a short time (usually no longer than 1-7 days) *in vitro* with several compounds in order to assess the impact of drugs on tissue architecture, necrosis and proliferation (S. Z. Martin et al. 2019). This technique maintains both tissue architecture and microenvironment, is far quicker than PDX drug treatment experiments and can simultaneously assess the effects of different compounds on the same tumour sample (Gavert et al. 2022; S. Z. Martin et al. 2019). Ex vivo culture has recently been improved with the use of vibratome sectioning to precisely and cleanly cut tumours, minimising slice size variation and disruption of tissue architecture (Kenerson et al. 2021; 2020). However, one downside of this technique is that the high variability of tissue quality between different patients in addition to variable tissue quality in the same sample due to areas of necrosis can often lead to highly variable results (S. Z. Martin et al. 2019).

A recent study reported successful 5 day *ex vivo* slice culture of 104 out of 108 (96.3%) resection or biopsy tissue from patients with a range of cancer types, including LMS, showing this technique is feasible for LMS tissue and going on to demonstrate that colorectal cancer *ex vivo* models can predict PDX model treatment response (Gavert et al. 2022). A unique application of ex vivo culture systems is the ability to simultaneously test tissue from various areas of tumour samples as well as healthy tissue in order to assess the extent of tumour specificity as well as intra-tumoural heterogeneity of drug response which would be invaluable in LMS research where both inter-tumoural and inter-tumoural molecular heterogeneity is commonly observed (Anderson et al. 2021). One of the limitations of these slice cultures is that tumour tissue will be evenly exposed to media and any drug or cell therapy added which is not representative of *in vivo* tumour

concentration gradients. Furthermore, current techniques using these slice cultures can only maintain viable tissue for one week or less, and therefore slice cultures are not suitable for long term proliferation assays (Kenerson et al. 2021; S. Z. Martin et al. 2019). However, slice cultures of LMS patient or PDX tissue could be a complementary assay to quickly assess candidate therapies and molecular responses before full *in vivo* assessment.

7.2 Future directions for chemotherapies and molecular targeted therapies in advanced LMS

7.2.1 Exploiting defective DNA repair pathways

As detailed in the introductory **chapter 1**, LMS tumours frequently harbour alterations in the HR associated genes and several clinical trials are now exploring the potential use of PARP inhibitors for advanced STS treatment based on pre-clinical evidence that LMS cell lines respond to such therapy (Pignochino et al. 2017). While BRCA1/2 mutations are well established as biomarkers of PARP inhibitor response, it is clear that alterations in other HR associated genes consistently lead to PARP inhibitor responses in the absence of BRCA1/2 mutations in other cancer types (Hodgson et al. 2018; Gruber et al. 2022). However, outside of BRCA1/2 deletions or loss of function, alterations in other HR components are less well-defined as patient selection criteria. Expanding patient selection for PARP inhibitor treatment could potentially benefit LMS patients, where a range of HR associated gene alterations are often observed (Chudasama et al. 2018; Hensley et al. 2020).

Although PARP inhibitors have achieved clinical success as monotherapies in other cancer types, combination of PARP inhibitors with chemotherapeutic agents in these cancer types has been met with limited clinical success, due to dose limiting haematologic toxicity (Plummer et al. 2013; 2008; Khan et al. 2011; Bendell et al. 2015). Despite the potential risk of toxicity, the assessment of combinatorial therapies to produce synergy in LMS is underway. One of the earliest studies reporting PARP inhibitor sensitivity in LMS cells *in vitro* showed that olaparib synergised with trabectedin treatment, even re-sensitising a chemo resistant LMS cell line to trabectedin (Pignochino et al. 2017). The authors went on to show that the degree of synergism was determined by PARP1 expression, with overexpression or silencing of PARP1 causing increased and decreased synergy respectively (Pignochino et al. 2017; 2021). However, another study reported that trabectedin only caused additive or even antagonistic effects when

instead combined with the PARP inhibitor rucaparib in different LMS cell lines suggesting either that the synergy of trabectedin and PARP inhibition is restricted to certain LMS models or that synergy is dependent on the specific PARP inhibitor used (Laroche et al. 2017). The TOMAS phase Ib trial combining trabectedin and olaparib in advanced bone and STS patients (30% of which were LMS patients) reported a partial response in only 12 of 50 patients, giving a response rate of 14%, although the subtype information of responding patients was not reported. Therefore future trials are awaited to confirm if this combination demonstrates efficacy specifically in LMS patients.

Several studies have demonstrated synergism between PARP inhibitors and the alkylating agent temozolomide in LMS cell lines. For example, it has been shown that temozolomide and niraparib produce synergistic effects in LMS cell lines, although the extent of synergistic effect varied depending on specific PARP inhibitor used as well as the cell line (H. Li et al. 2020; Vornicova et al. 2022). Temozolomide treatment causes alkylation of DNA which can be repaired via PARP1, thus an increased amount of PARP1 will be bound to DNA. If treated with a PARP inhibitor with high trapping ability, this will lead to an increase in DNA-PARP complexes compared to that if treated with PARP inhibitors alone (Murai, Zhang, et al. 2014). Combined PARP inhibition and temozolomide can also decrease the expression of the anti-apoptotic protein MCL-1 as well as enhance the activation of proapoptotic proteins BAX and BAK when compared to either monotherapy (Engert et al. 2015). Preliminary results from a phase II trial has demonstrated promising results, with a response rate of 23% at six months after treatment initiation for uterine LMS patients who have previously progressed on chemotherapy (Ingham et al. 2021). These results have led to a phase II/III clinical assessment of temozolomide with the PARP inhibitor olaparib in chemo refractory advanced uterine LMS patients (NCT05432791). Tumour tissue from these trials will undergo correlative analysis of BRCAness through whole exome sequencing of HR associated genes as well as Rad51 foci formation analysis as a functional marker of HR. Based on prior *in vitro* analysis of LMS response to PARP inhibition a correlation between PARP inhibitor response and HR deficiency is predicted (Anderson et al. 2021; Chudasama et al. 2018).

PARP inhibitors have also been combined with gemcitabine in other cancer types following reports that gemcitabine treatment increased DNA replication stress and stalled replication forks in cancer cells (Karnitz et al. 2005; Jacob et al. 2007; Hastak, Alli, and Ford 2010). However, dose limiting toxicity with this combination has been reported in pancreatic cancer patients (Bendell et al. 2015) . Nonetheless, due to the current clinical use of gemcitabine in LMS treatment pathways, combination with PARP inhibitors

represents a potentially beneficial novel combination for LMS patients and should be investigated in pre-clinical models (A. Gronchi et al. 2021).

A hypoxic microenvironment has been previously shown to contribute to impaired HR in breast cancer while leaving the NHEJ unaffected (Bindra et al. 2005). This impaired HR was further confirmed to be mediated via E2F dependent transcriptional repression of both *BRCA1* and *RAD51* which was induced by hypoxia, therefore, the use of anti-angiogenesis compounds including VEGF inhibitors was suggested as a possible method to potentiate a response to PARP inhibition (Bindra et al. 2005). On top of hypoxia induction, inhibition of VEGFR-3 or PDGFR has also reported to directly cause the downregulation of BRCA1/2 and Rad51 via E2F transcription factors in breast and ovarian cancer cells, causing PARP inhibitor sensitivity independent of hypoxia induction (Kaplan et al. 2019; Lim et al. 2014). As an already clinically approved VEGFR inhibitor for LMS, pazopanib should be tested *in vitro* to observe if this drug can modulate HR activity in LMS cells and lead to synergistic effects. If observed, this might be a possible method of inducing a BRCAness phenotype despite the absence of mutations in DDR associated genes, potentially expanding the number of patients gaining clinical benefit from pazopanib-PARP inhibitor treatment.

Going forward, further pre-clinical assessment of the impact of different DDR associated gene alterations on PARP inhibitor sensitivity should be conducted in LMS patient derived models, perhaps by first establishing a panel of HR deficient LMS models with differing gene alterations. Identifications of mutations predictive of response would allow for patient stratification in clinical trials and strengthen the argument for molecular profiling of LMS tumours upon disease diagnosis in order to guide treatment regimens.

One major issue facing PARP inhibitor treatment in other cancer types in the acquisition of resistance as with many targeted therapies (Dias et al. 2021). Multiple resistance mechanisms have been identified in cancers for which PARP inhibitor treatment has been approved, the most common being reversion mutations in *BRCA1/2*, leading to restoration of BRCA1/2 function and formation of Rad51 foci in response to DNA damage (Ter Brugge et al. 2016; Sakai et al. 2008). Here it has been suggested that patients with pathogenic *BRCA1/2* deletions causing frameshift mutations may be more likely to revert to wild type *BRCA1/2* compared to those harbouring missense mutations (Pettitt et al. 2020). Given that LMS tumours demonstrate a higher prevalence of *BRCA1/2* deleterious mutations compared to point mutations it is possible that reversion mutations may be a frequent mechanism of resistance to PARP inhibitors in LMS patients

(Chudasama et al. 2018; Hensley et al. 2020). Another known mechanism of resistance via HR restoration includes suppression of NHEJ, which can be mediated by the loss of p53-binding protein 1 (53BP1), a key molecule for the initiation of NHEJ and antagonistic to HR components (Bunting et al. 2010; Bouwman et al. 2010). Resistance to PARP inhibition can also occur via the stabilisation of stalled replication forks, which is mediated by modulation of several components involved in DNA remodelling such as Chromodomain helicase DNA-binding protein 4 (CHD4), Snf2 family proteins, components of the MRE nuclease complex as well as SLFN11, a protein involved in replication stress response (Guillemette et al. 2015; Taglialatela et al. 2017; Chaudhuri et al. 2016; Murai et al. 2016). Additionally, mutations in both the catalytic site of PARP and domains necessary for PARP-DNA trapping can cause loss of PARP inhibitor efficacy as shown in high density CRISPR-cas9 screening of PARP point mutations (Pettitt et al. 2018).

Alternatively, increased drug efflux via the upregulation of ABC transporter P-gp, can also lead to PARP inhibitor resistance (Jaspers et al. 2015). However, some PARP inhibitions such as veliparib and niraparib are poor substrates of P-gp and therefore may be more effective in patients who demonstrate P-gp mediated multi-drug resistance (Vaidyanathan et al. 2016). This may be particularly interesting to investigate in LMS models of patients who have progressed on prior doxorubicin treatment and demonstrate P-gp mediated multidrug resistance. Future work following the results in this thesis involves the generation of acquired PARP inhibitor resistant patient-derived cells, which is currently underway, or PDX models via *in vivo* dose escalation or even generating patient matched pre-and post-PARP inhibitor treatment models in order to identify candidate PARP inhibitor resistance mechanisms active in LMS and possible strategies to avoid or overcome the acquisition of resistance.

Beyond PARP inhibition, several LMS cell lines including the immortalised uterine LMS lines SK-UT-1 and SK-UT-1b have demonstrated sensitivity *in vitro* to inhibitors of other DDR components including CHK1, WEE1 or Ataxia telangiectasia and Rad3-related protein (ATR)*,* consistent with recurrent mutations in DDR associated genes observed in LMS tumours (Anderson et al. 2021; Chudasama et al. 2018; Rosenbaum et al. 2019; Cuppens et al. 2018). Additionally, *in vitro* and *in vivo* pre-clinical work has shown that CDK4/6 inhibitors are able to further sensitise Rb-positive LMS cells to WEE1 inhibition (Francis et al. 2017). Studies have also assessed the efficacy of DDR inhibitors in combination with genotoxic chemotherapies in order to potentiate responses. For example ATR inhibition sensitises *TP53* mutant LMS cells to gemcitabine, causing increase accumulation of DNA damage while preventing checkpoint activation seen

under gemcitabine monotherapy (Audrey Laroche-Clary et al. 2020). Based on these encouraging results, a phase II is underway to assess the safety and efficacy of the ATR inhibitor berzosertib with gemcitabine in patients with advanced LMS (NCT04807816). Meanwhile the combination of CHK1 inhibition with gemcitabine is also under clinical assessment following pre-clinical evidence of synergy in LMS cells and xenografts caused by the prevention of checkpoint activation and raised accumulation of DNA damage, although antagonistic effects were also observed in some cell lines (A. Laroche-Clary et al. 2018). A phase I study of the CHK1 inhibitor GDC-0575 with gemcitabine reported two STS patients with *TP53* mutations who had exceptional, long lasting responses, although dose limiting toxicities were also observed (A. Laroche-Clary et al. 2018; Italiano et al. 2018). A clear correlation of CHK1 inhibition-gemcitabine synergy with *TP53* mutation status has not yet been drawn due to small cohort sizes included in this study, therefore further *in vitro* assessment on the effects of P53 action on this combination is needed in LMS (Italiano et al. 2018).

7.2.2 Improving clinical application of PI3K-Akt-mTOR pathway inhibition in LMS

LMS tumours often show upregulation of the PI3K/Akt/mTOR pathway via *PTEN* alterations (Schaefer et al. 2021; Hensley et al. 2020; Cuppens, Annibali, et al. 2017; Cuppens et al. 2018). In 2017, the dual PI3K/mTOR inhibitor BEZ235 demonstrated anti-tumour activity in LMS PDX models which correlated with increased presence of protein S6 (p-S6) phosphorylated at serine 240. This phosphorylation site on p-S6 is a target of p70S6K downstream of mTOR activation, therefore suggesting that only tumours which demonstrate upregulated PI3K/mTOR activity would response to this treatment (Cuppens, Annibali, et al. 2017). Additionally a higher proportion of metastatic LMS patient tumours showed positive IHC staining for p-S6 phosphorylated at serine 240, with these patients showing shorter PFS compared to patient tumours which were negative for phosphorylated p-S6. This indicates that PI3K/mTOR inhibition might be particularly applicable for the treatment of aggressive metastatic lesions (Cuppens, Annibali, et al. 2017).

Future directions for the targeting of PI3K-Akt-mTOR pathway in LMS tumours will need to bear in mind clinical toxicity which has been observed in other cancer types (Massard et al. 2017; Wise-Draper et al. 2017; Salazar et al. 2018). Results from this study in

chapter 6 demonstrates that, *in vitro,* dual PI3K/mTOR inhibition starts to reduce cell viability at sub micromolar concentrations. Therefore, a possible way to avoid reduce clinical toxicity is by utilising low dose PI3K/mTOR inhibitors combined with other anti-cancer therapies in order to potentiate tumour specific responses. For example, in a fibrosarcoma cell line the mTOR inhibitor ridaforolimus synergised with the CDK4/6 inhibitor palbociclib (X. Wang et al. 2019). Meanwhile, one study previously showed that treatment with doxorubicin and BEZ235 lead to synergistic effects *in vitro* and a greater reduction of *in vivo* tumour growth compared to each monotherapy (Babichev et al. 2016). However the authors also reported via immunohistochemical staining that markers of proliferation or apoptosis were not statistically different between combination and monotherapy treated xenografts. Other evidence in leukaemia cells suggests that inhibiting the PI3K/Akt pathway can overcome multi-drug resistance by inducing cell cycle arrest, while downregulating anti-apoptotic protein B-cell lymphoma 2 (BCL-2) and upregulating pro-apoptotic protein Bcl-2-associated X protein (BAX) (Jie Li et al. 2021). Both a combination of low dose PI3K inhibition with other targeted therapies and with chemotherapies should be explored in LMS pre-clinical models. This would highlight candidate regimens to inform future clinical trials surrounding PI3K inhibition. Additionally, a recent study demonstrated that the Akt inhibitor MK-2206 can sensitise LMS cells and other STS models to doxorubicin specifically by targeting HR, leading to reduced Rad51 foci and enhanced DNA damage accumulation compared to doxorubicin treatment alone (Boichuk et al. 2020). Despite the modest response of PDX-derived LMS models to the MK-2206 shown in **chapter 6**, the combination of Akt inhibition and doxorubicin treatment could be further investigated in these models and it would be interesting to assess what impact HR deficiency status has on Akt inhibitor-doxorubicin synergy.

PI3K signalling has been implicated in DDR mechanisms including DNA damage detection as well as BRCA1/2 expression maintenance whereby inhibition of PI3K leads to HR deficiency as well as enhanced cell death via reduction of p53 binding protein 1 (53BP1) localisation (Y. H. Ibrahim et al. 2012; Juvekar et al. 2012). Additionally, mTOR inhibition can also potentiate the anti-tumour effects of PARP inhibition via the modulation of the histone methyltransferase SUV39H1, which plays a role in the DSB repair pathway (Mo et al. 2016). It was even demonstrated that combined PI3K/mTOR-PARP inhibition was still able to inhibit proliferation and upregulate apoptosis of BRCA1/2 wild type breast cancer cells (De et al. 2014). Although *PTEN* alterations were observed in these cells which was hypothesised to contribute to this combinatorial sensitivity (De et al. 2014). The combination of PI3K/mTOR inhibitors with PARP inhibitors has yet to

be explored in LMS but some evidence suggests that endometrial cancer cells with PTEN deficiency are particularly sensitive to PARP-PI3K inhibition, therefore uterine LMS patients which often display *PTEN* alterations may also benefit from this combination (Bian et al. 2018).

7.2.3 Emerging therapeutic targets in LMS

In order to proliferate indefinitely, cancer cells must continually elongate their telomeres which have been shortened after each successive division. The majority of cancer types utilise telomerase by telomerase reverse transcriptase (*TERT)* reactivation to achieve this, however some cancers utilise a telomerase independent, HR based mechanism of telomere maintenance, termed alternative lengthening of telomeres (ALT) (Barthel et al. 2017; Bryan et al. 1997; Dilley and Greenberg 2015). Interestingly, a study from 2015 showed that 59% of LMS tumours displayed ALT phenotypes by assessing telomere content and *TERT* mutation status (Liau et al. 2015). Furthermore, this study went on to show that ALT activation in LMS correlated with aggressive histological features and worse overall survival (Liau et al. 2015). A further study in 2018 even reported that 78% of LMS tumours are ALT positive by assessing markers of ALT such as C-circles, which are a unique DNA structures present during ALT mechanisms (Liau et al. 2015; Chudasama et al. 2018). Consistent with these findings, alterations in several genes involved in telomere maintenance have been detected including *ATRX, RB* Transcriptional Corepressor Like 2 *(RBL2)* and Speckled 100 kDa protein (*SP100),* of which *RBL2* and *SP100* deletions showed the strongest correlation with ALT activation (Chudasama et al. 2018). This mechanism of telomere maintenance is associated with high levels of DNA damage at telomeres and can lead to cell death if excessive, therefore inducing hyperactive ALT could potentially induce cell death selectively in ALT positive cells. This can be achieved by the stabilisation of G-quadruplex structures throughout telomeres undergoing ALT, which has recently shown to inhibit osteosarcoma cells *in vitro* by enhancing ALT and inducing DNA damage. The potential anti-tumour effect of G-quadruplex stabilisation should be tested in LMS models in order to assess efficacy in ALT positive and negative LMS.

Cuppens and co-workers have demonstrated that vasoactive intestinal peptide receptor 2 (*VIPR2*) was consistently affected in almost all LMS tumours tested (96%) with downregulated expression observed in 75% of tumours and deletions occurring in 37.5% of tumours (Cuppens et al. 2018). VIPR2 plays an important role in negative regulation of smooth muscle cell proliferation and therefore could potentially be a novel tumour

suppressor gene which is altered specifically in LMS tumours (Hilaire et al. 2010). Indeed, patients with low VIPR2 expression demonstrated worse clinical outcomes and additionally, treatment of SK-UT-1 LMS cells with a VIPR2 agonist lead to significantly reduced proliferation (Cuppens et al. 2018). Thus *VIPR2* may represent a novel tumour suppressor gene which is specifically lost in LMS cells and can also be therapeutically targeted. Agonists of VIPR2 could therefore be tested for anti-tumour efficacy in the LMS PDX-derived models generated in this thesis, especially in ICR-LMS-1 which shows a high expression of smooth muscle marker a-SMA.

7.3 Concluding remarks and future project directions

The prognosis of advanced LMS is poor and has remained largely unchanged in the past decade due to the lack of novel therapies able to outperform standard of care chemotherapy treatment. Treatment options for LMS patients who have progressed on chemotherapy regimens remains extremely limited and only one molecular targeted therapy, the multi-TKI inhibitor pazopanib, is currently approved for use in an advanced setting, highlighting the urgent need identify candidate drug targets to improve survival outcomes. However, one major challenge preventing such studies is the lack of well characterised pre-clinical models which can accurately recapitulate tumour biology and drug response phenotypes. Unfortunately, for this reason many candidate therapies shown to be efficacious in LMS cell lines are not translated into clinical efficacy. The need for improved patient-derived models of LMS is exacerbated by first: the inter-tumoural heterogeneity of disease, leading to variable clinical responses, and second: the rarity of the disease, meaning that clinical trials are difficult to set up, which increases the reliance on pre-clinical outcomes to accurately inform clinical studies.

By optimising and implementing a patient-derived model pipeline on STS biopsy samples, this work showed that biopsy samples are an effective starting material for the generation of patient-matched pre-clinical models, faithfully recapitulating patient tumour histology and proteomic profiles. PDX-derived cell cultures were also established that recapitulated characteristics of PDX and patient tumours and are therefore better models to use for pre-clinical studies of tumour drug response compared to conventional, immortalised cell lines. PDX-derived cell cultures and immortalised cell lines additionally showed distinct molecular changes associated with doxorubicin acquired resistance.

Utilising PDX-derived LMS cell cultures for targeted small molecule inhibitor screens, this work described a number of candidate pathways which can be therapeutically targeted in most, or a subset of advanced LMS tumours. The screen identified a shared sensitivity to dual PI3K/mTOR inhibition, as well as a sensitivity niclosamide treatment, an inhibitor of Wnt/β-catenin, mTOR, STAT3, NF-kB and Notch signalling pathways. This is the first study showing that LMS cells respond to niclosamide treatment *in vitro,* also demonstrating that this response occurs at concentrations well below the clinically relevant doses observed in other cancer types (Burock et al. 2018; Schweizer et al. 2018). Future work should assess the signalling pathways specifically effected by niclosamide treatment in all PDX-derived LMS cells derived in this study.

Another candidate drug identified from screening PDX-derived LMS cells was the PARP inhibitor talazoparib. Further investigation into the effect of prior DNA damaging chemotherapeutic agents on PARP inhibitor response is warranted although this work has shown both chemo-sensitive and chemo-resistant LMS cells display PARP inhibitor sensitivity. However several outstanding questions remain, first: to what extent do specific DDR defects in LMS cause PARP inhibitor sensitivity and can these be used as predictive biomarkers of response? Second: can LMS cells acquired resistance to PARP inhibition and if so, are these mechanisms specific to certain DDR mutants and third: can PARP inhibitors be combined with other molecular targeted therapies or chemotherapies to potentiate LMS tumour responses? These questions can be addressed by utilising the models derived in this study.

Chapter 8 - References

Abdolahi, Shahrokh, Zeinab Ghazvinian, Samad Muhammadnejad, Mahshid Saleh, Hamid Asadzadeh Aghdaei, and Kaveh Baghaei. 2022. "Patient-Derived Xenograft (PDX) Models, Applications and Challenges in Cancer Research." *Journal of Translational Medicine 2022 20:1* 20 (1): 1–15. https://doi.org/10.1186/S12967-022-03405-8.

Abeshouse, Adam, Clement Adebamowo, Sally N. Adebamowo, Rehan Akbani, Teniola Akeredolu, Adrian Ally, Matthew L. Anderson, et al. 2017. "Comprehensive and Integrated Genomic Characterization of Adult Soft Tissue Sarcomas." *Cell* 171 (4): 950-965.e28. https://doi.org/10.1016/j.cell.2017.10.014.

Abida, W., D. Campbell, A. Patnaik, B. Sautois, J. Shapiro, N.J. Vogelzang, A.H. Bryce, et al. 2019. "Preliminary Results from the TRITON2 Study of Rucaparib in Patients (Pts) with DNA Damage Repair (DDR)-Deficient Metastatic Castration-Resistant Prostate Cancer (MCRPC): Updated Analyses." *Annals of Oncology* 30 (5): v327–28. https://doi.org/10.1093/annonc/mdz248.003.

Abolhoda, Amir, Amy E. Wilson, Howard Ross, Peter V. Danenberg, Michael Burt, and Kathleen W. Scotto. 1999. "Rapid Activation of MDR1 Gene Expression in Human Metastatic Sarcoma after in Vivo Exposure to Doxorubicin." *Clinical Cancer Research* 5 (11): 3352–56.

Adjei, Isaac M., and Sharma Blanka. 2015. "Modulation of the Tumor Microenvironment for Cancer Treatment: A Biomaterials Approach." *Journal of Functional Biomaterials 2015, Vol. 6, Pages 81-103* 6 (1): 81–103. https://doi.org/10.3390/JFB6010081.

Ahn, Sung Yong, Nam Hee Kim, Kyungro Lee, Yong Hoon Cha, Ji Hye Yang, So Young Cha, Eunae Sandra Cho, et al. 2017. "Niclosamide Is a Potential Therapeutic for Familial Adenomatosis Polyposis by Disrupting Axin-GSK3 Interaction." *Oncotarget* 8 (19): 31842–55. https://doi.org/10.18632/ONCOTARGET.16252.

Alcoser, Sergio Y., David J. Kimmel, Suzanne D. Borgel, John P. Carter, Kelly M. Dougherty, and Melinda G. Hollingshead. 2011. "Real-Time PCR-Based Assay to Quantify the Relative Amount of Human and Mouse Tissue Present in Tumor Xenografts." *BMC Biotechnology* 11 (1): 1–8. https://doi.org/10.1186/1472-6750-11-124/TABLES/1.

Almeida, Jamie L., Kenneth D. Cole, and Anne L. Plant. 2016. "Standards for Cell Line Authentication and Beyond." *PLoS Biology* 14 (6). https://doi.org/10.1371/JOURNAL.PBIO.1002476.

Alston-Roberts, Christine, Rita Barallon, Steven R. Bauer, John Butler, Amanda Capes-Davis, Wilhelm G. Dirks, Eugene Elmore, et al. 2010. "Cell Line Misidentification: The Beginning of the End." *Nature Reviews Cancer 2010 10:6* 10 (6): 441–48. https://doi.org/10.1038/nrc2852.

Amdahl, Jordan, Stephanie C Manson, Robert Isbell, Ayman Chit, Jose Diaz, Lily Lewis, and Thomas E Delea. 2014. "Cost-Effectiveness of Pazopanib in Advanced Soft Tissue Sarcoma in the United Kingdom." *Sarcoma* 2014 (June): 481071. https://doi.org/10.1155/2014/481071.

American Cancer Society. 2018. "Risk Factors for Soft Tissue Sarcomas." 2018. https://www.cancer.org/cancer/soft-tissue-sarcoma/causes-risks-prevention/risk-factors.html.

Anderson, Nathaniel D., Yael Babichev, Fabio Fuligni, Federico Comitani, Mehdi Layeghifard, Rosemarie E. Venier, Stefan C. Dentro, et al. 2021. "Lineage-Defined Leiomyosarcoma Subtypes Emerge Years before Diagnosis and Determine Patient Survival." *Nature Communications 2021 12:1* 12 (1): 1–14. https://doi.org/10.1038/s41467-021-24677-6.

André, Fabrice, Eva Ciruelos, Gabor Rubovszky, Mario Campone, Sibylle Loibl, Hope S. Rugo, Hiroji Iwata, et al. 2019. " Alpelisib for PIK3CA -Mutated, Hormone Receptor–Positive Advanced Breast Cancer ." *New England Journal of Medicine* 380 (20): 1929–40. https://doi.org/10.1056/NEJMOA1813904/SUPPL_FILE/NEJMOA1813904_DATA-SHARING.PDF.

Annunziato, Stefano, Sjors M. Kas, Micha Nethe, Hatice Yücel, Jessica Del Bravo, Colin Pritchard, Rahmen Bin Ali, et al. 2016. "Modeling Invasive Lobular Breast Carcinoma by CRISPR/Cas9-Mediated Somatic Genome Editing of the Mammary Gland." *Genes & Development* 30 (12): 1470–80. https://doi.org/10.1101/GAD.279190.116.

Asano, Hiroshi, Toshiyuki Isoe, Yoichi M. Ito, Naoki Nishimoto, Yudai Watanabe, Saki Yokoshiki, and Hidemichi Watari. 2022. "Status of the Current Treatment Options and Potential Future Targets in Uterine Leiomyosarcoma: A Review." *Cancers 2022, Vol. 14, Page 1180* 14 (5): 1180. https://doi.org/10.3390/CANCERS14051180.

Asleh, Karama, Gian Luca Negri, Sandra E. Spencer Miko, Shane Colborne, Christopher S. Hughes, Xiu Q. Wang, Dongxia Gao, et al. 2022. "Proteomic Analysis of Archival Breast Cancer Clinical Specimens Identifies Biological Subtypes with Distinct Survival Outcomes." *Nature Communications 2022 13:1* 13 (1): 1–19. https://doi.org/10.1038/s41467-022-28524-0.

Babichev, Yael, Leah Kabaroff, Alessandro Datti, David Uehling, Methvin Isaac, Rima Al-awar, Michael Prakesch, et al. 2016. "PI3K/AKT/MTOR Inhibition in Combination with Doxorubicin Is an Effective Therapy for Leiomyosarcoma." *Journal of Translational Medicine* 14 (1): 1–12. https://doi.org/10.1186/S12967-016-0814-Z/FIGURES/6.

Bai, Chujie, Min Yang, Zhengfu Fan, Shu Li, Tian Gao, and Zhiwei Fang. 2015. "Associations of Chemo- and Radio-Resistant Phenotypes with the Gap Junction, Adhesion and Extracellular Matrix in a Three-Dimensional Culture Model of Soft Sarcoma." *Journal of Experimental and Clinical Cancer Research* 34 (1): 1–10. https://doi.org/10.1186/S13046-015-0175-0/FIGURES/5.

Bai, Y., J. Li, B. Fang, A. Edwards, G. Zhang, M. Bui, S. Eschrich, S. Altiok, J. Koomen, and E. B. Haura. 2012. "Phosphoproteomics Identifies Driver Tyrosine Kinases in Sarcoma Cell Lines and Tumors." *Cancer Research* 72 (10): 2501–11. https://doi.org/10.1158/0008-5472.CAN-11-3015.

Bairoch, Amos. 2018. "The Cellosaurus, a Cell-Line Knowledge Resource." *Journal of Biomolecular Techniques* 29 (2): 25–38. https://doi.org/10.7171/JBT.18-2902-002.

Ballinger, Mandy L., David L. Goode, Isabelle Ray-Coquard, Paul A. James, Gillian Mitchell, Eveline Niedermayr, Ajay Puri, et al. 2016. "Monogenic and Polygenic Determinants of Sarcoma Risk: An International Genetic Study." *The Lancet Oncology* 17 (9): 1261–71. https://doi.org/10.1016/S1470-2045(16)30147-4.

Balmus, Gabriel, Domenic Pilger, Julia Coates, Mukerrem Demir, Matylda Sczaniecka-Clift, Ana C. Barros, Michael Woods, et al. 2019. "ATM Orchestrates the DNA-Damage Response to Counter Toxic Non-Homologous End-Joining at Broken Replication Forks." *Nature Communications 2019 10:1* 10 (1): 1–18. https://doi.org/10.1038/s41467-018-07729-2.

Barthel, Floris P., Wei Wei, Ming Tang, Emmanuel Martinez-Ledesma, Xin Hu, Samirkumar B. Amin, Kadir C. Akdemir, et al. 2017. "Systematic Analysis of Telomere Length and Somatic Alterations in 31 Cancer Types." *Nature Genetics* 49 (3): 349–57. https://doi.org/10.1038/NG.3781.

Bassi, Giada, Silvia Panseri, Samuele Maria Dozio, Monica Sandri, Elisabetta Campodoni,

Massimiliano Dapporto, Simone Sprio, Anna Tampieri, and Monica Montesi. 2020. "Scaffold-Based 3D Cellular Models Mimicking the Heterogeneity of Osteosarcoma Stem Cell Niche." *Scientific Reports 2020 10:1* 10 (1): 1–12. https://doi.org/10.1038/s41598-020-79448-y.

Bathan, Andrew J., Anastasia Constantinidou, Seth M. Pollack, and Robin L. Jones. 2013. "Diagnosis, Prognosis, and Management of Leiomyosarcoma: Recognition of Anatomic Variants." *Current Opinion in Oncology* 25 (4): 384–89. https://doi.org/10.1097/CCO.0B013E3283622C77.

Baxter, Patricia A., Jack M. Su, Arzu Onar-Thomas, Catherine A. Billups, Xiao Nan Li, Tina Young Poussaint, Edward R. Smith, et al. 2020. "A Phase I/II Study of Veliparib (ABT-888) with Radiation and Temozolomide in Newly Diagnosed Diffuse Pontine Glioma: A Pediatric Brain Tumor Consortium Study." *Neuro-Oncology* 22 (6): 875–85. https://doi.org/10.1093/NEUONC/NOAA016.

Beck, A. H., C. H. Lee, D. M. Witten, B. C. Gleason, B. Edris, I. Espinosa, S. Zhu, et al. 2009. "Discovery of Molecular Subtypes in Leiomyosarcoma through Integrative Molecular Profiling." *Oncogene 2010 29:6* 29 (6): 845–54. https://doi.org/10.1038/onc.2009.381.

Belgiovine, Cristina, Roberta Frapolli, Manuela Liguori, Elisabeth Digifico, Federico Simone Colombo, Marina Meroni, Paola Allavena, and Maurizio D'Incalci. 2021. "Inhibition of Tumor-Associated Macrophages by Trabectedin Improves the Antitumor Adaptive Immunity in Response to Anti-PD-1 Therapy." *European Journal of Immunology* 51 (11): 2677–86. https://doi.org/10.1002/EJI.202149379.

Benassi, M. S., P. Ragazzini, G. Gamberi, M. R. Sollazzo, L. Molendini, C. Ferrari, M. Merli, T. Böhling, and P. Picci. 1998. "Adhesion Molecules in High-Grade Soft Tissue Sarcomas: Correlation to Clinical Outcome." *European Journal of Cancer* 34 (4): 496–502. https://doi.org/10.1016/S0959-8049(97)10097-1.

Bendell, Johanna, E. M. O'Reilly, M. R. Middleton, I. Chau, H. Hochster, A. Fielding, W. Burke, and H. Burris. 2015. "Phase I Study of Olaparib plus Gemcitabine in Patients with Advanced Solid Tumours and Comparison with Gemcitabine Alone in Patients with Locally Advanced/Metastatic Pancreatic Cancer." *Annals of Oncology* 26 (4): 804–11. https://doi.org/10.1093/annonc/mdu581.

Benitez, Anaid, Wenjun Liu, Anna Palovcak, Guanying Wang, Jaewon Moon, Kevin An, Anna Kim, et al. 2018. "FANCA Promotes DNA Double-Strand Break Repair by Catalyzing Single-Strand Annealing and Strand Exchange." *Molecular Cell* 71 (4): 621-628.e4. https://doi.org/10.1016/j.molcel.2018.06.030.

Benjamin, Robert S., and Andrew Futreal. 2016. "Are Sarcomas Hereditary?" *The Lancet Oncology* 17 (9): 1179–81. https://doi.org/10.1016/S1470-2045(16)30292-3.

Berrington De Gonzalez, Amy, Ethel Gilbert, Rochelle Curtis, Peter Inskip, Ruth Kleinerman, Lindsay Morton, Preetha Rajaraman, and Mark P. Little. 2013. "Second Solid Cancers after Radiation Therapy: A Systematic Review of the Epidemiologic Studies of the Radiation Dose-Response Relationship." *International Journal of Radiation Oncology, Biology, Physics* 86 (2): 224–33. https://doi.org/10.1016/J.IJROBP.2012.09.001.

Bian, X., J. Gao, F. Luo, C. Rui, T. Zheng, D. Wang, Y. Wang, et al. 2018. "PTEN Deficiency Sensitizes Endometrioid Endometrial Cancer to Compound PARP-PI3K Inhibition but Not PARP Inhibition as Monotherapy." *Oncogene* 37 (3). https://doi.org/10.1038/onc.2017.326.

Bindra, Ranjit S., Shannon L. Gibson, Alice Meng, Ulrica Westermark, Maria Jasin, Andrew J.

Pierce, Robert G. Bristow, Marie K. Classon, and Peter M. Glazer. 2005. "Hypoxia-Induced Down-Regulation of BRCA1 Expression by E2Fs." *Cancer Research* 65 (24): 11597–604. https://doi.org/10.1158/0008-5472.CAN-05-2119.

Bjerkehagen, Bodil, Sigbjørn Smeland, Lise Walberg, Sigmund Skjeldal, Kirsten Sundby Hall, Jahn M. Nesland, Milada Cvancarova Småstuen, et al. 2009. "Radiation-Induced Sarcoma: 25-Year Experience from The Norwegian Radium Hospital." *Https://Doi.Org/10.1080/02841860802047387* 47 (8): 1475–82. https://doi.org/10.1080/02841860802047387.

Blanke, Charles D., Cathryn Rankin, George D. Demetri, Christopher W. Ryan, Margaret Von Mehren, Robert S. Benjamin, A. Kevin Raymond, et al. 2008. "Phase III Randomized, Intergroup Trial Assessing Imatinib Mesylate at Two Dose Levels in Patients with Unresectable or Metastatic Gastrointestinal Stromal Tumors Expressing the Kit Receptor Tyrosine Kinase: S0033." *Journal of Clinical Oncology* 26 (4): 626–32. https://doi.org/10.1200/JCO.2007.13.4452.

Blay, J. Y., C. Honoré, E. Stoeckle, P. Meeus, M. Jafari, F. Gouin, P. Anract, et al. 2019. "Surgery in Reference Centers Improves Survival of Sarcoma Patients: A Nationwide Study." *Annals of Oncology* 30 (7): 1143–53. https://doi.org/10.1093/annonc/mdz124.

Blay, Jean Yves, Patrick Schöffski, Sebastian Bauer, Anders Krarup-Hansen, Charlotte Benson, David R. D'Adamo, Yan Jia, and Robert G. Maki. 2019. "Eribulin versus Dacarbazine in Patients with Leiomyosarcoma: Subgroup Analysis from a Phase 3, Open-Label, Randomised Study." *British Journal of Cancer* 120 (11): 1026–32. https://doi.org/10.1038/s41416-019-0462-1.

Blume-Jensen, Peter, and Tony Hunter. 2001. "Oncogenic Kinase Signalling." *Nature* 411 (6835): 355–65. https://doi.org/10.1038/35077225.

Boichuk, Sergei, Firuza Bikinieva, Ilmira Nurgatina, Pavel Dunaev, Elena Valeeva, Aida Aukhadieva, Alexey Sabirov, and Aigul Galembikova. 2020. "Inhibition of AKT-Signaling Sensitizes Soft Tissue Sarcomas (STS) and Gastrointestinal Stromal Tumors (GIST) to Doxorubicin via Targeting of Homology-Mediated DNA Repair." *International Journal of Molecular Sciences 2020, Vol. 21, Page 8842* 21 (22): 8842. https://doi.org/10.3390/IJMS21228842.

Bonetti, Andrea, Marta Zaninelli, Stefania Rodella, Annamaria Molino, Loris Sperotto, Quirino Piubello, Franco Bonetti, Rolando Nortilli, Monica Turazza, and Gian Luigi Cetto. 1996. "Tumor Proliferative Activity and Response to First-Line Chemotherapy in Advanced Breast Carcinoma." *Breast Cancer Research and Treatment 1996 38:3* 38 (3): 289–97. https://doi.org/10.1007/BF01806148.

Bono, Johann de, Joaquin Mateo, Karim Fizazi, Fred Saad, Neal Shore, Shahneen Sandhu, Kim N. Chi, et al. 2020. "Olaparib for Metastatic Castration-Resistant Prostate Cancer." *New England Journal of Medicine* 382 (22): 2091–2102. https://doi.org/10.1056/NEJMOA1911440/SUPPL_FILE/NEJMOA1911440_DATA-SHARING.PDF.

Bougeard, Gaëlle, Mariette Renaux-Petel, Jean Michel Flaman, Camille Charbonnier, Pierre Fermey, Muriel Belotti, Marion Gauthier-Villars, et al. 2015. "Revisiting Li-Fraumeni Syndrome From TP53 Mutation Carriers." *Journal of Clinical Oncology* 33 (21): 2345–52. https://doi.org/10.1200/JCO.2014.59.5728.

Bouwman, Peter, Amal Aly, Jose M. Escandell, Mark Pieterse, Jirina Bartkova, Hanneke Van Der Gulden, Sanne Hiddingh, et al. 2010. "53BP1 Loss Rescues BRCA1 Deficiency and Is

Associated with Triple-Negative and BRCA-Mutated Breast Cancers." *Nature Structural and Molecular Biology* 17 (6). https://doi.org/10.1038/nsmb.1831.

Bouwman, Peter, and Jos Jonkers. 2012. "The Effects of Deregulated DNA Damage Signalling on Cancer Chemotherapy Response and Resistance." *Nature Reviews. Cancer* 12 (9): 587–98. https://doi.org/10.1038/NRC3342.

Brady, Mary Susan, Jeffrey J. Gaynor, and Murray F. Brennan. 1992. "Radiation-Associated Sarcoma of Bone and Soft Tissue." *Archives of Surgery* 127 (12): 1379–85. https://doi.org/10.1001/ARCHSURG.1992.01420120013002.

Bramwell, Vivien H.C., Dale Anderson, and Manya L. Charette. 2000. "Doxorubicin-Based Chemotherapy for the Palliative Treatment of Adult with Locally Advanced or Metastatic Soft-Tissue Sarcoma:A Meta-Analysis and Clinical Practice Guideline." *Sarcoma* 4 (3): 103–12. https://doi.org/10.1080/13577140020008066.

Brandsma, Inger, and Dik C. Gent. 2012. "Pathway Choice in DNA Double Strand Break Repair: Observations of a Balancing Act." *Genome Integrity* 3 (1): 1–10. https://doi.org/10.1186/2041-9414-3-9/FIGURES/4.

Brem, Reto, and Janet Hall. 2005. "XRCC1 Is Required for DNA Single-Strand Break Repair in Human Cells." *Nucleic Acids Research* 33 (8): 2512–20. https://doi.org/10.1093/NAR/GKI543.

Brennan, Murray F., Cristina R. Antonescu, Nicole Moraco, and Samuel Singer. 2014. "Lessons Learned from the Study of 10,000 Patients with Soft Tissue Sarcoma." *Annals of Surgery* 260 (3): 416–22. https://doi.org/10.1097/SLA.0000000000000869.

Brenner, J. Chad, Felix Y. Feng, Sumin Han, Sonam Patel, Siddharth V. Goyal, Laura M. Bou-Maroun, Meilan Liu, et al. 2012. "PARP-1 Inhibition as a Targeted Strategy to Treat Ewing's Sarcoma." *Cancer Research* 72 (7): 1608–13. https://doi.org/10.1158/0008-5472.CAN-11-3648/650100/AM/PARP-1-INHIBITION-AS-A-TARGETED-STRATEGY-TO-TREAT.

Broad Institute. 2021. "DepMap Portal." 2021. https://depmap.org/portal/download/all/.

Brodin, Bertha A., Krister Wennerberg, Elisabet Lidbrink, Otte Brosjö, Swapnil Potdar, Jennifer N. Wilson, Limin Ma, et al. 2019. "Drug Sensitivity Testing on Patient-Derived Sarcoma Cells Predicts Patient Response to Treatment and Identifies c-Sarc Inhibitors as Active Drugs for Translocation Sarcomas." *British Journal of Cancer* 120 (4): 435–43. https://doi.org/10.1038/s41416-018-0359-4.

Brownhill, Samantha, Dena Cohen, and Sue Burchill. 2014. "Proliferation Index: A Continuous Model to Predict Prognosis in Patients with Tumours of the Ewing's Sarcoma Family." *PLoS ONE* 9 (8). https://doi.org/10.1371/JOURNAL.PONE.0104106.

Brugge, Petra Ter, Petra Kristel, Eline Van Der Burg, Ute Boon, Michiel De Maaker, Esther Lips, Lennart Mulder, et al. 2016. "Mechanisms of Therapy Resistance in Patient-Derived Xenograft Models of Brca1-Deficient Breast Cancer." *Journal of the National Cancer Institute* 108 (11). https://doi.org/10.1093/jnci/djw148.

Bruin, Maaike A.C., Gabe S. Sonke, Jos H. Beijnen, and Alwin D.R. Huitema. 2022. "Pharmacokinetics and Pharmacodynamics of PARP Inhibitors in Oncology." *Clinical Pharmacokinetics 2022*, October, 1–27. https://doi.org/10.1007/S40262-022-01167-6.

Bruland, Fodstad, and A. Pihl. 1985. "The Use of Multicellular Spheroids in Establishing Human Sarcoma Cell Lines In Vitro." *International Journal of Cancer* 35 (6): 793–98. https://doi.org/10.1002/IJC.2910350616.

Bryan, Tracy M., Anna Englezou, Luciano Dalla-Pozza, Melissa A. Dunham, and Roger R. Reddel. 1997. "Evidence for an Alternative Mechanism for Maintaining Telomere Length in Human Tumors and Tumor-Derived Cell Lines." *Nature Medicine 1997 3:11* 3 (11): 1271–74. https://doi.org/10.1038/nm1197-1271.

Bryant, Helen E., Eva Petermann, Niklas Schultz, Ann Sofie Jemth, Olga Loseva, Natalia Issaeva, Fredrik Johansson, Serena Fernandez, Peter McGlynn, and Thomas Helleday. 2009. "PARP Is Activated at Stalled Forks to Mediate Mre11-Dependent Replication Restart and Recombination." *The EMBO Journal* 28 (17): 2601–15. https://doi.org/10.1038/EMBOJ.2009.206.

Bryant, Helen E., Niklas Schultz, Huw D. Thomas, Kayan M. Parker, Dan Flower, Elena Lopez, Suzanne Kyle, Mark Meuth, Nicola J. Curtin, and Thomas Helleday. 2005. "Specific Killing of BRCA2-Deficient Tumours with Inhibitors of Poly(ADP-Ribose) Polymerase." *Nature* 434 (7035): 913–17. https://doi.org/10.1038/NATURE03443.

Bunting, Samuel F., Elsa Callén, Nancy Wong, Hua Tang Chen, Federica Polato, Amanda Gunn, Anne Bothmer, et al. 2010. "53BP1 Inhibits Homologous Recombination in Brca1-Deficient Cells by Blocking Resection of DNA Breaks." *Cell* 141 (2): 243–54. https://doi.org/10.1016/J.CELL.2010.03.012.

Burock, Susen, Severin Daum, Ulrich Keilholz, Konrad Neumann, Wolfgang Walther, and Ulrike Stein. 2018. "Phase II Trial to Investigate the Safety and Efficacy of Orally Applied Niclosamide in Patients with Metachronous or Sychronous Metastases of a Colorectal Cancer Progressing after Therapy: The NIKOLO Trial." *BMC Cancer* 18 (1): 1–7. https://doi.org/10.1186/S12885-018-4197-9/TABLES/1.

Burton, Gary Von, Cathy Rankin, Mark M. Zalupski, Glen M. Mills, Ernest C. Borden, and Antman Karen. 2006. "Phase II Trial of Gemcitabine as First Line Chemotherapy in Patients with Metastatic or Unresectable Soft Tissue Sarcoma." *American Journal of Clinical Oncology* 29 (1): 59–61. https://doi.org/10.1097/01.COC.0000195088.28956.DD.

Byrum, Andrea K., Alessandro Vindigni, and Nima Mosammaparast. 2019. "Defining and Modulating 'BRCAness.'" *Trends in Cell Biology* 29 (9): 740–51. https://doi.org/10.1016/J.TCB.2019.06.005.

Cairns, Rob A., Isaac S. Harris, and Tak W. Mak. 2011. "Regulation of Cancer Cell Metabolism." *Nature Reviews Cancer 2011 11:2* 11 (2): 85–95. https://doi.org/10.1038/nrc2981.

Calandrini, Camilla, Sander R. van Hooff, Irene Paassen, Dilara Ayyildiz, Sepide Derakhshan, M. Emmy M. Dolman, Karin P.S. Langenberg, et al. 2021. "Organoid-Based Drug Screening Reveals Neddylation as Therapeutic Target for Malignant Rhabdoid Tumors." *Cell Reports* 36 (8): 109568. https://doi.org/10.1016/j.celrep.2021.109568.

Cancer Research UK. 2017a. "Bone Sarcoma Incidence Statistics." 2017. https://www.cancerresearchuk.org/health-professional/cancer-statistics/statistics-by-cancer-type/bone-sarcoma/incidence#heading-Zero.

———. 2017b. "Cancer Incidence for Common Cancers." 2017. https://www.cancerresearchuk.org/health-professional/cancer-statistics/incidence/common-cancers-compared#heading-Zero.

———. 2017c. "Soft Tissue Sarcoma Incidence Statistics." 2017. https://www.cancerresearchuk.org/health-professional/cancer-statistics/statistics-by-cancer-type/soft-tissue-sarcoma/incidence#heading-Zero.

Capes-Davis, Amanda, Yvonne A. Reid, Margaret C. Kline, Douglas R. Storts, Ethan Strauss, Wilhelm G. Dirks, Hans G. Drexler, et al. 2013. "Match Criteria for Human Cell Line Authentication: Where Do We Draw the Line?" *International Journal of Cancer* 132 (11): 2510–19. https://doi.org/10.1002/IJC.27931.

Capes-Davis, Amanda, George Theodosopoulos, Isobel Atkin, Hans G. Drexler, Arihiro Kohara, Roderick A.F. MacLeod, John R. Masters, et al. 2010. "Check Your Cultures! A List of Cross-Contaminated or Misidentified Cell Lines." *International Journal of Cancer* 127 (1): 1–8. https://doi.org/10.1002/IJC.25242.

Carracedo, Arkaitz, Li Ma, Julie Teruya-Feldstein, Federico Rojo, Leonardo Salmena, Andrea Alimonti, Ainara Egia, et al. 2008. "Inhibition of MTORC1 Leads to MAPK Pathway Activation through a PI3K-Dependent Feedback Loop in Human Cancer." *The Journal of Clinical Investigation* 118 (9): 3065–74. https://doi.org/10.1172/JCI34739.

Casali, P G, N Abecassis, H T Aro, S Bauer, R Biagini, S Bielack, S Bonvalot, et al. 2018. "Soft Tissue and Visceral Sarcomas: ESMO-EURACAN Clinical Practice Guidelines for Diagnosis, Treatment and Follow-Up." *Annals of Oncology* 29 (Suppl 4): iv51–67. https://doi.org/10.1093/annonc/mdy096.

Casey, Mattie J., and Rodney A. Stewart. 2020. "Pediatric Cancer Models in Zebrafish." *Trends in Cancer* 6 (5): 407–18. https://doi.org/10.1016/j.trecan.2020.02.006.

Cattaruzza, Sabrina, Pier Andrea Nicolosi, Paola Braghetta, Laura Pazzaglia, Maria Serena Benassi, Piero Picci, Katia Lacrima, et al. 2013. "NG2/CSPG4–Collagen Type VI Interplays Putatively Involved in the Microenvironmental Control of Tumour Engraftment and Local Expansion." *Journal of Molecular Cell Biology* 5 (3): 176–93. https://doi.org/10.1093/JMCB/MJT010.

Cesarman, Ethel, Blossom Damania, Susan E. Krown, Jeffrey Martin, Mark Bower, and Denise Whitby. 2019. "Kaposi Sarcoma." *Nature Reviews. Disease Primers* 5 (1). https://doi.org/10.1038/S41572-019-0060-9.

Cesne, A. Le, J. Y. Blay, I. Judson, A. Van Oosterom, J. Verweij, J. Radford, P. Lorigan, et al. 2005. "Phase II Study of ET-743 in Advanced Soft Tissue Sarcomas: A European Organisation for the Research and Treatment of Cancer (EORTC) Soft Tissue and Bone Sarcoma Group Trial." *Journal of Clinical Oncology* 23 (3): 576–84. https://doi.org/10.1200/JCO.2005.01.180.

Cesne, A. Le, M. Van Glabbeke, P. J. Woll, V. H. Bramwell, P. G. Casali, H. J. Hoekstra, P. Reichardt, P. C. Hogendoorn, P. Hohenberger, and J. Y. Blay. 2008. "The End of Adjuvant Chemotherapy (AdCT) Era with Doxorubicin-Based Regimen in Resected High-Grade Soft Tissue Sarcoma (STS): Pooled Analysis of the Two STBSG-EORTC Phase III Clinical Trials." *Https://Doi.Org/10.1200/Jco.2008.26.15_suppl.10525* 26 (15_suppl): 10525–10525. https://doi.org/10.1200/JCO.2008.26.15_SUPPL.10525.

Cesne, Axel Le, Javier Martín-Broto, and Giovanni Grignani. 2022. "A Review of the Efficacy of Trabectedin as Second-Line Treatment of Advanced Soft Tissue Sarcoma." *Future Oncology*, September. https://doi.org/10.2217/FON-2022-0517/ASSET/IMAGES/LARGE/FIGURE1.JPEG.

Cha, Charles, Christina R. Antonescu, May Lynn Quan, Sandip Maru, Murray F. Brennan, J. Bradley Aust, Martin J. Heslin, and Lynn H. Harrison. 2004. "Long-Term Results with Resection of Radiation-Induced Soft Tissue Sarcomas." *Annals of Surgery* 239 (6): 903–10. https://doi.org/10.1097/01.SLA.0000128686.51815.8B.

Chadha, Madhumeeta, and Paul H. Huang. 2022. "Proteomic and Metabolomic Profiling in Soft

Tissue Sarcomas." *Current Treatment Options in Oncology 2022 23:1* 23 (1): 78–88. https://doi.org/10.1007/S11864-022-00947-3.

Chan, S. 2004. "Targeting the Mammalian Target of Rapamycin (MTOR): A New Approach to Treating Cancer." *British Journal of Cancer* 91 (8): 1420. https://doi.org/10.1038/SJ.BJC.6602162.

Chang, L., P. H. Graham, J. Hao, J. Ni, J. Bucci, P. J. Cozzi, J. H. Kearsley, and Y. Li. 2014. "PI3K/Akt/MTOR Pathway Inhibitors Enhance Radiosensitivity in Radioresistant Prostate Cancer Cells through Inducing Apoptosis, Reducing Autophagy, Suppressing NHEJ and HR Repair Pathways." *Cell Death & Disease* 5 (10). https://doi.org/10.1038/CDDIS.2014.415.

Chatterjee, Nimrat, and Graham C. Walker. 2017. "Mechanisms of DNA Damage, Repair, and Mutagenesis." *Environmental and Molecular Mutagenesis* 58 (5): 235–63. https://doi.org/10.1002/EM.22087.

Chaudhuri, Arnab Ray, Elsa Callen, Xia Ding, Ewa Gogola, Alexandra A. Duarte, Ji Eun Lee, Nancy Wong, et al. 2016. "Replication Fork Stability Confers Chemoresistance in BRCA-Deficient Cells." *Nature* 535 (7612): 382–87. https://doi.org/10.1038/NATURE18325.

Chen, Eleanor, Fionnuala O'Connell, and Christopher D.M. Fletcher. 2011. "Dedifferentiated Leiomyosarcoma: Clinicopathological Analysis of 18 Cases." *Histopathology* 59 (6): 1135–43. https://doi.org/10.1111/J.1365-2559.2011.04070.X.

Chen, T. R. 1988. "SK-UT-1B, a Human Tumorigenic Diploid Cell Line." *Cancer Genetics and Cytogenetics* 33 (1): 77–81. https://doi.org/10.1016/0165-4608(88)90052-0.

Chen, Zhongjian, Chenxi Yang, Zhenying Guo, Siyu Song, Yun Gao, Ding Wang, Weimin Mao, and Junping Liu. 2021. "A Novel PDX Modeling Strategy and Its Application in Metabolomics Study for Malignant Pleural Mesothelioma." *BMC Cancer* 21 (1): 1–15. https://doi.org/10.1186/S12885-021-08980-5/FIGURES/10.

Chi, Yihebali, Zhiwei Fang, Xiaonan Hong, Yang Yao, Ping Sun, Guowen Wang, Feng Du, et al. 2018. "Safety and Efficacy of Anlotinib, a Multikinase Angiogenesis Inhibitor, in Patients with Refractory Metastatic Soft-Tissue Sarcoma." *Clinical Cancer Research* 24 (21): 5233–38. https://doi.org/10.1158/1078-0432.CCR-17-3766.

Choi, Jungmin, Aranzazu Manzano, Weilai Dong, Stefania Bellone, Elena Bonazzoli, Luca Zammataro, Xiaotong Yao, et al. 2021. "Integrated Mutational Landscape Analysis of Uterine Leiomyosarcomas." *Proceedings of the National Academy of Sciences of the United States of America* 118 (15): e2025182118. https://doi.org/10.1073/PNAS.2025182118/SUPPL_FILE/PNAS.2025182118.SD15.XLSX.

Christowitz, Claudia, Tanja Davis, Ashwin Isaacs, Gustav Van Niekerk, Suzel Hattingh, and Anna Mart Engelbrecht. 2019. "Mechanisms of Doxorubicin-Induced Drug Resistance and Drug Resistant Tumour Growth in a Murine Breast Tumour Model." *BMC Cancer* 19 (1): 1–10. https://doi.org/10.1186/S12885-019-5939-Z/FIGURES/5.

Chudasama, Priya, Sadaf S. Mughal, Mathijs A. Sanders, Daniel Hübschmann, Inn Chung, Katharina I. Deeg, Siao Han Wong, et al. 2018. "Integrative Genomic and Transcriptomic Analysis of Leiomyosarcoma." *Nature Communications 2018 9:1* 9 (1): 1–15. https://doi.org/10.1038/s41467-017-02602-0.

Chudasama, Priya, Marcus Renner, Melanie Straub, Sadaf S. Mughal, Barbara Hutter, Zeynep Kosaloglu, Ron Schweßinger, et al. 2017. "Targeting Fibroblast Growth Factor Receptor 1 for Treatment of Soft-Tissue Sarcoma." *Clinical Cancer Research* 23 (4): 962–73.

https://doi.org/10.1158/1078-0432.CCR-16-0860.

Chung, Jongkyeong, Calvin J. Kuo, Gerald R. Crabtree, and John Blenis. 1992. "Rapamycin-FKBP Specifically Blocks Growth-Dependent Activation of and Signaling by the 70 Kd S6 Protein Kinases." *Cell* 69 (7): 1227–36. https://doi.org/10.1016/0092-8674(92)90643-Q.

Clevers, Hans. 2016. "Modeling Development and Disease with Organoids." *Cell* 165 (7): 1586–97. https://doi.org/10.1016/J.CELL.2016.05.082.

Colella, Gianluca, Flavio Fazioli, Michele Gallo, Annarosaria De Chiara, Gaetano Apice, Carlo Ruosi, Amelia Cimmino, and Filomena de Nigris. 2018. "Sarcoma Spheroids and Organoids—Promising Tools in the Era of Personalized Medicine." *International Journal of Molecular Sciences* 19 (2): 615. https://doi.org/10.3390/ijms19020615.

Coleman, Niamh, Bingnan Zhang, Lauren A. Byers, and Timothy A. Yap. 2020. "The Role of Schlafen 11 (SLFN11) as a Predictive Biomarker for Targeting the DNA Damage Response." *British Journal of Cancer 2020 124:5* 124 (5): 857–59. https://doi.org/10.1038/s41416-020-01202-y.

Coleman, Robert L., Amit M. Oza, Domenica Lorusso, Carol Aghajanian, Ana Oaknin, Andrew Dean, Nicoletta Colombo, et al. 2017. "Rucaparib Maintenance Treatment for Recurrent Ovarian Carcinoma after Response to Platinum Therapy (ARIEL3): A Randomised, Double-Blind, Placebo-Controlled, Phase 3 Trial." *The Lancet* 390 (10106): 1949–61. https://doi.org/10.1016/S0140-6736(17)32440-6.

Coley, H. M., M. W. Verrill, S. E. Gregson, D. E. Odell, C. Fisher, and I. R. Judson. 2000. "Incidence of P-Glycoprotein Overexpression and Multidrug Resistance (MDR) Reversal in Adult Soft Tissue Sarcoma." *European Journal of Cancer* 36 (7): 881–88. https://doi.org/10.1016/S0959-8049(00)00032-0.

Comandone, Alessandro, Fausto Petrelli, Antonella Boglione, and Sandro Barni. 2017. "Salvage Therapy in Advanced Adult Soft Tissue Sarcoma: A Systematic Review and Meta-Analysis of Randomized Trials." *The Oncologist* 22 (12): 1518. https://doi.org/10.1634/THEONCOLOGIST.2016-0474.

Conde, Carmen, Manuel Mark, F. Javier Oliver, Aline Huber, Gilbert De Murcia, and Josiane Ménissier-De Murcia. 2001. "Loss of Poly(ADP-Ribose) Polymerase-1 Causes Increased Tumour Latency in P53-Deficient Mice." *The EMBO Journal* 20 (13): 3535–43. https://doi.org/10.1093/EMBOJ/20.13.3535.

Conteduca, Vincenza, Sheng Yu Ku, Loredana Puca, Megan Slade, Luisa Fernandez, Judy Hess, Rohan Bareja, et al. 2020. "SLFN11 Expression in Advanced Prostate Cancer and Response to Platinum-Based Chemotherapy." *Molecular Cancer Therapeutics* 19 (5): 1157–64. https://doi.org/10.1158/1535-7163.MCT-19-0926/177205/AM/SLFN11-EXPRESSION-IN-ADVANCED-PROSTATE-CANCER-AND.

Corless, Christopher L., Christine M. Barnett, and Michael C. Heinrich. 2011. "Gastrointestinal Stromal Tumours: Origin and Molecular Oncology." *Nature Reviews. Cancer* 11 (12): 865–78. https://doi.org/10.1038/NRC3143.

Cornillet-Lefebvre, P., W. Cuccuini, V. Bardet, J. Tamburini, L. Gillot, N. Ifrah, P. Nguyen, et al. 2005. "Constitutive Phosphoinositide 3-Kinase Activation in Acute Myeloid Leukemia Is Not Due to P110δ Mutations." *Leukemia 2006 20:2* 20 (2): 374–76. https://doi.org/10.1038/sj.leu.2404054.

Cornillie, Jasmien, Agnieszka Wozniak, Haifu Li, Yannick Wang, Bram Boeckx, Yemarshet K.

Gebreyohannes, Jasmien Wellens, et al. 2019. "Establishment and Characterization of Histologically and Molecularly Stable Soft-Tissue Sarcoma Xenograft Models for Biological Studies and Preclinical Drug Testing." *Molecular Cancer Therapeutics* 18 (6): 1168–78. https://doi.org/10.1158/1535-7163.MCT-18-1045/87751/AM/ESTABLISHMENT-AND-CHARACTERIZATION-OF.

Cree, Ian A, Sharon Glaysher, and Alan L Harvey. 2010. "Efficacy of Anti-Cancer Agents in Cell Lines versus Human Primary Tumour Tissue." *Current Opinion in Pharmacology* 10 (4): 375–79. https://doi.org/10.1016/J.COPH.2010.05.001.

Croce, Sabrina, Agnes Ribeiro, Celine Brulard, Jean Christophe Noel, Frederic Amant, Eberhard Stoeckle, Mojgan Devouassoux-Shisheborah, et al. 2015. "Uterine Smooth Muscle Tumor Analysis by Comparative Genomic Hybridization: A Useful Diagnostic Tool in Challenging Lesions." *Modern Pathology 2015 28:7* 28 (7): 1001–10. https://doi.org/10.1038/modpathol.2015.3.

Cruz, C., M. Castroviejo-Bermejo, S. Gutiérrez-Enríquez, A. Llop-Guevara, Y. H. Ibrahim, A. Gris-Oliver, S. Bonache, et al. 2018. "RAD51 Foci as a Functional Biomarker of Homologous Recombination Repair and PARP Inhibitor Resistance in Germline BRCA-Mutated Breast Cancer." *Annals of Oncology* 29 (5): 1203. https://doi.org/10.1093/ANNONC/MDY099.

Cuppens, Tine, Daniela Annibali, An Coosemans, Jone Trovik, Natalja Te rHaar, Eva Colas, Angel Garcia-Jimenez, et al. 2017. "Potential Targets' Analysis Reveals Dual PI3K/MTOR Pathway Inhibition as a Promising Therapeutic Strategy for Uterine Leiomyosarcomas - An ENITEC Group Initiative." *Clinical Cancer Research* 23 (5): 1274–85. https://doi.org/10.1158/1078-0432.CCR-16-2149/8681/P/POTENTIAL-TARGETS-ANALYSIS-REVEALS-DUAL-PI3K-MTOR.

Cuppens, Tine, Jeroen Depreeuw, Daniela Annibali, Debby Thomas, Els Hermans, Ellen Gommé, Xuan Bich Trinh, et al. 2017. "Establishment and Characterization of Uterine Sarcoma and Carcinosarcoma Patient-Derived Xenograft Models." *Gynecologic Oncology* 146 (3): 538–45. https://doi.org/10.1016/J.YGYNO.2017.06.005.

Cuppens, Tine, Matthieu Moisse, Jeroen Depreeuw, Daniela Annibali, Eva Colas, Antonio Gil-Moreno, Jutta Huvila, et al. 2018. "Integrated Genome Analysis of Uterine Leiomyosarcoma to Identify Novel Driver Genes and Targetable Pathways." *International Journal of Cancer* 142 (6). https://doi.org/10.1002/ijc.31129.

D'Agostino, Stefania, Lucia Tombolan, Mattia Saggioro, Chiara Frasson, Elena Rampazzo, Stefania Pellegrini, Francesca Favaretto, et al. 2021. "Rhabdomyosarcoma Cells Produce Their Own Extracellular Matrix With Minimal Involvement of Cancer-Associated Fibroblasts: A Preliminary Study." *Frontiers in Oncology* 10 (January): 3202. https://doi.org/10.3389/FONC.2020.600980/BIBTEX.

D'Ambrosio, Lorenzo, Nathan Touati, Jean Yves Blay, Giovanni Grignani, Ronan Flippot, Anna M. Czarnecka, Sophie Piperno-Neumann, et al. 2020. "Doxorubicin plus Dacarbazine, Doxorubicin plus Ifosfamide, or Doxorubicin Alone as a First-Line Treatment for Advanced Leiomyosarcoma: A Propensity Score Matching Analysis from the European Organization for Research and Treatment of Cancer Soft Tissue and Bone Sarcoma Group." *Cancer* 126 (11): 2637–47. https://doi.org/10.1002/CNCR.32795.

D'Angelo, Emanuela, and Jaime Prat. 2010. "Uterine Sarcomas: A Review." *Gynecologic Oncology* 116 (1): 131–39. https://doi.org/10.1016/J.YGYNO.2009.09.023.

D'Ardenne, A. J., P. Kirkpatrick, and B. C. Sykes. 1984. "Distribution of Laminin, Fibronectin, and Interstitial Collagen Type III in Soft Tissue Tumours." *Journal of Clinical Pathology* 37 (8): 895–904. https://doi.org/10.1136/JCP.37.8.895.

D'Incalci, Maurizio, and Carlos M. Galmarini. 2010. "A Review of Trabectedin (ET-743): A Unique Mechanism of Action." *Molecular Cancer Therapeutics* 9 (8): 2157–63. https://doi.org/10.1158/1535-7163.MCT-10-0263/355076/P/A-REVIEW-OF-TRABECTEDIN-ET-743-A-UNIQUE-MECHANISM.

Dancsok, Amanda R., Dongxia Gao, Anna F. Lee, Sonja Eriksson Steigen, Jean-Yves Blay, David M. Thomas, Robert G. Maki, Torsten O. Nielsen, and Elizabeth G. Demicco. 2020. "Tumor-Associated Macrophages and Macrophage-Related Immune Checkpoint Expression in Sarcomas." *OncoImmunology* 9 (1): 1747340. https://doi.org/10.1080/2162402X.2020.1747340.

Dancsok, Amanda R., Nokitaka Setsu, Dongxia Gao, Jean Yves Blay, David Thomas, Robert G. Maki, Torsten O. Nielsen, and Elizabeth G. Demicco. 2019. "Expression of Lymphocyte Immunoregulatory Biomarkers in Bone and Soft-Tissue Sarcomas." *Modern Pathology* 32 (12): 1772–85. https://doi.org/10.1038/s41379-019-0312-y.

Das, Basudeb, Neha Jain, and Bibekanand Mallick. 2021. "PiR-39980 Mediates Doxorubicin Resistance in Fibrosarcoma by Regulating Drug Accumulation and DNA Repair." *Communications Biology 2021 4:1* 4 (1): 1–18. https://doi.org/10.1038/s42003-021-02844-1.

Davis, Anthony J., Benjamin P.C. Chen, and David J. Chen. 2014. "DNA-PK: A Dynamic Enzyme in a Versatile DSB Repair Pathway." *DNA Repair* 17 (May): 21–29. https://doi.org/10.1016/J.DNAREP.2014.02.020.

De, Pradip, Yuling Sun, Jennifer H. Carlson, Lori S. Friedman, Brian R. Leyland-Jones, and Nandini Dey. 2014. "Doubling Down on the PI3K-AKT-MTOR Pathway Enhances the Antitumor Efficacy of PARP Inhibitor in Triple Negative Breast Cancer Model beyond BRCA-Ness." *Neoplasia* 16 (1): 43-W19. https://doi.org/10.1593/NEO.131694.

Dei Tos, Angelo P., Roberta Maestro, Claudio Doglioni, Sara Piccinin, Duilio Della Libera, Mauro Boiocchi, and Christopher D.M. Fletcher. 1996. "Tumor Suppressor Genes and Related Molecules in Leiomyosarcoma." *The American Journal of Pathology* 148 (4): 1037. /pmc/articles/PMC1861534/?report=abstract.

Demetri, George D., Sant P. Chawla, Isabelle Ray-Coquard, Axel Le Cesne, Arthur P. Staddon, Mohammed M. Milhem, Nicolas Penel, et al. 2013. "Results of an International Randomized Phase III Trial of the Mammalian Target of Rapamycin Inhibitor Ridaforolimus Versus Placebo to Control Metastatic Sarcomas in Patients after Benefit from Prior Chemotherapy." *Journal of Clinical Oncology* 31 (19): 2485–92. https://doi.org/10.1200/JCO.2012.45.5766.

Demetri, George D., Margaret Von Mehren, Robin L. Jones, Martee L. Hensley, Scott M. Schuetze, Arthur Staddon, Mohammed Milhem, et al. 2016. "Efficacy and Safety of Trabectedin or Dacarbazine for Metastatic Liposarcoma or Leiomyosarcoma After Failure of Conventional Chemotherapy: Results of a Phase III Randomized Multicenter Clinical Trial." *Journal of Clinical Oncology* 34 (8): 786. https://doi.org/10.1200/JCO.2015.62.4734.

Demicco, Elizabeth G., Genevieve M. Boland, Kari J.Brewer Savannah, Kristelle Lusby, Eric D. Young, Davis Ingram, Kelsey L. Watson, et al. 2015. "Progressive Loss of Myogenic Differentiation in Leiomyosarcoma Has Prognostic Value." *Histopathology* 66 (5): 627–38. https://doi.org/10.1111/HIS.12466.

Demichev, Vadim, Christoph B. Messner, Spyros I. Vernardis, Kathryn S. Lilley, and Markus Ralser. 2020. "DIA-NN: Neural Networks and Interference Correction Enable Deep Proteome Coverage in High Throughput." *Nature Methods* 17 (1): 41–44.

https://doi.org/10.1038/S41592-019-0638-X.

Dias, Mariana Paes, Sarah C. Moser, Shridar Ganesan, and Jos Jonkers. 2021. "Understanding and Overcoming Resistance to PARP Inhibitors in Cancer Therapy." *Nature Reviews Clinical Oncology*. https://doi.org/10.1038/s41571-021-00532-x.

Dijkstra, Krijn K., Chiara M. Cattaneo, Fleur Weeber, Myriam Chalabi, Joris van de Haar, Lorenzo F. Fanchi, Maarten Slagter, et al. 2018. "Generation of Tumor-Reactive T Cells by Co-Culture of Peripheral Blood Lymphocytes and Tumor Organoids." *Cell* 174 (6): 1586-1598.e12. https://doi.org/10.1016/j.cell.2018.07.009.

Dileo, Palma, Jeffrey A. Morgan, David Zahrieh, Jayesh Desai, Jeanine M. Salesi, David C. Harmon, M. Travis Quigley, Kathleen Polson, George D. Demetri, and Suzanne George. 2007. "Gemcitabine and Vinorelbine Combination Chemotherapy for Patients with Advanced Soft Tissue Sarcomas." *Cancer* 109 (9): 1863–69. https://doi.org/10.1002/CNCR.22609.

Dilley, Robert L., and Roger A. Greenberg. 2015. "ALTernative Telomere Maintenance and Cancer." *Trends in Cancer* 1 (2): 145. https://doi.org/10.1016/J.TRECAN.2015.07.007.

Dodd, Rebecca D., Leonor Añó, Jordan M. Blum, Zhizhong Li, David Van Mater, and David G. Kirsch. 2015. "Methods to Generate Genetically Engineered Mouse Models of Soft Tissue Sarcoma." *Methods in Molecular Biology* 1267 (January): 283–95. https://doi.org/10.1007/978-1-4939-2297-0_13.

Doi, Toshihiko, Kenji Tamura, Yuko Tanabe, Kan Yonemori, Takayuki Yoshino, Nozomu Fuse, Makoto Kodaira, et al. 2015. "Phase 1 Pharmacokinetic Study of the Oral Pan-AKT Inhibitor MK-2206 in Japanese Patients with Advanced Solid Tumors." *Cancer Chemotherapy and Pharmacology* 76 (2): 409. https://doi.org/10.1007/S00280-015-2810-Z.

Domenici, Giacomo, Rodrigo Eduardo, Helena Castillo-Ecija, Gorka Orive, Ángel Montero Carcaboso, and Catarina Brito. 2021. "PDX-Derived Ewing's Sarcoma Cells Retain High Viability and Disease Phenotype in Alginate Encapsulated Spheroid Cultures." *Cancers* 13 (4): 1–18. https://doi.org/10.3390/CANCERS13040879.

Dreyling, Martin, Armando Santoro, Luigina Mollica, Sirpa Leppä, George Follows, Georg Lenz, Won Seog Kim, et al. 2020. "Long-Term Safety and Efficacy of the PI3K Inhibitor Copanlisib in Patients with Relapsed or Refractory Indolent Lymphoma: 2-Year Follow-up of the CHRONOS-1 Study." *American Journal of Hematology* 95 (4): 362–71. https://doi.org/10.1002/AJH.25711.

Driehuis, Else, Kai Kretzschmar, and Hans Clevers. 2020. "Establishment of Patient-Derived Cancer Organoids for Drug-Screening Applications." *Nature Protocols 2020 15:10* 15 (10): 3380–3409. https://doi.org/10.1038/s41596-020-0379-4.

Drost, Jarno, and Hans Clevers. 2018. "Organoids in Cancer Research." *Nature Reviews Cancer*. Nature Publishing Group. https://doi.org/10.1038/s41568-018-0007-6.

Du, Zhenfang, and Christine M. Lovly. 2018. "Mechanisms of Receptor Tyrosine Kinase Activation in Cancer." *Molecular Cancer* 17 (1): 58. https://doi.org/10.1186/s12943-018-0782-4.

Duval, Kayla, Hannah Grover, Li Hsin Han, Yongchao Mou, Adrian F. Pegoraro, Jeffery Fredberg, and Zi Chen. 2017. "Modeling Physiological Events in 2D vs. 3D Cell Culture." *Physiology* 32 (4): 266–77. https://doi.org/10.1152/PHYSIOL.00036.2016/ASSET/IMAGES/LARGE/PHY0041703840003.JPEG.

Ebbing, Eva A., Amber P. Van Der Zalm, Anne Steins, Aafke Creemers, Simone Hermsen, Rosa

Rentenaar, Michelle Klein, et al. 2019. "Stromal-Derived Interleukin 6 Drives Epithelial-to-Mesenchymal Transition and Therapy Resistance in Esophageal Adenocarcinoma." *Proceedings of the National Academy of Sciences of the United States of America* 116 (6). https://doi.org/10.1073/pnas.1820459116.

Edris, Badreddin, Jonathan A. Fletcher, Robert B. West, Matt Van De Rijn, and Andrew H. Beck. 2012. "Comparative Gene Expression Profiling of Benign and Malignant Lesions Reveals Candidate Therapeutic Compounds for Leiomyosarcoma." *Sarcoma* 2012. https://doi.org/10.1155/2012/805614.

Emmerich, Denise, Tomasz Zemojtel, Jochen Hecht, Peter Krawitz, Malte Spielmann, Jirko Kühnisch, Karolina Kobus, et al. 2015. "Somatic Neurofibromatosis Type 1 (NF1) Inactivation Events in Cutaneous Neurofibromas of a Single NF1 Patient." *European Journal of Human Genetics* 23 (6): 870. https://doi.org/10.1038/EJHG.2014.210.

Engert, Florian, Cornelius Schneider, Lilly Magdalena Weib, Marie Probst, and Simone Fulda. 2015. "PARP Inhibitors Sensitize Ewing Sarcoma Cells to Temozolomide-Induced Apoptosis via the Mitochondrial Pathway." *Molecular Cancer Therapeutics* 14 (12): 2818–30. https://doi.org/10.1158/1535-7163.MCT-15-0587/87066/AM/PARP-INHIBITORS-SENSITIZE-EWING-SARCOMA-CELLS-TO.

Farid, Mohamad, Elizabeth G. Demicco, Roberto Garcia, Linda Ahn, Pamela R. Merola, Angela Cioffi, and Robert G. Maki. 2014. "Malignant Peripheral Nerve Sheath Tumors." *The Oncologist* 19 (2): 193. https://doi.org/10.1634/THEONCOLOGIST.2013-0328.

Farid, Mohamad, and Joanne Ngeow. 2016. "Sarcomas Associated With Genetic Cancer Predisposition Syndromes: A Review." *The Oncologist* 21 (8): 1002. https://doi.org/10.1634/THEONCOLOGIST.2016-0079.

Farmer, Hannah, Huala McCabe, Christopher J. Lord, Andrew H.J. Tutt, Damian A. Johnson, Tobias B. Richardson, Manuela Santarosa, et al. 2005. "Targeting the DNA Repair Defect in BRCA Mutant Cells as a Therapeutic Strategy." *Nature* 434 (7035): 917–21. https://doi.org/10.1038/NATURE03445.

Fedier, André, Nadia Maggi, Alessandra Tozzi, Muriel Disler, Ricardo Coelho, Francis Jacob, and Viola Heinzelmann-Schwarz. 2022. "Exposure to Escalating Olaparib Does Not Induce Acquired Resistance to PARPi and to Other Chemotherapeutic Compounds in Ovarian Cancer Cell Lines." *International Journal of Oncology* 61 (1): 1–14. https://doi.org/10.3892/IJO.2022.5379/HTML.

Fell, Victoria L., and Caroline Schild-Poulter. 2015. "The Ku Heterodimer: Function in DNA Repair and Beyond." *Mutation Research/Reviews in Mutation Research* 763 (January): 15–29. https://doi.org/10.1016/J.MRREV.2014.06.002.

Ferrari, Stefan0, H Regina Bandi, J A N Hofsteenge, Bernd M Bussians, and George Thomas5. 1991. "Mitogen-Activated 70K S6 Kinase. Identification of in Vitro 40 S Ribosomal S6 Phosphorylation Sites." 266 (33): 22770–75. https://doi.org/10.1016/S0021-9258(18)54634-2.

Ferry-Galow, Katherine V., Vivekananda Datta, Hala R. Makhlouf, John Wright, Bradford J. Wood, Elliot Levy, Etta D. Pisano, et al. 2018. "What Can Be Done to Improve Research Biopsy Quality in Oncology Clinical Trials?" *Journal of Oncology Practice* 14 (11): e722–28. https://doi.org/10.1200/JOP.18.00092.

Filipiak-Duliban, Aleksandra, Klaudia Brodaczewska, Arkadiusz Kajdasz, and Claudine Kieda. 2022. "Spheroid Culture Differentially Affects Cancer Cell Sensitivity to Drugs in Melanoma

and RCC Models." *International Journal of Molecular Sciences* 23 (3): 1166. https://doi.org/10.3390/IJMS23031166/S1.

Fisher, Anna E. O., Helfrid Hochegger, Shunichi Takeda, and Keith W. Caldecott. 2007. "Poly(ADP-Ribose) Polymerase 1 Accelerates Single-Strand Break Repair in Concert with Poly(ADP-Ribose) Glycohydrolase." *Molecular and Cellular Biology* 27 (15): 5597–5605. https://doi.org/10.1128/MCB.02248-06/ASSET/03F97ECD-BDFB-4BDE-88DB-38266B28DE1A/ASSETS/GRAPHIC/ZMB0150769040006.JPEG.

Fleming, Ronald A. 1997. "An Overview of Cyclophosphamide and Ifosfamide Pharmacology." *Pharmacotherapy: The Journal of Human Pharmacology and Drug Therapy* 17 (5P2): 146S-154S. https://doi.org/10.1002/J.1875-9114.1997.TB03817.X.

Fleuren, Emmy D.G., Myrella Vlenterie, Winette T.A. Van Der Graaf, Melissa H.S. Hillebrandt-Roeffen, James Blackburn, Xiuquan Ma, Howard Chan, et al. 2017. "Phosphoproteomic Profiling Reveals ALK and MET as Novel Actionable Targets across Synovial Sarcoma Subtypes." *Cancer Research* 77 (16): 4279–92. https://doi.org/10.1158/0008-5472.CAN-16-2550/662527/P/PHOSPHOPROTEOMIC-PROFILING-REVEALS-ALK-AND-MET-AS.

Fogh, J., J. M. Fogh, and T. Orfeo. 1977. "One Hundred and Twenty Seven Cultured Human Tumor Cell Lines Producing Tumors in Nude Mice." *Journal of the National Cancer Institute*. J Natl Cancer Inst. https://doi.org/10.1093/jnci/59.1.221.

Fok, Jacqueline H.L., Antonio Ramos-Montoya, Mercedes Vazquez-Chantada, Paul W.G. Wijnhoven, Valeria Follia, Neil James, Paul M. Farrington, et al. 2019. "AZD7648 Is a Potent and Selective DNA-PK Inhibitor That Enhances Radiation, Chemotherapy and Olaparib Activity." *Nature Communications 2019 10:1* 10 (1): 1–15. https://doi.org/10.1038/s41467-019-12836-9.

Forrester, Steven J., Daniel S. Kikuchi, Marina S. Hernandes, Qian Xu, and Kathy K. Griendling. 2018. "Reactive Oxygen Species in Metabolic and Inflammatory Signaling." *Circulation Research* 122 (6): 877–902. https://doi.org/10.1161/CIRCRESAHA.117.311401/-/DC1.

Fourneaux, Benjamin, Aurélien Bourdon, Bérengère Dadone, Carlo Lucchesi, Scott R. Daigle, Elodie Richard, Audrey Laroche-Clary, François Le Loarer, and Antoine Italiano. 2019. "Identifying and Targeting Cancer Stem Cells in Leiomyosarcoma: Prognostic Impact and Role to Overcome Secondary Resistance to PI3K/MTOR Inhibition." *Journal of Hematology & Oncology* 12 (1): 11. https://doi.org/10.1186/s13045-018-0694-1.

Fourneaux, Benjamin, Vanessa Chaire, Carlo Lucchesi, Marie Karanian, Raphael Pineau, Audrey Laroche-Clary, Antoine Italiano, et al. 2016. "Dual Inhibition of the PI3K/AKT/MTOR Pathway Suppresses the Growth of Leiomyosarcomas but Leads to ERK Activation through MTORC2: Biological and Clinical Implications." *Oncotarget* 8 (5): 7878–90. https://doi.org/10.18632/ONCOTARGET.13987.

———. 2017. "Dual Inhibition of the PI3K/AKT/MTOR Pathway Suppresses the Growth of Leiomyosarcomas but Leads to ERK Activation through MTORC2: Biological and Clinical Implications." *Oncotarget* 8 (5): 7878–90. https://doi.org/10.18632/oncotarget.13987.

Francis, Ashleigh M., Angela Alexander, Yanna Liu, Smruthi Vijayaraghavan, Kwang Hui Low, Dong Yang, Tuyen Bui, et al. 2017. "CDK4/6 Inhibitors Sensitize Rb-Positive Sarcoma Cells to Wee1 Kinase Inhibition through Reversible Cell-Cycle Arrest." *Molecular Cancer Therapeutics* 16 (9): 1751–64. https://doi.org/10.1158/1535-7163.MCT-17-0040.

Frezza, Anna Maria, Silvia Stacchiotti, and Alessandro Gronchi. 2017. "Systemic Treatment in Advanced Soft Tissue Sarcoma: What Is Standard, What Is New." *BMC Medicine*. BioMed

Central Ltd. https://doi.org/10.1186/s12916-017-0872-y.

Fujii, Hiromasa, Kanya Honoki, Toshifumi Tsujiuchi, Akira Kido, Kazuhiro Yoshitani, and Yoshinori Takakura. 2009. "Sphere-Forming Stem-like Cell Populations with Drug Resistance in Human Sarcoma Cell Lines." *International Journal of Oncology* 34 (5): 1381–86. https://doi.org/10.3892/IJO_00000265/HTML.

Fujii, Masayuki, and Toshiro Sato. 2020. "Somatic Cell-Derived Organoids as Prototypes of Human Epithelial Tissues and Diseases." *Nature Materials 2020 20:2* 20 (2): 156–69. https://doi.org/10.1038/s41563-020-0754-0.

Gaebler, Manuela, Alessandra Silvestri, Peter Reichardt, Eva Wardelmann, Guido Gambara, Johannes Haybaeck, Philipp Stroebel, Maya Niethard, Gerrit Erdmann, and Christian R. Regenbrecht. 2019. "Patient-Derived Sarcoma Models: First Results from the SARQMA Study." *Cancer Research* 79 (13_Supplement): 469–469. https://doi.org/10.1158/1538-7445.AM2019-469.

Galili, Naomi, Richard J. Davis, William J. Fredericks, Sunil Mukhopadhyay, Frank J. Rauscher, Beverly S. Emanuel, Giovanni Rovera, and Frederic G. Barr. 1993. "Fusion of a Fork Head Domain Gene to PAX3 in the Solid Tumour Alveolar Rhabdomyosarcoma." *Nature Genetics* 5 (3): 230–35. https://doi.org/10.1038/NG1193-230.

Gallego, Borja, Dzohara Murillo, Verónica Rey, Carmen Huergo, Óscar Estupiñán, Aida Rodríguez, Juan Tornín, and René Rodríguez. 2022. "Addressing Doxorubicin Resistance in Bone Sarcomas Using Novel Drug-Resistant Models." *International Journal of Molecular Sciences* 23 (12). https://doi.org/10.3390/IJMS23126425.

Gamboa, Adriana C., Alessandro Gronchi, and Kenneth Cardona. 2020. "Soft-tissue Sarcoma in Adults: An Update on the Current State of Histiotype-specific Management in an Era of Personalized Medicine." *CA: A Cancer Journal for Clinicians* 70 (3): 200–229. https://doi.org/10.3322/caac.21605.

Ganiatsas, Soula, Renee Dow, Anne Thompson, Brenda Schulman, and Doris Germain. 2001. "A Splice Variant of Skp2 Is Retained in the Cytoplasm and Fails to Direct Cyclin D1 Ubiquitination in the Uterine Cancer Cell Line SK-UT." *Oncogene* 20 (28): 3641–50. https://doi.org/10.1038/SJ.ONC.1204501.

Garcia-Carbonero, R., J. G. Supko, J. Manola, M. V. Seiden, D. Hannon, D. P. Ryan, M. T. Quigley, et al. 2004. "Phase II and Pharmacokinetic Study of Ecteinascidin 743 in Patients with Progressive Sarcomas of Soft Tissues Refractory to Chemotherapy." *Journal of Clinical Oncology* 22 (8): 1480–90. https://doi.org/10.1200/JCO.2004.02.098.

Garcia-Ortega, Dorian Yarih, Sara Aileen Cabrera-Nieto, Haydee Sarai Caro-Sánchez, and Marlid Cruz-Ramos. 2022. "An Overview of Resistance to Chemotherapy in Osteosarcoma and Future Perspectives." *Cancer Drug Resistance* 5 (3): 762–93. https://doi.org/10.20517/CDR.2022.18.

Gartler, Stanley M. 1968. "Apparent HeLa Cell Contamination of Human Heteroploid Cell Lines." *Nature 1968 217:5130* 217 (5130): 750–51. https://doi.org/10.1038/217750a0.

Gaumann, Andreas K.A., Hannes C.A. Drexler, Sven A. Lang, Oliver Stoeltzing, Simone Diermeier-Daucher, Elisabeth Buchdunger, Jeanette Wood, Guido Bold, and Georg Breier. 2014. "The Inhibition of Tyrosine Kinase Receptor Signalling in Leiomyosarcoma Cells Using the Small Molecule Kinase Inhibitor PTK787/ZK222584 (Vatalanib®)." *International Journal of Oncology* 45 (6): 2267–77. https://doi.org/10.3892/IJO.2014.2683/HTML.

Gavert, Nancy, Yaara Zwang, Roi Weiser, Orli Greenberg, Sharon Halperin, Oded Jacobi, Giuseppe Mallel, et al. 2022. "Ex Vivo Organotypic Cultures for Synergistic Therapy Prioritization Identify Patient-Specific Responses to Combined MEK and Src Inhibition in Colorectal Cancer." *Nature Cancer 2021 3:2* 3 (2): 219–31. https://doi.org/10.1038/s43018-021-00325-2.

Geenen, Jill J.J., Sabine C. Linn, Jos H. Beijnen, and Jan H.M. Schellens. 2018. "PARP Inhibitors in the Treatment of Triple-Negative Breast Cancer." *Clinical Pharmacokinetics* 57 (4): 427–37. https://doi.org/10.1007/S40262-017-0587-4.

Gennaro, Nicolò, Sophie Reijers, Annemarie Bruining, Christina Messiou, Rick Haas, Piergiuseppe Colombo, Zuhir Bodalal, Regina Beets-Tan, Winan van Houdt, and Winette T.A. van der Graaf. 2021. "Imaging Response Evaluation after Neoadjuvant Treatment in Soft Tissue Sarcomas: Where Do We Stand?" *Critical Reviews in Oncology/Hematology* 160 (April): 103309. https://doi.org/10.1016/J.CRITREVONC.2021.103309.

George, Suzanne, Constance Barysauskas, César Serrano, Titilope Oduyebo, Jose A. Rauh-Hain, Marcela G. Del Carmen, George D. Demetri, and Michael G. Muto. 2014. "Retrospective Cohort Study Evaluating the Impact of Intraperitoneal Morcellation on Outcomes of Localized Uterine Leiomyosarcoma." *Cancer* 120 (20): 3154–58. https://doi.org/10.1002/CNCR.28844.

Giacinti, C., and A. Giordano. 2006. "RB and Cell Cycle Progression." *Oncogene 2006 25:38* 25 (38): 5220–27. https://doi.org/10.1038/sj.onc.1209615.

Giard, Donald J., Stuart A. Aaronson, George J. Todaro, Paul Arnstein, John H. Kersey, Harvey Dosik, and Wade P. Parks. 1973. "In Vitro Cultivation of Human Tumors: Establishment of Cell Lines Derived From a Series of Solid Tumors." *JNCI: Journal of the National Cancer Institute* 51 (5): 1417–23. https://doi.org/10.1093/JNCI/51.5.1417.

Gingrich, Alicia A., Sarah B. Bateni, Arta M. Monjazeb, Morgan A. Darrow, Steven W. Thorpe, Amanda R. Kirane, Richard J. Bold, and Robert J. Canter. 2017. "Neoadjuvant Radiotherapy Is Associated with R0 Resection and Improved Survival for Patients with Extremity Soft Tissue Sarcoma Undergoing Surgery: A National Cancer Database Analysis." *Annals of Surgical Oncology 2017 24:11* 24 (11): 3252–63. https://doi.org/10.1245/S10434-017-6019-8.

Gladdy, Rebecca A., Li Xuan Qin, Nicole Moraco, Narasimhan P. Agaram, Murray F. Brennan, and Samuel Singer. 2013. "Predictors of Survival and Recurrence in Primary Leiomyosarcoma." *Annals of Surgical Oncology* 20 (6): 1851–57. https://doi.org/10.1245/S10434-013-2876-Y.

Gobbo, Marina Guimarães, Gláucia Maria de Mendonça Fernandes, Rafael Fernandes-Ferreira, Lennon Pereira Caires, Heloisa Cristina Caldas, Débora Aparecida Pires de Campos Zuccari, Newton Antonio Bordin-Junior, Giovana Aparecida Gonçalves Vidotti, and Doroteia Rossi Silva Souza. 2022. "Evaluation of Doxorubicin in Three-Dimensional Culture of Breast Cancer Cells and the Response in PI3K/AKT/PTEN Signaling Pathways: A Pilot Study." *Https://Doi.Org/10.1080/03630242.2022.2085842* 62 (6): 467–75. https://doi.org/10.1080/03630242.2022.2085842.

Godon, Camille, Fabrice P. Cordelières, Denis Biard, Nicole Giocanti, Frédérique Mégnin-Chanet, Janet Hall, and Vincent Favaudon. 2008. "PARP Inhibition versus PARP-1 Silencing: Different Outcomes in Terms of Single-Strand Break Repair and Radiation Susceptibility." *Nucleic Acids Research* 36 (13): 4454–64. https://doi.org/10.1093/NAR/GKN403.

Golan, Talia, Pascal Hammel, Michele Reni, Eric Van Cutsem, Teresa Macarulla, Michael J. Hall, Joon-Oh Park, et al. 2019. " Maintenance Olaparib for Germline BRCA -Mutated Metastatic

Pancreatic Cancer ." *New England Journal of Medicine* 381 (4): 317–27. https://doi.org/10.1056/NEJMOA1903387/SUPPL_FILE/NEJMOA1903387_DATA-SHARING.PDF.

Gong, Xue, Chao Lin, Jian Cheng, Jiansheng Su, Hang Zhao, Tianlin Liu, Xuejun Wen, and Peng Zhao. 2015. "Generation of Multicellular Tumor Spheroids with Microwell-Based Agarose Scaffolds for Drug Testing." *PloS One* 10 (6). https://doi.org/10.1371/JOURNAL.PONE.0130348.

González-Martín, Antonio, Bhavana Pothuri, Ignace Vergote, René DePont Christensen, Whitney Graybill, Mansoor R. Mirza, Colleen McCormick, et al. 2019. "Niraparib in Patients with Newly Diagnosed Advanced Ovarian Cancer." *New England Journal of Medicine* 381 (25): 2391–2402. https://doi.org/10.1056/NEJMOA1910962/SUPPL_FILE/NEJMOA1910962_DATA-SHARING.PDF.

Gopinathan, Aarthi, Jennifer P. Morton, Duncan I. Jodrell, and Owen J. Sansom. 2015. "GEMMs as Preclinical Models for Testing Pancreatic Cancer Therapies." *Disease Models & Mechanisms* 8 (10): 1185–1200. https://doi.org/10.1242/DMM.021055.

Gottfried, Oren N., David H. Viskochil, and William T. Couldwell. 2010. "Neurofibromatosis Type 1 and Tumorigenesis: Molecular Mechanisms and Therapeutic Implications." *Neurosurgical Focus* 28 (1): E8. https://doi.org/10.3171/2009.11.FOCUS09221.

Gottipati, Ponnari, Barbara Vischioni, Niklas Schultz, Joyce Solomons, Helen E. Bryant, Tatjana Djureinovic, Natalia Issaeva, Kate Sleeth, Ricky A. Sharma, and Thomas Helleday. 2010. "Poly(ADP-Ribose) Polymerase Is Hyperactivated in Homologous Recombination-Defective Cells." *Cancer Research* 70 (13): 5389–98. https://doi.org/10.1158/0008-5472.CAN-09-4716/656165/P/POLY-ADP-RIBOSE-POLYMERASE-IS-HYPERACTIVATED-IN.

Gounder, Mrinal M., Narasimhan P. Agaram, Sally E. Trabucco, Victoria Robinson, Richard A. Ferraro, Sherri Z. Millis, Anita Krishnan, et al. 2022. "Clinical Genomic Profiling in the Management of Patients with Soft Tissue and Bone Sarcoma." *Nature Communications 2022 13:1* 13 (1): 1–15. https://doi.org/10.1038/s41467-022-30496-0.

Graaf, Winette TA van der, Jean-Yves Blay, Sant P Chawla, Dong-Wan Kim, Binh Bui-Nguyen, Paolo G Casali, Patrick Schöffski, et al. 2012. "Pazopanib for Metastatic Soft-Tissue Sarcoma (PALETTE): A Randomised, Double-Blind, Placebo-Controlled Phase 3 Trial." *The Lancet* 379 (9829): 1879–86. https://doi.org/10.1016/S0140-6736(12)60651-5.

Graaff, Marieke A. De, Marije A.J. De Rooij, Brendy E.W.M. Van Den Akker, Hans Gelderblom, Frederic Chibon, Jean Michel Coindre, Adrian Marino-Enriquez, Jonathan A. Fletcher, Anne Marie Cleton-Jansen, and Judith V.M.G. Bovée. 2016. "Inhibition of Bcl-2 Family Members Sensitises Soft Tissue Leiomyosarcomas to Chemotherapy." *British Journal of Cancer 2016 114:11* 114 (11): 1219–26. https://doi.org/10.1038/bjc.2016.117.

Grantab, Rama, Shankar Sivananthan, and Ian F. Tannock. 2006. "The Penetration of Anticancer Drugs through Tumor Tissue as a Function of Cellular Adhesion and Packing Density of Tumor Cells." *Cancer Research* 66 (2): 1033–39. https://doi.org/10.1158/0008-5472.CAN-05-3077.

Grignani, Giovanni, Lorenzo D'Ambrosio, Ymera Pignochino, Emanuela Palmerini, Massimo Zucchetti, Paola Boccone, Sandra Aliberti, et al. 2018. "Trabectedin and Olaparib in Patients with Advanced and Non-Resectable Bone and Soft-Tissue Sarcomas (TOMAS): An Open-Label, Phase 1b Study from the Italian Sarcoma Group." *The Lancet Oncology* 19 (10): 1360–71. https://doi.org/10.1016/S1470-2045(18)30438-8.

Gril, Brunilde, Diane Palmieri, Yong Qian, Talha Anwar, Lilia Ileva, Marcelino Bernardo, Peter Choyke, David J. Liewehr, Seth M. Steinberg, and Patricia S. Steeg. 2011. "The B-Raf Status of Tumor Cells May Be a Significant Determinant of Both Antitumor and Anti-Angiogenic Effects of Pazopanib in Xenograft Tumor Models." *PLOS ONE* 6 (10): e25625. https://doi.org/10.1371/JOURNAL.PONE.0025625.

Gril, Brunilde, Diane Palmieri, Yong Qian, Dee Dee Smart, Lilia Ileva, David J. Liewehr, Seth M. Steinberg, and Patricia S. Steeg. 2011. "Pazopanib Reveals a Role for Tumor Cell B-Raf in the Prevention of HER2+ Breast Cancer Brain Metastasis." *Clinical Cancer Research* 17 (1): 142–53. https://doi.org/10.1158/1078-0432.CCR-10-1603/83513/AM/PAZOPANIB-REVEALS-A-ROLE-FOR-TUMOR-CELL-B-RAF-IN.

Gril, Brunilde, Diane Palmieri, Yongzhen Qian, Talha Anwar, David J. Liewehr, Seth M. Steinberg, Zoraida Andreu, et al. 2013. "Pazopanib Inhibits the Activation of PDGFRβ-Expressing Astrocytes in the Brain Metastatic Microenvironment of Breast Cancer Cells." *American Journal of Pathology* 182 (6): 2368–79. https://doi.org/10.1016/j.ajpath.2013.02.043.

Gronchi, A., A. B. Miah, A. P. Dei Tos, N. Abecassis, J. Bajpai, S. Bauer, R. Biagini, et al. 2021. "Soft Tissue and Visceral Sarcomas: ESMO–EURACAN–GENTURIS Clinical Practice Guidelines for Diagnosis, Treatment and Follow-Up☆." *Annals of Oncology* 32 (11): 1348–65. https://doi.org/10.1016/J.ANNONC.2021.07.006.

Gronchi, Alessandro, Emanuela Palmerini, Vittorio Quagliuolo, Javier Martin Broto, Antonio Lopez Pousa, Giovanni Grignani, Antonella Brunello, et al. 2020. "Neoadjuvant Chemotherapy in High-Risk Soft Tissue Sarcomas: Final Results of a Randomized Trial From Italian (ISG), Spanish (GEIS), French (FSG), and Polish (PSG) Sarcoma Groups." *Journal of Clinical Oncology* 38 (19): 2178–86. https://doi.org/10.1200/JCO.19.03289.

Gruber, Joshua J., Anosheh Afghahi, Kirsten Timms, Alyssa DeWees, Wyatt Gross, Vasily N. Aushev, Hsin Ta Wu, et al. 2022. "A Phase II Study of Talazoparib Monotherapy in Patients with Wild-Type BRCA1 and BRCA2 with a Mutation in Other Homologous Recombination Genes." *Nature Cancer 2022 3:10* 3 (10): 1181–91. https://doi.org/10.1038/s43018-022-00439-1.

Grünewald, Thomas GP, Marta Alonso, Sofia Avnet, Ana Banito, Stefan Burdach, Florencia Cidre-Aranaz, Gemma Di Pompo, et al. 2020. "Sarcoma Treatment in the Era of Molecular Medicine." *EMBO Molecular Medicine* 12 (11): e11131. https://doi.org/10.15252/EMMM.201911131.

Guillemette, Shawna, Ryan W. Serra, Min Peng, Janelle A. Hayes, Panagiotis A. Konstantinopoulos, Michael R. Green, Michael R. Green, and Sharon B. Cantor. 2015. "Resistance to Therapy in BRCA2 Mutant Cells Due to Loss of the Nucleosome Remodeling Factor CHD4." *Genes & Development* 29 (5): 489–94. https://doi.org/10.1101/GAD.256214.114.

Guillen, Katrin P., Maihi Fujita, Andrew J. Butterfield, Sandra D. Scherer, Matthew H. Bailey, Zhengtao Chu, Yoko S. DeRose, et al. 2022. "A Human Breast Cancer-Derived Xenograft and Organoid Platform for Drug Discovery and Precision Oncology." *Nature Cancer 2022 3:2* 3 (2): 232–50. https://doi.org/10.1038/s43018-022-00337-6.

Guillou, L., J. M. Coindre, F. Bonichon, B. B. Nguyen, P. Terrier, F. Collin, M. O. Vilain, et al. 2016. "Comparative Study of the National Cancer Institute and French Federation of Cancer Centers Sarcoma Group Grading Systems in a Population of 410 Adult Patients with Soft Tissue Sarcoma." *Https://Doi.Org/10.1200/JCO.1997.15.1.350* 15 (1): 350–62. https://doi.org/10.1200/JCO.1997.15.1.350.

Guo, Xiangqian, Vickie Y. Jo, Anne M. Mills, Shirley X. Zhu, Cheng Han Lee, Inigo Espinosa, Marisa R. Nucci, et al. 2015. "Clinically Relevant Molecular Subtypes in Leiomyosarcoma." *Clinical Cancer Research* 21 (15): 3501–11. https://doi.org/10.1158/1078-0432.CCR-14-3141/86546/AM/CLINICALLY-RELEVANT-MOLECULAR-SUBTYPES-IN.

Gupta, Abhishekh, Prson Gautam, Krister Wennerberg, and Tero Aittokallio. 2020. "A Normalized Drug Response Metric Improves Accuracy and Consistency of Anticancer Drug Sensitivity Quantification in Cell-Based Screening." *Communications Biology 2020 3:1* 3 (1): 1–12. https://doi.org/10.1038/s42003-020-0765-z.

Gutierrez, Alejandro, Eric L. Snyder, Adrian Marino-Enriquez, Yi Xiang Zhang, Stefano Sioletic, Elena Kozakewich, Ruta Grebliunaite, et al. 2011. "Aberrant AKT Activation Drives Well-Differentiated Liposarcoma." *Proceedings of the National Academy of Sciences of the United States of America* 108 (39). https://doi.org/10.1073/pnas.1106127108.

Gutierrez, Wade R., Amanda Scherer, Gavin R. McGivney, Qierra R. Brockman, Vickie Knepper-Adrian, Emily A. Laverty, Grace A. Roughton, and Rebecca D. Dodd. 2021. "Divergent Immune Landscapes of Primary and Syngeneic Kras-Driven Mouse Tumor Models." *Scientific Reports 2021 11:1* 11 (1): 1–14. https://doi.org/10.1038/s41598-020-80216-1.

Gutmann, David H., Rosalie E. Ferner, Robert H. Listernick, Bruce R. Korf, Pamela L. Wolters, and Kimberly J. Johnson. 2017. "Neurofibromatosis Type 1." *Nature Reviews Disease Primers* 3 (February). https://doi.org/10.1038/nrdp.2017.4.

Hafner, Marc, Mario Niepel, Mirra Chung, and Peter K. Sorger. 2016. "Growth Rate Inhibition Metrics Correct for Confounders in Measuring Sensitivity to Cancer Drugs." *Nature Methods* 13 (6): 521–27. https://doi.org/10.1038/nmeth.3853.

Hajdu, Steven I. 1981. "Soft Tissue Sarcomas: Classification and Natural History." *CA: A Cancer Journal for Clinicians* 31 (5): 271–80. https://doi.org/10.3322/CANJCLIN.31.5.271.

Hajdu, Steven I, Harry Kozakewich, Lawrence Helson, and Edward J Beattie. 1981. "Growth Pattern and Differentiation of Human Soft Tissue Sarcomas in Nude Mice." *Cancer*, January. https://doi.org/10.1002/1097-0142.

Halaoui, Ruba, Carlis Rejon, Sudipa June Chatterjee, Joseph Szymborski, Sarkis Meterissian, William J. Muller, Atilla Omeroglu, and Luke McCaffrey. 2017. "Progressive Polarity Loss and Luminal Collapse Disrupt Tissue Organization in Carcinoma." *Genes and Development* 31 (15): 1573–87. https://doi.org/10.1101/GAD.300566.117/-/DC1.

Harlow, Matt L., Maggie H. Chasse, Elissa A. Boguslawski, Katie M. Sorensen, Jenna M. Gedminas, Susan M. Kitchen-Goosen, Scott B. Rothbart, et al. 2019. "Trabectedin Inhibits EWS-FLI1 and Evicts SWI/SNF from Chromatin in a Schedule-Dependent Manner." *Clinical Cancer Research* 25 (11): 3417–29. https://doi.org/10.1158/1078-0432.CCR-18-3511/74111/AM/TRABECTEDIN-INHIBITS-EWS-FLI1-AND-EVICTS-SWI-SNF.

Hastak, Kedar, Elizabeth Alli, and James M. Ford. 2010. "Synergistic Chemosensitivity of Triple-Negative Breast Cancer Cell Lines to Poly(ADP-Ribose) Polymerase Inhibition, Gemcitabine, and Cisplatin." *Cancer Research* 70 (20): 7970–80. https://doi.org/10.1158/0008-5472.CAN-09-4521/649380/AM/SYNERGISTIC-CHEMOSENSITIVITY-OF-TRIPLE-NEGATIVE.

Hattori, Emi, Rieko Oyama, and Tadashi Kondo. 2019. "Systematic Review of the Current Status of Human Sarcoma Cell Lines." *Cells* 8 (2). https://doi.org/10.3390/CELLS8020157.

Hayasaka, Naotaka, Kohichi Takada, Hajime Nakamura, Yohei Arihara, Yutaka Kawano, Takahiro Osuga, Kazuyuki Murase, et al. 2019. "Combination of Eribulin plus AKT Inhibitor Evokes

Synergistic Cytotoxicity in Soft Tissue Sarcoma Cells." *Scientific Reports 2019 9:1* 9 (1): 1–8. https://doi.org/10.1038/s41598-019-42300-z.

Helleday, Thomas. 2011. "The Underlying Mechanism for the PARP and BRCA Synthetic Lethality: Clearing up the Misunderstandings." *Molecular Oncology* 5 (4): 387–93. https://doi.org/10.1016/J.MOLONC.2011.07.001.

Hemming, Matthew L., Patrick Bhola, Michael A. Loycano, Justin A. Anderson, Madeleine L. Taddei, Leona A. Doyle, Elizaveta Lavrova, et al. 2022. "Preclinical Modeling of Leiomyosarcoma Identifies Susceptibility to Transcriptional CDK Inhibitors through Antagonism of E2F-Driven Oncogenic Gene Expression." *Clinical Cancer Research* 28 (11): 2397–2408. https://doi.org/10.1158/1078-0432.CCR-21-3523/688346/AM/PRECLINICAL-MODELING-OF-LEIOMYOSARCOMA-IDENTIFIES.

Hemming, Matthew L., Changyu Fan, Chandrajit P. Raut, George D. Demetri, Scott A. Armstrong, Ewa Sicinska, and Suzanne George. 2020. "Oncogenic Gene-Expression Programs in Leiomyosarcoma and Characterization of Conventional, Inflammatory, and Uterogenic Subtypes." *Molecular Cancer Research* 18 (9): 1302–14. https://doi.org/10.1158/1541-7786.MCR-20-0197/81785/AM/ONCOGENIC-GENE-EXPRESSION-PROGRAMS-IN.

Hensley, Martee L., John A. Blessing, Koen DeGeest, Ovadia Abulafia, Peter G. Rose, and Howard D. Homesley. 2008. "Fixed-Dose Rate Gemcitabine plus Docetaxel as Second-Line Therapy for Metastatic Uterine Leiomyosarcoma: A Gynecologic Oncology Group Phase II Study." *Gynecologic Oncology* 109 (3): 323–28. https://doi.org/10.1016/j.ygyno.2008.02.024.

Hensley, Martee L., John A. Blessing, Robert Mannel, and Peter G. Rose. 2008. "Fixed-Dose Rate Gemcitabine plus Docetaxel as First-Line Therapy for Metastatic Uterine Leiomyosarcoma: A Gynecologic Oncology Group Phase II Trial." *Gynecologic Oncology* 109 (3): 329–34. https://doi.org/10.1016/j.ygyno.2008.03.010.

Hensley, Martee L., Shweta S. Chavan, David B. Solit, Rajmohan Murali, Robert Soslow, Sarah Chiang, Achim A. Jungbluth, et al. 2020. "Genomic Landscape of Uterine Sarcomas Defined through Prospective Clinical Sequencing." *Clinical Cancer Research* 26 (14): 3881–88. https://doi.org/10.1158/1078-0432.CCR-19-3959/15421/AM/GENOMIC-LANDSCAPE-OF-UTERINE-SARCOMAS-DEFINED.

Hensley, Martee L., Robert Maki, E. Venkatraman, Gennifer Geller, Meghan Lovegren, Carol Aghajanian, Paul Sabbatini, William Tong, Richard Barakat, and David R. Spriggs. 2002. "Gemcitabine and Docetaxel in Patients with Unresectable Leiomyosarcoma: Results of a Phase II Trial." *Journal of Clinical Oncology* 20 (12): 2824–31. https://doi.org/10.1200/JCO.2002.11.050.

Hernando, Eva, Elizabeth Charytonowicz, Maria E. Dudas, Silvia Menendez, Igor Matushansky, Joslyn Mills, Nicholas D. Socci, et al. 2007. "The AKT-MTOR Pathway Plays a Critical Role in the Development of Leiomyosarcomas." *Nature Medicine 2007 13:6* 13 (6): 748–53. https://doi.org/10.1038/nm1560.

Hilaire, Rose Claire, Subramanyam N. Murthya, Philip J. Kadowitza, and James R. Jeter. 2010. "Role of VPAC1 and VPAC2 in VIP Mediated Inhibition of Rat Pulmonary Artery and Aortic Smooth Muscle Cell Proliferation." *Peptides* 31 (8): 1517–22. https://doi.org/10.1016/J.PEPTIDES.2010.04.024.

Hoang, Ngoc T., Luis A. Acevedo, Michael J. Mann, and Bhairavi Tolani. 2018. "A Review of Soft-Tissue Sarcomas: Translation of Biological Advances into Treatment Measures." *Cancer Management and Research*. Dove Medical Press Ltd. https://doi.org/10.2147/CMAR.S159641.

Hodgson, Darren R., Brian A. Dougherty, Zhongwu Lai, Anitra Fielding, Lynda Grinsted, Stuart Spencer, Mark J. O'Connor, et al. 2018. "Candidate Biomarkers of PARP Inhibitor Sensitivity in Ovarian Cancer beyond the BRCA Genes." *British Journal of Cancer 2018 119:11* 119 (11): 1401–9. https://doi.org/10.1038/s41416-018-0274-8.

Hoff, D. D. von, M. W. Layard, P. Basa, H. L. Davis, A. L. Von Hoff, M. Rozencweig, and F. M. Muggia. 1979. "Risk Factors for Doxorubicin-Induced Congestive Heart Failure." *Annals of Internal Medicine* 91 (5): 710–17. https://doi.org/10.7326/0003-4819-91-5-710.

Honkala, Alexander, Sanjay V. Malhotra, Shivaani Kummar, and Melissa R. Junttila. 2021. "Harnessing the Predictive Power of Preclinical Models for Oncology Drug Development." *Nature Reviews Drug Discovery 2021 21:2* 21 (2): 99–114. https://doi.org/10.1038/s41573-021-00301-6.

Honoki, Kanya. 2010. "Do Stem-like Cells Play a Role in Drug Resistance of Sarcomas?" *Expert Review of Anticancer Therapy* 10 (2): 261–70. https://doi.org/10.1586/ERA.09.184.

Honoki, Kanya, Hiromasa Fujii, Atsushi Kubo, Akira Kido, Toshio Mori, Yasuhito Tanaka, and Toshifumi Tsujiuchi. 2010. "Possible Involvement of Stem-like Populations with Elevated ALDH1 in Sarcomas for Chemotherapeutic Drug Resistance." *Oncology Reports* 24 (2): 501–5. https://doi.org/10.3892/OR_00000885.

Hopkins, Todd A., William B. Ainsworth, Paul A. Ellis, Cherrie K. Donawho, Enrico L. DiGiammarino, Sanjay C. Panchal, Vivek C. Abraham, et al. 2019. "PARP1 Trapping by PARP Inhibitors Drives Cytotoxicity in Both Cancer Cells and Healthy Bone Marrow." *Molecular Cancer Research* 17 (2): 409–19. https://doi.org/10.1158/1541-7786.MCR-18-0138/81784/AM/PARP1-TRAPPING-BY-PARP-INHIBITORS-DRIVES.

Horvai, Andrew E., Sandy Devries, Ritu Roy, Richard J. O'Donnell, and Frederic Waldman. 2009. "Similarity in Genetic Alterations between Paired Well-Differentiated and Dedifferentiated Components of Dedifferentiated Liposarcoma." *Modern Pathology 2009 22:11* 22 (11): 1477–88. https://doi.org/10.1038/modpathol.2009.119.

Hosaka, Seiichi, Keisuke Horiuchi, Masaki Yoda, Robert Nakayama, Takahide Tohmonda, Michiro Susa, Masaya Nakamura, Kazuhiro Chiba, Yoshiaki Toyama, and Hideo Morioka. 2012. "A Novel Multi-Kinase Inhibitor Pazopanib Suppresses Growth of Synovial Sarcoma Cells through Inhibition of the PI3K-AKT Pathway." *Journal of Orthopaedic Research* 30 (9): 1493–98. https://doi.org/10.1002/JOR.22091.

Howe, Kerstin, Matthew D. Clark, Carlos F. Torroja, James Torrance, Camille Berthelot, Matthieu Muffato, John E. Collins, et al. 2013. "The Zebrafish Reference Genome Sequence and Its Relationship to the Human Genome." *Nature 2013 496:7446* 496 (7446): 498–503. https://doi.org/10.1038/nature12111.

Hu-Lowe, Dana D., Helen Y. Zou, Maren L. Grazzini, Max E. Hallin, Grant R. Wickman, Karin Amundson, Jeffrey H. Chen, et al. 2008. "Nonclinical Antiangiogenesis and Antitumor Activities of Axitinib (AG-013736), an Oral, Potent, and Selective Inhibitor of Vascular Endothelial Growth Factor Receptor Tyrosine Kinases 1, 2, 3." *Clinical Cancer Research* 14 (22): 7272–83. https://doi.org/10.1158/1078-0432.CCR-08-0652.

Hu, Jie, Uma N.M. Rao, Suhagi Jasani, Vineesh Khanna, Kenneth Yaw, and Urvashi Surti. 2005. "Loss of DNA Copy Number of 10q Is Associated with Aggressive Behavior of Leiomyosarcomas: A Comparative Genomic Hybridization Study." *Cancer Genetics and Cytogenetics* 161 (1): 20–27. https://doi.org/10.1016/J.CANCERGENCYTO.2005.01.011.

Hu, Mei, Garth L. Nicolson, Jonathan C. Trent, Dihua Yu, Lianglin Zhang, Aiqing Lang, Ann Killary,

Lee M. Ellis, Corazon D. Bucana, and Raphael E. Pollock. 2002. "Characterization of 11 Human Sarcoma Cell Strains." *Cancer* 95 (7): 1569–76. https://doi.org/10.1002/CNCR.10879.

Huang, Jianguo, Mark Chen, Melodi Javid Whitley, Hsuan Cheng Kuo, Eric S. Xu, Andrea Walens, Yvonne M. Mowery, et al. 2017. "Generation and Comparison of CRISPR-Cas9 and Cre-Mediated Genetically Engineered Mouse Models of Sarcoma." *Nature Communications 2017 8:1* 8 (1): 1–11. https://doi.org/10.1038/ncomms15999.

Huang, Ling, Bruno Bockorny, Indranil Paul, Dipikaa Akshinthala, Pierre Oliver Frappart, Omar Gandarilla, Arindam Bose, et al. 2020. "PDX-Derived Organoids Model in Vivo Drug Response and Secrete Biomarkers." *JCI Insight* 5 (21). https://doi.org/10.1172/JCI.INSIGHT.135544.

Huang, Paul H., Rebecca Cook, Georgia Zoumpoulidou, Maciej T. Luczynski, and Sibylle Mittnacht. 2016. "Retinoblastoma Family Proteins: New Players in DNA Repair by Non-Homologous End-Joining." *Https://Doi.Org/10.1080/23723556.2015.1053596* 3 (2). https://doi.org/10.1080/23723556.2015.1053596.

Hughes, Chris S., Lynne M. Postovit, and Gilles A. Lajoie. 2010. "Matrigel: A Complex Protein Mixture Required for Optimal Growth of Cell Culture." *PROTEOMICS* 10 (9): 1886–90. https://doi.org/10.1002/PMIC.200900758.

Huxham, Lynsey A., Alastair H. Kyle, Jennifer H.E. Baker, Lani K. Nykilchuk, and Andrew I. Minchinton. 2004. "Microregional Effects of Gemcitabine in HCT-116 Xenografts." *Cancer Research* 64 (18): 6537–41. https://doi.org/10.1158/0008-5472.CAN-04-0986.

Ibrahim, Ayon, Nora Yucel, Boa Kim, and Zoltan Arany. 2020. "Local Mitochondrial ATP Production Regulates Endothelial Fatty Acid Uptake and Transport." *Cell Metabolism* 32 (2): 309-319.e7. https://doi.org/10.1016/J.CMET.2020.05.018.

Ibrahim, Yasir H., Celina García-García, Violeta Serra, Lei He, Kristine Torres-Lockhart, Aleix Prat, Pilar Anton, et al. 2012. "PI3K Inhibition Impairs BRCA1/2 Expression and Sensitizes BRCA-Proficient Triple-Negative Breast Cancer to PARP Inhibition." *Cancer Discovery* 2 (11): 1036–47. https://doi.org/10.1158/2159-8290.CD-11-0348/42119/AM/PI3K-INHIBITION-IMPAIRS-BRCA1-2-EXPRESSION-AND.

Ignatius, Myron S., Eleanor Chen, Natalie M. Elpek, Adam Z. Fuller, Inês M. Tenente, Ryan Clagg, Sali Liu, et al. 2012. "In Vivo Imaging of Tumor-Propagating Cells, Regional Tumor Heterogeneity, and Dynamic Cell Movements in Embryonal Rhabdomyosarcoma." *Cancer Cell* 21 (5). https://doi.org/10.1016/j.ccr.2012.03.043.

Ikoma, Naruhiko, Keila E. Torres, Heather Y. Lin, Vinod Ravi, Christina L. Roland, Gary N. Mann, Kelly K. Hunt, Janice N. Cormier, and Barry W. Feig. 2017. "Recurrence Patterns of Retroperitoneal Leiomyosarcoma and Impact of Salvage Surgery." *Journal of Surgical Oncology* 116 (3): 313–19. https://doi.org/10.1002/JSO.24667.

Imamura, Yoshinori, Toru Mukohara, Yohei Shimono, Yohei Funakoshi, Naoko Chayahara, Masanori Toyoda, Naomi Kiyota, et al. 2015. "Comparison of 2D- and 3D-Culture Models as Drug-Testing Platforms in Breast Cancer." *Oncology Reports* 33 (4): 1837–43. https://doi.org/10.3892/OR.2015.3767/HTML.

Imle, Roland, Felix K.F. Kommoss, and Ana Banito. 2021. "Preclinical in Vivo Modeling of Pediatric Sarcoma—Promises and Limitations." *Journal of Clinical Medicine* 10 (8): 1578. https://doi.org/10.3390/JCM10081578/S1.

Ingham, Matthew, Jacob B. Allred, Katherine Gano, Suzanne George, Steven Attia, Melissa Amber Burgess, Mahesh Seetharam, et al. 2021. "NCI Protocol 10250: A Phase II Study of Temozolomide and Olaparib for the Treatment of Advanced Uterine Leiomyosarcoma." *Journal of Clinical Oncology* 39 (15_suppl): 11506–11506. https://doi.org/10.1200/JCO.2021.39.15_SUPPL.11506.

Italiano, Antoine, J. R. Infante, G. I. Shapiro, K. N. Moore, P. M. LoRusso, E. Hamilton, S. Cousin, et al. 2018. "Phase I Study of the Checkpoint Kinase 1 Inhibitor GDC-0575 in Combination with Gemcitabine in Patients with Refractory Solid Tumors." *Annals of Oncology* 29 (5): 1304–11. https://doi.org/10.1093/annonc/mdy076.

Italiano, Antoine, Michèle Kind, Eberhard Stoeckle, Natalie Jones, Jean Michel Coindre, and Binh Bui. 2011. "Temsirolimus in Advanced Leiomyosarcomas: Patterns of Response and Correlation with the Activation of the Mammalian Target of Rapamycin Pathway." *Anti-Cancer Drugs* 22 (5): 463–67. https://doi.org/10.1097/CAD.0B013E3283442074.

Jacob, Dietmar A., Marcus Bahra, Jan M. Langrehr, Sabine Boas-Knoop, Robert Stefaniak, John Davis, Guido Schumacher, Steffen Lippert, and Ulf P. Neumann. 2007. "Combination Therapy of Poly (ADP-Ribose) Polymerase Inhibitor 3-Aminobenzamide and Gemcitabine Shows Strong Antitumor Activity in Pancreatic Cancer Cells." *Journal of Gastroenterology and Hepatology* 22 (5): 738–48. https://doi.org/10.1111/J.1440-1746.2006.04496.X.

Janku, Filip. 2017. "Phosphoinositide 3-Kinase (PI3K) Pathway Inhibitors in Solid Tumors: From Laboratory to Patients." *Cancer Treatment Reviews* 59 (September): 93–101. https://doi.org/10.1016/J.CTRV.2017.07.005.

Jaspers, Janneke E., Wendy Sol, Ariena Kersbergen, Andreas Schlicker, Charlotte Guyader, Guotai Xu, Lodewyk Wessels, Piet Borst, Jos Jonkers, and Sven Rottenberg. 2015. "BRCA2-Deficient Sarcomatoid Mammary Tumors Exhibit Multidrug Resistance." *Cancer Research* 75 (4): 732–41. https://doi.org/10.1158/0008-5472.CAN-14-0839.

Jenkins, Russell W., Amir R. Aref, Patrick H. Lizotte, Elena Ivanova, Susanna Stinson, Chensheng W. Zhou, Michaela Bowden, et al. 2018. "Ex Vivo Profiling of PD-1 Blockade Using Organotypic Tumor Spheroids." *Cancer Discovery* 8 (2): 196–215. https://doi.org/10.1158/2159-8290.CD-17-0833/333263/AM/EX-VIVO-PROFILING-OF-PD-1-BLOCKADE-USING.

Jensen, Ryan B., Aura Carreira, and Stephen C. Kowalczykowski. 2010. "Purified Human BRCA2 Stimulates RAD51-Mediated Recombination." *Nature 2010 467:7316* 467 (7316): 678–83. https://doi.org/10.1038/nature09399.

Jenson, Hal B., Charles T. Leach, Kenneth L. Mcclain, Vijay V. Joshi, Brad H. Pollock, Richard T. Parmley, Ellen Gould Chadwick, and Sharon B. Murphy. 2009. "Benign and Malignant Smooth Muscle Tumors Containing Epstein-Barr Virus in Children with AIDS." *Https://Doi.Org/10.3109/10428199709059684* 27 (3–4): 303–14. https://doi.org/10.3109/10428199709059684.

Jeong, Sung Baek, Ji Hye Im, Jeong Hoon Yoon, Quyen Thu Bui, Sung Chul Lim, Joon Myong Song, Yumi Shim, Jieun Yun, Janghee Hong, and Keon Wook Kang. 2018. "Essential Role of Polo-like Kinase 1 (Plk1) Oncogene in Tumor Growth and Metastasis of Tamoxifen-Resistant Breast Cancer." *Molecular Cancer Therapeutics* 17 (4): 825–37. https://doi.org/10.1158/1535-7163.MCT-17-0545/86718/AM/ESSENTIAL-ROLE-OF-POLO-LIKE-KINASE-1-PLK1-ONCOGENE.

Jia, Yiyang, Zhentong Wei, Songling Zhang, Bai Yang, and Yunfeng Li. 2022. "Instructive Hydrogels for Primary Tumor Cell Culture: Current Status and Outlook." *Advanced Healthcare*

Materials 11 (12): 2102479. https://doi.org/10.1002/ADHM.202102479.

Jian, Mi, Li Ren, Li Ren, Guodong He, Guodong He, Qi Lin, Qi Lin, et al. 2020. "A Novel Patient-Derived Organoids-Based Xenografts Model for Preclinical Drug Response Testing in Patients with Colorectal Liver Metastases." *Journal of Translational Medicine* 18 (1): 234. https://doi.org/10.1186/S12967-020-02407-8.

Jiang, Guojuan, Wanglong Deng, Yang Liu, and Chengde Wang. 2020. "General Mechanism of JQ1 in Inhibiting Various Types of Cancer." *Molecular Medicine Reports* 21 (3): 1021–34. https://doi.org/10.3892/MMR.2020.10927/HTML.

Jiao, Qinlian, Lei Bi, Yidan Ren, Shuliang Song, Qin Wang, and Yun-shan Wang. 2018. "Advances in Studies of Tyrosine Kinase Inhibitors and Their Acquired Resistance." *Molecular Cancer* 17 (1): 36. https://doi.org/10.1186/s12943-018-0801-5.

Jones, Devin M., Kaitlin A. Read, and Kenneth J. Oestreich. 2020. "Dynamic Roles for IL-2–STAT5 Signaling in Effector and Regulatory CD4+ T Cell Populations." *The Journal of Immunology* 205 (7): 1721–30. https://doi.org/10.4049/JIMMUNOL.2000612.

Jones, Robin L. 2014. "Utility of Dexrazoxane for the Reduction of Anthracycline-Induced Cardiotoxicity." *Http://Dx.Doi.Org/10.1586/14779072.6.10.1311* 6 (10): 1311–17. https://doi.org/10.1586/14779072.6.10.1311.

Jonigk, Danny, F. Laenger, L. Maegel, N. Izykowski, J. Rische, C. Tiede, C. Klein, B. Maecker-Kolhoff, H. Kreipe, and K. Hussein. 2012. "Molecular and Clinicopathological Analysis of Epstein-Barr Virus–Associated Posttransplant Smooth Muscle Tumors." *American Journal of Transplantation* 12 (7): 1908–17. https://doi.org/10.1111/J.1600-6143.2012.04011.X.

Jonsson, Philip, Chaitanya Bandlamudi, Michael L. Cheng, Preethi Srinivasan, Shweta S. Chavan, Noah D. Friedman, Ezra Y. Rosen, et al. 2019. "Tumour Lineage Shapes BRCA-Mediated Phenotypes." *Nature* 571 (7766): 576–79. https://doi.org/10.1038/S41586-019-1382-1.

Judson, Ian, Jaap Verweij, Hans Gelderblom, Jörg T. Hartmann, Patrick Schöffski, Jean Yves Blay, J. Martijn Kerst, et al. 2014. "Doxorubicin Alone versus Intensified Doxorubicin plus Ifosfamide for First-Line Treatment of Advanced or Metastatic Soft-Tissue Sarcoma: A Randomised Controlled Phase 3 Trial." *The Lancet Oncology* 15 (4): 415–23. https://doi.org/10.1016/S1470-2045(14)70063-4.

Jun, Eunsung, Seung Mo Hong, Hyun Ju Yoo, Moon Bo Kim, Ji Sun Won, Soyeon An, In Kyong Shim, Suhwan Chang, Robert M. Hoffman, and Song Cheol Kim. 2018. "Genetic and Metabolic Comparison of Orthotopic and Heterotopic Patient-Derived Pancreatic-Cancer Xenografts to the Original Patient Tumors." *Oncotarget* 9 (8): 7867. https://doi.org/10.18632/ONCOTARGET.23567.

Jungbluth, Achim A., Cristina R. Antonescu, Klaus J. Busam, Kristin Iversen, Denise Kolb, Keren Coplan, Yao T. Chen, Elisabeth Stockert, Marc Ladanyi, and Lloyd J. Old. 2001. "Monophasic and Biphasic Synovial Sarcomas Abundantly Express Cancer/Testis Antigen NY-ESO-1 but Not MAGE-A1 or CT7." *International Journal of Cancer* 94 (2): 252–56. https://doi.org/10.1002/ijc.1451.

Juvekar, Ashish, Laura N. Burga, Hai Hu, Elaine P. Lunsford, Yasir H. Ibrahim, Judith Balmañà, Anbazhagan Rajendran, et al. 2012. "Combining a PI3K Inhibitor with a PARP Inhibitor Provides an Effective Therapy for BRCA1-Related Breast Cancer." *Cancer Discovery* 2 (11): 1048–63. https://doi.org/10.1158/2159-8290.CD-11-0336/42092/AM/COMBINING-A-PI3K-INHIBITOR-WITH-A-PARP-INHIBITOR.

Kale, Justin, Elizabeth J. Osterlund, and David W. Andrews. 2017. "BCL-2 Family Proteins: Changing Partners in the Dance towards Death." *Cell Death & Differentiation 2018 25:1* 25 (1): 65–80. https://doi.org/10.1038/cdd.2017.186.

Kallen, Michael E., and Jason L. Hornick. 2021. "The 2020 WHO Classification: What's New in Soft Tissue Tumor Pathology?" *American Journal of Surgical Pathology* 45 (1): 1–23. https://doi.org/10.1097/PAS.0000000000001552.

Kaplan, Alanna R., Susan E. Gueble, Yanfeng Liu, Sebastian Oeck, Hoon Kim, Zhong Yun, and Peter M. Glazer. 2019. "Cediranib Suppresses Homology-Directed DNA Repair through down-Regulation of BRCA1/2 and RAD51." *Science Translational Medicine* 11 (492). https://doi.org/10.1126/SCITRANSLMED.AAV4508.

Karki, Prashant, Vahideh Angardi, Juan C. Mier, and Mehmet A. Orman. 2022. "A Transient Metabolic State in Melanoma Persister Cells Mediated by Chemotherapeutic Treatments." *Frontiers in Molecular Biosciences* 8 (January): 1398. https://doi.org/10.3389/FMOLB.2021.780192/BIBTEX.

Karnitz, Larry M., Karen S. Flatten, Jill M. Wagner, David Loegering, Jennifer S. Hackbarth, Sonnet J. H. Arlander, Benjamin T. Vroman, et al. 2005. "Gemcitabine-Induced Activation of Checkpoint Signaling Pathways That Affect Tumor Cell Survival." *Molecular Pharmacology* 68 (6): 1636–44. https://doi.org/10.1124/MOL.105.012716.

Kasper, Bernd, Annie Achee, Kathrin Schuster, Roger Wilson, Gerard van Oortmerssen, Rebecca A. Gladdy, Matthew L. Hemming, et al. 2021. "Unmet Medical Needs and Future Perspectives for Leiomyosarcoma Patients—A Position Paper from the National LeioMyoSarcoma Foundation (NLMSF) and Sarcoma Patients EuroNet (SPAEN)." *Cancers 2021, Vol. 13, Page 886* 13 (4): 886. https://doi.org/10.3390/CANCERS13040886.

Kasper, Bernd, Stefan Sleijfer, Saskia Litière, Sandrine Marreaud, Jaap Verweij, Rachel Hodge, Sebastian Bauer, J. Martijn Kerst, and Winette T.A. Van der Graaf. 2014. "Long-Term Responders and Survivors on Pazopanib for Advanced Soft Tissue Sarcomas: Subanalysis of Two European Organisation for Research and Treatment of Cancer (EORTC) Clinical Trials 62043 and 62072." *Annals of Oncology* 25 (3): 719–24. https://doi.org/10.1093/annonc/mdt586.

Kato, Sumie, Natalia Espinoza, Soledad Lange, Manuel Villalón, Mauricio Cuello, and Gareth I. Owen. 2008. "Characterization and Phenotypic Variation with Passage Number of Cultured Human Endometrial Adenocarcinoma Cells." *Tissue and Cell* 40 (2): 95–102. https://doi.org/10.1016/J.TICE.2007.09.007.

Kaufman, Bella, Ronnie Shapira-Frommer, Rita K. Schmutzler, M. William Audeh, Michael Friedlander, Judith Balmaña, Gillian Mitchell, et al. 2015. "Olaparib Monotherapy in Patients with Advanced Cancer and a Germline BRCA1/2 Mutation." *Journal of Clinical Oncology* 33 (3): 244–50. https://doi.org/10.1200/JCO.2014.56.2728.

Kaur, Gurvinder, and Jannette M. Dufour. 2012. "Cell Lines: Valuable Tools or Useless Artifacts." *Spermatogenesis* 2 (1): 1–5. https://doi.org/10.4161/SPMG.19885.

Kawaguchi, Kei, Kentaro Igarashi, Takashi Murakami, Tasuku Kiyuna, Scott D. Nelson, Sarah M. Dry, Yunfeng Li, et al. 2017. "Combination of Gemcitabine and Docetaxel Regresses Both Gastric Leiomyosarcoma Proliferation and Invasion in an Imageable Patient-Derived Orthotopic Xenograft (IPDOX) Model." *Cell Cycle* 16 (11). https://doi.org/10.1080/15384101.2017.1314406.

Kawai, Akira, James Woodruff, John H. Healey, Murray F. Brennan, Cristina R. Antonescu, and

Marc Ladanyi. 1998. "SYT-SSX Gene Fusion as a Determinant of Morphology and Prognosis in Synovial Sarcoma." *The New England Journal of Medicine* 338 (3): 153–60. https://doi.org/10.1056/NEJM199801153380303.

Kawano, Satoshi, Makoto Asano, Yusuke Adachi, and Junji Matsui. 2016. "Antimitotic and Non-Mitotic Effects of Eribulin Mesilate in Soft Tissue Sarcoma." *Anticancer Research* 36 (4).

Kendall, Genevieve C., Sarah Watson, Lin Xu, Collette A. Lavigne, Whitney Murchison, Dinesh Rakheja, Stephen X. Skapek, Franck Tirode, Olivier Delattre, and James F. Amatruda. 2018. "PAX3-FOXO1 Transgenic Zebrafish Models Identify HES3 as a Mediator of Rhabdomyosarcoma Tumorigenesis." *ELife* 7 (June). https://doi.org/10.7554/ELIFE.33800.

Kenerson, Heidi L., Kevin M. Sullivan, Kevin P. Labadie, Venu G. Pillarisetty, and Raymond S. Yeung. 2021. "Protocol for Tissue Slice Cultures from Human Solid Tumors to Study Therapeutic Response." *STAR Protocols* 2 (2): 100574. https://doi.org/10.1016/J.XPRO.2021.100574.

Kenerson, Heidi L., Kevin M. Sullivan, Yongwoo D. Seo, Kathryn M. Stadeli, Cigdem Ussakli, Xiaowei Yan, Chris Lausted, et al. 2020. "Tumor Slice Culture as a Biologic Surrogate of Human Cancer." *Annals of Translational Medicine* 8 (4): 114–114. https://doi.org/10.21037/atm.2019.12.88.

Kenny, Paraic A, Genee Y Lee, Connie A Myers, Richard M Neve, Jeremy R Semeiks, Paul T Spellman, Katrin Lorenz, et al. 2007. "The Morphologies of Breast Cancer Cell Lines in Three-Dimensional Assays Correlate with Their Profiles of Gene Expression." *Molecular Oncology* 1 (1): 84–96. https://doi.org/10.1016/j.molonc.2007.02.004.

Khan, O. A., M. Gore, P. Lorigan, J. Stone, A. Greystoke, W. Burke, J. Carmichael, et al. 2011. "A Phase I Study of the Safety and Tolerability of Olaparib (AZD2281, KU0059436) and Dacarbazine in Patients with Advanced Solid Tumours." *British Journal of Cancer 2011 104:5* 104 (5): 750–55. https://doi.org/10.1038/bjc.2011.8.

Kim, Hee Kyung, Sun Young Kim, Su Jin Lee, Mihyeon Kang, Seung Tae Kim, Jiryeon Jang, Oliver Rath, et al. 2016. "BEZ235 (PIK3/MTOR Inhibitor) Overcomes Pazopanib Resistance in Patient-Derived Refractory Soft Tissue Sarcoma Cells." *Translational Oncology* 9 (3): 197–202. https://doi.org/10.1016/j.tranon.2016.03.008.

Kim, Seon Young, Sang Jin Kim, Byoung Joo Kim, So Young Rah, Mo Chung Sung, Mie Jae Im, and Uh Hyun Kim. 2006. "Doxorubicin-Induced Reactive Oxygen Species Generation and Intracellular Ca2+increase Are Reciprocally Modulated in Rat Cardiomyocytes." *Experimental & Molecular Medicine 2006 38:5* 38 (5): 535–45. https://doi.org/10.1038/emm.2006.63.

King, M. L., M. E. Lindberg, G. R. Stodden, H. Okuda, S. D. Ebers, A. Johnson, A. Montag, E. Lengyel, J. A. Maclean, and K. Hayashi. 2015. "WNT7A/β-Catenin Signaling Induces FGF1 and Influences Sensitivity to Niclosamide in Ovarian Cancer." *Oncogene* 34 (26): 3452–62. https://doi.org/10.1038/ONC.2014.277.

Kirik, Ufuk, Karin Hansson, Morten Krogh, Mats Jönsson, Mef Nilbert, Peter James, and Ana Carneiro. 2014. "Discovery-Based Protein Expression Profiling Identifies Distinct Subgroups and Pathways in Leiomyosarcomas." *Molecular Cancer Research* 12 (12): 1729–39. https://doi.org/10.1158/1541-7786.MCR-14-0072/80676/AM/DISCOVERY-BASED-PROTEIN-EXPRESSION-PROFILING.

Kirilin, Evgeny M., Timur I. Fetisov, Natalia I. Moiseeva, Ekaterina A. Lesovaya, Lidia A. Laletina, Leyla F. Makhmudova, Angelika E. Manikaylo, et al. 2022. "Soft Tissue Sarcoma Study:

Association of Genetic Alterations in the Apoptosis Pathways with Chemoresistance to Doxorubicin." *Cancers 2022, Vol. 14, Page 1796* 14 (7): 1796. https://doi.org/10.3390/CANCERS14071796.

Kleinman, Hynda K., and George R. Martin. 2005. "Matrigel: Basement Membrane Matrix with Biological Activity." *Seminars in Cancer Biology* 15 (5): 378–86. https://doi.org/10.1016/J.SEMCANCER.2005.05.004.

Kodack, David P., Anna F. Farago, Anahita Dastur, Matthew A. Held, Leila Dardaei, Luc Friboulet, Friedrich von Flotow, et al. 2017. "Primary Patient-Derived Cancer Cells and Their Potential for Personalized Cancer Patient Care." *Cell Reports* 21 (11): 3298–3309. https://doi.org/10.1016/j.celrep.2017.11.051.

Kodama, Michiko, Hiroko Shimura, Jean C. Tien, Justin Y. Newberg, Takahiro Kodama, Zhubo Wei, Roberto Rangel, et al. 2021. "Sleeping Beauty Transposon Mutagenesis Identifies Genes Driving the Initiation and Metastasis of Uterine Leiomyosarcoma." *Cancer Research* 81 (21): 5413–24. https://doi.org/10.1158/0008-5472.CAN-21-0356/670878/AM/SLEEPING-BEAUTY-TRANSPOSON-MUTAGENESIS-IDENTIFIES.

Koga, Yoshikatsu, and Atsushi Ochiai. 2019. "Systematic Review of Patient-Derived Xenograft Models for Preclinical Studies of Anti-Cancer Drugs in Solid Tumors." *Cells* 8 (5). https://doi.org/10.3390/CELLS8050418.

Kopper, Oded, Chris J. de Witte, Kadi Lõhmussaar, Jose Espejo Valle-Inclan, Nizar Hami, Lennart Kester, Anjali Vanita Balgobind, et al. 2019. "An Organoid Platform for Ovarian Cancer Captures Intra- and Interpatient Heterogeneity." *Nature Medicine 2019 25:5* 25 (5): 838–49. https://doi.org/10.1038/s41591-019-0422-6.

Köstler, W. J., T. Brodowicz, Y. Attems, M. Hejna, S. Tomek, G. Amann, W. C.C. Fiebiger, Ch Wiltschke, M. Krainer, and Ch C. Zielinski. 2001. "Docetaxel as Rescue Medication in Anthracycline- and Ifosfamide-Resistant Locally Advanced or Metastatic Soft Tissue Sarcoma: Results of a Phase II Trial." *Annals of Oncology* 12 (9): 1281–88. https://doi.org/10.1023/A:1012272007146.

Kostov, Stoyan, Yavor Kornovski, Vesela Ivanova, Deyan Dzhenkov, Dimitar Metodiev, Rafał Watrowski, Yonka Ivanova, et al. 2021. "New Aspects of Sarcomas of Uterine Corpus—A Brief Narrative Review." *Clinics and Practice 2021, Vol. 11, Pages 878-900* 11 (4): 878–900. https://doi.org/10.3390/CLINPRACT11040103.

Kruiswijk, Flore, Christiaan F. Labuschagne, and Karen H. Vousden. 2015. "P53 in Survival, Death and Metabolic Health: A Lifeguard with a Licence to Kill." *Nature Reviews Molecular Cell Biology 2015 16:7* 16 (7): 393–405. https://doi.org/10.1038/nrm4007.

Kummar, Shivaani, Robert Kinders, Martin E. Gutierrez, Larry Rubinstein, Ralph E. Parchment, Lawrence R. Phillips, Uping Ji, et al. 2009. "Phase 0 Clinical Trial of the Poly (ADP-Ribose) Polymerase Inhibitor ABT-888 in Patients with Advanced Malignancies." *Journal of Clinical Oncology : Official Journal of the American Society of Clinical Oncology* 27 (16): 2705–11. https://doi.org/10.1200/JCO.2008.19.7681.

Kunz-Schughart, Leoni A., Marina Kreutz, and Ruth Knuechel. 1998. "Multicellular Spheroids: A Three-Dimensional in Vitro Culture System to Study Tumour Biology." *International Journal of Experimental Pathology* 79 (1): 1–23. https://doi.org/10.1046/J.1365-2613.1998.00051.X.

Kuo, Calvin J., Jongkyeong Chung, David F. Fiorentino, W. Michael Flanagan, John Blenis, and Gerald R. Crabtree. 1992. "Rapamycin Selectively Inhibits Interleukin-2 Activation of P70

S6 Kinase." *Nature 1992 358:6381* 358 (6381): 70–73. https://doi.org/10.1038/358070a0.

Kyle, Alastair H., Lynsey A. Huxham, Devon M. Yeoman, and Andrew I. Minchinton. 2007. "Limited Tissue Penetration of Taxanes: A Mechanism for Resistance in Solid Tumors." *Clinical Cancer Research* 13 (9): 2804–10. https://doi.org/10.1158/1078-0432.CCR-06-1941.

Lamm, Wolfgang, Camilla Natter, Sophie Schur, Wolfgang J. Köstler, Alexander Reinthaller, Michael Krainer, Christoph Grimm, et al. 2014. "Distinctive Outcome in Patients with Non-Uterine and Uterine Leiomyosarcoma." *BMC Cancer* 14 (1): 1–11. https://doi.org/10.1186/1471-2407-14-981/FIGURES/6.

Laplante, Mathieu, and David M. Sabatini. 2012. "MTOR Signaling in Growth Control and Disease." *Cell* 149 (2): 274–93. https://doi.org/10.1016/J.CELL.2012.03.017.

Lapointe, Jacques, Chunde Li, John P. Higgins, Matt Van De Rijn, Eric Bair, Kelli Montgomery, Michelle Ferrari, et al. 2004. "Gene Expression Profiling Identifies Clinically Relevant Subtypes of Prostate Cancer." *Proceedings of the National Academy of Sciences of the United States of America* 101 (3): 811–16. https://doi.org/10.1073/PNAS.0304146101/SUPPL_FILE/04146FIG6LEGEND.HTML.

Laroche-Clary, A., C. Lucchesi, C. Rey, S. Verbeke, A. Bourdon, V. Chaire, M. P. Algéo, et al. 2018. "CHK1 Inhibition in Soft-Tissue Sarcomas: Biological and Clinical Implications." *Annals of Oncology* 29 (4): 1023–29. https://doi.org/10.1093/annonc/mdy039.

Laroche-Clary, Audrey, Vanessa Chaire, Stéphanie Verbeke, Marie Paule Algéo, Andrei Malykh, François Le Loarer, and Antoine Italiano. 2020. "ATR Inhibition Broadly Sensitizes Soft-Tissue Sarcoma Cells to Chemotherapy Independent of Alternative Lengthening Telomere (ALT) Status." *Scientific Reports* 10 (1). https://doi.org/10.1038/S41598-020-63294-Z.

Laroche, Audrey, Vanessa Chaire, François Le Loarer, Marie Paule Algéo, Christophe Rey, Kevin Tran, Carlo Lucchesi, and Antoine Italiano. 2017. "Activity of Trabectedin and the PARP Inhibitor Rucaparib in Soft-Tissue Sarcomas." *Journal of Hematology and Oncology* 10 (1): 1–10. https://doi.org/10.1186/S13045-017-0451-X/FIGURES/5.

Law, Nathan C., Morris F. White, and Mary E. Hunzicker-Dunn. 2016. "G Protein-Coupled Receptors (GPCRs) That Signal via Protein Kinase A (PKA) Cross-Talk at Insulin Receptor Substrate 1 (IRS1) to Activate the Phosphatidylinositol 3-Kinase (PI3K)/AKT Pathway." *Journal of Biological Chemistry* 291 (53): 27160–69. https://doi.org/10.1074/JBC.M116.763235.

Lee, Alex T J, Robin L Jones, and Paul H Huang. 2019. "Pazopanib in Advanced Soft Tissue Sarcomas." *Signal Transduction and Targeted Therapy* 4: 16. https://doi.org/10.1038/s41392-019-0049-6.

Lee, Jeongwu, Svetlana Kotliarova, Yuri Kotliarov, Aiguo Li, Qin Su, Nicholas M. Donin, Sandra Pastorino, et al. 2006. "Tumor Stem Cells Derived from Glioblastomas Cultured in BFGF and EGF More Closely Mirror the Phenotype and Genotype of Primary Tumors than Do Serum-Cultured Cell Lines." *Cancer Cell* 9 (5): 391–403. https://doi.org/10.1016/J.CCR.2006.03.030.

Lee, Ming Cheng, Yin Kai Chen, Yih Jen Hsu, and Bor Ru Lin. 2020. "Niclosamide Inhibits the Cell Proliferation and Enhances the Responsiveness of Esophageal Cancer Cells to Chemotherapeutic Agents." *Oncology Reports* 43 (2). https://doi.org/10.3892/or.2019.7449.

Lemmon, Mark A., and Joseph Schlessinger. 2010. "Cell Signaling by Receptor Tyrosine Kinases." *Cell* 141 (7): 1117–34. https://doi.org/10.1016/J.CELL.2010.06.011.

LeSavage, Bauer L., Riley A. Suhar, Nicolas Broguiere, Matthias P. Lutolf, and Sarah C. Heilshorn. 2022. "Next-Generation Cancer Organoids." *Nature Materials* 21 (2): 143–59. https://doi.org/10.1038/S41563-021-01057-5.

Leu, Kirsten M., Leo J. Ostruszka, Donna Shewach, Mark Zalupski, Vernon Sondak, J. Sybil Biertnann, Julia Shin Jung Lee, Carol Couwlier, Krisinda Palazzolo, and Laurence H. Baker. 2004. "Laboratory and Clinical Evidence of Synergistic Cytotoxicity of Sequential Treament with Gemcitabine Followed by Docetaxel in the Treatment of Sarcoma." *Journal of Clinical Oncology* 22 (9): 1706–12. https://doi.org/10.1200/JCO.2004.08.043.

Li, Hongyi, Jian Tu, Zhiqiang Zhao, Lijuan Chen, Yueting Qu, Hongbo Li, Hao Yao, et al. 2020. "Molecular Signatures of BRCAness Analysis Identifies PARP Inhibitor Niraparib as a Novel Targeted Therapeutic Strategy for Soft Tissue Sarcomas." *Theranostics* 10 (21): 9477–94. https://doi.org/10.7150/THNO.45763.

Li, Jie, Xiaozi Wang, Chuanbao Ma, Shasha Xu, Mengyao Xu, Jie Yang, Ruicang Wang, and Liying Xue. 2021. "Dual PI3K/MTOR Inhibitor NVP-BEZ235 Decreases the Proliferation of Doxorubicin-Resistant K562 Cells." *Molecular Medicine Reports* 23. https://doi.org/10.3892/MMR.2021.11940.

Li, Jing, Sang Gyun Kim, and John Blenis. 2014. "Rapamycin: One Drug, Many Effects." *Cell Metabolism* 19 (3): 373–79. https://doi.org/10.1016/j.cmet.2014.01.001.

Liao, Hongwei, Fang Ji, Thomas Helleday, and Songmin Ying. 2018. "Mechanisms for Stalled Replication Fork Stabilization: New Targets for Synthetic Lethality Strategies in Cancer Treatments." *EMBO Reports* 19 (9): e46263. https://doi.org/10.15252/EMBR.201846263.

Liau, Jau Yu, Jia Huei Tsai, Yung Ming Jeng, Jen Chieh Lee, Hung Han Hsu, and Ching Yao Yang. 2015. "Leiomyosarcoma with Alternative Lengthening of Telomeres Is Associated with Aggressive Histologic Features, Loss of ATRX Expression, and Poor Clinical Outcome." *American Journal of Surgical Pathology* 39 (2). https://doi.org/10.1097/PAS.0000000000000324.

Liberzon, Arthur, Chet Birger, Helga Thorvaldsdóttir, Mahmoud Ghandi, Jill P. Mesirov, and Pablo Tamayo. 2015. "The Molecular Signatures Database (MSigDB) Hallmark Gene Set Collection." *Cell Systems* 1 (6): 417–25. https://doi.org/10.1016/J.CELS.2015.12.004.

Lim, Jaeyoung, Kun Yang, Barbie Taylor-Harding, W. Ruprecht Wiedemeyer, and Ronald J. Buckanovich. 2014. "VEGFR3 Inhibition Chemosensitizes Ovarian Cancer Stemlike Cells through Down-Regulation of BRCA1 and BRCA2." *Neoplasia* 16 (4): 343-353.e2. https://doi.org/10.1016/J.NEO.2014.04.003.

Lin, Jun, Lin Chen, Wenqian Jiang, Huilian Zhang, Yang Shi, and Weiwen Cai. 2019. "Rapid Detection of Low-Level HeLa Cell Contamination in Cell Culture Using Nested PCR." *Journal of Cellular and Molecular Medicine* 23 (1): 227–36. https://doi.org/10.1111/JCMM.13923.

Lin, Kevin K., Maria I. Harrell, Amit M. Oza, Ana Oaknin, Isabelle Ray-Coquard, Anna V. Tinker, Elena Helman, et al. 2019. "BRCA Reversion Mutations in Circulating Tumor DNA Predict Primary and Acquired Resistance to the PARP Inhibitor Rucaparib in High-Grade Ovarian Carcinoma." *Cancer Discovery* 9 (2): 210–19. https://doi.org/10.1158/2159-8290.CD-18-0715/42875/AM/BRCA-REVERSION-MUTATIONS-IN-CIRCULATING-TUMOR-DNA.

Lin, Szu Ting, Hsiu Chuan Chou, Shing Jyh Chang, Yi Wen Chen, Ping Chiang Lyu, Wen Ching Wang,

Margaret Dah Tsyr Chang, and Hong Lin Chan. 2012. "Proteomic Analysis of Proteins Responsible for the Development of Doxorubicin Resistance in Human Uterine Cancer Cells." *Journal of Proteomics* 75 (18): 5822–47. https://doi.org/10.1016/J.JPROT.2012.07.047.

Linch, Mark, Aisha B. Miah, Khin Thway, Ian R. Judson, and Charlotte Benson. 2014. "Systemic Treatment of Soft-Tissue Sarcoma - Gold Standard and Novel Therapies." *Nature Reviews Clinical Oncology*. Nature Publishing Group. https://doi.org/10.1038/nrclinonc.2014.26.

Liston, Dane R., and Myrtle Davis. 2017. "Clinically Relevant Concentrations of Anticancer Drugs: A Guide for Nonclinical Studies." *Clinical Cancer Research* 23 (14): 3489. https://doi.org/10.1158/1078-0432.CCR-16-3083.

Litton, Jennifer K., Hope S. Rugo, Johannes Ettl, Sara A. Hurvitz, Anthony Gonçalves, Kyung-Hun Lee, Louis Fehrenbacher, et al. 2018. "Talazoparib in Patients with Advanced Breast Cancer and a Germline BRCA Mutation." *The New England Journal of Medicine* 379 (8): 753–63. https://doi.org/10.1056/NEJMOA1802905.

Liu, Jiaye, Pengfei Li, Ling Wang, Meng Li, Zhouhong Ge, Lisanne Noordam, Ruby Lieshout, et al. 2021. "Cancer-Associated Fibroblasts Provide a Stromal Niche for Liver Cancer Organoids That Confers Trophic Effects and Therapy Resistance." *CMGH* 11 (2): 407–31. https://doi.org/10.1016/j.jcmgh.2020.09.003.

Liu, Libao, Lei Huang, Jinyuan He, Songwang Cai, Yimin Weng, Shaohong Huang, and Shaohong Ma. 2019. "PTEN Inhibits Non-Small Cell Lung Cancer Cell Growth by Promoting G0/G1 Arrest and Cell Apoptosis." *Oncology Letters* 17 (1): 1333–40. https://doi.org/10.3892/OL.2018.9719/HTML.

Liu, Ping, Thankiah Sudhaharan, Rosita M L Koh, Ling C Hwang, Sohail Ahmed, Ichiro N Maruyama, and Thorsten Wohland. 2007. "Investigation of the Dimerization of Proteins from the Epidermal Growth Factor Receptor Family by Single Wavelength Fluorescence Cross-Correlation Spectroscopy." *Biophysical Journal* 93 (2): 684–98. https://doi.org/10.1529/biophysj.106.102087.

Liu, Xuefeng, Virginie Ory, Sandra Chapman, Hang Yuan, Chris Albanese, Bhaskar Kallakury, Olga A. Timofeeva, et al. 2012. "ROCK Inhibitor and Feeder Cells Induce the Conditional Reprogramming of Epithelial Cells." *The American Journal of Pathology* 180 (2): 599. https://doi.org/10.1016/J.AJPATH.2011.10.036.

Liu, Zhixian, Qingrong Sun, and Xiaosheng Wang. 2017. "PLK1, A Potential Target for Cancer Therapy." *Translational Oncology* 10 (1): 22–32. https://doi.org/10.1016/J.TRANON.2016.10.003.

Lohiya, Garima, and Dhirendra S. Katti. 2021. "A Synergistic Combination of Niclosamide and Doxorubicin as an Efficacious Therapy for All Clinical Subtypes of Breast Cancer." *Cancers* 13 (13): 3299. https://doi.org/10.3390/CANCERS13133299/S1.

Loi, Sherene, Nicolas Sirtaine, Fanny Piette, Roberto Salgado, Giuseppe Viale, Françoise Van Eenoo, Ghizlane Rouas, et al. 2013. "Prognostic and Predictive Value of Tumor-Infiltrating Lymphocytes in a Phase III Randomized Adjuvant Breast Cancer Trial in Node-Positive Breast Cancer Comparing the Addition of Docetaxel to Doxorubicin with Doxorubicin-Based Chemotherapy: BIG 02-98." *Journal of Clinical Oncology* 31 (7): 860–67. https://doi.org/10.1200/JCO.2011.41.0902.

Loizos, Nick, Yan Xu, Jim Huber, Meilin Liu, Dan Lu, Bridget Finnerty, Robin Rolser, et al. 2005. "Targeting the Platelet-Derived Growth Factor Receptor Alpha with a Neutralizing Human

Monoclonal Antibody Inhibits the Growth of Tumor Xenografts: Implications as a Potential Therapeutic Target." *Molecular Cancer Therapeutics* 4 (3): 369–79. https://doi.org/10.1158/1535-7163.MCT-04-0114.

Longley, D. B., and P. G. Johnston. 2005. "Molecular Mechanisms of Drug Resistance." *The Journal of Pathology* 205 (2): 275–92. https://doi.org/10.1002/PATH.1706.

Lord, Christopher J., and Alan Ashworth. 2017. "PARP Inhibitors: Synthetic Lethality in the Clinic." *Science (New York, N.Y.)* 355 (6330): 1152–58. https://doi.org/10.1126/SCIENCE.AAM7344.

Lorigan, Paul, Jaap Verweij, Zsuzsa Papai, Sjoerd Rodenhuis, Axel Le Cesne, Michael G. Leahy, John A. Radford, et al. 2007. "Phase III Trial of Two Investigational Schedules of Ifosfamide Compared with Standard-Dose Doxorubicin in Advanced or Metastatic Soft Tissue Sarcoma: A European Organisation for Research and Treatment of Cancer Soft Tissue and Bone Sarcoma Group Study." *Journal of Clinical Oncology* 25 (21): 3144–50. https://doi.org/10.1200/JCO.2006.09.7717.

Loskutov, Juergen, Manuela Regenbrecht, Saskia Scharf, Philipp Stroebel, Maya Niethard, Christoph Reinhard, and Christian Regenbrecht. 2021. "Patient-Derived 3D Sarcoma Model - Robust System for Sarcoma Research and Personalized Therapy Selection." *Cancer Research* 81 (13_Supplement): 2980–2980. https://doi.org/10.1158/1538-7445.AM2021-2980.

Lovitt, Carrie J., Todd B. Shelper, and Vicky M. Avery. 2018. "Doxorubicin Resistance in Breast Cancer Cells Is Mediated by Extracellular Matrix Proteins." *BMC Cancer* 18 (1): 1–11. https://doi.org/10.1186/S12885-017-3953-6/FIGURES/6.

Magg, Thomas, Tilmann Schober, Christoph Walz, Julia Ley-Zaporozhan, Fabio Facchetti, Christoph Klein, and Fabian Hauck. 2018. "Epstein-Barr Virus+ Smooth Muscle Tumors as Manifestation of Primary Immunodeficiency Disorders." *Frontiers in Immunology* 9 (FEB): 368. https://doi.org/10.3389/FIMMU.2018.00368/BIBTEX.

Maki, Robert G., J. Kyle Wathen, Shreyaskumar R. Patel, Dennis A. Priebat, Scott H. Okuno, Brian Samuels, Michael Fanucchi, et al. 2007. "Randomized Phase II Study of Gemcitabine and Docetaxel Compared with Gemcitabine Alone in Patients with Metastatic Soft Tissue Sarcomas: Results of Sarcoma Alliance for Research through Collaboration Study 002 [Corrected]." *Journal of Clinical Oncology* 25 (19): 2755–63. https://doi.org/10.1200/JCO.2006.10.4117.

Mamane, Yaël, Emmanuel Petroulakis, Liwei Rong, Kaori Yoshida, Lian Wee Ler, and Nahum Sonenberg. 2004. "EIF4E – from Translation to Transformation." *Oncogene 2004 23:18* 23 (18): 3172–79. https://doi.org/10.1038/sj.onc.1207549.

Mañas, Adriana, Kristina Aaltonen, Natalie Andersson, Karin Hansson, Aleksandra Adamska, Alexandra Seger, Hiroaki Yasui, et al. 2022. "Clinically Relevant Treatment of PDX Models Reveals Patterns of Neuroblastoma Chemoresistance." *Science Advances* 8 (43): eabq4617. https://doi.org/10.1126/SCIADV.ABQ4617/SUPPL_FILE/SCIADV.ABQ4617_DATA_FILES_S2_AND_S3.ZIP.

Mancuso, Roberta, Renato Biffi, Marilena Valli, Monica Bellinvia, Tourlaki Athanasia, Silvia Ferrucci, Lucia Brambilla, et al. 2008. "HHV8 a Subtype Is Associated with Rapidly Evolving Classic Kaposi's Sarcoma." *Journal of Medical Virology* 80 (12): 2153–60. https://doi.org/10.1002/JMV.21322.

Manning, Brendan D., and Alex Toker. 2017. "AKT/PKB Signaling: Navigating the Network." *Cell*

169 (3): 381. https://doi.org/10.1016/J.CELL.2017.04.001.

Manning, G, D B Whyte, R Martinez, T Hunter, and S Sudarsanam. 2002. "The Protein Kinase Complement of the Human Genome." *Science (New York, N.Y.)* 298 (5600): 1912–34. https://doi.org/10.1126/science.1075762.

Manzella, Gabriele, Leonie D. Schreck, Willemijn B. Breunis, Jan Molenaar, Hans Merks, Frederic G. Barr, Wenyue Sun, et al. 2020. "Phenotypic Profiling with a Living Biobank of Primary Rhabdomyosarcoma Unravels Disease Heterogeneity and AKT Sensitivity." *Nature Communications 2020 11:1* 11 (1): 1–15. https://doi.org/10.1038/s41467-020-18388-7.

Mao, Zhiyong, Michael Bozzella, Andrei Seluanov, and Vera Gorbunova. 2008. "DNA Repair by Nonhomologous End Joining and Homologous Recombination during Cell Cycle in Human Cells." *Http://Dx.Doi.Org/10.4161/Cc.7.18.6679* 7 (18): 2902–6. https://doi.org/10.4161/CC.7.18.6679.

Marisa, Laetitia, Aurélien de Reyniès, Alex Duval, Janick Selves, Marie Pierre Gaub, Laure Vescovo, Marie Christine Etienne-Grimaldi, et al. 2013. "Gene Expression Classification of Colon Cancer into Molecular Subtypes: Characterization, Validation, and Prognostic Value." *PLOS Medicine* 10 (5): e1001453. https://doi.org/10.1371/JOURNAL.PMED.1001453.

Martin-Broto, Javier, Maria Lopez-Alvarez, David S. Moura, Rafael Ramos, Paola Collini, Cleofe Romagosa, Silvia Bague, et al. 2021. "Predictive Value of MRP-1 in Localized High-Risk Soft Tissue Sarcomas: A Translational Research Associated to ISG-STS 1001 Randomized Phase III Trial." *Molecular Cancer Therapeutics* 20 (12): 2539–52. https://doi.org/10.1158/1535-7163.MCT-21-0315/673432/AM/PREDICTIVE-VALUE-OF-MRP-1-IN-LOCALIZED-HIGH-RISK.

Martin-Liberal, Juan, Antonio López-Pousa, Javier Martínez-Trufero, Javier Martín-Broto, Ricardo Cubedo, Javier Lavernia, Andrés Redondo, et al. 2017. "Phase II Study of Gemcitabine Plus Sirolimus in Previously Treated Patients with Advanced Soft-Tissue Sarcoma: A Spanish Group for Research on Sarcomas (GEIS) Study." *Targeted Oncology 2017 13:1* 13 (1): 81–87. https://doi.org/10.1007/S11523-017-0539-9.

Martin, Dietmar E., and Michael N. Hall. 2005. "The Expanding TOR Signaling Network." *Current Opinion in Cell Biology* 17 (2): 158–66. https://doi.org/10.1016/J.CEB.2005.02.008.

Martin, Steve Z., Daniel C. Wagner, Nina Hörner, David Horst, Hauke Lang, Katrin E. Tagscherer, and Wilfried Roth. 2019. "Ex Vivo Tissue Slice Culture System to Measure Drug-Response Rates of Hepatic Metastatic Colorectal Cancer." *BMC Cancer* 19 (1): 1–14. https://doi.org/10.1186/S12885-019-6270-4/FIGURES/6.

Massard, Christophe, Kim Nguyen Chi, Daniel Castellano, Johann de Bono, Gwenaelle Gravis, Luc Dirix, Jean Pascal Machiels, et al. 2017. "Phase Ib Dose-Finding Study of Abiraterone Acetate plus Buparlisib (BKM120) or Dactolisib (BEZ235) in Patients with Castration-Resistant Prostate Cancer." *European Journal of Cancer* 76 (May): 36–44. https://doi.org/10.1016/j.ejca.2017.01.024.

May, Eugenie Wong Soon, Szu Ting Lin, Chi Chen Lin, Jo Fan Chang, Eric Hung, Yi Wen Lo, Li Hsun Lin, et al. 2014. "Identification of Up- and down-Regulated Proteins in Doxorubicin-Resistant Uterine Cancer Cells: Reticulocalbin-1 Plays a Key Role in the Development of Doxorubicin-Associated Resistance." *Pharmacological Research* 90 (December): 1–17. https://doi.org/10.1016/J.PHRS.2014.08.007.

Mbatani, Nomonde, Alexander B. Olawaiye, and Jaime Prat. 2018. "Uterine Sarcomas." *International Journal of Gynecology & Obstetrics* 143 (October): 51–58.

https://doi.org/10.1002/IJGO.12613.

McDermott, Martina, Alex J. Eustace, Steven Busschots, Laura Breen, John Crown, Martin Clynes, Norma O'Donovan, and Britta Stordal. 2014. "In Vitro Development of Chemotherapy and Targeted Therapy Drug-Resistant Cancer Cell Lines: A Practical Guide with Case Studies." *Frontiers in Oncology* 4. https://doi.org/10.3389/FONC.2014.00040.

Meister, Michael T, Marian J A Groot Koerkamp, Terezinha de Souza, Willemijn B Breunis, Ewa Frazer-Mendelewska, Mariël Brok, Jeff DeMartino, et al. 2022. "Mesenchymal Tumor Organoid Models Recapitulate Rhabdomyosarcoma Subtypes." *EMBO Molecular Medicine* 14 (10): e16001. https://doi.org/10.15252/EMMM.202216001.

Mellor, Howard R., and Richard Callaghan. 2011. "Accumulation and Distribution of Doxorubicin in Tumour Spheroids: The Influence of Acidity and Expression of P-Glycoprotein." *Cancer Chemotherapy and Pharmacology 2011 68:5* 68 (5): 1179–90. https://doi.org/10.1007/S00280-011-1598-8.

Mendes-Pereira, Ana M., Sarah A. Martin, Rachel Brough, Afshan McCarthy, Jessica R. Taylor, Jung Sik Kim, Todd Waldman, Christopher J. Lord, and Alan Ashworth. 2009. "Synthetic Lethal Targeting of PTEN Mutant Cells with PARP Inhibitors." *EMBO Molecular Medicine* 1 (6–7): 315. https://doi.org/10.1002/EMMM.200900041.

Menezes, Daniel L., Pietro Taverna, Michael R. Jensen, Tinya Abrams, Darrin Stuart, Guoying Karen Yu, David Duhl, et al. 2012. "The Novel Oral Hsp90 Inhibitor NVP-HSP990 Exhibits Potent and Broad-Spectrum Antitumor Activities in Vitro and in Vivo." *Molecular Cancer Therapeutics* 11 (3): 730–39. https://doi.org/10.1158/1535-7163.MCT-11-0667.

Merimsky, Ofer, Isaac Meller, Gidon Flusser, Yehuda Kollender, Josephine Issakov, Miriam Weil-Ben-Arush, Eyal Fenig, et al. 2000. "Gemcitabine in Soft Tissue or Bone Sarcoma Resistant to Standard Chemotherapy: A Phase II Study." *Cancer Chemotherapy and Pharmacology 2000 45:2* 45 (2): 177–81. https://doi.org/10.1007/S002800050027.

Merry, Eve, Khin Thway, Robin L. Jones, and Paul H. Huang. 2021. "Predictive and Prognostic Transcriptomic Biomarkers in Soft Tissue Sarcomas." *Npj Precision Oncology 2021 5:1* 5 (1): 1–8. https://doi.org/10.1038/s41698-021-00157-4.

Milighetti, Martina, Lukas Krasny, Alex T.J. Lee, Gabriele Morani, Cornelia Szecsei, Yingtong Chen, Nafia Guljar, et al. 2021. "Proteomic Profiling of Soft Tissue Sarcomas with SWATH Mass Spectrometry." *Journal of Proteomics* 241 (June). https://doi.org/10.1016/J.JPROT.2021.104236.

Mishra, Rosalin, Hima Patel, Samar Alanazi, Mary Kate Kilroy, and Joan T. Garrett. 2021. "PI3K Inhibitors in Cancer: Clinical Implications and Adverse Effects." *International Journal of Molecular Sciences 2021, Vol. 22, Page 3464* 22 (7): 3464. https://doi.org/10.3390/IJMS22073464.

Mito, Jeffrey K., Devarati Mitra, Constance M. Barysauskas, Adrián Mariño-Enriquez, Elizabeth A. Morgan, Christopher D.M. Fletcher, Chandrajit P. Raut, Elizabeth H. Baldini, and Leona A. Doyle. 2019. "A Comparison of Outcomes and Prognostic Features for Radiation-Associated Angiosarcoma of the Breast and Other Radiation-Associated Sarcomas." *International Journal of Radiation Oncology, Biology, Physics* 104 (2): 425–35. https://doi.org/10.1016/J.IJROBP.2019.01.082.

Mitra, Abhisek, Lopa Mishra, and Shulin Li. 2013. "Technologies for Deriving Primary Tumor Cells for Use in Personalized Cancer Therapy." *Trends in Biotechnology* 31 (6): 347–54. https://doi.org/10.1016/J.TIBTECH.2013.03.006.

Miwa, Shinji, Yong Zhang, Kyung Eun Baek, Fuminari Uehara, Shuya Yano, Mako Yamamoto, Yukihiko Hiroshima, et al. 2014. "Inhibition of Spontaneous and Experimental Lung Metastasis of Soft-Tissue Sarcoma by Tumor-Targeting Salmonella Typhimurium A1-R." *Oncotarget* 5 (24): 12849. https://doi.org/10.18632/ONCOTARGET.2561.

Miyoshi, Hiroyuki, Hisatsugu Maekawa, Fumihiko Kakizaki, Tadayoshi Yamaura, Kenji Kawada, Yoshiharu Sakai, M. Mark Taketo, et al. 2018. "An Improved Method for Culturing Patient-Derived Colorectal Cancer Spheroids." *Oncotarget* 9 (31): 21950–64. https://doi.org/10.18632/ONCOTARGET.25134.

Mo, Wei, Qingxin Liu, Curtis Chun Jen Lin, Hui Dai, Yang Peng, Yulong Liang, Guang Peng, et al. 2016. "MTOR Inhibitors Suppress Homologous Recombination Repair and Synergize with PARP Inhibitors via Regulating SUV39H1 in BRCA-Proficient Triple-Negative Breast Cancer." *Clinical Cancer Research* 22 (7): 1699–1712. https://doi.org/10.1158/1078-0432.CCR-15-1772/268567/AM/MTOR-INHIBITORS-SUPPRESS-HOMOLOGOUS-RECOMBINATION.

Monk, Bradley J., Domenica Lorusso, Antoine Italiano, Stan B. Kaye, Miguel Aracil, Adnan Tanović, and Maurizio D'Incalci. 2016. "Trabectedin as a Chemotherapy Option for Patients with BRCA Deficiency." *Cancer Treatment Reviews* 50 (November): 175–82. https://doi.org/10.1016/j.ctrv.2016.09.009.

Moore Dalal, Kimberly, Cristina R. Antonescu, Ronald P. DeMatteo, and Robert G. Maki. 2008. "EBV-Associated Smooth Muscle Neoplasms: Solid Tumors Arising in the Presence of Immunosuppression and Autoimmune Diseases." *Sarcoma* 2008. https://doi.org/10.1155/2008/859407.

Moritake, Hiroshi, Yusuke Saito, Daisuke Sawa, Naoki Sameshima, Ai Yamada, Mariko Kinoshita, Sachiyo Kamimura, Takao Konomoto, and Hiroyuki Nunoi. 2019. "TAE226, a Dual Inhibitor of Focal Adhesion Kinase and Insulin-like Growth Factor-I Receptor, Is Effective for Ewing Sarcoma." *Cancer Medicine* 8 (18): 7809–21. https://doi.org/10.1002/CAM4.2647.

Moura, David S., Maria Peña-Chilet, Juan Antonio Cordero Varela, Ramiro Alvarez-Alegret, Carolina Agra-Pujol, Francisco Izquierdo, Rafael Ramos, et al. 2021. "A DNA Damage Repair Gene-Associated Signature Predicts Responses of Patients with Advanced Soft-Tissue Sarcoma to Treatment with Trabectedin." *Molecular Oncology* 15 (12): 3691–3705. https://doi.org/10.1002/1878-0261.12996.

Moynahan, Mary Ellen, Joanne W. Chiu, Beverly H. Koller, and Maria Jasint. 1999. "Brca1 Controls Homology-Directed DNA Repair." *Molecular Cell* 4 (4): 511–18. https://doi.org/10.1016/S1097-2765(00)80202-6.

Munoz-Garcia, Javier, Camille Jubelin, Aurélie Loussouarn, Matisse Goumard, Laurent Griscom, Axelle Renodon-Cornière, Marie Françoise Heymann, and Dominique Heymann. 2021. "In Vitro Three-Dimensional Cell Cultures for Bone Sarcomas." *Journal of Bone Oncology* 30 (October): 100379. https://doi.org/10.1016/J.JBO.2021.100379.

Murai, Junko, Ying Feng, Guoying K. Yu, Yuanbin Ru, Sai Wen Tang, Yuqiao Shen, and Yves Pommier. 2016. "Resistance to PARP Inhibitors by SLFN11 Inactivation Can Be Overcome by ATR Inhibition." *Oncotarget* 7 (47): 76534–50. https://doi.org/10.18632/ONCOTARGET.12266.

Murai, Junko, Shar Yin N. Huang, Benu Brata Das, Amelie Renaud, Yiping Zhang, James H. Doroshow, Jiuping Ji, Shunichi Takeda, and Yves Pommier. 2012. "Trapping of PARP1 and PARP2 by Clinical PARP Inhibitors." *Cancer Research* 72 (21): 5588–99. https://doi.org/10.1158/0008-5472.CAN-12-2753.

Murai, Junko, Shar Yin N. Huang, Amèlie Renaud, Yiping Zhang, Jiuping Ji, Shunichi Takeda, Joel Morris, Beverly Teicher, James H. Doroshow, and Yves Pommier. 2014. "Stereospecific PARP Trapping by BMN 673 and Comparison with Olaparib and Rucaparib." *Molecular Cancer Therapeutics* 13 (2): 433–43. https://doi.org/10.1158/1535-7163.MCT-13-0803/85892/AM/STEREOSPECIFIC-PARP-TRAPPING-BY-BMN-673-AND.

Murai, Junko, Yiping Zhang, Joel Morris, Jiuping Ji, Shunichi Takeda, James H. Doroshow, and Yves Pommier. 2014. "Rationale for Poly(ADP-Ribose) Polymerase (PARP) Inhibitors in Combination Therapy with Camptothecins or Temozolomide Based on PARP Trapping versus Catalytic Inhibition." *Journal of Pharmacology and Experimental Therapeutics* 349 (3): 408–16. https://doi.org/10.1124/JPET.113.210146.

Muriithi, Wanjiru, Lucy Wanjiku Macharia, Carlos Pilotto Heming, Juliana Lima Echevarria, Atunga Nyachieo, Paulo Niemeyer Filho, and Vivaldo Moura Neto. 2020. "ABC Transporters and the Hallmarks of Cancer: Roles in Cancer Aggressiveness beyond Multidrug Resistance." *Cancer Biology & Medicine* 17 (2): 253. https://doi.org/10.20892/J.ISSN.2095-3941.2019.0284.

Nacev, Benjamin A., Francisco Sanchez-Vega, Shaleigh A. Smith, Cristina R. Antonescu, Evan Rosenbaum, Hongyu Shi, Cerise Tang, et al. 2022. "Clinical Sequencing of Soft Tissue and Bone Sarcomas Delineates Diverse Genomic Landscapes and Potential Therapeutic Targets." *Nature Communications 2022 13:1* 13 (1): 1–15. https://doi.org/10.1038/s41467-022-30453-x.

Nair, Jayasree S., and Gary K. Schwartz. 2015. "Inhibition of Polo like Kinase 1 in Sarcomas Induces Apoptosis That Is Dependent on Mcl-1 Suppression." *Cell Cycle* 14 (19): 3101. https://doi.org/10.1080/15384101.2015.1078033.

Nakamura, Tomoki, Akihiko Matsumine, Takao Matsubara, Kunihiro Asanuma, Astumasa Uchida, and Akihiro Sudo. 2011. "Clinical Impact of the Tumor Volume Doubling Time on Sarcoma Patients with Lung Metastases." *Clinical & Experimental Metastasis* 28 (8): 819–25. https://doi.org/10.1007/S10585-011-9413-9.

Namatame, Nachi, Naomi Tamaki, Yuya Yoshizawa, Mutsumi Okamura, Yumiko Nishimura, Kanami Yamazaki, Miwa Tanaka, et al. 2018. "Antitumor Profile of the PI3K Inhibitor ZSTK474 in Human Sarcoma Cell Lines." *Oncotarget* 9 (80): 35141. https://doi.org/10.18632/ONCOTARGET.26216.

Neal, James T., Xingnan Li, Junjie Zhu, Valeria Giangarra, Caitlin L. Grzeskowiak, Jihang Ju, Iris H. Liu, et al. 2018. "Organoid Modeling of the Tumor Immune Microenvironment." *Cell* 175 (7): 1972-1988.e16. https://doi.org/10.1016/j.cell.2018.11.021.

Ng, Felicia, Shayne Boucher, Susie Koh, Konduru S.R. Sastry, Lucas Chase, Uma Lakshmipathy, Cleo Choong, et al. 2008. "PDGF, TGF-β, and FGF Signaling Is Important for Differentiation and Growth of Mesenchymal Stem Cells (MSCs): Transcriptional Profiling Can Identify Markers and Signaling Pathways Important in Differentiation of MSCs into Adipogenic, Chondrogenic, and Osteogenic Lineages." *Blood* 112 (2): 295–307. https://doi.org/10.1182/BLOOD-2007-07-103697.

Nguyen, Kim Bich, and Stefani Spranger. 2020. "Modulation of the Immune Microenvironment by Tumor-Intrinsic Oncogenic Signaling." *The Journal of Cell Biology* 219 (1). https://doi.org/10.1083/JCB.201908224.

Nishida, Toshirou, Masahiko Tsujimoto, Tsuyoshi Takahashi, Seiichi Hirota, Jean Yves Blay, and Mari Wataya-Kaneda. 2016. "Gastrointestinal Stromal Tumors in Japanese Patients with Neurofibromatosis Type I." *Journal of Gastroenterology* 51 (6): 571–78.

https://doi.org/10.1007/S00535-015-1132-6/FIGURES/2.

Nitiss, John L. 2009. "Targeting DNA Topoisomerase II in Cancer Chemotherapy." *Nature Reviews. Cancer* 9 (5): 338. https://doi.org/10.1038/NRC2607.

Nogales, Vanesa, William C. Reinhold, Sudhir Varma, Anna Martinez-Cardus, Catia Moutinho, Sebastian Moran, Holger Heyn, et al. 2015. "Epigenetic Inactivation of the Putative DNA/RNA Helicase SLFN11 in Human Cancer Confers Resistance to Platinum Drugs." *Oncotarget* 7 (3): 3084–97. https://doi.org/10.18632/ONCOTARGET.6413.

Noguchi, Rei, Yuki Yoshimatsu, Takuya Ono, Akane Sei, Kaoru Hirabayashi, Iwao Ozawa, Kazutaka Kikuta, and Tadashi Kondo. 2020. "Establishment and Characterization of NCC-LMS2-C1—a Novel Patient-Derived Cancer Cell Line of Leiomyosarcoma." *Human Cell 2020 34:1* 34 (1): 279–88. https://doi.org/10.1007/S13577-020-00443-6.

Nunes, Ana S., Andreia S. Barros, Elisabete C. Costa, André F. Moreira, and Ilídio J. Correia. 2019. "3D Tumor Spheroids as in Vitro Models to Mimic in Vivo Human Solid Tumors Resistance to Therapeutic Drugs." *Biotechnology and Bioengineering* 116 (1): 206–26. https://doi.org/10.1002/bit.26845.

O'Reilly, Kathryn E., Fredi Rojo, Qing Bai She, David Solit, Gordon B. Mills, Debra Smith, Heidi Lane, et al. 2006. "MTOR Inhibition Induces Upstream Receptor Tyrosine Kinase Signaling and Activates Akt." *Cancer Research* 66 (3): 1500–1508. https://doi.org/10.1158/0008-5472.CAN-05-2925.

Ogawa, Katsuhiko, Motoi Oguchi, Hirohiko Yamabe, Yasuaki Nakashima, and Yoshihiro Hamashima. 1986. "Distribution of Collagen Type IV in Soft Tissue Tumors: An Immunohistochemical Study." *Cancer* 58 (2). https://doi.org/10.1002/1097-0142(19860715)58:2<269::AID-CNCR2820580212>3.0.CO;2-7.

Ognjanovic, Simona, Magali Olivier, Tracy L. Bergemann, and Pierre Hainaut. 2012. "Sarcomas in TP53 Germline Mutation Carriers." *Cancer* 118 (5): 1387–96. https://doi.org/10.1002/CNCR.26390.

Okkenhaug, Klaus, and Bart Vanhaesebroeck. 2003. "PI3K in Lymphocyte Development, Differentiation and Activation." *Nature Reviews Immunology 2003 3:4* 3 (4): 317–30. https://doi.org/10.1038/nri1056.

Okuno, Scott, Howard Bailey, Michelle R. Mahoney, Douglas Adkins, William Maples, Tom Fitch, David Ettinger, Charles Erlichman, and Jann N. Sarkaria. 2011. "A Phase 2 Study of Temsirolimus (CCI-779) in Patients with Soft Tissue Sarcomas." *Cancer* 117 (15): 3468–75. https://doi.org/10.1002/CNCR.25928.

Oliva, Esther. 2015. "Practical Issues in Uterine Pathology from Banal to Bewildering: The Remarkable Spectrum of Smooth Muscle Neoplasia." *Modern Pathology 2016 29:1* 29 (1): S104–20. https://doi.org/10.1038/modpathol.2015.139.

Ong, Kong Wee, Marissa Teo, Victor Lee, Danny Ong, Ann Lee, Suai Tan Chieh, A. Vathsala, and Han Chong Toh. 2009. "Expression of EBV Latent Antigens, Mammalian Target of Rapamycin, and Tumor Suppression Genes in EBV-Positive Smooth Muscle Tumors: Clinical and Therapeutic Implications." *Clinical Cancer Research* 15 (17): 5350–58. https://doi.org/10.1158/1078-0432.CCR-08-2979/346841/P/EXPRESSION-OF-EBV-LATENT-ANTIGENS-MAMMALIAN-TARGET.

oosterwijk, J. G. Van, B. Herpers, D. Meijer, I. H. Briaire-de bruijn, A. M. Cleton-jansen, H. Gelderblom, B. Van de water, and J. V.M.G. Bée. 2012. "Restoration of Chemosensitivity

for Doxorubicin and Cisplatin in Chondrosarcoma in Vitro: BCL-2 Family Members Cause Chemoresistance." *Annals of Oncology* 23 (6): 1617–26. https://doi.org/10.1093/annonc/mdr512.

Oshi, Masanori, Stephanie Newman, Yoshihisa Tokumaru, Li Yan, Ryusei Matsuyama, Itaru Endo, Matthew H.G. Katz, and Kazuaki Takabe. 2020. "High G2m Pathway Score Pancreatic Cancer Is Associated with Worse Survival, Particularly after Margin-Positive (R1 or R2) Resection." *Cancers* 12 (10). https://doi.org/10.3390/cancers12102871.

Outani, Hidetatsu, Takaaki Tanaka, Toru Wakamatsu, Yoshinori Imura, Kenichiro Hamada, Nobuhito Araki, Kazuyuki Itoh, Hideki Yoshikawa, and Norifumi Naka. 2014. "Establishment of a Novel Clear Cell Sarcoma Cell Line (Hewga-CCS), and Investigation of the Antitumor Effects of Pazopanib on Hewga-CCS." *BMC Cancer* 14 (1): 1–12. https://doi.org/10.1186/1471-2407-14-455/TABLES/1.

Oza, Amit M., Anna V. Tinker, Ana Oaknin, Ronnie Shapira-Frommer, Iain A. McNeish, Elizabeth M. Swisher, Isabelle Ray-Coquard, et al. 2017. "Antitumor Activity and Safety of the PARP Inhibitor Rucaparib in Patients with High-Grade Ovarian Carcinoma and a Germline or Somatic BRCA1 or BRCA2 Mutation: Integrated Analysis of Data from Study 10 and ARIEL2." *Gynecologic Oncology* 147 (2): 267–75. https://doi.org/10.1016/j.ygyno.2017.08.022.

Ozturk, Sukru, Cansu Gorgun, Sevtap Gokalp, Seda Vatansever, and Aylin Sendemir. 2020. "Development and Characterization of Cancer Stem Cell-Based Tumoroids as an Osteosarcoma Model." *Biotechnology and Bioengineering* 117 (8): 2527–39. https://doi.org/10.1002/BIT.27381.

Palubeckaitė, Ieva, Sanne Venneker, Inge H. Briaire-de Bruijn, Brendy E. van den Akker, Augustinus D. Krol, Hans Gelderblom, and Judith V.M.G. Bovée. 2020. "Selection of Effective Therapies Using Three-Dimensional in Vitro Modeling of Chondrosarcoma." *Frontiers in Molecular Biosciences* 7 (December): 438. https://doi.org/10.3389/FMOLB.2020.566291/BIBTEX.

Pan, Cuiping, Chanchal Kumar, Sebastian Bohl, Ursula Klingmueller, and Matthias Mann. 2009. "Comparative Proteomic Phenotyping of Cell Lines and Primary Cells to Assess Preservation of Cell Type-Specific Functions." *Molecular and Cellular Proteomics* 8 (3): 443–50. https://doi.org/10.1074/mcp.M800258-MCP200.

Pankova, Valeriya, Khin Thway, Robin L. Jones, and Paul H. Huang. 2021. "The Extracellular Matrix in Soft Tissue Sarcomas: Pathobiology and Cellular Signalling." *Frontiers in Cell and Developmental Biology* 9 (December): 3374. https://doi.org/10.3389/FCELL.2021.763640/BIBTEX.

Pasquali, Sandro, Emanuela Palmerini, Vittorio Quagliuolo, Javier Martin-Broto, Antonio Lopez-Pousa, Giovanni Grignani, Antonella Brunello, et al. 2022. "Neoadjuvant Chemotherapy in High-Risk Soft Tissue Sarcomas: A Sarculator-Based Risk Stratification Analysis of the ISG-STS 1001 Randomized Trial." *Cancer* 128 (1): 85–93. https://doi.org/10.1002/CNCR.33895.

Patel, Anand G., Jann N. Sarkaria, and Scott H. Kaufmann. 2011. "Nonhomologous End Joining Drives Poly(ADP-Ribose) Polymerase (PARP) Inhibitor Lethality in Homologous Recombination-Deficient Cells." *Proceedings of the National Academy of Sciences of the United States of America* 108 (8): 3406–11. https://doi.org/10.1073/PNAS.1013715108/SUPPL_FILE/PNAS.201013715SI.PDF.

Patel, Krish, Alexey V. Danilov, and John M. Pagel. 2019. "Duvelisib for CLL/SLL and Follicular Non-Hodgkin Lymphoma." *Blood* 134 (19): 1573–77. https://doi.org/10.1182/BLOOD.2019001795.

Patel, S. R., V. Gandhi, J. Jenkins, N. Papadopolous, M. A. Burgess, C. Plager, W. Plunkett, and R. S. Benjamin. 2001. "Phase II Clinical Investigation of Gemcitabine in Advanced Soft Tissue Sarcomas and Window Evaluation of Dose Rate on Gemcitabine Triphosphate Accumulation." *Journal of Clinical Oncology* 19 (15): 3483–89. https://doi.org/10.1200/JCO.2001.19.15.3483.

Patwardhan, Parag P., Kathryn S. Ivy, Elgilda Musi, Elisa de Stanchina, and Gary K. Schwartz. 2016. "Significant Blockade of Multiple Receptor Tyrosine Kinases by MGCD516 (Sitravatinib), a Novel Small Molecule Inhibitor, Shows Potent Anti-Tumor Activity in Preclinical Models of Sarcoma." *Oncotarget* 7 (4): 4093–4109. https://doi.org/10.18632/ONCOTARGET.6547.

Paull, Tanya T., Emmy P. Rogakou, Vikky Yamazaki, Cordula U. Kirchgessner, Martin Gellert, and William M. Bonner. 2000. "A Critical Role for Histone H2AX in Recruitment of Repair Factors to Nuclear Foci after DNA Damage." *Current Biology* 10 (15): 886–95. https://doi.org/10.1016/S0960-9822(00)00610-2.

Pautier, P., A. Floquet, C. Chevreau, N. Penel, C. Guillemet, C. Delcambre, D. Cupissol, et al. 2021. "A Single-Arm Multicentre Phase II Trial of Doxorubicin in Combination with Trabectedin in the First-Line Treatment for Leiomyosarcoma with Long-Term Follow-up and Impact of Cytoreductive Surgery." *ESMO Open* 6 (4). https://doi.org/10.1016/j.esmoop.2021.100209.

Pautier, P., A. Italiano, S. Piperno-Neumann, C.M. Chevreau, N. Penel, D. Cupissol, P. Boudou Rouquette, et al. 2021. "LBA59 LMS-04 Study: A Randomised, Multicenter, Phase III Study Comparing Doxorubicin Alone versus Doxorubicin with Trabectedin Followed by Trabectedin in Non-Progressive Patients as First-Line Therapy, in Patients with Metastatic or Unresectable Leiomyosarcoma - A French Sarcoma Group Study." *Annals of Oncology* 32 (September): S1335–36. https://doi.org/10.1016/j.annonc.2021.08.2139.

Pautier, Patricia, Anne Floquet, Christine Chevreau, Nicolas Penel, Cécile Guillemet, Corinne Delcambre, Didier Cupissol, et al. 2015. "Trabectedin in Combination with Doxorubicin for First-Line Treatment of Advanced Uterine or Soft-Tissue Leiomyosarcoma (LMS-02): A Non-Randomised, Multicentre, Phase 2 Trial." *The Lancet Oncology* 16 (4): 457–64. https://doi.org/10.1016/S1470-2045(15)70070-7.

Pautier, Patricia, Anne Floquet, Nicolas Penel, Sophie Piperno-Neumann, Nicolas Isambert, Annie Rey, Emmanuelle Bompas, et al. 2012. "Randomized Multicenter and Stratified Phase II Study of Gemcitabine Alone Versus Gemcitabine and Docetaxel in Patients with Metastatic or Relapsed Leiomyosarcomas: A Fédération Nationale Des Centres de Lutte Contre Le Cancer (FNCLCC) French Sarcoma Group Study (TAXOGEM Study)." *The Oncologist* 17 (9): 1213–20. https://doi.org/10.1634/THEONCOLOGIST.2011-0467.

Pautier, Patricia, Antoine ITALIANO, Sophie PIPERNO-NEUMANN, Christine CHEVREAU, Nicolas PENEL, Nelly Firmin, Pascaline Boudou-Rouquette, et al. 2022. "Doxorubicin Alone versus Doxorubicin with Trabectedin Followed by Trabectedin Alone as First-Line Therapy for Metastatic or Unresectable Leiomyosarcoma (LMS-04): A Randomised, Multicentre, Open-Label Phase 3 Trial." *The Lancet Oncology* 23 (8): 1044–54. https://doi.org/10.1016/S1470-2045(22)00380-1.

Pedra Nobre, Silvana, Martee L. Hensley, Melody So, Qin C. Zhou, Alexia Iasonos, Mario M. Leitao, Jennifer Ducie, et al. 2021. "The Impact of Tumor Fragmentation in Patients with Stage I Uterine Leiomyosarcoma on Patterns of Recurrence and Oncologic Outcome." *Gynecologic Oncology* 160 (1): 99. https://doi.org/10.1016/J.YGYNO.2020.10.020.

Penel, N., M. Van Glabbeke, S. Marreaud, M. Ouali, J. Y. Blay, and P. Hohenberger. 2011. "Testing New Regimens in Patients with Advanced Soft Tissue Sarcoma: Analysis of Publications from the Last 10 Years." *Annals of Oncology* 22 (6): 1266–72. https://doi.org/10.1093/annonc/mdq608.

Penel, N., A. Italiano, N. Isambert, E. Bompas, G. Bousquet, and F. Duffaud. 2009. "Factors Affecting the Outcome of Patients with Metastatic Leiomyosarcoma Treated with Doxorubicin-Containing Chemotherapy." *Annals of Oncology* 21 (6): 1361–65. https://doi.org/10.1093/annonc/mdp485.

Perut, Francesca, Francesca V. Sbrana, Sofia Avnet, Angelo De Milito, and Nicola Baldini. 2018. "Spheroid-Based 3D Cell Cultures Identify Salinomycin as a Promising Drug for the Treatment of Chondrosarcoma." *Journal of Orthopaedic Research®* 36 (8): 2305–12. https://doi.org/10.1002/JOR.23880.

Pervaiz, Nabeel, Nigel Colterjohn, Forough Farrokhyar, Richard Tozer, Alvaro Figueredo, and Michelle Ghert. 2008. "A Systematic Meta-Analysis of Randomized Controlled Trials of Adjuvant Chemotherapy for Localized Resectable Soft-Tissue Sarcoma." *Cancer* 113 (3): 573–81. https://doi.org/10.1002/CNCR.23592.

Pettitt, Stephen J., Jessica R. Frankum, Marco Punta, Stefano Lise, John Alexander, Yi Chen, Timothy A. Yap, Syed Haider, Andrew N.J. Tutt, and Christopher J. Lord. 2020. "Clinical Brca1/2 Reversion Analysis Identifies Hotspot Mutations and Predicted Neoantigens Associated with Therapy Resistance." *Cancer Discovery* 10 (10): 1475–88. https://doi.org/10.1158/2159-8290.CD-19-1485/333449/AM/CLINICAL-BRCA1-2-REVERSION-ANALYSIS-IDENTIFIES.

Pettitt, Stephen J., Dragomir B. Krastev, Inger Brandsma, Amy Dréan, Feifei Song, Radoslav Aleksandrov, Maria I. Harrell, et al. 2018. "Genome-Wide and High-Density CRISPR-Cas9 Screens Identify Point Mutations in PARP1 Causing PARP Inhibitor Resistance." *Nature Communications* 9 (1). https://doi.org/10.1038/s41467-018-03917-2.

Pham, Nhu An, Nikolina Radulovich, Emin Ibrahimov, Sebastiao N. Martins-Filho, Quan Li, Melania Pintilie, Jessica Weiss, et al. 2021. "Patient-Derived Tumor Xenograft and Organoid Models Established from Resected Pancreatic, Duodenal and Biliary Cancers." *Scientific Reports 2021 11:1* 11 (1): 1–12. https://doi.org/10.1038/s41598-021-90049-1.

Philip, Charles André, Ido Laskov, Marie Claude Beauchamp, Maud Marques, Oreekha Amin, Joanna Bitharas, Roy Kessous, et al. 2017. "Inhibition of PI3K-AKT-MTOR Pathway Sensitizes Endometrial Cancer Cell Lines to PARP Inhibitors." *BMC Cancer* 17 (1): 1–11. https://doi.org/10.1186/S12885-017-3639-0/FIGURES/4.

Phillips, Edward, Robin L. Jones, Paul Huang, and Antonia Digklia. 2022. "Efficacy of Eribulin in Soft Tissue Sarcomas." *Frontiers in Pharmacology* 0 (March): 1104. https://doi.org/10.3389/FPHAR.2022.869754.

Pickup, Michael W, Janna K Mouw, and Valerie M Weaver. 2014. "The Extracellular Matrix Modulates the Hallmarks of Cancer." *EMBO Reports* 15 (12): 1243–53. https://doi.org/10.15252/EMBR.201439246.

Pienta, Kenneth J. 2001. "Preclinical Mechanisms of Action of Docetaxel and Docetaxel Combinations in Prostate Cancer." *Seminars in Oncology* 28 (4 Suppl 15): 3–7. https://doi.org/10.1016/S0093-7754(01)90148-4.

Pignochino, Ymera, Federica Capozzi, Lorenzo D'Ambrosio, Carmine Dell'Aglio, Marco Basiricò, Marta Canta, Annalisa Lorenzato, et al. 2017. "PARP1 Expression Drives the Synergistic

Antitumor Activity of Trabectedin and PARP1 Inhibitors in Sarcoma Preclinical Models." *Molecular Cancer* 16 (1): 1–15. https://doi.org/10.1186/S12943-017-0652-5/FIGURES/6.

Pignochino, Ymera, Giovanni Crisafulli, Giorgia Giordano, Alessandra Merlini, Enrico Berrino, Maria Laura Centomo, Giulia Chiabotto, et al. 2021. "Parp1 Inhibitor and Trabectedin Combination Does Not Increase Tumor Mutational Burden in Advanced Sarcomas—a Preclinical and Translational Study." *Cancers* 13 (24). https://doi.org/10.3390/CANCERS13246295/S1.

Piha-Paul, Sarina A., Matthew H. Taylor, Daniel Spitz, Lee Schwartzberg, J. Thaddeus Beck, Todd M. Bauer, Funda Meric-Bernstam, et al. 2019. "Efficacy and Safety of Buparlisib, a PI3K Inhibitor, in Patients with Malignancies Harboring a PI3K Pathway Activation: A Phase 2, Open-Label, Single-Arm Study." *Oncotarget* 10 (60): 6526. https://doi.org/10.18632/ONCOTARGET.27251.

Plaat, B E, H Hollema, W M Molenaar, G H Torn Broers, J Pijpe, M F Mastik, H J Hoekstra, E van den Berg, R J Scheper, and W T van der Graaf. 2000. "Soft Tissue Leiomyosarcomas and Malignant Gastrointestinal Stromal Tumors: Differences in Clinical Outcome and Expression of Multidrug Resistance Proteins." *Journal of Clinical Oncology* 18 (18): 3211–20. https://doi.org/10.1200/JCO.2000.18.18.3211.

Plummer, Ruth, Christopher Jones, Mark Middleton, Richard Wilson, Jeffrey Evans, Anna Olsen, Nicola Curtin, et al. 2008. "Phase I Study of the Poly(ADP-Ribose) Polymerase Inhibitor, AG014699, in Combination with Temozolomide in Patients with Advanced Solid Tumors." *Clinical Cancer Research* 14 (23): 7917–23. https://doi.org/10.1158/1078-0432.CCR-08-1223.

Plummer, Ruth, Paul Lorigan, Neil Steven, Lucy Scott, Mark R. Middleton, Richard H. Wilson, Evan Mulligan, et al. 2013. "A Phase II Study of the Potent PARP Inhibitor, Rucaparib (PF-01367338, AG014699), with Temozolomide in Patients with Metastatic Melanoma Demonstrating Evidence of Chemopotentiation." *Cancer Chemotherapy and Pharmacology 2013 71:5* 71 (5): 1191–99. https://doi.org/10.1007/S00280-013-2113-1.

Plunkett, W., P. Huang, and V. Gandhi. 1995. "Preclinical Characteristics of Gemcitabine." *Anti-Cancer Drugs* 6 Suppl 6 (SUPPL. 6): 7–13. https://doi.org/10.1097/00001813-199512006-00002.

Podar, Klaus, Giovanni Tonon, Martin Sattler, Yu Tsu Tai, Steven LeGouill, Hiroshi Yasui, Kenji Ishitsuka, et al. 2006. "The Small-Molecule VEGF Receptor Inhibitor Pazopanib (GW786034B) Targets Both Tumor and Endothelial Cells in Multiple Myeloma." *Proceedings of the National Academy of Sciences of the United States of America* 103 (51): 19478–83. https://doi.org/10.1073/PNAS.0609329103/SUPPL_FILE/09329FIG6.PDF.

Pommier, Yves, Elisabetta Leo, Hongliang Zhang, and Christophe Marchand. 2010. "DNA Topoisomerases and Their Poisoning by Anticancer and Antibacterial Drugs." *Chemistry & Biology* 17 (5): 421–33. https://doi.org/10.1016/J.CHEMBIOL.2010.04.012.

Price, Daniel J., J. Russell Grove, Victor Calvo, Joseph Avruch, and Barbara E. Bierer. 1992. "Rapamycin-Induced Inhibition of the 70-Kilodalton S6 Protein Kinase." *Science* 257 (5072): 973–77. https://doi.org/10.1126/SCIENCE.1380182.

Primeau, Andrew J., Augusto Rendon, David Hedley, Lothar Lilge, and Ian F. Tannock. 2005. "The Distribution of the Anticancer Drug Doxorubicin in Relation to Blood Vessels in Solid Tumors." *Clinical Cancer Research* 11 (24): 8782–88. https://doi.org/10.1158/1078-0432.CCR-05-1664.

Przybyl, Joanna, Jacob J. Chabon, Lien Spans, Kristen N. Ganjoo, Sujay Vennam, Aaron M. Newman, Erna Forgo, et al. 2018. "Combination Approach for Detecting Different Types of Alterations in Circulating Tumor DNA in Leiomyosarcoma." *Clinical Cancer Research* 24 (11): 2688–99. https://doi.org/10.1158/1078-0432.CCR-17-3704/15257/AM/COMBINATION-APPROACH-FOR-DETECTING-DIFFERENT-TYPES.

Pujade-Lauraine, Eric, Jonathan A. Ledermann, Frédéric Selle, Val Gebski, Richard T. Penson, Amit M. Oza, Jacob Korach, et al. 2017. "Olaparib Tablets as Maintenance Therapy in Patients with Platinum-Sensitive, Relapsed Ovarian Cancer and a BRCA1/2 Mutation (SOLO2/ENGOT-Ov21): A Double-Blind, Randomised, Placebo-Controlled, Phase 3 Trial." *The Lancet. Oncology* 18 (9): 1274–84. https://doi.org/10.1016/S1470-2045(17)30469-2.

Raish, Mohammad, Mohsin Khurshid, Mushtaq Ahmad Ansari, Pankaj Kumar Chaturvedi, Su Mi Bae, Jang Heub Kim, Eun Kyung Park, Dong Chun Park, and Woong Shick Ahn. 2012. "Analysis of Molecular Cytogenetic Alterations in Uterine Leiomyosarcoma by Array-Based Comparative Genomic Hybridization." *Journal of Cancer Research and Clinical Oncology 2012 138:7* 138 (7): 1173–86. https://doi.org/10.1007/S00432-012-1182-6.

Rao, Trisha, Jill J. Ranger, Harvey W. Smith, Sonya H. Lam, Lewis Chodosh, and William J. Muller. 2014. "Inducible and Coupled Expression of the Polyomavirus Middle T Antigen and Cre Recombinase in Transgenic Mice: An in Vivo Model for Synthetic Viability in Mammary Tumour Progression." *Breast Cancer Research* 16 (1): 1–14. https://doi.org/10.1186/BCR3603/TABLES/1.

Raphael, Benjamin J., Ralph H. Hruban, Andrew J. Aguirre, Richard A. Moffitt, Jen Jen Yeh, Chip Stewart, A. Gordon Robertson, et al. 2017. "Integrated Genomic Characterization of Pancreatic Ductal Adenocarcinoma." *Cancer Cell* 32 (2): 185-203.e13. https://doi.org/10.1016/J.CCELL.2017.07.007/ATTACHMENT/80C14F16-B71C-486D-906A-9E50A53F88B3/MMC10.XLSX.

Rascio, Federica, Federica Spadaccino, Maria Teresa Rocchetti, Giuseppe Castellano, Giovanni Stallone, Giuseppe Stefano Netti, and Elena Ranieri. 2021. "The Pathogenic Role of PI3K/AKT Pathway in Cancer Onset and Drug Resistance: An Updated Review." *Cancers 2021, Vol. 13, Page 3949* 13 (16): 3949. https://doi.org/10.3390/CANCERS13163949.

Raudvere, Uku, Liis Kolberg, Ivan Kuzmin, Tambet Arak, Priit Adler, Hedi Peterson, and Jaak Vilo. 2019. "G:Profiler: A Web Server for Functional Enrichment Analysis and Conversions of Gene Lists (2019 Update)." *Nucleic Acids Research* 47 (W1): W191–98. https://doi.org/10.1093/NAR/GKZ369.

Rebbeck, Timothy R., Tara M. Friebel, Eitan Friedman, Ute Hamann, Dezheng Huo, Ava Kwong, Edith Olah, et al. 2018. "Mutational Spectrum in a Worldwide Study of 29,700 Families with BRCA1 or BRCA2 Mutations." *Human Mutation* 39 (5): 593–620. https://doi.org/10.1002/HUMU.23406.

Rebelo de Almeida, Cátia, Raquel Valente Mendes, Anna Pezzarossa, Joaquim Gago, Carlos Carvalho, António Alves, Vitor Nunes, et al. 2020. "Zebrafish Xenografts as a Fast Screening Platform for Bevacizumab Cancer Therapy." *Communications Biology 2020 3:1* 3 (1): 1–13. https://doi.org/10.1038/s42003-020-1015-0.

Redpath, Nicholas T., Emily J. Foulstone, and Christopher G. Proud. 1996. "Regulation of Translation Elongation Factor-2 by Insulin via a Rapamycin-Sensitive Signalling Pathway." *The EMBO Journal* 15 (9): 2291–97. https://doi.org/10.1002/J.1460-2075.1996.TB00582.X.

Rees, Douglas C., Eric Johnson, and Oded Lewinson. 2009. "ABC Transporters: The Power to Change." *Nature Reviews. Molecular Cell Biology* 10 (3): 218.

https://doi.org/10.1038/NRM2646.

Rey, Veronica, Sofia T. Menendez, Oscar Estupiñan, Aida Rodriguez, Laura Santos, Juan Tornin, Lucia Martinez-Cruzado, et al. 2019. "New Chondrosarcoma Cell Lines with Preserved Stem Cell Properties to Study the Genomic Drift During In Vitro/In Vivo Growth." *Journal of Clinical Medicine* 8 (4): 455. https://doi.org/10.3390/JCM8040455.

Risbridger, Gail P., Mitchell G. Lawrence, and Renea A. Taylor. 2020. "PDX: Moving Beyond Drug Screening to Versatile Models for Research Discovery." *Journal of the Endocrine Society* 4 (11). https://doi.org/10.1210/JENDSO/BVAA132.

Roberts, Maureen E., Jason T. Aynardi, and Christina S. Chu. 2018. "Uterine Leiomyosarcoma: A Review of the Literature and Update on Management Options." *Gynecologic Oncology* 151 (3): 562–72. https://doi.org/10.1016/J.YGYNO.2018.09.010.

Robin, Thibault, Amanda Capes-Davis, and Amos Bairoch. 2020. "CLASTR: The Cellosaurus STR Similarity Search Tool - A Precious Help for Cell Line Authentication." *International Journal of Cancer* 146 (5): 1299–1306. https://doi.org/10.1002/IJC.32639.

Robson, M. E., N. Tung, P. Conte, S. A. Im, E. Senkus, B. Xu, N. Masuda, et al. 2019. "OlympiAD Final Overall Survival and Tolerability Results: Olaparib versus Chemotherapy Treatment of Physician's Choice in Patients with a Germline BRCA Mutation and HER2-Negative Metastatic Breast Cancer." *Annals of Oncology* 30 (4): 558–66. https://doi.org/10.1093/annonc/mdz012.

Rogakou, Emmy P., Duane R. Pilch, Ann H. Orr, Vessela S. Ivanova, and William M. Bonner. 1998. "DNA Double-Stranded Breaks Induce Histone H2AX Phosphorylation on Serine 139." *Journal of Biological Chemistry* 273 (10): 5858–68. https://doi.org/10.1074/jbc.273.10.5858.

Romero-López, Mónica, Andrew L. Trinh, Agua Sobrino, Michaela M.S. Hatch, Mark T. Keating, Cristhian Fimbres, David E. Lewis, et al. 2017. "Recapitulating the Human Tumor Microenvironment: Colon Tumor-Derived Extracellular Matrix Promotes Angiogenesis and Tumor Cell Growth." *Biomaterials* 116 (February): 118–29. https://doi.org/10.1016/J.BIOMATERIALS.2016.11.034.

Ronson, George E., Ann Liza Piberger, Martin R. Higgs, Anna L. Olsen, Grant S. Stewart, Peter J. McHugh, Eva Petermann, and Nicholas D. Lakin. 2018. "PARP1 and PARP2 Stabilise Replication Forks at Base Excision Repair Intermediates through Fbh1-Dependent Rad51 Regulation." *Nature Communications 2018 9:1* 9 (1): 1–12. https://doi.org/10.1038/s41467-018-03159-2.

Rööser, B, H Pettersson, and T Alvegård. 1987. "Growth Rate of Pulmonary Metastases from Soft Tissue Sarcoma." *Acta Oncologica* 26 (3): 189–92. https://doi.org/10.3109/02841868709091429.

Rosa, Fausto, Claudio Fiorillo, Antonio Pio Tortorelli, Alejandro Martin Sánchez, Guido Costamagna, Giovanni Battista Doglietto, and Sergio Alfieri. 2016. "Surgical Management of Retroperitoneal Soft Tissue Sarcomas: Role of Curative Resection." *The American Surgeon* 82 (2): 128–33. https://doi.org/10.1177/000313481608200215.

Rosai, Juan, Mans Akerman, Paola Dal Cin, Ivo DeWever, Christopher D.M. Fletcher, Nils Mandahl, Fredrik Mertens, et al. 1996. "Combined Morphologic and Karyotypic Study of 59 Atypical Lipomatous Tumors. Evaluation of Their Relationship and Differential Diagnosis with Other Adipose Tissue Tumors (a Report of the CHAMP Study Group)." *The American Journal of Surgical Pathology* 20 (10): 1182–89. https://doi.org/10.1097/00000478-

199610000-00002.

Rosenbaum, Evan, Philip Jonsson, Kenneth Seier, Ping Chi, Mark Andrew Dickson, Mrinal M. Gounder, Ciara Marie Kelly, et al. 2019. "DNA Damage Response Pathway Alterations and Clinical Outcome in Leiomyosarcoma." *Journal of Clinical Oncology* 37 (15_suppl): 11048–11048. https://doi.org/10.1200/JCO.2019.37.15_SUPPL.11048.

Rosenbaum, Evan, Philip Jonsson, Kenneth Seier, Li-Xuan Qin, Ping Chi, Mark Dickson, Mrinal Gounder, et al. 2020. "Clinical Outcome of Leiomyosarcomas With Somatic Alteration in Homologous Recombination Pathway Genes." *Https://Doi.Org/10.1200/PO.20.00122*, no. 4 (November): 1350–60. https://doi.org/10.1200/PO.20.00122.

Rosenberger, George, Ching Chiek Koh, Tiannan Guo, Hannes L. Röst, Petri Kouvonen, Ben C. Collins, Moritz Heusel, et al. 2014. "A Repository of Assays to Quantify 10,000 Human Proteins by SWATH-MS." *Scientific Data* 1 (1): 1–15. https://doi.org/10.1038/sdata.2014.31.

Ross, Christina, Karol Szczepanek, Maxwell Lee, Howard Yang, Cody J. Peer, Jessica Kindrick, Priya Shankarappa, et al. 2020. "Metastasis-Specific Gene Expression in Autochthonous and Allograft Mouse Mammary Tumor Models: Stratification and Identification of Targetable Signatures." *Molecular Cancer Research* 18 (9). https://doi.org/10.1158/1541-7786.MCR-20-0046.

Rothkamm, Kai, Martin Kü, Penny A Jeggo, and Markus Löbrich. 2001. "Radiation-Induced Genomic Rearrangements Formed by Nonhomologous End-Joining of DNA Double-Strand Breaks 1." *CANCER RESEARCH* 61: 3886–93. http://aacrjournals.org/cancerres/article-pdf/61/10/3886/2484982/ch100103886.pdf.

Russell, Tara A., Mark A. Eckardt, Takashi Murakami, Irmina A. Elliott, Kei Kawaguchi, Tasuku Kiyuna, Kentaro Igarashi, et al. 2017. "Clinical Factors That Affect the Establishment of Soft Tissue Sarcoma Patient-Derived Orthotopic Xenografts: A University of California, Los Angeles, Sarcoma Program Prospective Clinical Trial." *JCO Precision Oncology*, no. 1. https://doi.org/10.1200/po.17.00071.

Ryan, Christopher W., Ofer Merimsky, Mark Agulnik, Jean Yves Blay, Scott M. Schuetze, Brian A. Van Tine, Robin L. Jones, et al. 2016. "PICASSO III: A Phase III, Placebo-Controlled Study of Doxorubicin with or without Palifosfamide in Patients with Metastatic Soft Tissue Sarcoma." *Journal of Clinical Oncology* 34 (32): 3898–3905. https://doi.org/10.1200/JCO.2016.67.6684.

Ryu, Hyun Hee, Minkyung Kang, Jinsil Park, Sung Hye Park, and Yong Seok Lee. 2019. "Enriched Expression of NF1 in Inhibitory Neurons in Both Mouse and Human Brain." *Molecular Brain* 12 (1): 1–5. https://doi.org/10.1186/S13041-019-0481-0/FIGURES/1.

Sachs, Norman, Joep de Ligt, Oded Kopper, Ewa Gogola, Gergana Bounova, Fleur Weeber, Anjali Vanita Balgobind, et al. 2018. "A Living Biobank of Breast Cancer Organoids Captures Disease Heterogeneity." *Cell* 172 (1–2): 373-386.e10. https://doi.org/10.1016/j.cell.2017.11.010.

Sachs, Norman, Angelos Papaspyropoulos, Domenique D Zomer-van Ommen, Inha Heo, Lena Böttinger, Dymph Klay, Fleur Weeber, et al. 2019. "Long-term Expanding Human Airway Organoids for Disease Modeling." *The EMBO Journal* 38 (4). https://doi.org/10.15252/embj.2018100300.

Sakai, Wataru, Elizabeth M. Swisher, Beth Y. Karlan, Mukesh K. Agarwal, Jake Higgins, Cynthia Friedman, Emily Villegas, et al. 2008. "Secondary Mutations as a Mechanism of Cisplatin

Resistance in BRCA2-Mutated Cancers." *Nature* 451 (7182). https://doi.org/10.1038/nature06633.

Salawu, Abdulazeez, Malee Fernando, David Hughes, Malcolm W R Reed, Penella Woll, Claire Greaves, Chris Day, Meshal Alhajimohammed, and Karen Sisley. 2016. "Establishment and Molecular Characterisation of Seven Novel Soft-Tissue Sarcoma Cell Lines." *British Journal of Cancer* 115 (9): 1058–68. https://doi.org/10.1038/bjc.2016.259.

Salazar, Ramon, Rocio Garcia-Carbonero, Steven K Libutti, Andrew E Hendifar, Ana Custodio, Rosine Guimbaud, Catherine Lombard-Bohas, et al. 2018. "Phase II Study of BEZ235 versus Everolimus in Patients with Mammalian Target of Rapamycin Inhibitor-Naïve Advanced Pancreatic Neuroendocrine Tumors." *The Oncologist* 23 (7): 766-e90. https://doi.org/10.1634/THEONCOLOGIST.2017-0144.

Salerno, Manuela, Sofia Avnet, Gloria Bonuccelli, Adriana Eramo, Ruggero De Maria, Marco Gambarotti, Gabriella Gamberi, and Nicola Baldini. 2013. "Sphere-Forming Cell Subsets with Cancer Stem Cell Properties in Human Musculoskeletal Sarcomas." *International Journal of Oncology* 43 (1): 95–102. https://doi.org/10.3892/ijo.2013.1927.

Sanada, Sakiko, Kimio Ushijima, Hiroyuki Yanai, Yoshiki Mikami, Yoshihiro Ohishi, Hiroaki Kobayashi, Hironori Tashiro, Mikio Mikami, Shingo Miyamoto, and Hidetaka Katabuchi. 2022. "A Critical Review of 'Uterine Leiomyoma' with Subsequent Recurrence or Metastasis: A Multicenter Study of 62 Cases." *The Journal of Obstetrics and Gynaecology Research* 48 (12). https://doi.org/10.1111/JOG.15426.

Sargos, Paul, Marie Pierre Sunyach, Anne Ducassou, Carmen Llacer, Carine A. Bellera, Audrey Michot, Thibaud Valentin, et al. 2022. "Preliminary Results of a Phase IB Study of Olaparib with Concomitant Radiotherapy in Locally Advanced/Unresectable Soft-Tissue Sarcoma from the French Sarcoma Group." *Journal of Clinical Oncology* 40 (16_suppl): 11522–11522. https://doi.org/10.1200/JCO.2022.40.16_SUPPL.11522.

Sartori, Alessandro A., Claudia Lukas, Julia Coates, Martin Mistrik, Shuang Fu, Jiri Bartek, Richard Baer, Jiri Lukas, and Stephen P. Jackson. 2007. "Human CtIP Promotes DNA End Resection." *Nature 2007 450:7169* 450 (7169): 509–14. https://doi.org/10.1038/nature06337.

Sathe, Anuja, Géraldine Chalaud, Immanuel Oppolzer, Kit Yeng Wong, Margarita von Busch, Sebastian C. Schmid, Zhichao Tong, et al. 2018. "Parallel PI3K, AKT and MTOR Inhibition Is Required to Control Feedback Loops That Limit Tumor Therapy." *PLoS ONE* 13 (1). https://doi.org/10.1371/journal.pone.0190854.

Sato, Toshiro, Robert G. Vries, Hugo J. Snippert, Marc Van De Wetering, Nick Barker, Daniel E. Stange, Johan H. Van Es, et al. 2009. "Single Lgr5 Stem Cells Build Crypt-Villus Structures in Vitro without a Mesenchymal Niche." *Nature 2009 459:7244* 459 (7244): 262–65. https://doi.org/10.1038/nature07935.

Satoh, Masahiko S., and Tomas Lindahl. 1992. "Role of Poly(ADP-Ribose) Formation in DNA Repair." *Nature* 356 (6367): 356–58. https://doi.org/10.1038/356356A0.

Savina, Marion, Axel Le Cesne, Jean Yves Blay, Isabelle Ray-Coquard, Olivier Mir, Maud Toulmonde, Sophie Cousin, et al. 2017. "Patterns of Care and Outcomes of Patients with METAstatic Soft Tissue SARComa in a Real-Life Setting: The METASARC Observational Study." *BMC Medicine* 15 (1): 1–11. https://doi.org/10.1186/S12916-017-0831-7/FIGURES/3.

Schaefer, Inga Marie, Meijun Z. Lundberg, Elizabeth G. Demicco, Joanna Przybyl, Magdalena Matusiak, Frédéric Chibon, Davis R. Ingram, et al. 2021. "Relationships between Highly

Recurrent Tumor Suppressor Alterations in 489 Leiomyosarcomas." *Cancer* 127 (15). https://doi.org/10.1002/cncr.33542.

Schmucker, Stephane, and Izabela Sumara. 2014. "Molecular Dynamics of PLK1 during Mitosis." *Molecular & Cellular Oncology* 1 (2). https://doi.org/10.1080/23723548.2014.954507.

Schneider, Johann W., and Dirk P. Dittmer. 2017. "Diagnosis and Treatment of Kaposi Sarcoma." *American Journal of Clinical Dermatology 2017 18:4* 18 (4): 529–39. https://doi.org/10.1007/S40257-017-0270-4.

Schoenwolf, Gary C., Steven B. Bleyl, Philip R. Brauer, and Philippa H. Francis-West. 2020. "Larsen's Human Embryology ," November. https://www.elsevier.com/books/larsens-human-embryology/schoenwolf/978-0-323-69604-3.

Schöffski, Patrick, Isabelle Laure Ray-Coquard, Angela Cioffi, Nguyen Bin Bui, Sebastian Bauer, Joerg Thomas Hartmann, Anders Krarup-Hansen, et al. 2011. "Activity of Eribulin Mesylate in Patients with Soft-Tissue Sarcoma: A Phase 2 Study in Four Independent Histological Subtypes." *The Lancet Oncology* 12 (11): 1045–52. https://doi.org/10.1016/S1470-2045(11)70230-3.

Schoffski, Patrick, Britt Van Renterghem, Jasmien Cornillie, Yannick Wang, Yemarshet Kelemework Gebreyohannes, Che-Jui Lee, Jasmien Wellens, et al. 2019. "XenoSarc: A Comprehensive Platform of Patient-Derived Xenograft (PDX) Models of Soft Tissue Sarcoma (STS) for Early Drug Testing." *Journal of Clinical Oncology* 5 (October): 37–37. https://doi.org/10.1200/JGO.2019.5.SUPPL.37.

Schuth, Sebastian, Solange Le Blanc, Teresa G. Krieger, Julia Jabs, Miriam Schenk, Nathalia A. Giese, Markus W. Büchler, Roland Eils, Christian Conrad, and Oliver Strobel. 2022. "Patient-Specific Modeling of Stroma-Mediated Chemoresistance of Pancreatic Cancer Using a Three-Dimensional Organoid-Fibroblast Co-Culture System." *Journal of Experimental and Clinical Cancer Research* 41 (1): 1–14. https://doi.org/10.1186/S13046-022-02519-7/FIGURES/5.

Schütte, Moritz, Thomas Risch, Nilofar Abdavi-Azar, Karsten Boehnke, Dirk Schumacher, Marlen Keil, Reha Yildiriman, et al. 2017. "Molecular Dissection of Colorectal Cancer in Pre-Clinical Models Identifies Biomarkers Predicting Sensitivity to EGFR Inhibitors." *Nature Communications 2017 8:1* 8 (1): 1–19. https://doi.org/10.1038/ncomms14262.

Schweizer, Michael T., Kathleen Haugk, Jožefa S. McKiernan, Roman Gulati, Heather H. Cheng, Jessica L. Maes, Ruth F. Dumpit, et al. 2018. "A Phase I Study of Niclosamide in Combination with Enzalutamide in Men with Castration-Resistant Prostate Cancer." *PLoS ONE* 13 (6). https://doi.org/10.1371/JOURNAL.PONE.0198389.

Scurr, Michelle. 2011. "Histology-Driven Chemotherapy in Soft Tissue Sarcomas." *Current Treatment Options in Oncology 2011 12:1* 12 (1): 32–45. https://doi.org/10.1007/S11864-011-0140-X.

Seale, Patrick, Bryan Bjork, Wenli Yang, Shingo Kajimura, Sherry Chin, Shihuan Kuang, Anthony Scimè, et al. 2008. "PRDM16 Controls a Brown Fat/Skeletal Muscle Switch." *Nature* 454 (7207): 961. https://doi.org/10.1038/NATURE07182.

Seddon, Beatrice, Sandra J. Strauss, Jeremy Whelan, Michael Leahy, Penella J. Woll, Fiona Cowie, Christian Rothermundt, et al. 2017. "Gemcitabine and Docetaxel versus Doxorubicin as First-Line Treatment in Previously Untreated Advanced Unresectable or Metastatic Soft-Tissue Sarcomas (GeDDiS): A Randomised Controlled Phase 3 Trial." *The Lancet Oncology* 18 (10): 1397–1410. https://doi.org/10.1016/S1470-2045(17)30622-8.

Sekulovski, Nikola, James A. MacLean, Sambasiva R. Bheemireddy, Zhifeng Yu, Hiroshi Okuda, Cindy Pru, Kyle N. Plunkett, Martin Matzuk, and Kanako Hayashi. 2021. "Niclosamide's Potential Direct Targets in Ovarian Cancer." *Biology of Reproduction* 105 (2): 403–12. https://doi.org/10.1093/BIOLRE/IOAB071.

Seligson, Nathan D., Esko A. Kautto, Edward N. Passen, Colin Stets, Amanda E. Toland, Sherri Z. Millis, Christian F. Meyer, John L. Hays, and James L. Chen. 2019. "BRCA1/2 Functional Loss Defines a Targetable Subset in Leiomyosarcoma." *The Oncologist* 24 (7): 973–79. https://doi.org/10.1634/THEONCOLOGIST.2018-0448.

Seligson, Nathan D., Joy Tang, Dexter X. Jin, Monica P. Bennett, Julia A. Elvin, Kiley Graim, John L. Hays, Sherri Z. Millis, Wayne O. Miles, and James L. Chen. 2022. "Drivers of Genomic Loss of Heterozygosity in Leiomyosarcoma Are Distinct from Carcinomas." *Npj Precision Oncology 2022 6:1* 6 (1): 1–8. https://doi.org/10.1038/s41698-022-00271-x.

Serra, Violeta, Ben Markman, Maurizio Scaltriti, Pieter J.A. Eichhorn, Vanesa Valero, Marta Guzman, Maria Luisa Botero, et al. 2008. "NVP-BEZ235, a Dual PI3K/MTOR Inhibitor, Prevents PI3K Signaling and Inhibits the Growth of Cancer Cells with Activating PI3K Mutations." *Cancer Research* 68 (19). https://doi.org/10.1158/0008-5472.CAN-08-1385.

Serrano, Cesar, and Suzanne George. 2013. "Leiomyosarcoma." *Hematology/Oncology Clinics of North America* 27 (5): 957–74. https://doi.org/10.1016/J.HOC.2013.07.002.

Shai, Ruty, Tao Shi, Thomas J. Kremen, Steve Horvath, Linda M. Liau, Timothy F. Cloughesy, Paul S. Mischel, and Stanley F. Nelson. 2003. "Gene Expression Profiling Identifies Molecular Subtypes of Gliomas." *Oncogene 2003 22:31* 22 (31): 4918–23. https://doi.org/10.1038/sj.onc.1206753.

Shammas, Natalie, Tiffany Yang, Alireza Abidi, Malaika Amneus, and Melissa Hodeib. 2022. "Clinical Use of PARP Inhibitor in Recurrent Uterine Leiomyosarcoma with Presence of a Somatic BRCA2 Mutation." *Gynecologic Oncology Reports* 42 (August): 2352–5789. https://doi.org/10.1016/J.GORE.2022.101044.

Sharma, Sheetal, Shweta Takyar, Stephanie C. Manson, Sarah Powell, and Nicolas Penel. 2013. "Efficacy and Safety of Pharmacological Interventions in Second- or Later-Line Treatment of Patients with Advanced Soft Tissue Sarcoma: A Systematic Review." *BMC Cancer* 13 (1): 1–21. https://doi.org/10.1186/1471-2407-13-385/TABLES/6.

Shen, Qi, Wei Feng, Michael S. Long, Xiuzhen Duan, Siraya Jaijakul, Cesar A. Arias, Robert E. Brown, and Bihong Zhao. 2011. "Multicentric Hepatic EBV-Associated Smooth Muscle Tumors in an AIDS Patient: A Case Report, Investigation of MTOR Activation and Review of the Literature." *International Journal of Clinical and Experimental Pathology* 4 (4): 421. /pmc/articles/PMC3093067/.

Shen, Rui, Bo Liu, Xuesen Li, Tengbo Yu, Kuishuai Xu, and Jinfeng Ma. 2021. "Development and Validation of an Immune Gene-Set Based Prognostic Signature for Soft Tissue Sarcoma." *BMC Cancer* 21 (1): 1–14. https://doi.org/10.1186/S12885-021-07852-2/FIGURES/8.

Shihabi, Ahmad Al, Peyton J. Tebon, Jomjit Chantharasamee, Huyen T. Nguyen, Sara Sartini, Ardalan Davarifar, Nasrin Tavanaie, et al. 2022. "A Pipeline for Functional Precision Medicine in Bone and Soft Tissue Sarcoma Organoids." *Cancer Research* 82 (12_Supplement): 3078–3078. https://doi.org/10.1158/1538-7445.AM2022-3078.

Siebert, Jakob, Michaela Schneider, Daniela Reuter-Schmitt, Julia Würtemberger, Annette Neubüser, Wolfgang Driever, Simone Hettmer, and Friedrich G. Kapp. 2023. "Rhabdomyosarcoma Xenotransplants in Zebrafish Embryos." *Pediatric Blood & Cancer* 70

(1): e30053. https://doi.org/10.1002/PBC.30053.

Sleijfer, Stefan, Monia Ouali, Martine van Glabbeke, Anders Krarup-Hansen, Sjoerd Rodenhuis, Axel Le Cesne, Pancras C.W. Hogendoorn, Jaap Verweij, and Jean Yves Blay. 2010. "Prognostic and Predictive Factors for Outcome to First-Line Ifosfamide-Containing Chemotherapy for Adult Patients with Advanced Soft Tissue Sarcomas: An Exploratory, Retrospective Analysis on Large Series from the European Organization for Research and Treatment of Cancer-Soft Tissue and Bone Sarcoma Group (EORTC-STBSG)." *European Journal of Cancer* 46 (1): 72–83. https://doi.org/10.1016/J.EJCA.2009.09.022.

Smith, Jennifer A., Leslie Wilson, Olga Azarenko, Xiaojie Zhu, Bryan M. Lewis, Bruce A. Littlefield, and Mary Ann Jordan. 2010. "Eribulin Binds at Microtubule Ends to a Single Site on Tubulin to Suppress Dynamic Instability." *Biochemistry* 49 (6): 1331–37. https://doi.org/10.1021/BI901810U/ASSET/IMAGES/MEDIUM/BI-2009-01810U_0003.GIF.

Song, Min Sup, Leonardo Salmena, and Pier Paolo Pandolfi. 2012. "The Functions and Regulation of the PTEN Tumour Suppressor." *Nature Reviews Molecular Cell Biology 2012 13:5* 13 (5): 283–96. https://doi.org/10.1038/nrm3330.

Sonobe, H., Y. Manabe, M. Furihata, J. Iwata, T. Oka, Y. Ohtsuki, H. Mizobuchi, H. Yamamoto, O. Kumano, and S. Abe. 1992. "Establishment and Characterization of a New Human Synovial Sarcoma Cell Line, HS-SY-II." *Laboratory Investigation; a Journal of Technical Methods and Pathology* 67 (4): 498–505. https://europepmc.org/article/med/1331610.

Sørlie, Therese, Charles M. Perou, Robert Tibshirani, Turid Aas, Stephanie Geisler, Hilde Johnsen, Trevor Hastie, et al. 2001. "Gene Expression Patterns of Breast Carcinomas Distinguish Tumor Subclasses with Clinical Implications." *Proceedings of the National Academy of Sciences of the United States of America* 98 (19): 10869–74. https://doi.org/10.1073/PNAS.191367098/SUPPL_FILE/INDEX.HTML.

Souren, Nicole Y, Norbert E Fusenig, Stefanie Heck, Wilhelm G Dirks, Amanda Capes-Davis, Franca Bianchini, and Christoph Plass. 2022. "Cell Line Authentication: A Necessity for Reproducible Biomedical Research." *The EMBO Journal* 41 (14): e111307. https://doi.org/10.15252/EMBJ.2022111307.

Stacchiotti, Silvia, Anna Maria Frezza, Jean Yves Blay, Elizabeth H. Baldini, Sylvie Bonvalot, Judith V.M.G. Bovée, Dario Callegaro, et al. 2021. "Ultra-Rare Sarcomas: A Consensus Paper from the Connective Tissue Oncology Society Community of Experts on the Incidence Threshold and the List of Entities." *Cancer* 127 (16): 2934–42. https://doi.org/10.1002/CNCR.33618.

Stebbing, Justin, Keren Paz, Gary K. Schwartz, Leonard H. Wexler, Robert Maki, Raphael E. Pollock, Ronnie Morris, et al. 2014. "Patient-Derived Xenografts for Individualized Care in Advanced Sarcoma." *Cancer* 120 (13): 2006–15. https://doi.org/10.1002/CNCR.28696.

Steffensen, Karina Dahl, Parvin Adimi, and Anders Jakobsen. 2017. "Veliparib Monotherapy to Patients With BRCA Germ Line Mutation and Platinum-Resistant or Partially Platinum-Sensitive Relapse of Epithelial Ovarian Cancer: A Phase I/II Study." *International Journal of Gynecologic Cancer* 27 (9): 1842–49. https://doi.org/10.1097/IGC.0000000000001089.

Stiller, C. A., A. Trama, D. Serraino, S. Rossi, C. Navarro, M. D. Chirlaque, N. Zielonk, et al. 2013. "Descriptive Epidemiology of Sarcomas in Europe: Report from the RARECARE Project." *European Journal of Cancer* 49 (3): 684–95. https://doi.org/10.1016/J.EJCA.2012.09.011.

Sulzmaier, Florian J., Christine Jean, and David D. Schlaepfer. 2014. "FAK in Cancer: Mechanistic Findings and Clinical Applications." *Nature Reviews Cancer 2014 14:9* 14 (9): 598–610.

https://doi.org/10.1038/nrc3792.

Sun, Hua, Song Cao, R. Jay Mashl, Chia Kuei Mo, Simone Zaccaria, Michael C. Wendl, Sherri R. Davies, et al. 2021. "Comprehensive Characterization of 536 Patient-Derived Xenograft Models Prioritizes Candidates for Targeted Treatment." *Nature Communications 2021 12:1* 12 (1): 1–20. https://doi.org/10.1038/s41467-021-25177-3.

Szucs, Zoltan, Khin Thway, Cyril Fisher, Ramesh Bulusu, Anastasia Constantinidou, Charlotte Benson, Winette T.A. Van Der Graaf, and Robin L. Jones. 2017. "Molecular Subtypes of Gastrointestinal Stromal Tumors and Their Prognostic and Therapeutic Implications." *Future Oncology*. https://doi.org/10.2217/fon-2016-0192.

Taglialatela, Angelo, Silvia Alvarez, Giuseppe Leuzzi, Vincenzo Sannino, Lepakshi Ranjha, Jen Wei Huang, Chioma Madubata, et al. 2017. "Restoration of Replication Fork Stability in BRCA1- and BRCA2-Deficient Cells by Inactivation of SNF2-Family Fork Remodelers." *Molecular Cell* 68 (2): 414-430.e8. https://doi.org/10.1016/J.MOLCEL.2017.09.036.

Tan, Valerie P., and Shigeki Miyamoto. 2016. "Nutrient-Sensing MTORC1: Integration of Metabolic and Autophagic Signals." *Journal of Molecular and Cellular Cardiology* 95 (June): 31. https://doi.org/10.1016/J.YJMCC.2016.01.005.

Tang, L., W. Yu, Y. Wang, H. Li, and Z. Shen. 2019. "Anlotinib Inhibits Synovial Sarcoma by Targeting GINS1: A Novel Downstream Target Oncogene in Progression of Synovial Sarcoma." *Clinical & Translational Oncology* 21 (12): 1624–33. https://doi.org/10.1007/S12094-019-02090-2.

Tap, William D., Robin L. Jones, Brian A. Van Tine, Bartosz Chmielowski, Anthony D. Elias, Douglas Adkins, Mark Agulnik, et al. 2016. "Olaratumab and Doxorubicin versus Doxorubicin Alone for Treatment of Soft-Tissue Sarcoma: An Open-Label Phase 1b and Randomised Phase 2 Trial." *The Lancet* 388 (10043): 488–97. https://doi.org/10.1016/S0140-6736(16)30587-6.

Tap, William D., Andrew J. Wagner, Patrick Schöffski, Javier Martin-Broto, Anders Krarup-Hansen, Kristen N. Ganjoo, Chueh Chuan Yen, et al. 2020. "Effect of Doxorubicin Plus Olaratumab vs Doxorubicin Plus Placebo on Survival in Patients With Advanced Soft Tissue Sarcomas: The ANNOUNCE Randomized Clinical Trial." *JAMA* 323 (13): 1266–76. https://doi.org/10.1001/JAMA.2020.1707.

Tascilar, Metin, Walter J. Loos, Caroline Seynaeve, Jaap Verweij, and Stefan Sleijfer. 2007. "The Pharmacologic Basis of Ifosfamide Use in Adult Patients with Advanced Soft Tissue Sarcomas." *The Oncologist* 12 (11): 1351–60. https://doi.org/10.1634/THEONCOLOGIST.12-11-1351.

Taylor, Barry S., Jordi Barretina, Robert G. Maki, Cristina R. Antonescu, Samuel Singer, and Marc Ladanyi. 2011. "Advances in Sarcoma Genomics and New Therapeutic Targets." *Nature Reviews Cancer 2011 11:8* 11 (8): 541–57. https://doi.org/10.1038/nrc3087.

Tegze, Bálint, Zoltán Szállási, Irén Haltrich, Zsófia Pénzváltó, Zsuzsa Tóth, István Likó, and Balázs Gyorffy. 2012. "Parallel Evolution under Chemotherapy Pressure in 29 Breast Cancer Cell Lines Results in Dissimilar Mechanisms of Resistance." *PLOS ONE* 7 (2): e30804. https://doi.org/10.1371/JOURNAL.PONE.0030804.

Teicher, Beverly A., Eric Polley, Mark Kunkel, David Evans, Thomas Silvers, Rene Delosh, Julie Laudeman, et al. 2015. "Sarcoma Cell Line Screen of Oncology Drugs and Investigational Agents Identifies Patterns Associated with Gene and MicroRNA Expression." *Molecular Cancer Therapeutics* 14 (11): 2452. https://doi.org/10.1158/1535-7163.MCT-15-0074.

Thanapprapasr, Duangmani, Rebecca A. Previs, Wei Hu, Cristina Ivan, Guillermo N. Armaiz-Pena, Piotr L. Dorniak, Jean M. Hansen, et al. 2015. "PTEN Expression as a Predictor of Response to Focal Adhesion Kinase Inhibition in Uterine Cancer." *Molecular Cancer Therapeutics* 14 (6): 1466–75. https://doi.org/10.1158/1535-7163.MCT-14-1077/86080/AM/PTEN-EXPRESSION-AS-A-PREDICTOR-OF-RESPONSE-TO.

The Jackson Laboratory. 2022. "Patient-Derived Xenograft Models." 2022. https://www.jax.org/jax-mice-and-services/in-vivo-pharmacology/oncology-services/pdx-tumors.

Thorpe, Lauren M., Haluk Yuzugullu, and Jean J. Zhao. 2015. "PI3K in Cancer: Divergent Roles of Isoforms, Modes of Activation, and Therapeutic Targeting." *Nature Reviews. Cancer* 15 (1): 7. https://doi.org/10.1038/NRC3860.

Thway, K. 2009. "Pathology of Soft Tissue Sarcomas." *Clinical Oncology* 21 (9): 695–705. https://doi.org/10.1016/j.clon.2009.07.016.

Tian, Wei, Guowen Wang, Jilong Yang, Yi Pan, and Yulin Ma. 2013. "Prognostic Role of E-Cadherin and Vimentin Expression in Various Subtypes of Soft Tissue Leiomyosarcomas." *Medical Oncology (Northwood, London, England)* 30 (1). https://doi.org/10.1007/S12032-012-0401-Y.

Tilson, Samantha G., Elizabeth M. Haley, Ursula L. Triantafillu, David A. Dozier, Catherine P. Langford, G. Yancey Gillespie, Yonghyun Kim, and Anita B. Hjelmeland. 2015. "ROCK Inhibition Facilitates In Vitro Expansion of Glioblastoma Stem-Like Cells." *PLoS ONE* 10 (7). https://doi.org/10.1371/JOURNAL.PONE.0132823.

Tiriac, Hervé, Pascal Belleau, Dannielle D. Engle, Dennis Plenker, Astrid Deschênes, Tim D.D. Somerville, Fieke E.M. Froeling, et al. 2018. "Organoid Profiling Identifies Common Responders to Chemotherapy in Pancreatic Cancer." *Cancer Discovery* 8 (9): 1112–29. https://doi.org/10.1158/2159-8290.CD-18-0349/42871/AM/ORGANOID-PROFILING-IDENTIFIES-COMMON-RESPONDERS-TO.

Tomlinson, James, Sanford H. Barsky, Scott Nelson, Samuel Singer, Behnaz Pezeshki, Maggie C. Lee, Frederick Eilber, and Mai Nguyen. 1999. "Different Patterns of Angiogenesis in Sarcomas and Carcinomas." *Clinical Cancer Research* 5 (11).

Trucco, Matteo M., Christian F. Meyer, Katherine A. Thornton, Preeti Shah, Allen R. Chen, Breelyn A. Wilky, Maria A. Carrera-Haro, et al. 2018. "A Phase II Study of Temsirolimus and Liposomal Doxorubicin for Patients with Recurrent and Refractory Bone and Soft Tissue Sarcomas." *Clinical Sarcoma Research 2018 8:1* 8 (1): 1–9. https://doi.org/10.1186/S13569-018-0107-9.

Tusher, Virginia Goss, Robert Tibshirani, and Gilbert Chu. 2001. "Significance Analysis of Microarrays Applied to the Ionizing Radiation Response." *Proceedings of the National Academy of Sciences of the United States of America* 98 (9). https://doi.org/10.1073/pnas.091062498.

Tyanova, Stefka, Tikira Temu, Pavel Sinitcyn, Arthur Carlson, Marco Y. Hein, Tamar Geiger, Matthias Mann, and Jürgen Cox. 2016. "The Perseus Computational Platform for Comprehensive Analysis of (Prote)Omics Data." *Nature Methods 2016 13:9* 13 (9): 731–40. https://doi.org/10.1038/nmeth.3901.

Ueda, Shigeto, Toshiaki Saeki, Hideki Takeuchi, Takashi Shigekawa, Tomohiko Yamane, Ichiei Kuji, and Akihiko Osaki. 2016. "In Vivo Imaging of Eribulin-Induced Reoxygenation in Advanced Breast Cancer Patients: A Comparison to Bevacizumab." *British Journal of Cancer*

2016 114:11 114 (11): 1212–18. https://doi.org/10.1038/bjc.2016.122.

Vaidyanathan, Aparajitha, Lynne Sawers, Anne Louise Gannon, Probir Chakravarty, Alison L. Scott, Susan E. Bray, Michelle J. Ferguson, and Gillian Smith. 2016. "ABCB1 (MDR1) Induction Defines a Common Resistance Mechanism in Paclitaxel- and Olaparib-Resistant Ovarian Cancer Cells." *British Journal of Cancer* 115 (4): 431–41. https://doi.org/10.1038/BJC.2016.203.

Vanhaesebroeck, Bart, Julie Guillermet-Guibert, Mariona Graupera, and Benoit Bilanges. 2010. "The Emerging Mechanisms of Isoform-Specific PI3K Signalling." *Nature Reviews Molecular Cell Biology 2010 11:5* 11 (5): 329–41. https://doi.org/10.1038/nrm2882.

Vanhaesebroeck, Bart, Len Stephens, and Phillip Hawkins. 2012. "PI3K Signalling: The Path to Discovery and Understanding." *Nature Reviews Molecular Cell Biology 2012 13:3* 13 (3): 195–203. https://doi.org/10.1038/nrm3290.

Venkatraman, L., J. R. Goepel, K. Steele, S. P. Dobbs, R. W. Lyness, and W. G. McCluggage. 2003. "Soft Tissue, Pelvic, and Urinary Bladder Leiomyosarcoma as Second Neoplasm Following Hereditary Retinoblastoma." *Journal of Clinical Pathology* 56 (3): 233. https://doi.org/10.1136/JCP.56.3.233.

Verma, Mohit K., Julia Clemens, Lisa Burzenski, Stephen B. Sampson, Michael A. Brehm, Dale L. Greiner, and Leonard D. Shultz. 2017. "A Novel Hemolytic Complement-Sufficient NSG Mouse Model Supports Studies of Complement-Mediated Antitumor Activity In Vivo." *Journal of Immunological Methods* 446 (July): 47. https://doi.org/10.1016/J.JIM.2017.03.021.

Verma, Subhash C., and Erle S. Robertson. 2003. "Molecular Biology and Pathogenesis of Kaposi Sarcoma-Associated Herpesvirus." *FEMS Microbiology Letters* 222 (2): 155–63. https://doi.org/10.1016/S0378-1097(03)00261-1.

Vernardis, Spyros I., Konstantinos Terzoudis, Nicki Panoskaltsis, and Athanasios Mantalaris. 2017. "Human Embryonic and Induced Pluripotent Stem Cells Maintain Phenotype but Alter Their Metabolism after Exposure to ROCK Inhibitor." *Scientific Reports 2017 7:1* 7 (1): 1–11. https://doi.org/10.1038/srep42138.

Verschoor, Arie Jan, Saskia Litière, Sandrine Marréaud, Ian Judson, Maud Toulmonde, Eva Wardelmann, Axel LeCesne, and Hans Gelderblom. 2020. "Survival of Soft Tissue Sarcoma Patients after Completing Six Cycles of First-Line Anthracycline Containing Treatment: An EORTC-STBSG Database Study." *Clinical Sarcoma Research 2020 10:1* 10 (1): 1–9. https://doi.org/10.1186/S13569-020-00137-5.

Verweij, Jaap, Paolo G. Casali, John Zalcberg, Axel LeCesne, Peter Reichardt, Jean Yves Blay, Rolf Issels, et al. 2004. "Progression-Free Survival in Gastrointestinal Stromal Tumours with High-Dose Imatinib: Randomised Trial." *Lancet* 364 (9440): 1127–34. https://doi.org/10.1016/S0140-6736(04)17098-0.

Vidula, Neelima, Taronish Dubash, Michael S. Lawrence, Antoine Simoneau, Andrzej Niemierko, Erica Blouch, Becky Nagy, et al. 2020. "Identification of Somatically Acquired BRCA1/2 Mutations by CfDNA Analysis in Patients with Metastatic Breast Cancer." *Clinical Cancer Research* 26 (18): 4852–62. https://doi.org/10.1158/1078-0432.CCR-20-0638.

Villar, Victor Hugo, Oliver Vögler, Jordi Martínez-Serra, Rafael Ramos, Silvia Calabuig-Fariñas, Antonio Gutiérrez, Francisca Barceló, Javier Martín-Broto, and Regina Alemany. 2012. "Nilotinib Counteracts P-Glycoprotein-Mediated Multidrug Resistance and Synergizes the Antitumoral Effect of Doxorubicin in Soft Tissue Sarcomas." *PLOS ONE* 7 (5): e37735.

https://doi.org/10.1371/JOURNAL.PONE.0037735.

Vita, Alessandro De, Federica Recine, Giacomo Miserocchi, Federica Pieri, Chiara Spadazzi, Claudia Cocchi, Silvia Vanni, et al. 2021. "The Potential Role of the Extracellular Matrix in the Activity of Trabectedin in UPS and L-Sarcoma: Evidences from a Patient-Derived Primary Culture Case Series in Tridimensional and Zebrafish Models." *Journal of Experimental & Clinical Cancer Research : CR* 40 (1). https://doi.org/10.1186/S13046-021-01963-1.

Voissiere, Aurelien, Elodie Jouberton, Elise Maubert, Francoise Degoul, Caroline Peyrode, Jean Michel Chezal, and Elisabeth Miot-Noirault. 2017. "Development and Characterization of a Human Three-Dimensional Chondrosarcoma Culture for in Vitro Drug Testing." *PloS One* 12 (7). https://doi.org/10.1371/JOURNAL.PONE.0181340.

Vokurka, Martin, Lukáš Lacina, Jan Brábek, Michal Kolář, Yi Zhen Ng, and Karel Smetana. 2022. "Cancer-Associated Fibroblasts Influence the Biological Properties of Malignant Tumours via Paracrine Secretion and Exosome Production." *International Journal of Molecular Sciences* 23 (2): 23. https://doi.org/10.3390/IJMS23020964.

Volkova, Maria, and Raymond Russell. 2012. "Anthracycline Cardiotoxicity: Prevalence, Pathogenesis and Treatment." *Current Cardiology Reviews* 7 (4): 214–20. https://doi.org/10.2174/157340311799960645.

Vornicova, Olga, Yael Babichev, Rima Al-awar, Richard Marcellus, Albiruni Ryan Abdul Razak, and Rebecca Anne Gladdy. 2022. "Synergistic Activity of PARP Inhibitors (PARPi) in Combination with Standard Chemotherapy (CTx) in Leiomyosarcoma." *Journal of Clinical Oncology* 40 (16_suppl): 11560–11560. https://doi.org/10.1200/JCO.2022.40.16_SUPPL.11560.

Wan, X., B. Harkavy, N. Shen, P. Grohar, and L. J. Helman. 2006. "Rapamycin Induces Feedback Activation of Akt Signaling through an IGF-1R-Dependent Mechanism." *Oncogene 2007 26:13* 26 (13): 1932–40. https://doi.org/10.1038/sj.onc.1209990.

Wang, Chengzhi, Xiaoqing Zhou, Hongjuan Xu, Xiaqing Shi, Jinfeng Zhao, Manyi Yang, Lihua Zhang, et al. 2018. "Niclosamide Inhibits Cell Growth and Enhances Drug Sensitivity of Hepatocellular Carcinoma Cells via STAT3 Signaling Pathway." *Journal of Cancer* 9 (22): 4150–55. https://doi.org/10.7150/JCA.26948.

Wang, Haiwei, Xinrui Wang, Liangpu Xu, Ji Zhang, and Hua Cao. 2020. "Integrated Analysis of the E2F Transcription Factors across Cancer Types." *Oncology Reports* 43 (4): 1133–46. https://doi.org/10.3892/OR.2020.7504/HTML.

Wang, Jian, Xiaoye Lv, Xiutian Guo, Yanbo Dong, Peipei Peng, Fang Huang, Peng Wang, et al. 2021. "Feedback Activation of STAT3 Limits the Response to PI3K/AKT/MTOR Inhibitors in PTEN-Deficient Cancer Cells." *Oncogenesis 2021 10:1* 10 (1): 1–12. https://doi.org/10.1038/s41389-020-00292-w.

Wang, Lin Hong, Mei Xu, Luo Qin Fu, Xiao Yi Chen, and Fan Yang. 2018. "The Antihelminthic Niclosamide Inhibits Cancer Stemness, Extracellular Matrix Remodeling, and Metastasis through Dysregulation of the Nuclear β-Catenin/c-Myc Axis in OSCC." *Scientific Reports 2018 8:1* 8 (1): 1–13. https://doi.org/10.1038/s41598-018-30692-3.

Wang, Minli, Weizhong Wu, Wenqi Wu, Bustanur Rosidi, Lihua Zhang, Huichen Wang, and George Iliakis. 2006. "PARP-1 and Ku Compete for Repair of DNA Double Strand Breaks by Distinct NHEJ Pathways." *Nucleic Acids Research* 34 (21): 6170–82. https://doi.org/10.1093/NAR/GKL840.

Wang, Xiaochun, David Goldstein, Philip Crowe, and Jia-Lin Yang. 2019. "Abstract 3907: Synergistic Effect of Targeting Both CDK4/6 and MTORin Sarcoma Cell Lines." *Cancer Research* 79 (13_Supplement): 3907–3907. https://doi.org/10.1158/1538-7445.AM2019-3907.

Watanabe, K., T. Tajino, M. Sekiguchi, and T. Suzuki. 2000. "H-Caldesmon as a Specific Marker for Smooth Muscle TumorsComparison With Other Smooth Muscle Markers in Bone Tumors." *American Journal of Clinical Pathology* 113 (5): 663–68. https://doi.org/10.1309/JNQX-F4KM-Q0Q0-7XK8.

Watanabe, Kiichi, Morio Ueno, Daisuke Kamiya, Ayaka Nishiyama, Michiru Matsumura, Takafumi Wataya, Jun B. Takahashi, et al. 2007. "A ROCK Inhibitor Permits Survival of Dissociated Human Embryonic Stem Cells." *Nature Biotechnology 2007 25:6* 25 (6): 681–86. https://doi.org/10.1038/nbt1310.

Waters, Crystal A., Natasha T. Strande, John M. Pryor, Christina N. Strom, Piotr Mieczkowski, Martin D. Burkhalter, Sehyun Oh, et al. 2014. "The Fidelity of the Ligation Step Determines How Ends Are Resolved during Nonhomologous End Joining." *Nature Communications 2014 5:1* 5 (1): 1–11. https://doi.org/10.1038/ncomms5286.

Weichselbaum, Ralph R., Hemant Ishwaran, Taewon Yoon, Dimitry S.A. Nuyten, Samuel W. Baker, Nikolai Khodarev, Andy W. Su, et al. 2008. "An Interferon-Related Gene Signature for DNA Damage Resistance Is a Predictive Marker for Chemotherapy and Radiation for Breast Cancer." *Proceedings of the National Academy of Sciences of the United States of America* 105 (47): 18490–95. https://doi.org/10.1073/PNAS.0809242105/SUPPL_FILE/0809242105SI.PDF.

WHO classification of tumor editorial board. 2020. *Soft Tissue and Bone Tumours*. *International Agency for Research on Cancer*. Vol. 3.

Wilding, Christopher P, Mark L Elms, Ian Judson, Aik-Choon Tan, Robin L Jones, and Paul H Huang. 2019. "The Landscape of Tyrosine Kinase Inhibitors in Sarcomas: Looking beyond Pazopanib." *Expert Review of Anticancer Therapy* 19 (11): 971–91. https://doi.org/10.1080/14737140.2019.1686979.

Wilhelm, Scott M., Jacques Dumas, Lila Adnane, Mark Lynch, Christopher A. Carter, Gunnar Schütz, Karl Heinz Thierauch, and Dieter Zopf. 2011. "Regorafenib (BAY 73-4506): A New Oral Multikinase Inhibitor of Angiogenic, Stromal and Oncogenic Receptor Tyrosine Kinases with Potent Preclinical Antitumor Activity." *International Journal of Cancer* 129 (1). https://doi.org/10.1002/ijc.25864.

Wise-Draper, Trisha M., Ganesh Moorthy, Mohamad A. Salkeni, Nagla Abdel Karim, Hala Elnakat Thomas, Carol A. Mercer, M. Shalaan Beg, et al. 2017. "A Phase Ib Study of the Dual PI3K/MTOR Inhibitor Dactolisib (BEZ235) Combined with Everolimus in Patients with Advanced Solid Malignancies." *Targeted Oncology* 12 (3): 323–32. https://doi.org/10.1007/S11523-017-0482-9/FIGURES/3.

Woll, Penella J., Peter Reichardt, Axel Le Cesne, Sylvie Bonvalot, Alberto Azzarelli, Harald J. Hoekstra, Michael Leahy, et al. 2012. "Adjuvant Chemotherapy with Doxorubicin, Ifosfamide, and Lenograstim for Resected Soft-Tissue Sarcoma (EORTC 62931): A Multicentre Randomised Controlled Trial." *The Lancet Oncology* 13 (10): 1045–54. https://doi.org/10.1016/S1470-2045(12)70346-7.

Wong, Jocelyn P., Jason R. Todd, Martina A. Finetti, Frank McCarthy, Malgorzata Broncel, Simon Vyse, Maciej T. Luczynski, et al. 2016. "Dual Targeting of PDGFRα and FGFR1 Displays Synergistic Efficacy in Malignant Rhabdoid Tumors." *Cell Reports* 17 (5): 1265–75.

https://doi.org/10.1016/J.CELREP.2016.10.005.

Xia, Fen, Danielle G. Taghian, Jeffrey S. DeFrank, Zhao Chong Zeng, Henning Willers, George Iliakis, and Simon N. Powell. 2001. "Deficiency of Human BRCA2 Leads to Impaired Homologous Recombination but Maintains Normal Nonhomologous End Joining." *Proceedings of the National Academy of Sciences of the United States of America* 98 (15): 8644–49. https://doi.org/10.1073/PNAS.151253498/ASSET/20D9CD60-D04B-482F-AA84-221347626011/ASSETS/GRAPHIC/PQ1512534005.JPEG.

Xie, Chengying, Xiaozhe Wan, Haitian Quan, Mingyue Zheng, Li Fu, Yun Li, and Liguang Lou. 2018. "Preclinical Characterization of Anlotinib, a Highly Potent and Selective Vascular Endothelial Growth Factor Receptor-2 Inhibitor." *Cancer Science* 109 (4): 1207–19. https://doi.org/10.1111/CAS.13536.

Xue, Xiaoyu, Steven Raynard, Valeria Busygina, Akhilesh K. Singh, and Patrick Sung. 2013. "Role of Replication Protein A in Double Holliday Junction Dissolution Mediated by the BLM-Topo IIIα-RMI1-RMI2 Protein Complex." *Journal of Biological Chemistry* 288 (20): 14221–27. https://doi.org/10.1074/JBC.M113.465609.

Yaeger, Rona, Walid K. Chatila, Marla D. Lipsyc, Jaclyn F. Hechtman, Andrea Cercek, Francisco Sanchez-Vega, Gowtham Jayakumaran, et al. 2018. "Clinical Sequencing Defines the Genomic Landscape of Metastatic Colorectal Cancer." *Cancer Cell* 33 (1): 125-136.e3. https://doi.org/10.1016/J.CCELL.2017.12.004/ATTACHMENT/A573C216-11E2-47ED-AD64-AD660B40C229/MMC5.XLSX.

Yan, Chuan, Dalton C. Brunson, Qin Tang, Daniel Do, Nicolae A. Iftimia, John C. Moore, Madeline N. Hayes, et al. 2019. "Visualizing Engrafted Human Cancer and Therapy Responses in Immunodeficient Zebrafish." *Cell* 177 (7): 1903-1914.e14. https://doi.org/10.1016/j.cell.2019.04.004.

Yang, Fan, Christopher J. Kemp, and Steven Henikoff. 2013. "Doxorubicin Enhances Nucleosome Turnover around Promoters." *Current Biology* 23 (9): 782–87. https://doi.org/10.1016/j.cub.2013.03.043.

Yang, Jia-Lin, Romi Das Gupta, David Goldstein, and Philip J Crowe. 2017. "Significance of Phosphorylated Epidermal Growth Factor Receptor and Its Signal Transducers in Human Soft Tissue Sarcoma." *International Journal of Molecular Sciences* 18 (6). https://doi.org/10.3390/ijms18061159.

Yang, Jilong, Xiaoling Du, Kexin Chen, Antti Ylipää, Alexander J.F. Lazar, Jonathan Trent, Dina Lev, et al. 2009. "Genetic Aberrations in Soft Tissue Leiomyosarcoma." *Cancer Letters* 275 (1): 1. https://doi.org/10.1016/J.CANLET.2008.06.013.

Yang, Jilong, James A. Eddy, Yuan Pan, Andrea Hategan, Ioan Tabus, Yingmei Wang, David Cogdell, et al. 2010. "Integrated Proteomics and Genomics Analysis Reveals a Novel Mesenchymal to Epithelial Reverting Transition in Leiomyosarcoma through Regulation of Slug." *Molecular & Cellular Proteomics* 9 (11): 2405–13. https://doi.org/10.1074/MCP.M110.000240.

Yang, Jing, Ji Nie, Xuelei Ma, Yuquan Wei, Yong Peng, and Xiawei Wei. 2019. "Targeting PI3K in Cancer: Mechanisms and Advances in Clinical Trials." *Molecular Cancer 2019 18:1* 18 (1): 1–28. https://doi.org/10.1186/S12943-019-0954-X.

Yang, Qingshan, Prexy Modi, Terry Newcomb, Christophe Quéva, and Varsha Gandhi. 2015. "Idelalisib: First-in-Class PI3K Delta Inhibitor for the Treatment of Chronic Lymphocytic Leukemia, Small Lymphocytic Leukemia, and Follicular Lymphoma." *Clinical Cancer*

Research 21 (7): 1537–42. https://doi.org/10.1158/1078-0432.CCR-14-2034.

Yeh, Liang Tsai, Chiao Wen Lin, Ko Hsiu Lu, Yi Hsien Hsieh, Chao Bin Yeh, Shun Fa Yang, and Jia Sin Yang. 2022. "Niclosamide Suppresses Migration and Invasion of Human Osteosarcoma Cells by Repressing TGFBI Expression via the ERK Signaling Pathway." *International Journal of Molecular Sciences* 23 (1): 484. https://doi.org/10.3390/IJMS23010484/S1.

Yi, Young, Young Mi Woo, Kyu Ho Hwang, Hyun Sil Kim, and Sang Hyeong Lee. 2021. "Niclosamide and Pyrvinium Are Both Potential Therapeutics for Osteosarcoma, Inhibiting Wnt–Axin2–Snail Cascade." *Cancers* 13 (18). https://doi.org/10.3390/CANCERS13184630/S1.

Yoon, Hyunho, Chih Min Tang, Sudeep Banerjee, Antonio L. Delgado, Mayra Yebra, Jacob Davis, and Jason K. Sicklick. 2021. "TGF-B1-Mediated Transition of Resident Fibroblasts to Cancer-Associated Fibroblasts Promotes Cancer Metastasis in Gastrointestinal Stromal Tumor." *Oncogenesis* 10 (2). https://doi.org/10.1038/s41389-021-00302-5.

Yoon, Sam S., Neil H. Segal, Peter J. Park, Kara Y. Detwiller, Namali T. Fernando, Sandra W. Ryeom, Murray F. Brennan, and Samuel Singer. 2006. "Angiogenic Profile of Soft Tissue Sarcomas Based on Analysis of Circulating Factors and Microarray Gene Expression." *Journal of Surgical Research* 135 (2): 282–90. https://doi.org/10.1016/J.JSS.2006.01.023.

Yovine, A., M. Riofrio, J. Y. Blay, E. Brain, J. Alexandre, C. Kahatt, A. Taamma, et al. 2004. "Phase II Study of Ecteinascidin-743 in Advanced Pretreated Soft Tissue Sarcoma Patients." *Journal of Clinical Oncology* 22 (5): 890–99. https://doi.org/10.1200/JCO.2004.05.210.

Yu, Xinyi, Feng Liu, Liyi Zeng, Fang He, Ruyi Zhang, Shujuan Yan, Zongyue Zeng, et al. 2018. "Niclosamide Exhibits Potent Anticancer Activity and Synergizes with Sorafenib in Human Renal Cell Cancer Cells." *Cellular Physiology and Biochemistry* 47 (3). https://doi.org/10.1159/000490140.

Yuan, Jin, Xiaoyang Li, and Shengji Yu. 2021. "Molecular Targeted Therapy for Advanced or Metastatic Soft Tissue Sarcoma." *Cancer Control : Journal of the Moffitt Cancer Center* 28 (November): 1–20. https://doi.org/10.1177/10732748211038424.

Zhan, Maocheng, Dihua Yu, Aiqing Lang, Lan Li, and Raphael E Pollock. 2001. "Wild Type P53 Sensitizes Soft Tissue Sarcoma Cells to Doxorubicin by Down-Regulating Multidrug Resistance-1 Expression." https://doi.org/10.1002/1097-0142.

Zhang, Chen, Juan Gao, Shanshan Lu, Yinli Zhang, and Honglan Zhu. 2021. "Uterine Smooth Muscle Tumors of Uncertain Malignant Potential (STUMP): A Retrospective Study in a Single Center." *European Journal of Obstetrics, Gynecology, and Reproductive Biology* 265 (October): 74–79. https://doi.org/10.1016/J.EJOGRB.2021.08.010.

Zhang, Jing, Quan Tian, and Shu-Feng Zhou. 2008. "Clinical Pharmacology of Cyclophosphamide and Ifosfamide." *Current Drug Therapy* 1 (1): 55–84. https://doi.org/10.2174/157488506775268515.

Zhang, Sui, Xiaobing Liu, Tasneem Bawa-Khalfe, Long Sheng Lu, Yi Lisa Lyu, Leroy F. Liu, and Edward T.H. Yeh. 2012. "Identification of the Molecular Basis of Doxorubicin-Induced Cardiotoxicity." *Nature Medicine 2012 18:11* 18 (11): 1639–42. https://doi.org/10.1038/nm.2919.

Zhang, Zhiwei, Chenggong Sun, Chengcheng Li, Xinlin Jiao, Brannan B. Griffin, Samina Dongol, Huan Wu, et al. 2020. "Upregulated MELK Leads to Doxorubicin Chemoresistance and M2 Macrophage Polarization via the MiR-34a/JAK2/STAT3 Pathway in Uterine

Leiomyosarcoma." *Frontiers in Oncology* 10 (April): 453. https://doi.org/10.3389/fonc.2020.00453.

Zhang, Zhiying, Kaiwen Hu, Tasuku Kiyuna, Kentaro Miyake, Kei Kawaguchi, Kentaro Igarashi, Scott D. Nelson, Yunfeng Li, Shree Ram Singh, and Robert M. Hoffman. 2019. "A Patient-Derived Orthotopic Xenograft (PDOX) Nude-Mouse Model Precisely Identifies Effective and Ineffective Therapies for Recurrent Leiomyosarcoma." *Pharmacological Research* 142 (April): 169–75. https://doi.org/10.1016/J.PHRS.2019.02.021.

Zhao, Jihe. 2016. "Cancer Stem Cells and Chemoresistance: The Smartest Survives the Raid." *Pharmacology & Therapeutics* 160 (April): 145. https://doi.org/10.1016/J.PHARMTHERA.2016.02.008.

Zhao, Liqun, and Baolin Zhang. 2017. "Doxorubicin Induces Cardiotoxicity through Upregulation of Death Receptors Mediated Apoptosis in Cardiomyocytes." *Scientific Reports 2017 7:1* 7 (1): 1–11. https://doi.org/10.1038/srep44735.

Zheng, Yuan-Yin, Xiao-Bin Liu, Ying-Yu Mao, and Mao-Hua Lin. 2020. "Smooth Muscle Tumor of Uncertain Malignant Potential (STUMP): A Clinicopathologic Analysis of 26 Cases." *International Journal of Clinical and Experimental Pathology* 13 (4): 818. /pmc/articles/PMC7191150/.

Zhu, Min, Hongchang Zhao, Oliver Limbo, and Paul Russell. 2018. "Mre11 Complex Links Sister Chromatids to Promote Repair of a Collapsed Replication Fork." *Proceedings of the National Academy of Sciences of the United States of America* 115 (35): 8793–98. https://doi.org/10.1073/PNAS.1808189115/SUPPL_FILE/PNAS.1808189115.SAPP.PDF.

Zumwalde, Nicholas A., Jill D. Haag, Deepak Sharma, Jennifer A. Mirrielees, Lee G. Wilke, Michael N. Gould, and Jenny E. Gumperz. 2016. "Analysis of Immune Cells from Human Mammary Ductal Epithelial Organoids Reveals Vδ2+ T Cells That Efficiently Target Breast Carcinoma Cells in the Presence of Bisphosphonate." *Cancer Prevention Research* 9 (4): 305–16. https://doi.org/10.1158/1940-6207.CAPR-15-0370-T/36196/AM/ANALYSIS-OF-IMMUNE-CELLS-FROM-HUMAN-MAMMARY-DUCTAL.